MULTI-PROXY RECONSTRUCTIONS OF HOLOCENE ENVIRONMENTAL CHANGE AND CATCHMENT BIOGEOCHEMISTRY USING ALGAL PIGMENTS AND STABLE ISOTOPES PRESERVED IN LAKE SEDIMENT FROM BAFFIN ISLAND AND ICELAND

by

CHRISTOPHER ROTH FLORIAN

B.A., University of Colorado, 2007

A thesis submitted to the

Faculty of the Graduate School of the

University of Colorado in partial fulfillment

of the requirement for the degree of

Doctor of Philosophy

Department of Geological Sciences

2016

This thesis entitled:

Multi-proxy reconstructions of Holocene environmental change and catchment biogeochemistry using algal pigments and stable isotopes preserved in lake sediment from Baffin Island and Iceland

has been approved for the Department of Geological Sciences

Gifford H. Miller

Áslaug Geirsdóttir

Date_____

The final copy of this thesis has been examined by the signatories, and we find that both the content and the form meet acceptable presentation standards of scholarly work in the above mentioned discipline.

Florian, Christopher Roth (Ph.D., Geological Sciences)

Multi-proxy reconstructions of Holocene environmental change and catchment biogeochemistry using algal pigments and stable isotopes preserved in lake sediment from Baffin Island and Iceland

Thesis directed by Professors Gifford H. Miller and Áslaug Geirsdóttir

Lake sediments provide a continuous record of environmental change, integrating information about multiple biogeochemical processes occurring within the lake and catchment. Much of this is recorded by the chemical characteristics of sedimentary organic matter, which can be used as a proxy for past conditions. This dissertation examines Holocene lake sediment records from Baffin Island and Iceland, which, as a result of Arctic amplification feedbacks, are particularly sensitive to changes in climate. We integrated sedimentary algal pigments with more commonly used proxies such as stable isotopes, C:N ratio, and biogenic silica in order to derive a more complete understanding of local climate history and catchment biogeochemistry. Contrasting modern climate conditions between the Eastern Canadian Arctic and Iceland allows us to examine proxy response across different environments.

The climate records developed in this study broadly agree with other regional records, with coherent shifts in biogeochemical proxies occurring in response to Holocene climate evolution. The nature, magnitude, and timing of proxy response vary between locations, underscoring the need to account for the distinct environmental factors of each lake system when reconstructing climate history. This study is the first to develop Holocene records of sedimentary algal pigments in each study area which distinctly characterize changes in lacustrine algal group assemblage through time. In Baffin Island, green algae and higher plants are most abundant

during the early Holocene, with increased diatom relative abundance during the late Holocene and Little Ice Age. This is followed by a return to increased green algae and higher plants during recent times. This pattern is not replicated in Icelandic lakes, where cyanobacteria show the strongest temperature response and are more abundant during warm times. More complete progression of seasonal algal group succession during longer ice-free seasons is the proposed mechanism controlling algal group relative abundance. Recent trends in Icelandic lakes from this study do not show as strong of a response to Anthropogenic warming as on Baffin Island, where many proxies abruptly return to a Holocene Thermal Maximum-like state. The results of this dissertation characterize the biogeochemical regimes which occur during climatic extremes of the Holocene, and can be used to predict future conditions influencing water quality and the carbon cycle in a warming Arctic.

ACKNOWLEDGMENTS

I wish to thank my advisors Giff Miller and Áslaug Geirsdóttir for their guidance, teaching, expertise, and having allowed me the freedom to pursue analytical methods new to our research group; my committee members Julio Sepúlveda, Tom Marchitto, Jim White, and Diane McKnight for their thought provoking questions, comments and advice given during committee meetings and the comprehensive exam; Billy D'Andrea and Jostein Bakke for serving as opponents during the University of Iceland defense; Marilyn Fogel for allowing me to spend months running samples in her lab and teaching me about isotope biogeochemistry; Zoe Sigle for analyzing nearly all of the FTIR-BSi samples; Steve DeVogel for keeping the lab running smoothly and teaching me how to use an HPLC; Rolfe Vinebrooke and Mark Graham for assisting me with the development of algal pigment methodologies at INSTAAR; Thorvaldur Thordarson for assistance with tephra identification; Sveinbjörn Steinthórsson and Thorsteinn Jónsson for excellent field work assistance; John Andrews, Anne Jennings, Scott Lehman, Alex Wolfe and Yarrow Axford for scientific discussions; Sarah Spaulding and Mark Edlund for teaching all about diatoms; fellow graduate students Sarah Crump, Sydney Gunnarson, Darren Larsen, Kurt Refsnider, Kate Zalzal, Simon Pendleton, Leif Anderson, Ben Schupack, Celene Blair, and David Harning for discussion, advice, and friendship; and especially Amy Steiker for her support, encouragement, and willingness to edit many documents over the years.

Salary was provided by the Doctoral Grant of the University of Iceland and NSF grant ARC-0909347. This research was made possible by NSF grant ARC-0909347, RANNIS grant of Excellence #141573-051 and several grants awarded to Áslaug Geirsdóttir from the University of Iceland Research Fund.

CONTENTS

CHAPTER 3: CATCHMENT GEOMETRY INFLUENCES PROXY RESPONSE IN LATE HOLOCENE RECORDS FROM TWO PROXIMAL LAKES LOCATED IN NORTH ICELAND

TABLE

FIGURE

CHAPTER 1

1.1. INTRODUCTION

Temperature and moisture availability are key controls over biological processes and both of these factors are directly dependent on climatic conditions. Because of this, changes in climate favor certain species or groups of organisms (Blois et al. 2013). This relationship also impacts the success of human civilization, which is dependent on agriculture, the availability of water, and is vulnerable to extreme events. Therefore, past changes in climate are predicted to have impacted societies (e.g. Buntgen et al. 2011; D'Andrea et al. 2011). Reconstructing the Earth's past climate is essential for understanding the range of conditions that we can expect in the future, and more importantly, how rapidly climate transitions might occur (Overpeck and Cole 2006). Using the same relationship between climate and biology stated above, we can make the assumption that changes in climate will lead to a shift in the makeup of biological communities over time at a particular location. Additional factors that influence biological communities are nutrients, availability of a carbon source, and environmental parameters such as pH. These factors may also be directly or indirectly altered through changes in climatic conditions. Therefore, by reconstructing past abundances of various organisms, along with developing an understanding of the climatic and environmental factors controlling their populations, we can use a record of biological communities and associated biogeochemical history of a specific location as a proxy for changes in past climate. This dissertation relies on this core principal to develop climate records from biogeochemical information stored in the organic matter of lake sediments.

While the range in Holocene climatic conditions is less than that occurred over long timescales, it has long been recognized that significant variability has occurred (e.g. Mayewski et

al. 2004 and references therein). Abrupt, non-linear responses to monotonic orbital-driven insolation changes provide information about the sensitivity points of the climate system (Mayewski et al. 2004; Wanner et al. 2011; Geirsdóttir et al. 2013). Numerous high-quality archives are available which record environmental conditions during the Holocene, allowing for high spatial and temporal resolution and making possible the study of mechanisms causing spatiotemporal variability (e.g. Kaufman et al. 2004). Human-caused alterations to the Earth system are now ubiquitous, and the impacts are distinct enough to characterize the Anthropocene as a new geological epoch (Zalasiewicz et al. 2011; Wolfe et al. 2013). Although no exact analogue exists for the Anthropocene during the Holocene because of different forcing mechanisms, understanding the nature of Holocene climate events is the best-possible way to make the future projections needed to successfully anticipate and adapt to change.

Particularly important is constraining Arctic climate history, as it is these environments that will undergo the most rapid change of greatest magnitude as a result of the positive feedbacks associated with loss of snow and ice cover (Serreze and Francis 2006; Serreze and Barry 2011). Lacustrine environments in the Arctic will experience decreasing duration of ice cover, elevated maximum summer temperature, and alteration of mixing regimes (Smol et al. 2005; Smol and Douglas 2007). Studying the past changes that have occurred in Arctic lakes provides a record of climate events and information about how these lakes will evolve with future warming. This lacustrine biological response to climate is relevant for two main reasons. First, we are dependent on the condition of global fresh waters for drinking and food production. Projected increases in temperature may lead to deterioration of water quality due to toxic algal blooms (Paerl and Paul 2012), increased sediment load, reduced dissolved oxygen (Whitehead et al. 2009) and declining fisheries (Berkes and Jolly 2001); local communities will need to adapt to

these future changes. The second major implication of changes in Arctic lacustrine productivity is the potential of these environments to act as a source or sink of atmospheric carbon. The role of Arctic lakes in the global carbon cycle is not well constrained (Sobek et al. 2014), and climate plays a role in determining the balance between lake respiration and sediment carbon accumulation from aquatic and terrestrial primary productivity (Leng and Anderson 2014). Although fresh water carbon storage in sediment represents a small portion of the global carbon cycle (Cole et al. 2007), rates of carbon burial in high latitude lakes have increased in recent times and are projected to become increasingly important with future climate change (Heathcote et al. 2015).

This dissertation utilizes lake sediment cores from Baffin Island and Iceland to reconstruct climate and biogeochemical histories using similar suites of biological proxies across locations with contrasting mean climate state. The results of this study will provide a better understanding of the Holocene climate history of Baffin Island and Iceland, as well as how lacustrine biogeochemistry changed in response to climate events.

1.2. STUDY SITES

As a region of strong temperature gradients, and a primary pathway of northward heat advection by ocean currents and atmospheric circulation, North Atlantic climate is sensitive to change and reflects large-scale processes of global significance. This dissertation examines field sites from Baffin Island, in the western North Atlantic, and northern Iceland in the central North Atlantic. The environments at these nearly equivalent latitudes are distinctly contrasting due to the southwest to northeast trajectory of poleward heat transport, which has a lesser influence on Baffin Island climate compared to that of Iceland.

The western North Atlantic and eastern Canadian Arctic are characterized by extreme cold, with mean annual air temperatures (1957-1990) 90 km northwest of the study site at Cape Hooper, Nunavut -11.9 ºC; 2.3 ºC during summer (JJA) and -16.6 ºC during the non-summer months. Precipitation is low (~273 mm yr^{-1}), mostly falling as snow. The summer season is short, with freezing temperatures and snow occurring for 9.5 months of the year (Environment Canada 2016). Landscape vegetation cover is comprised of sparse heath tundra. The cold temperatures of this region are partially attributable to the influence of exported polar waters of the Baffin Current (Muench 1971) and widespread development of sea ice in Baffin Bay, where sea ice is present to some degree in all months except August and September (Tang et al. 2004).

Iceland, in the central North Atlantic, has a maritime climate with higher mean annual air temperature and precipitation than Baffin Island. Icelandic climate is characterized by relatively warm conditions as a result of heat transport from lower latitudes by regional oceanic and atmospheric circulation. North Iceland has a colder and more variable climate than southern Iceland (Einarsson 1993). Mean annual air temperatures in the study area were ~2.5 ºC between AD 1956 and 1990 (http://en.vedur.is/Medaltalstoflur-txt/Hraun_352_med6190.txt). The climate is variable, with the standard deviation of inter-annual variability greater than 1.3 ºC (Einarsson 1993). The Icelandic low, located south west of Iceland, is a persistent area of low pressure that dominates the regional atmospheric circulation (Serreze et al. 1997), bringing frequent wind and precipitation to the island. The coldest conditions in Iceland occur when sea ice, exported from Arctic Ocean, reaches the north coast (Einarsson 1984). Prevailing wind direction is variable and largely determines the temperature, with warm moist conditions characterizing a southwest wind and dry cold conditions during northeast winds. Precipitation type is variable, as rain can occur in the winter, with snow only making up 50-70% of winter precipitation at sea level in north

Iceland. Because of this, the duration of complete snow cover can vary from weeks to months (Einarsson 1984). Vegetation cover in northwest Iceland is dominated by heathlands of *Betula nana, Empetrum nigrum, Salix sp., Rachometrium* mosses, and various grasses and herbs (Arnalds 2015).

1.3. QUESTIONS MOTIVATING THIS DISSERTATION

This dissertation aims to answer several long-standing questions that have been the subject of multiple of past studies. These questions remain open, as a complete characterization of past environments and climatic conditions is nearly impossible to obtain. Increased spatial density of proxy records, the discovery of high-quality archives, and advances in methodology all continue to provide more complete answers to the questions below:

1) Was the evolution of Holocene climate linear, or punctuated by times of rapid change? Did spatial variability, timing, and magnitude of major climate events differ between the western and central sectors of the North Atlantic?

2) How are changes in lake and catchment biogeochemistry related to climate events?

1.4. RESEARCH METHODS AND GOALS

This dissertation utilizes lake sediment cores as archives of past change. Lake sediment incorporates minerogenic and organic material from within-lake and catchment sources into a continuous archive, which can often be precisely dated and sampled at high temporal resolution. Additionally, lakes are abundant, and suitable field sites often found in the desired region of study. Information is gained from lake sediment cores by examining various proxies, each of which records information about a specific process in the lake-watershed system. The proxies

used in this study are: algal pigments, carbon and nitrogen stable isotopes and elemental ratios, FTIRS-inferred biogenic silica, diatom species assemblages, total organic carbon, and magnetic susceptibility.

Algal pigments are isoprenoid organic molecules produced by all algae and higher plants and function to both harvest energy from sunlight and protect against damage from excess light. While all contain the primary photosynthetic pigment chlorophyll *a*, each lineage of algae is characterized by a different suite of accessory pigments. The pigments discussed in this dissertation fall into two major classes, chloropigments, which have a porphyrin ring containing a chelated Mg (Rowan 1989), and carotenoids, which are composed of a 40-carbon chain of conjugated double bonds. The chelated magnesium complex and conjugated double bonds contain weakly held electrons that absorb light energy.

While chloropigments can be specific to algal lineages, the much greater diversity of carotenoids makes them more suited for use as biomarkers. This dissertation focuses on pigments from the following groups: green algae (Chlorophyta), green plants (Plantae), diatoms (Bacillariophyta), chrysophytes (Chrysophyta) and cyanobacteria (Cyanophyta). Based on pigment composition, these groups of algae can be separated into three categories: the green algae/plants, diatoms and chrysophytes, and cyanobacteria. The pigment composition of green algae and higher plants consists primarily of the chlorophylls *a* and *b*, and the carotenoids violaxanthin, neoxanthin, lutein, and β carotene (Bianchi and Finlay 1990; Jeffery et al. 1997). Of these pigments, chlorophyll *b*, violaxanthin, neoxanthin and lutein are distinct and can be used for taxonomic reconstructions. Diatoms and chrysophtes share a similar pigment composition, consisting of chlorophylls *a* and *c*, fucoxanthin, diatoxanthin, diadinoxanthin, and β carotene (Stauber and Jeffery 1988; Jeffery et al. 1997; Leavitt and Hodgson 2001). Fucoxanthin,

diatoxanthin and diadinoxanthin are diagnostic of these groups. Cyanobacteria have a particularly diverse pigment composition, many of which are diagnostic: chlorophyll *a*, canthaxanthin, echinenone, myxoxanthophyll, zeaxanthin, scytonemin, oscillaxanthin, aphanizophyll, and β carotene (Nichols 1973; Jeffery et al. 1997; Leavitt and Hodgson 2001). Pigments can be solvent extracted from the water column, algal mats, and sediment, then chromatographically separated to quantitatively assess algal group abundance.

Due to their weakly held electrons, pigments can be easily degraded by exposure to high temperature, light, oxygen, and heterotrophy. The most stable pigments have relatively simple and unreactive functional groups (Bianchi et al. 1993; Leavitt and Hodgson 2001). Because of the immediate degradation process that begins upon algal cell death, the most complete pigment-inferred algal assemblages are developed from samples of filtered lake or ocean water and live algal mats. Sedimentary archives are variably suitable for reconstructing past algal abundances. Stratified lakes with anoxic bottom waters will retain the most similar pigment composition to that of the water column. Because stratified lakes are often difficult to find in desired field areas, paleolimnological studies using algal pigments focus on the most stable pigments as well as pigment degradation products. Once degraded, carotenoids are converted to *cis*-isomers and then to colorless compounds after alteration of the conjugated system of double bonds (Leavitt et al. 1993; Leavitt et al. 2001; Reuss and Conley 2005). Chloropigments are degraded into stable pheophytins through the loss of the central Mg^{2+}, or pheophorbides through the loss of the phytol chain (Hendry 1987; Scheer 1991; Leavitt 1993; Jeffery et al. 1997; Leavitt and Hodgson 2001). Once buried in the sediment below the active surface layer, pigments are stable on geological timescales allowing for the reconstruction of past algal group abundance (Leavitt and Hodgson 2001).

Elemental ratios of carbon and nitrogen in sedimentary organic matter can be used to gain information about organic matter source, aquatic productivity, and biogeochemical processes (Meyers and Teranes 2001). Plant structural material is dominated by carbon-rich cellulose, lignin, and polysaccharides; therefore rigid structures will have a high C:N. In contrast, proteins, amino acids, and chlorophyll contain nitrogen. Algae produce the least amount of structural material, and therefore have the lowest C:N, followed by aquatic macrophyte plants and soils, plant leaves, and woody material. The relative proportion of each of these materials in lake sediment determines the bulk C:N value (Meyers 1994; Meyers and Lallier-Vergès 1999; Meyers and Teranes 2001). For example, change in past source of organic matter from algae to terrigenous will be seen as an increase in C:N. The amount material contributed by each source of organic matter it determined by both the biomass and efficiency of transport to the sediment. C:N has been used to reconstruct watershed deforestation (Kaushal and Binford 1999), terrestrial vegetation changes (Lamb et al. 2004), soil erosion (Geirsdóttir et al. 2009b), and aquatic macrophyte plant abundance (Briner et al. 2006). Post-depositional microbial alteration of sediment organic matter can also lead to changes in C:N. Nitrogen-containing compounds are often labile, being preferentially degraded by microbes, and sedimentary nitrate can then be reduced to N_2 gas by denitrifying bacteria. As a result of this, in young lake sediments, there is often an increase in C:N with depth as labile nitrogen is removed. Unless the study focuses on recent (~100 yr.) limnological changes, or there have been large changes in the redox state of the bottom water, the impact of these processes on the sediment record are probably minimal as sedimentary values all represent the end result of these early diagenetic alterations. In this dissertation, all changes in C:N are therefore assumed to be due to variability of organic matter source.

The mass dependent fractionation of stable isotopes records information about a broad range of biological and chemical processes. Biological processes discriminate against the heavier isotope (Fogel and Cifuentes 1993), and the degree of fractionation varies between organisms and environmental conditions. This allows for the study of organic matter source, biogeochemistry and environmental conditions during the formation and deposition of organic matter. Ratios of isotope abundance are expressed in delta notation where $\delta = ((R_{sample}/R_{standard})-1) \times 1000$. Isotopic data is reported relative to the V-PDB ($\delta^{13}C$) and Air ($\delta^{15}N$) standards. In this dissertation, records of carbon and nitrogen isotopes in bulk organic matter are developed for each study site. Carbon isotopes of organic matter in lake sediment are controlled by changing organic matter source (Meyers 1994; Wolfe et al. 1999; Wang and Wooller 2006), aquatic productivity which can reduce concentrations of $CO_{2(aq)}$ (Hodell and Schelske 1998; Brenner et al. 1999), and the utilization of HCO_3^- over $CO_{2(aq)}$ during photosynthesis by algae and aquatic plants (Hollander and Mackenzie 1991; Hassan et al. 1997). Nitrogen isotopes in lake sediment are more complex to interpret (reviewed by Talbot 2001), and generally require cross comparison with other proxies to determine the most likely driver of variability. Paleo and modern limnological studies have utilized nitrogen isotope records to examine past aquatic productivity (e.g. Gu et al. 1996; Teranes and Bernasconi 2000), nitrogen biogeochemisty (Wolfe et al. 1999; Teranes and Bernasconi 2000; Hu et al. 2001; Jones et al. 2004; Patione et al. 2006; and many others), and lake fertilization due to anthropogenic and animal inputs (Wolfe et al. 2001; Michelutti et al. 2009; Holtgrieve et al. 2011; Wolfe et al. 2013).

Diatoms (Bacillariophyta) are algae that create distinctly patterned siliceous cell walls, which persist in the sediment and are identifiable to the species level (Battarbee et al. 2001). Their great diversity and frequently narrow tolerance to environmental conditions make diatom

species assemblages excellent paleoenvironmental indicators. Notable uses of diatom assemblages in paleolimnology are reconstruction of water chemistry parameters such as pH and conductivity (Wolfe 2003; Michelutti et al. 2007), phosphorous availability and eutrophication (Bradshaw and Anderson 2001), lake water level change (Wolin et al. 1999) and, less robustly in freshwater than marine environments, summer temperature (Rosén et al. 2000; Bigler and Hall 2003). The response of diatom assemblages to environmental parameters is determined by development of regional transfer functions (e.g. Joynt and Wolfe 2001). Diatom species have shown a marked response to recent changes in climate and nutrient input, this change in assemblage is one of the defining expressions of the Anthropocene in lake sediment archives (Antoniades et al. 2005; Smol et al. 2005; Wolfe et al. 2013)

Biogenic silica (BSi), which is comprised of the sedimentary concentration of siliceous microfossils produced primarily by diatoms and chrysophytes (Douglas and Smol 1999), is used to estimate within-lake algal productivity (Conley and Schelske 2001). There is often a strong link between algal productivity and climate, and biogenic silica concentrations have been shown to co-vary with temperature change in some lakes (Blass et al. 2007; McKay et al. 2008). In this dissertation, changes in BSi are attributed to diatom production and dilution by variable sedimentation rate, together representing qualitative change in environmental conditions as in other regional studies (Geirsdóttir et al. 2009b).

This dissertation is the first to employ algal pigments to address the long-standing questions discussed above. When used together with more traditional proxies, sedimentary algal pigments allow for a more complete characterization of paleolimnological changes. Detailed cross validation and comparison of multiple proxies is often the only way to precisely interpret

past variability. The proxy comparisons of this dissertation will assist the interpretation of future lake sediment records in the region.

The goals of this dissertation are:

1) Evaluate algal pigments as an environmental proxy in Arctic lakes, where they have been underutilized
2) Use pigments as part of a multi-proxy study to derive high-resolution records of Holocene climate from lakes on Baffin Island and Iceland
3) Compare these records to evaluate catchment and regional scale differences in proxy response and climate history

1.5. DISSERTATION OVERVIEW

The introduction has attempted to briefly explain the techniques used and provide the necessary context to understand how this study is relevant to the broader field of research. Chapters 2 through 4 are presented as individual, stand-alone manuscripts. Chapter 2 presents a multi-proxy study of a sediment core from Qivitu Highlands Lake located on Baffin Island in the eastern Canadian Arctic. Part of this study included the development of laboratory techniques to analyze algal pigments at INSTAAR. Chapter 2 is followed by an addendum, which describes several data sets are each lacking a key element required for a publication. These data sets may be used in future studies and are presented here to make the information accessible. Chapter 3 compares two late Holocene records from Icelandic lakes Torfdalsvatn and Bæjarvötn, using an identical suite of proxies, which show varying response despite similar climate history. Chapter 4

presents a complete Holocene record from Torfdalsvatn. The conclusions of this dissertation aim to summarize major findings and put these in a broader perspective.

CHAPTER 2

Algal pigments in Arctic lake sediments record biogeochemical changes due to Holocene climate variability and anthropogenic global change

As published in the Journal of Paleolimnology

Christopher R. Florian[1,2*], Gifford H. Miller[1], Marilyn L. Fogel[3], Alexander P. Wolfe[4], Rolf D. Vinebrooke[4], Áslaug Geirsdóttir[2]

[1]Institute of Arctic and Alpine Research and Department of Geological Sciences, University of Colorado, Boulder, CO 80309-0450, USA

[2] Institute of Earth Sciences, University of Iceland, Sturlugata 7, Reykjavík 101, Iceland

[3] School of Natural Science, University of California, Merced, CA 95343, USA

[4] Department of Biological Sciences, University of Alberta, Edmonton, AB, Canada T6G 2E9

2.1. ABSTRACT

In order to better constrain the limnological impacts from recent climate change relative to those of the Holocene, we developed a high-resolution multi-proxy paleoenvironmental record from a small lake on eastern Baffin Island, Arctic Canada. Carbon and nitrogen elemental and isotopic compositions from sediment organic matter, algal pigments, and diatom assemblages are

integrated to provide robust indices of paleoclimatic variability. In particular, the ratio between individual carotenoid pigments (lutein:diatoxanthin) reveals a shift in dominant primary production from 'green' taxa (chlorophytes, higher plants, and bryophytes) during the Holocene Thermal Maximum (HTM) to 'brown' taxa (diatoms and chrysophytes) over the mid- to late Holocene. Green pigment abundance appears most sensitive to mean summer temperatures, and their increased relative abundance in the past serves as an indicator of warm times. Regionally, the HTM occurred shortly after local deglaciation (10 ka), persisting until ~7 ka. This timing agrees with that revealed by chironomid assemblages and ice core records elsewhere in the Canadian Arctic, but is significantly earlier than suggestions from palynology on Baffin Island. This study provides additional evidence that this discrepancy represents the ecesis for higher plant dispersal and colonization on distal, freshly deglaciated landscapes. Pigment and diatom data indicate that mid Holocene cooling began between 7 and 6 ka, intensifying after 3 ka. All proxies show pronounced change after 1.5 ka, with the greatest divergence from average Holocene values occurring during the Little Ice Age (LIA), supporting the growing consensus that the LIA was the coldest multi-centennial interval of the Holocene. In the 20th century, most proxies, including sedimentary carotenoid ratios, abruptly returned to a similar state as the Holocene Thermal Maximum, while diatom species assemblages present a more muted response. This underscores that anthropogenic alteration of the Earth system has created conditions with no exact analog in the past 10,000 years. Collectively, these results add new information on the dimensions of Arctic lake responses to Holocene climate change, which in turn can be used to reconcile paleoclimate reconstructions from diverse proxies.

2.2. INTRODUCTION

The extent and persistence of Arctic snow and ice cover can influence climate on a global scale (Serreze and Francis 2006; Miller et al. 2012), yet also produces profound local impacts on nutrient cycling and biological communities in Arctic lakes and watersheds (Wolfe 2002; Smol et al. 2005; Michelutti et al. 2007). It is this relationship that allows the reconstruction of past climate based on changes in organic matter characteristics and microfossil assemblages preserved in Arctic lake sediments. Understanding the nature of Holocene paleoclimatic events at high spatial and temporal resolution is necessary to disentangle the variability of climatic evolution across the Arctic (Kaufman et al. 2004). Much information is gained about the functioning of the Earth's climate system by examining the variable regional responses to a spatially homogenous forcing, such as insolation along bands of equal latitude.

The eastern Canadian Arctic has long been recognized as an important region for the study of past climate (Andrews et al. 1972; Hughen et al. 2000; Miller et al. 2005; Briner et al. 2006; Besonen et al. 2008; Axford et al. 2009). Because other continuous high-resolution climate archives (such as ice sheets) are relatively sparse, the sediment archived in the abundant lakes of the region can be used to fill gaps in spatial coverage of climate records (Smol 2008).

A wide range of climate proxies from lake sediments has been used to reconstruct late Quaternary climates across the eastern Canadian Arctic, including quantifications of minerogenic input to lakes (Moore et al. 2001; Thomas and Briner 2008) and diatom species assemblages (Wolfe 1994; Wolfe and Härtling 1996; Wolfe 2003; Antoniades et al. 2005; Smol et al. 2005; Michelutti et al. 2007; Podritske and Gajewski 2007; Wilson et al. 2012). Recent multiproxy records (Briner et al. 2006; Axford et al. 2009; Thomas et al. 2011) have exploited carbon and

nitrogen elemental concentrations and isotopic ratios to shed new light on linkages between regional Holocene climate history and aquatic biogeochemistry.

Algal groups have variable tolerances for environmental conditions and are predicted to respond differentially to Holocene climate evolution (Smol and Cumming 2000). Sedimentary pigments provide a means to reconstruct the abundance of taxonomic groups that do not leave morphological remains. These pigments can be used to differentiate contributions from green algae, higher plants, and mosses, from those originating from diatom and chrysophyte production (Leavitt and Hodgson 2001). For example, the ratio between the xanthophyll carotenoids lutein and diatoxanthin is predicted to track such changes over time. Lutein and diatoxanthin are similarly stable because they both lack the 5,6-epoxide group that makes pigments such as fucoxanthin particularly unstable (Bianchi et al. 1993; Leavitt and Hodgson 2001). The similar structure, and thus stability, of these compounds allows a ratio to be used without diagenetic artifacts biasing the signal.

The goal of this study is to further refine the timing and magnitude of regional Holocene climate change by integrating more commonly used geochemical and biological properties with algal pigments. We employ multiple proxies of organic matter provenance and algal biomarkers, with diatom microfossil assemblage composition included to provide an independent proxy to help deconvolve the geochemical proxy signals. Although sedimentary pigments have been used extensively in temperate and Antarctic paleolimnological studies (Leavitt et al. 1997; Hodgson et al. 2004; Tani et al 2009; Hede et al. 2010), they have seen limited use in studies of Arctic lakes (Leavitt et al. 2003). By combining sedimentary pigments with geochemical and microfossil techniques, we present a multiproxy record of the past 10 ka which allows for a comprehensive understanding of past lacustrine bio-productivity and inferred climate history.

2.2.1. Regional Holocene Climate

The coastal lowlands of eastern Baffin Island were deglaciated as early as 14 ka (Dyke et al. 2002; Miller et al. 2005; Briner et al. 2007), but local glaciers persisted in the interior highlands until substantially later. The timing of the onset of the regional Holocene Thermal Maximum (HTM) remains contentious. Chironomid species assemblages (Briner et al. 2006; Axford et al. 2009) show peak warmth occurring 10 to 8.5 ka. The record from the Agassiz Ice Cap (Fisher et al. 2012) shows a similar timing, with peak melt occurring between 11 and 9 ka and remaining elevated until ~6.5 ka. However, palynological records from Baffin Island sediment cores suggest that peak warmth occurred much later, with maximum pollen concentrations occurring at approximately 6 ka while other proxies in the same cores point to earlier peak warmth (Miller et al. 2005). Regional syntheses of HTM timing such as Kaufman et al. (2004), rely on the integration of multiple proxies, some of which may have an inherent delayed response to a change in climate. The apparent discrepancy in HTM timing highlights the importance of selecting proxies that are responsive and representative of climate changes.

As the strength of summer insolation decreased, Neoglacial cooling began at ~5.5 ka and became more severe after 2 ka as shown by both decreases in lacustrine productivity as well as the growth of plateau ice caps (Miller et al. 2005, Miller et al. 2013). The culmination of Neoglacial cooling occurred during the Little Ice Age (LIA; ~1250-1850 AD) and is recognized throughout the North Atlantic as the coldest summers in the last 8 ka (Miller et al. 2010). In the last century, anthropogenic emission of greenhouse gasses has led to summer temperatures greater than any other century of the Holocene (Miller et al. 2013).

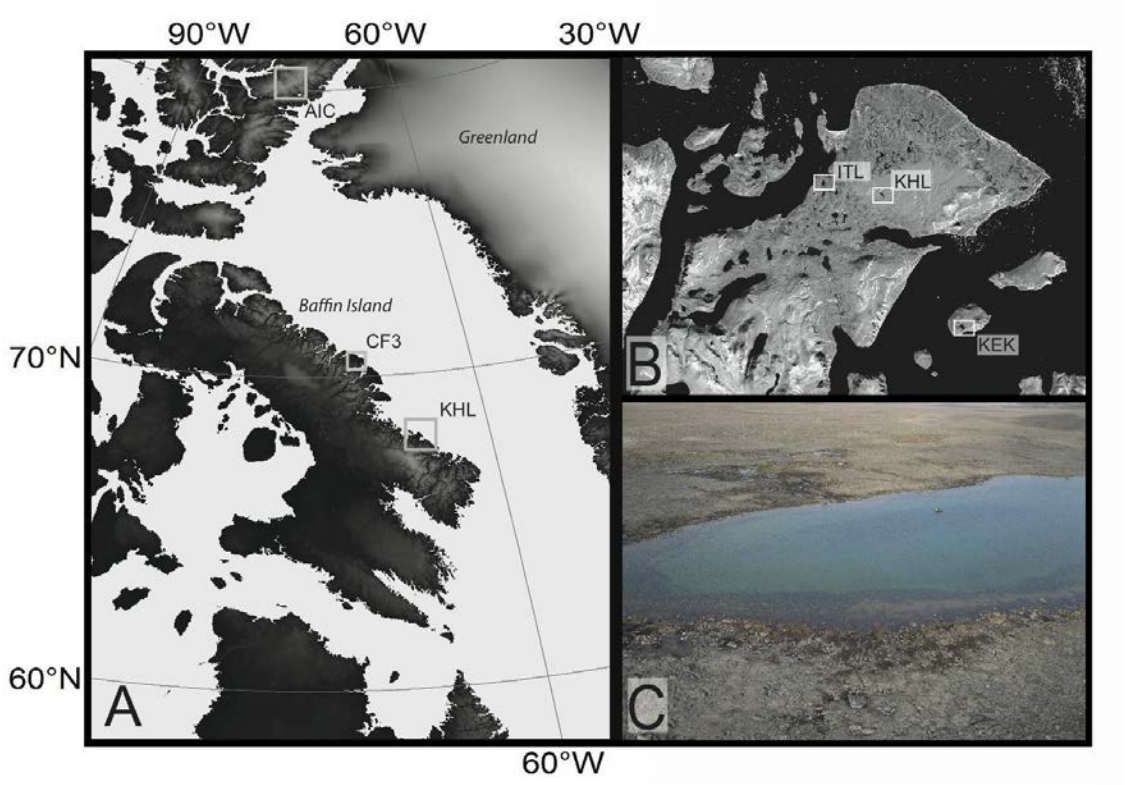

Figure 2.1. (A) The eastern North Atlantic showing the locations of proxy records discussed. KHL=Qivitu Highlands Lake, CF3=Clyde Foreland lake 3, AIC=Agassiz Ice Cap. (B) Qivitu Peninsula showing KHL, Itiliq Lake (ITL), and Kekerturnak Lake (KEK). (C) An aerial photograph of KHL during 2010 coring, note coring platform for coring location and scale.

2.2.2. Study Site

Qivitu Highlands Lake (hereafter: KHL after the earlier spelling as Kivitoo) is located on the forelands of the Qivitu Peninsula of eastern central Baffin Island, Nunavut, Arctic Canada (Fig. 1). It is a small (~0.3 km^2), shallow (3.75 m) lake, 100 m asl., with a small catchment (~1 km^2) and two trickling inlets. The lake surface is frozen as thick ice most of the year, with an estimated modern ice-free season of ~2.5 months from mid-June until September. Because of its shallowness, it experiences relatively warm summer water temperatures but has little thermal

inertia, cooling off quickly in late summer. Sparse vegetation fills crevices between till boulders in the catchment, with limited soil development. Mosses and lichens predominate with scattered shrub willow (*Salix*) and heaths (e.g. *Cassiope* and *Empetrum*).

2.3. MATERIALS AND METHODS

2.3.1. Modern Sampling

Lake water parameters were measured in the field (August 2010) using a Hydrolab multi-sensor probe and are listed in Table 1. Modern samples were collected to characterize the isotopic composition of various organic matter sources in the catchment. These consisted of lake margin soils (5-15 meters from the lake shore), aquatic moss from the littoral zone, aquatic moss from the central basin of the lake, and two plankton tows (Table 2). Plankton tows were conducted by pulling a fine (43 µm) mesh net across several transects of the lake at a depth of <1 m below the lake surface.

Table 2.1

Depth (m)	Specific conductivity ($\mu S \cdot cm^{-1}$)	pH	Dissolved oxygen ($mg \cdot L^{-1}$)
0	14	6.4	13.4
0.5	14	6.3	13.1
1	14	6.3	13.1
1.5	14	6.2	12.7
2	14	6.2	12.9
2.5	14	6.2	12.1
3	13	6.1	11.8
3.5	13	6.1	12.6

Table 2.1. Modern lake-water parameters measured at Qivitu Highlands Lake during August 2010.

Sample type	**$\delta^{15}N$ (‰)**	**%N**	**$\delta^{13}C$ (‰)**	**%C**	**C:N**
SOIL	-1.2	0.10	-24.7	5.0	41
SOIL	3.2	0.60	-26.3	9.8	19
SOIL	3.0	0.04	-25.5	0.6	20
TERRESTRIAL PLANT AVG (*n*=8)	-1.6 ±3.6	1.8 ±1.6	-26.9 ±1.21	43 ±10	48 ±29
MOSS (shallow water)	0.4	0.70	-20.1	20	36
MOSS (deep water)	0.6	0.90	-22.3	22	27
MOSS (deep water)	1.3	1.0	-23.1	26	30
PLANKTON	6.8	5.7	-30.9	44	9.0
PLANKTON	6.2	4.5	-30.5	33	8.5

Table 2.2. Isotopic composition of modern samples collected in and around KHL in summer 2010. These samples characterize the sources of organic matter to lake sediments.

2.3.2. Sediment Cores

Sediment cores from KHL were taken during three field seasons. A meter-long core, 95KHL-02, was recovered in 1995 and a macrofossil date at the contact with basal sandy diamicton provides a minimum age for local deglaciation (Table 3). A 60-cm surface core (05KHL-01-2), which did not recover the entire sediment package, was entirely extruded and subsampled in the field at high resolution in 2005. A 74-cm-long sediment core (KHL10-2A), visually identical to 95KHL-02, was recovered using a hammer-driven piston corer from an anchored raft platform in August 2010. An adjacent surface c-ore (KHL10-2B) with intact sediment-water interface was recovered and carefully extruded in the field at 0.25 to 0.5-cm-resolution to preserve the most recent part of the record. The composite sediment stratigraphy comprises 70 cm of organic-rich gyttja underlain by sandy glacial diamicton. When split, the top 3 cm as well as the bottom 44 cm of gyttja were dark and reduced, with diffuse transitions to a lighter, oxidized layer in between. A macrophyte layer occurs at 36 cm composite depth, just below the transition between reduced and oxidized sediment. The upper several cm of the 2010 surface core has high water content (93% at 1 cm), and thus permits high-resolution sampling of the last century.

2.3.3. Sediment Chronology

The chronology of the uppermost sediments was developed from the excess ^{210}Pb profile measured by a-spectroscopy at MyCore scientific, Ontario, Canada on 05KHL-2 (Fig. 2). The ^{210}Pb chronology was calculated using the Constant Rate of Supply (CRS) model (Appleby and Oldfield 1978), and transferred to the 2010 core by matching organic matter proxies (TOC, carbon and nitrogen stable isotopes) from the two cores to determine a tie-in point where only

background (supported) ^{210}Pb remains. Carbon isotopes show the strongest signal at the tie-in point, shown for each core in Figure 2. This tie-in point, at 1870 AD, was given an uncertainty of 30 years to account for limitations in the method of splicing the two records.

Macrofossils of aquatic mosses were sampled from the core wherever possible to develop a radiocarbon chronology for the remainder of the core. Although rare, macrofossils were recovered at 14.5 cm, 27.5 cm, and 36 cm depth, and dated by ^{14}C. The basal age of this core was determined by dating the humic acid fraction (Abbott and Stafford 1996) of bulk sediment at 65.5 cm, 4.5 cm above the contact between organic sediment and glacial diamicton (Table 3). This date is consistent with the stratigraphically deeper basal macrofossil date of 95KHL-02. Although humic material is typically older than the date of sedimentation due to an age reservoir in the catchment, the paucity of relict organic material on deglaciation leads to little age offset in the sediment shortly following deglaciation (Wolfe et al. 2004). All radiocarbon samples were processed at the Radiocarbon Laboratory of the Institute of Arctic and Alpine Research. The CLAM software package (Blaauw 2010), which integrates the Intcal 09 ^{14}C calibration (Reimer et al. 2009) was used to develop an age-depth model using a smooth spline (Fig. 2), which incorporates all radiocarbon ages as well as the 1870 ±30 AD ^{210}Pb derived age control point.

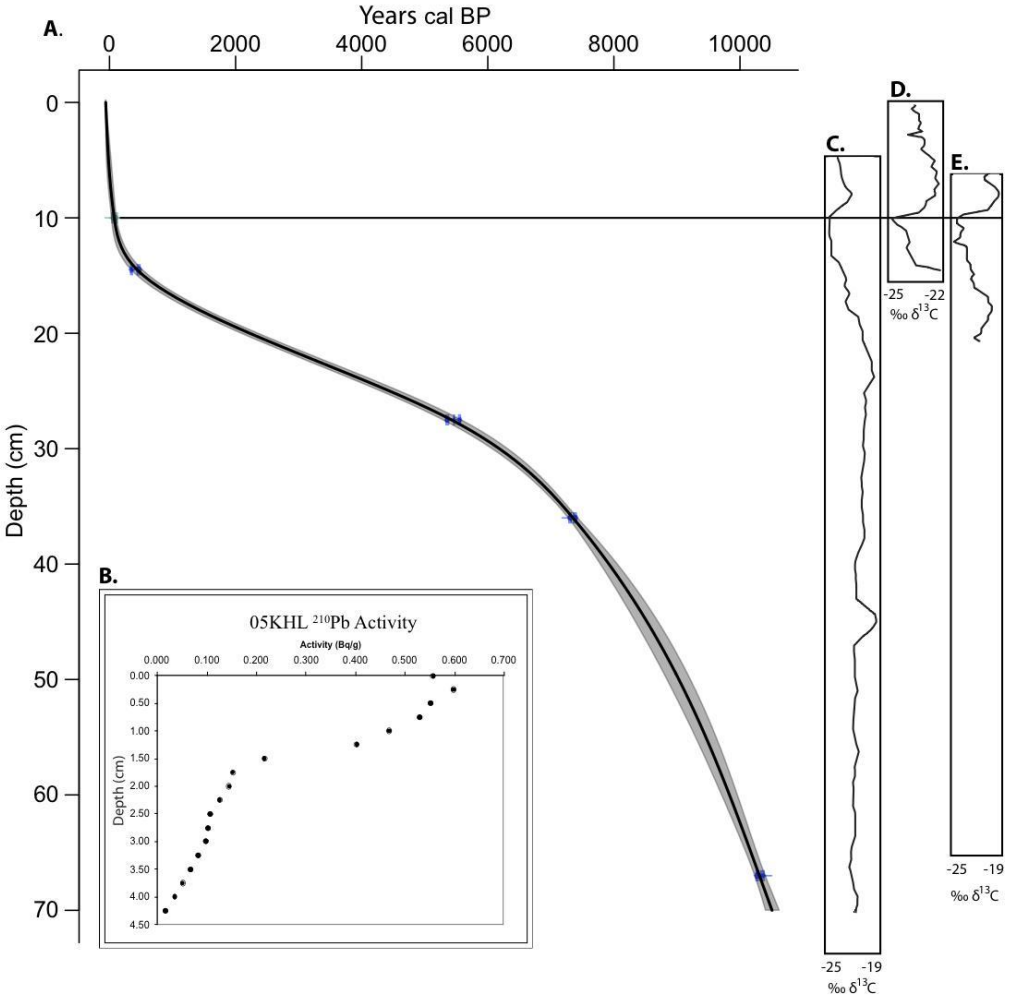

Figure 2.2. (A) Smoothed spline age model for KHL10 created using the program CLAM (Blaauw 2010). (B) The steep decline in unsupported ^{210}Pb in 05KHL shows that post-depositional mixing of the surface sediment has been minimal. (C) KHL10-2A-1N-01, (D) KHL10-2B-1B-1, and (E) 05KHL-2 showing the tie-in point for each core determined by characteristic proxy value. Carbon isotopic composition is shown here, however the same tie-in point is also obtained by using nitrogen isotopes or $TOC_{\%}$. Differences in the resolution and rate of change of proxy values are attributed to varying sediment density of each core.

Core	Depth (cm)	Material dated	^{14}C age (years BP)	$\delta^{13}C$	Calibrated 2-sigma age range (years BP)	AMS result number
KHL10-2B	14.5	Macrofossil	370 ± 20	-22.7	322-499	CURL-13518
KHL10-2A	27.5	Macrofossil	4720 ± 25	-17.9	5328-5880	CURL-14026
KHL10-2A	36.0	Macrofossil	6405 ± 25	-26.1	7273-7417	CURL-12695
KHL10-2A	65.5	Humic acids	9160 ± 25	-20.6	10241-10399	CURL-14020
95KHL-02	99-101	Macrofossil	9500 ± 60		10585-11085	CURL-2207

Table 2.3. Radiocarbon ages from KHL, processed at the Radiocarbon Laboratory of the Institute of Arctic and Alpine Research.

2.3.4. Sediment Geochemistry

Total organic carbon (TOC) and total nitrogen (N), as well as their stable isotopes, were measured on lyophilized homogenized bulk sediment at the Carnegie Institution of Washington's Geophysical Laboratory in Washington, DC. After being weighed into tin capsules, the samples were loaded into the autosampler of a CE NC 2500 Elemental Analyzer and combusted in an oxidation column at 1020 °C. CO_2 and N_2 were separated by gas chromatography and measured for concentration and isotopic composition by a Finnigan Delta V Plus isotope ratio mass spectrometer. An acetanilide standard was measured every 12^{th} sample and used to correct for drift. Isotopic data is reported in standard delta notation relative to the V-PDB ($d^{13}C$) and Air ($d^{15}N$) standards, and have analytical precision of ±<0.2‰ for both $d^{13}C$ and $d^{15}N$ values, estimated from duplicate analyses.

2.3.5. Algal Pigments

Algal pigments were measured at continuous half-centimeter resolution at the Institute of Arctic and Alpine Research following the methodology described in Leavitt and Hodgson (2001) pp. 305-306, using an Agilent 1200 series HPLC with an Eclipse XDB C18 15-cm column. The archive half of KHL10-2A was used for pigment analysis because it was sealed, stored cold, and not visibly oxidized at the time of sampling. All subsamples were kept frozen under nitrogen until the time of measurement. Freeze-dried subsamples of varying mass were extracted immediately upon lyophilization in 5 mL of 80:15:5 acetone:methanol:water solvent mixture in an amber vial, which was flushed with nitrogen and sealed. Samples were sonicated for 30 seconds to disperse the sediment, then stored at -10°C for 24 hours. After the extraction was complete, samples were filtered through a 0.2 µm PTFE syringe filter, which was then flushed with three milliliters of acetone to insure complete recovery of pigment. This extract was evaporated to dryness under N_2, after which a known volume of rehydration solution (acetone, methanol, and ion pairing reagent) was added and an aliquot transferred to a refrigerated autosampler. Pigments were identified and quantified by a Diode Array Spectrophotometer (DAD) calibrated with standards from DHI, Denmark. Carotenoids were quantified using the area under peaks in a trace at 435 nm. Because lutein and zeaxanthin co-elute using our methodology, identity and purity of the lutein peak was confirmed by examining the absorbance spectrum of this peak for each sample. Lutein has a deeper 'trough' between the second two absorbance peaks which are also slightly offset from those of zeaxanthin, occurring at slightly shorter wavelengths. Specifically, on our system, the second peak of the lutein spectrum occurs

at 445 nm, the trough at 460 nm and the third peak at 472 nm. The ratio of the height of the first peak to the height of the trough is 1.31. For zeaxanthin, the second peak occurs at 450 nm, the trough at 468 nm and the third peak at 476 nm. The ratio between the height of the second peak and the trough for zeaxanthin is 1.17. Spectra from all chromatograms were examined to assure that the peak quantified did not show evidence of zeaxanthin. Co-elution with carotenoids prohibited quantification of chlorins using the DAD, therefore chlorins were measured by fluorescence (excitation = 435 nm, emission = 667 nm). Pigment concentrations were normalized to the organic carbon content of the sediment to reduce apparent variability due to changing minerogenic inputs to the lake.

2.3.6. Diatom Preparation and Counting

Diatom microfossils were enumerated at 1-cm resolution using the same subsamples used for stable isotope and elemental analysis. Organic matter was digested using 30% hydrogen peroxide heated to approximately 90ºC overnight. Samples were then centrifuged and rinsed three times with distilled water. Clean diatoms were suspended in distilled water and several drops were placed on a microscope slide coverslip. These were allowed to dry and then mounted using ZRAX, a high refractive index mounting media. At least 300 diatom valves were identified per sample based on taxonomy and nomenclature following the Baffin Island flora of Wolfe (2003) and Wilson et al. (2012). Due to the variable nature of diatom preservation in this core, valves that were visibly dissolved (and not identifiable) were counted along with intact valves. Those levels where partially dissolved valves reached ~40% or more of the 300 counted were not included in our reconstructions to avoid any potential bias. Baffin Island transfer function

calibration data of Joynt and Wolfe (2001) was entered into the C2 program version 1.7 (Juggins 2011) to develop a pH transfer function. Diatom diversity is expressed in Hill's N2 index, also calculated by the C2 program. Biogenic silica (BSi) was measured to provide an indication of diatom abundance, but was not used for climate reconstruction.

2.3.7. Data Analysis

Statistical analysis of the dataset was performed using Principal Component Analysis (PCA) on a correlation matrix using the princomp function in the R environment (R Development Core Team 2010). PCA was conducted on two separate data sets: the geochemical data that spans the entire record, and the diatom taxonomic data, which is limited to the past 6 ka due to preservational constraints. The geochemical PCA data set contains all proxies measured, with the exception of BSi, which was excluded due to the lower temporal resolution of analysis. The diatom PCA was performed using a combination of simplified species data along with diatom preservation and Hill's N2 diversity index. Diatom inferred pH was excluded because the transfer function results are directly obtained from the species data. All principal components used in the study are significant as determined by the broken stick model performed by the bstick function within R. PCA factor scores were plotted through time to obtain a simplified proxy summary curve.

2.4. RESULTS

2.4.1. Chronology

The ^{210}Pb profile (Fig. 2) shows monotonic decay back to background levels, indicating little mixing of the upper sediments despite the shallowness of the lake. This gives confidence that surface sediments are not prone to redistribution by bioturbation or wave action. The small size of the lake limits the depth of wave action, and maximum winter lake ice is less than 2 m, so ice disturbance is unlikely. Surface sediment of the 2010 core was less dense than that of the 2005 core, with approximately twice the sediment depth represented by equal mass.

Radiocarbon dates (Table 3) increase with depth without age reversals and the basal ages of the 1995 and 2010 cores are similar. The slightly older date from the base of 95KHL indicates the onset of organic sedimentation occurring prior to ~10.6 ka. High sedimentation rates in the early Holocene rapidly decrease in the mid to late Holocene (Fig. 2, 3). Low sedimentation rates persist until the top of the core where lower sediment densities cause an apparent increase of mass accumulation rates. Although the age-depth relationship increases at the top of the core, the mass accumulation rate remains low, reaching a minimum between 1250 and 1850 AD. An increase in the mass accumulation rate occurs after 1850 AD.

2.4.2. Sediment Geochemistry

Total organic carbon ($TOC_{\%}$) content of KHL sediments ranges from 3.8 to 13%, with a stable maximum between 8.5 and 1.5 ka (Fig. 3). Between the start of organic sedimentation and 8.5 ka, $TOC_{\%}$ increases, associated with decreased minerogenic input. After 1.5 ka, $TOC_{\%}$

rapidly drops into a pronounced trough, reaching a minimum (3.8% at 1500 AD), which persists until a sharp recovery to 13% in the 20th century. Due to the large changes in sediment accumulation rate, organic carbon flux is quite different than $TOC_{\%}$. Organic carbon flux is greatest immediately following deglaciation, which then decreases but remains high until 7 ka. After 7 ka the flux of organic carbon gradually decreases until stabilizing at 5 ka, remaining at a low level (0.045 g cm^{-2} yr^{-1}) through the rest of the mid Holocene and reaching a minimum of 0.011 g cm^{-2} yr^{-1} during the LIA. Carbon flux increases during the 20th century, returning to similar values as in the early Holocene. Within-lake algal organic matter has low C:N (~9), while terrestrial organic matter is typically high (20-80), and aquatic mosses are intermediate (27-36; Table 2). C:N in bulk lake sediment ranges between 11.0 and 15.3, indicating that the sediment organic matter is composed of a varying mixture of terrestrial, aquatic macrophyte, and algal sources (Fig. 3). C:N values are highest during the early part of the record, with the maximum value occurring at 9.8 ka. There is a subsequent decrease in C:N until it stabilizes (~12.8) at 7 ka. C:N undergoes a slight rise between 7 ka and 2.2 ka, followed by a decrease. This decrease steepens at about 1400 AD and reaches a minimum value (~11) at 1870 AD, after which it rebounds sharply (~12.8) in the 20th century.

Carbon isotopic composition becomes steadily more enriched from the beginning of the record to ca. 3 ka, when $\delta^{13}C$ reaches its highest value (-20.4‰; Fig 3). Subsequently $\delta^{13}C$ becomes increasingly depleted, gradually at first, then more rapidly after 1500 AD, reaching its lowest value (-24.6‰) at 1870 AD, which coincides with the C:N minimum. Nitrogen isotopic composition closely tracks the $\delta^{13}C$ variability between 8 and 3 ka, but the two isotopic systems decouple and trend in opposite directions after 3 ka. A pronounced positive excursion of $\delta^{15}N$ occurs during the LIA with values reaching 2.2‰, contemporaneous with the lowest values of

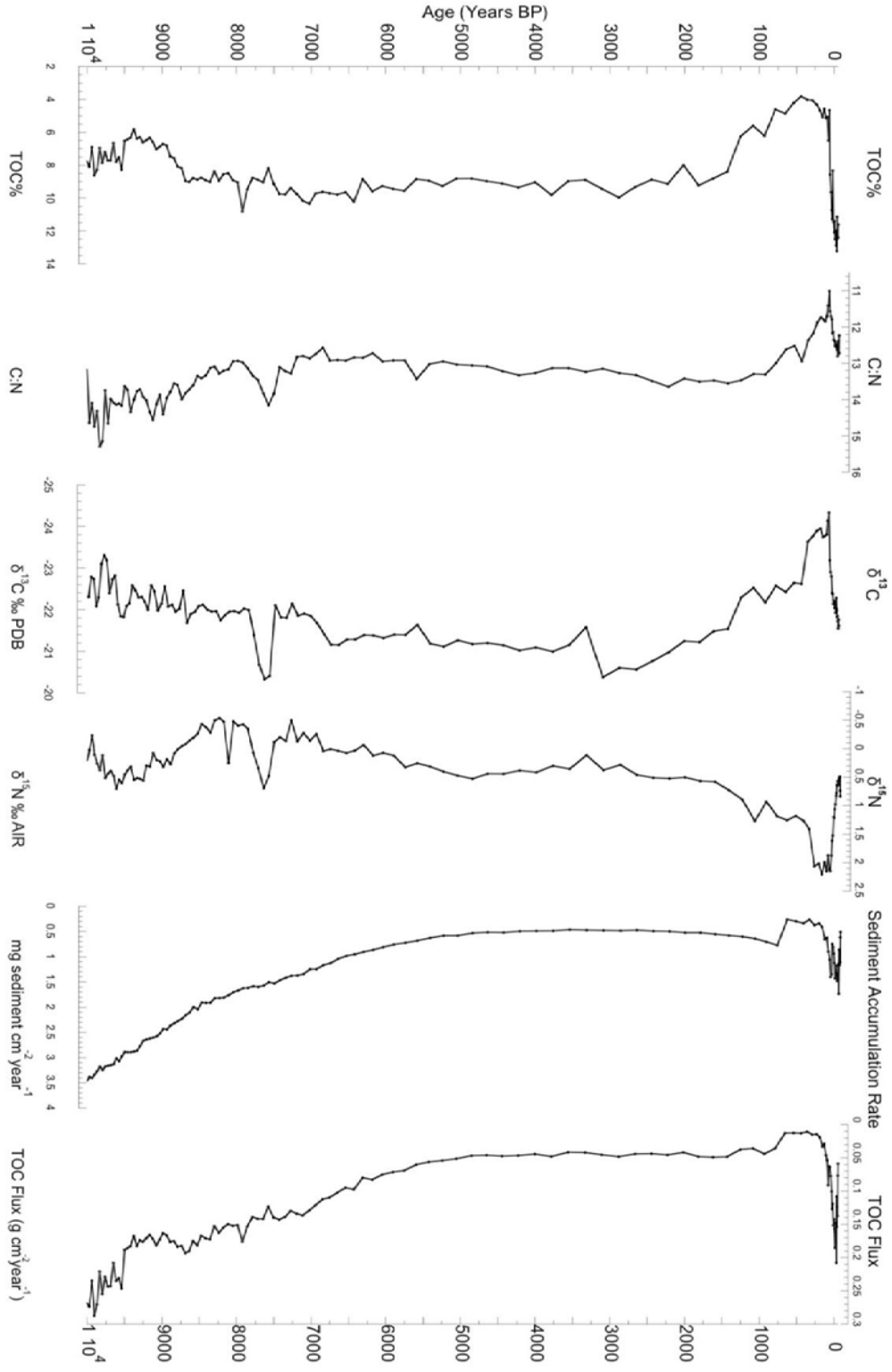

Figure 2.3. Organic carbon percent, carbon to nitrogen atomic ratio, and isotopes along with fluxes of bulk sediment and organic carbon.

C:N and $\delta^{13}C$ (Fig. 3). During the 20th century, sediment $\delta^{15}N$ rapidly declines from the high values seen in the LIA to ~0.5-0.8‰.

2.4.3. Algal Pigments

Algal pigment concentrations show large changes throughout the record. Because chlorins are not taxonomically specific, we focus on the two most abundant and continuously-preserved xanthophyll carotenoids, lutein and diatoxanthin. While the former is produced primarily by higher plants and chlorophyte algae, the latter is produced exclusively by siliceous ochrophyte algae (diatoms and chrysophytes). Lutein is the most abundant carotenoid in the sediment between 10 and 7.5 ka. This is captured as the lutein to diatoxanthin ratio (L:D) in Figure 4. Between 7.5 and 5 ka L:D gradually decreases, indicating the relative depletion of lutein-producing taxa from the watershed. After 5 ka, L:D remains consistently low, with elevated diatoxanthin concentration persisting during the late Neoglacial and LIA. In the 20th century, the relative contribution of lutein sharply rebounds with the L:D returning to HTM values.Variable preservation of pigments down core does not appear to be controlling observed trends. Concentrations of both lutein and diatoxanthin at the top of the core are relatively low and increase down core, which gives confidence that there has been minimal post-depositional diagenesis of these two carotenoids. The ratio of chlorophyll *a* to its degradation products (pheophytin *a* and pheophorbide *a*) is variable throughout the record but is not correlated with any factors that are expected to demonstrate a change in pigment preservation (such as

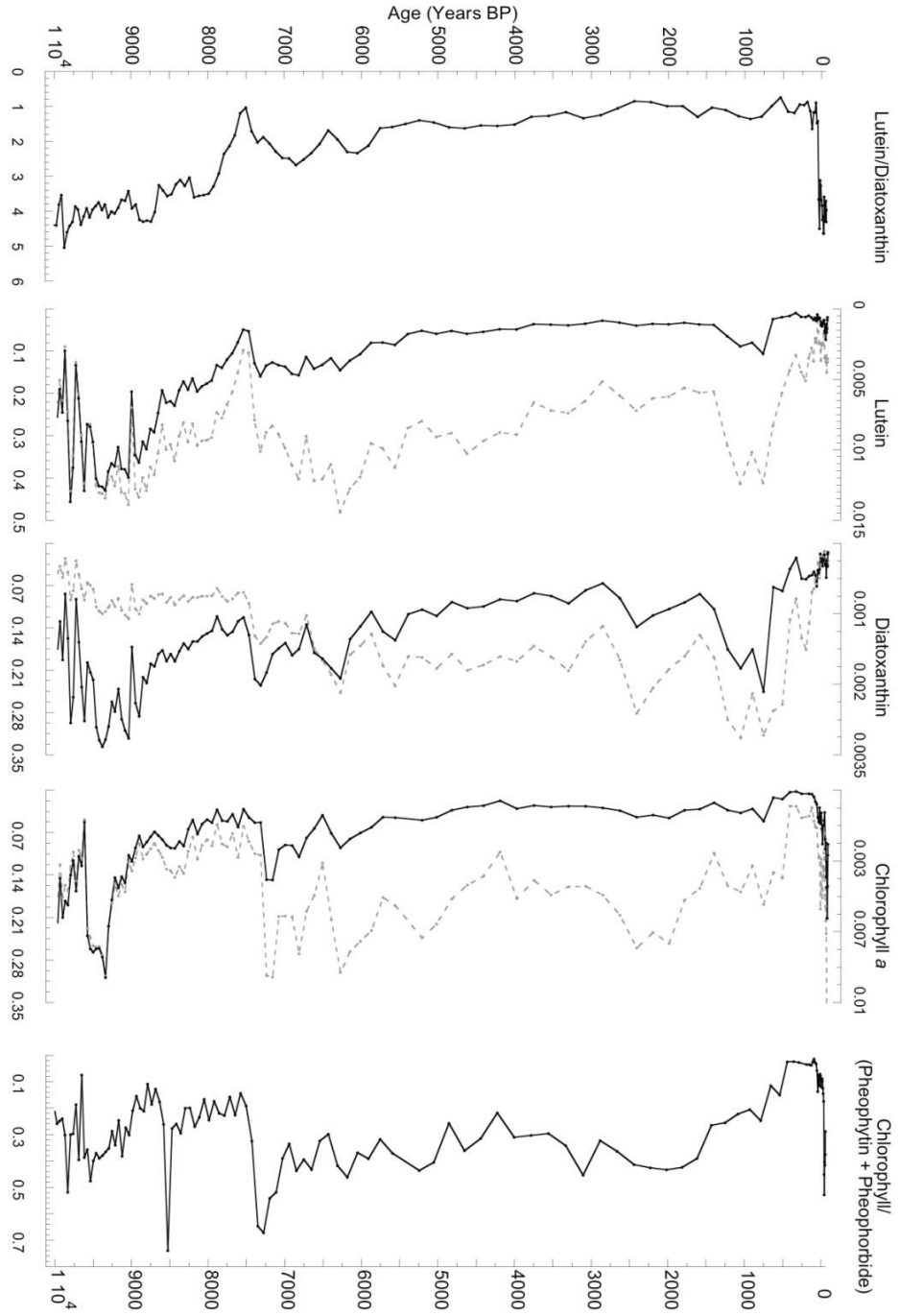

Figure 2.4. Sedimentary carotenoid concentration and flux along with chlorophyll *a* and a ratio of chlorophyll *a* to pheophytin *a* and pheophorbide *a* indicating the type and magnitude of lacustrine primary productivity. Lutein to diatoxanthin ratio shows the relative contribution of diatoms and chrysophytes (diatoxanthin) and green algae, bryophytes, and higher plants (lutein). For plots with two axes, solid lines represent pigment flux in μg mg C^{-1} $year^{-1}$ (upper axis) while dashed lines indicate pigment concentration in μg mg C^{-1} (lower axis).

sedimentation rate, TOC flux, or total chlorophyll *a* flux). Therefore, this ratio does not seem to be indicative of total pigment preservation but potentially reflects variably preserved aquatic and terrestrial pigment sources (Fig. 3, 5).

2.4.4. Diatom Assemblage Change

Diatoms are present, well-preserved, and abundant in the uppermost portion of the core but become progressively less well-preserved with depth. Preservation declines between 1 and 6 ka (Fig. 5). Before 6.5 ka, over 40% of valves show significant dissolution and were not enumerated. Valves were considered partially dissolved only when a non-identifiable fragment consisting of a sternum, central nodule, fascia or hyaline areas was tapered and thinner than that of an intact valve. Diatom microfossils are extremely rare in sediments older than ~8 ka. The greatest number of taxa occurs in the surface sediments, with many taxa (*Discostella* spp., *Cymbella gaeumannii* Meister, *Nitzchia* spp. and *Eunotia exigua* Rabenhorst) not seen other than in the top several centimeters of the core. The LIA sediments are dominated by *Aulacoseira* species along with *Pinnularia biceps* Gregory. There is a transition from the mid-Holocene fragilaroid taxa (primarily *Stauroforma exiguiformis* (Lange-Bertalot) R.J.Flower, V.J.Jones & F.E.Round) to the LIA-type diatoms beginning at about 3 ka (Fig. 5). This transition is gradual until a threshold is reached (likely pH-driven) just after 2 ka, when *Aulacoseira perglabra* (Østrup) E.Y.Haworth becomes dominant.

Biogenic silica (BSi) captures changes in the accumulation of diatom silica to the lake's sediment, regardless of whether or not individual valves subsequently dissolve in the sediment column. BSi indicates that the flux of diatom valves was highest during the early Holocene even though diatoms valves are not well preserved in that part of the core. Due to the large difference

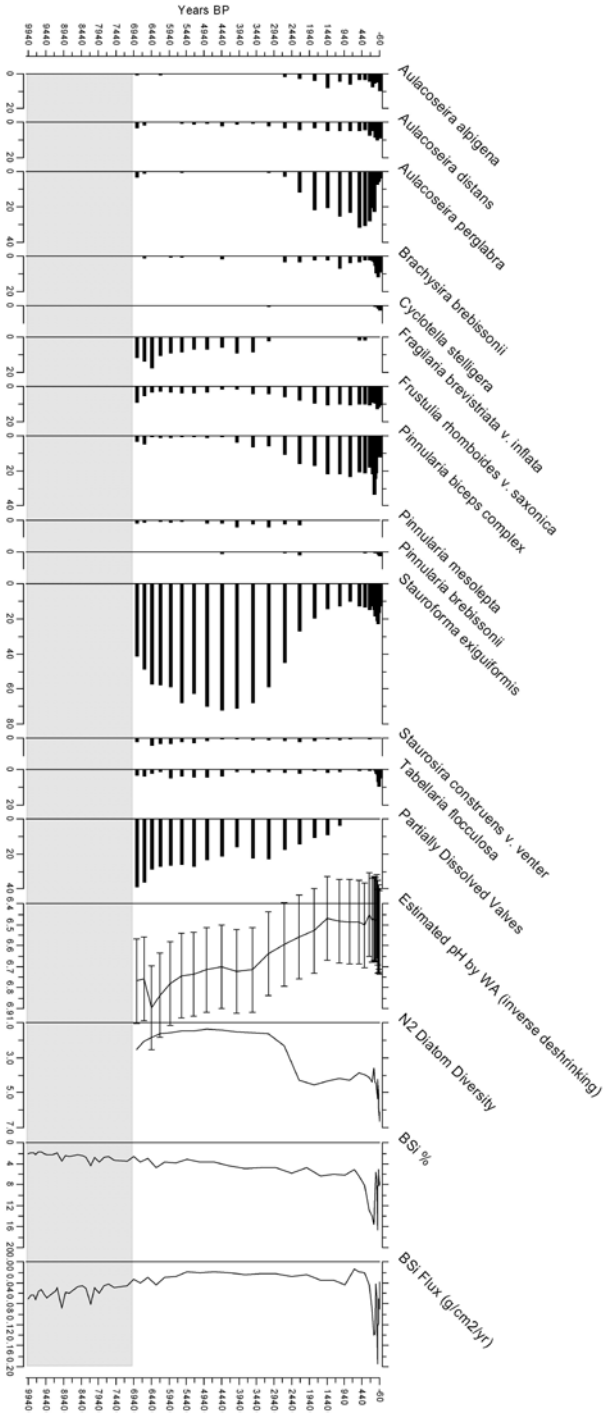

Figure 2.5. Dominant diatom taxa of the last 6.5 ka, the interval in which they were relatively well preserved. Partially dissolved valves are plotted to show decreasing valve preservation with increasing depth/age. Lake water pH was reconstructed using the calibration data set of Joynt and Wolfe (2001) and a transfer function calculated using the C2 program (Juggins, 2011). Hill's N2 diversity shows increasing diversity in recent sediments. N2 was also calculated using the C2 program. Grey shading indicates the interval of poor diatom preservation.

in silica per diatom frustule between fragilaroid taxa and *Aulacoseira*, as well as the potential for dissolved silica leaching from the sediment, BSi appears not to be a sufficiently reliable measurement of diatom abundance to be used in this climate reconstruction.

2.5. DISCUSSION

In this study, we have utilized algal pigment assemblages, organic matter bulk stable isotopes, and algal microfossils (which are all produced and deposited within the catchment) from the KHL sediment record as a means to provide a better understanding of past regional climate-driven environmental change. The proxy data show coherent trends and reveal climate states based on the sensitivity of each proxy measured. Additionally, the major climate states of the last 10 ka are uniquely characterized, with clearly distinguishable biogeochemical regimes observed in the time periods 10-7 ka and 2 ka to 1900 AD, with a transitional state occurring in between. The most recent century appears similar to the early Holocene in all proxies except diatom species assemblages, which are unique with respect to those observed earlier in the record.

2.5.1. Pigment and Diatom Preservation

Algal pigment preservation needs to be carefully considered in any study utilizing sedimentary pigments, which are inherently unstable. This is due to the nature of the light-absorbing chromophore and associated weakly held electrons. Factors that decrease pigment preservation are exposure to high light, temperature, oxygen, and heterotrophic consumption,

which are all highest in the water column and in the active layer at the sediment-water interface (Leavitt and Hodgson 2001). Pigments will be best preserved when they are quickly deposited and buried in the sediment column. The shallow depth of the lake and the high concentration of sedimentary pigments suggest that much of the pigment is sourced form benthic algae and macrophyte plants rather than from phytoplankton in the water column. Benthic pigments would be more quickly buried and removed from conditions favorable for degradation. The residence time of pigments in the active sediment layer depends on the sediment accumulation rate. Because there is a large reduction in accumulation rate over the KHL record, there is the potential for this to overprint the climatic signal contained in the pigment record. Pigment concentration, however, is actually higher during times of low sediment accumulation rate, suggesting that preservation is always high, and dilution by non-pigment organic material is a predominant control on sedimentary pigment abundance (Fig. 3). Additionally, there is no first order decrease in pigment concentration through time, indicating that in this environment, pigments remain stable once buried for at least the duration of the record. This shows that while there may have been small changes in pigment preservation over the Holocene, the climate signal of the pigment record in this core is reliable and not overprinted by degradation.

Changes in diatom preservation down-core are likely due to post-depositional processes that lead to elevated pH in sediment pore water, rather than dissolution due to lake water chemistry at the sediment water interface. Diatom dissolution is enhanced in waters with high pH, temperature, and low dissolved silica (Lewin 1961; Ryves et al. 2001). Although pH was possibly higher in the early Holocene, as reconstructed in other nearby lakes (Michelutti et al. 2007; Wilson et al. 2012), it was probably not sufficiently high to dissolve biogenic silica at the sediment water interface. Similar bedrock and lake morphology suggest that Holocene pH values

at KHL should be roughly the same as those at lake CF3, which had an early Holocene diatom-inferred pH of ~8.0 without significant evidence of dissolved valves (Michelutti et al. 2007). The presence of measureable biogenic silica (BSi, Fig. 5) in sediments without visible diatoms leads us to believe that the dissolution occurred post-deposition and after removal from the active upper sediment layer. This would allow dissolved silica to be trapped in sediment pore water. The reduction in diatom preservation occurs at the same depth at which sediments become black and presumably more strongly anoxic due to increased organic matter content. Processes such as denitrification and sulfate reduction in anoxic sediment can elevate the pH of the pore water due to hydroxide and bicarbonate ions produced, leading to *in situ* silica dissolution (Drtil et al. 1995; Warthmann et al. 2000). Elevated sediment organic matter encourages both denitrification and sulfate reduction, as heterotrophic respiration will deplete pore water oxygen and lead to the use of these alternate electron acceptors.

2.5.2. Early Holocene (10-7 ka)

The HTM occurred at this site between 10 and 7 ka and is distinctly characterized by most proxies. HTM organic matter has C:N above 11, low $\delta^{13}C$, high chlorophyll concentrations, high L:D ratio, and the lack of well-preserved diatoms. In Baffin Island lake catchments, due to the minimal terrestrial vegetation cover, high C:N can be interpreted as either a greater proportion of terrestrial to aquatic organic matter (Thomas et al. 2011), or a greater contribution from aquatic macrophyte mosses (Briner et al. 2006). Modern samples from the lake catchment (Table 2) show that terrigenous soil (C:N 20-40) and lacustrine mosses (C:N 27-36) are not readily distinguished by this measure. $\delta^{13}C$ can aid in this distinction (Wang and Wooller 2006).

Terrestrial and algal organic matter have consistently lighter carbon isotopic composition than that derived from aquatic macrophytes (Meyers and Teranes 2001; Wang and Wooller 2006). Modern terrestrial plants and soil collected near KHL are consistent with this, with plants averaging -26.9‰ (n=8, σ=1.21) and soils -25.5‰ (n=3, σ=0.8) (Table 2). High C:N coupled with light $\delta^{13}C$ suggest early Holocene conditions were characterized by a greater flux of allochthonous organic matter to the lake due to relatively abundant terrestrial biomass.

2.5.3. Mid Holocene (7 ka to 2 ka)

After the peak HTM warmth TOC flux is greatly reduced, becoming low and stable after 6 ka. This reflects an overall decline in biological productivity with the onset of mid Holocene cooling. The gradual rise of $\delta^{13}C$ and $\delta^{15}N$ between 8 and 3 ka suggests increasing abundance of aquatic macrophytes until 3 ka, when a decoupling of the correlation between $\delta^{13}C$ and $\delta^{15}N$ shows a shift toward algae as the predominant organic matter source to the lake.

An increase in diatoxanthin concentration relative to lutein indicates a shift in primary production characteristics in and around the lake. This is interpreted as a reduction of contributions from green algae, macrophytes, and higher plants after the HTM, with increasing relative abundance of diatoms as Neoglacial cooling begins. This in turn suggests that the 'green' taxa are more sensitive than diatoms to changing climate. L:D reaches a decreased value by 5 ka, indicating that higher plants and green algae were greatly reduced following the initial mid-Holocene cooling. Diatoxanthin flux remains high during the LIA, suggesting that diatom abundance may be more influenced by water chemistry or lake ontogeny than temperature. Additionally, diatom growth is often characterized by early-season blooms, which then become

silicon-limited before the end of ice-free conditions. Length of growing season is likely more limiting than nutrient availability for green plants, which grow slowly throughout the season and in some cases retain biomass from one season to the next. Because of this, diatom productivity is less sensitive to length of summer than higher plants or aquatic macrophytes. This is important to note as many studies have used diatom abundance to reconstruct total lake productivity, which is unlikely to accurately reflect total aquatic production.

The onset of continuous diatom preservation occurs after the end of the HTM, as organic matter flux decreases, suggesting that the post-depositional processes that led to the dissolution of diatoms were linked to this warm interval. Diatom preservation in KHL sediments can thus be interpreted as another piece of evidence for the termination of HTM conditions and onset of Holocene cooling between 7 and 6.5 ka. Improved diatom preservation, along with the change in color of the sediment (5.7-5.5 ka), represents a further transition in the lake basin in response to intensified mid Holocene cooling. During the mid Holocene, many of the organic matter proxies show relative stability, indicating an unchanging source. Contrastingly, the diatom record reveals significant changes in the lake basin during this time. The pH transfer function reveals a mid-Holocene pH of around 6.8, remaining relatively stable until 3 ka when a decrease in pH is indicated by the replacement of fragilaroid taxa by *Aulacoseira*. Although pH is not directly dependent on climate, an increase in the duration of ice cover and the associated buildup of carbonic acid in the lake water has been cited as a predominant driver of pH changes over the Holocene in poorly buffered Arctic lakes (Wolfe 2002; Michelutti et al. 2007). This diatom assemblage change indicates a pronounced increase in the duration of lake ice cover after ~3 ka.

2.5.4. Late Holocene (2 ka BP to ~1900 AD)

All organic matter proxies show that the biggest change in sediment properties from their mean Holocene state since the end of the last glaciation occurred during the LIA. A sharp decline in C:N, more negative $\delta^{13}C$, and more positive $\delta^{15}N$ shows an increasing relative contribution of algal organic matter, reaching its maximum during the late LIA. These characteristics all suggest a dominantly aquatic provenance for sediment organic matter. This requires that the landscape was nearly barren of plants or that prolonged frozen conditions prevented the mobilization of soil.

2.5.5. Anthropocene (~1900 AD to present)

Subsequently, many proxies from 20th–century sediments return to similar values as those recorded during the HTM. L:D shows the return of 'green' algae and plant predominance. C:N and carbon flux are elevated, indicating higher productivity and greater influx of terrestrial organic matter. Diatom assemblages, however, did not return to an assemblage similar to earlier in the record, indicating different environmental conditions to that of the mid Holocene. The rise of *Discostella* and assemblage diversification is similar to that observed by Smol et al. (2005) at many Arctic sites. Many of these assemblage changes were observed without associated changes in water chemistry and are linked to changes in air temperature. The rise of *Discostella* likely indicates warmer temperatures and reduced ice cover at KHL in the last century. We also note that sediment proxies from KHL provide a detailed and compelling expression of the Holocene-Anthropocene transition (Wolfe et al. 2013). During the 20th century, sediment $\delta^{15}N$ declines

markedly, corresponding with trends observed across much of the Arctic that reflect anthropogenic nitrogen deposition (Holtgrieve et al. 2011). In many cases (e.g. L:D, C:N, and carbon flux), peak values attained during the HTM have been reached or exceeded in sediments deposited during recent decades, ultimately implying that recent warming has reached temperatures not consistently encountered since the early Holocene.

2.5.6. PCA Analysis

Plotting PCA component values through time was used to summarize multiple proxies and develop a composite proxy curve (Fig. 6,7). The two principal components that explained the greatest proportion of variance were examined for each data set. Component one from the geochemical data explains 46.3% of the total variance and is primarily controlled by the anticorrelation between $\delta^{15}N$ and sedimentation rate, C:N, L:D and other pigment fluxes. This principal component is interpreted as primarily representing length of ice-free season and summer temperature. Geochemical component two explains 23.8% of the total variance, controlled by the inverse correlation of $\delta^{15}N$ with $\delta^{13}C$, $TOC_{\%}$, and (chlorophyll *a* / pheophytin *a* + pheophorbide *a*). The diatom data component one (not shown) explains 67.5% of the variance and is driven by the late Holocene diversification of assemblages. Diatom component two represents the shift in assemblages during the LIA. This component explains 18.8% of the variability and is possibly related to summer temperature.

Both geochemical PCA component 1 and the diatom data derived component 2 likely represent signals of climatic change rather than the within-lake thresholds that drive the other principal components. The PCA component 1 plot (Fig. 7) highlights the HTM, as well as the major

departures from the average climate of the Holocene-the late Neoglacial (after 2 ka) and LIA (1400-1900 AD). Anthropogenic influence on climate is recorded as a dramatic rise in PCA component 1, rapidly returning to a similar state as the HTM. PCA 2 (of the diatom data) differs in that most of the change occurs between 3.0 and 1.2 ka, and is a response to Neoglacial intensification rather than the LIA maximum. Multiproxy records have the advantage of including the unique point of sensitivity of each proxy. If only the geochemical record was examined, environmental change occurring during this interval would not have been detected.

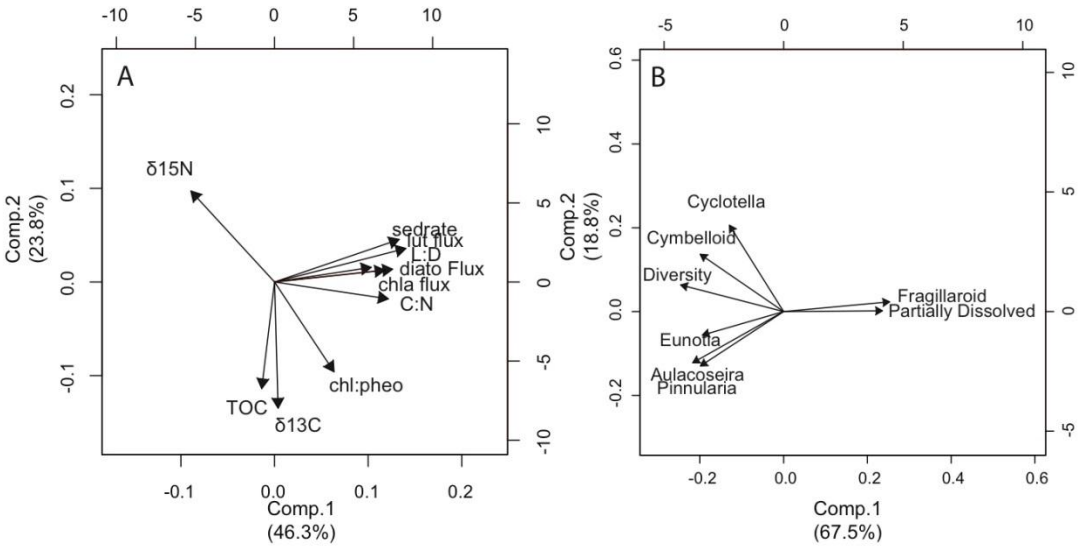

Figure 2.6. Principal component biplots of components one and two for the geochemical (A) and diatom (B) data.

2.5.7. Comparison with Regional Records

Chironomid-inferred summer air temperatures from lake CF3, ~300 km north of KHL and in a similar setting (Briner et al. 2006), and Agassiz Ice Cap melt (Fisher et al. 2012) show a distinct

HTM shortly after deglaciation, contemporaneous with the summer insolation maximum. Good agreement in the timing of the warm period at both of these sites with proxy records presented here strongly support an HTM between ~10 and 7 ka across eastern Baffin Island (Fig. 7). An early HTM conflicts with the HTM timing shown by pollen records, such as those presented in Miller et al. (1999; 2005), which suggest that thermophilous vegetation communities only developed ~2 ka after peak summer temperature. We propose a similar conclusion to that of Miller et al. (2005) to explain the discrepancy between pollen and lacustrine apparent peak warmth: the delayedresponse of higher terrestrial plants reflects the combined influences of residual Laurentide ice and long migration distances, thereby delaying higher plant ecesis. Vegetation succession in other Arctic sites has been relatively rapid since the end of the LIA, with mature tundra developing in as little as 100 years in a site on Svalbard (Prach and Rachlewicz 2012). Because it has been shown that plants are able to rapidly colonize nearby freshly deglaciated landscapes, we place more of an emphasis on migrational constraints rather than pedogenesis as the limiting factor to terrestrial plant community development. A comparison of proxy based global temperature anomalies presented by Marcott et al. (2013) implies that the Baffin Island HTM was considerably earlier than the global average, while the LIA timing was synchronous with the global average (Fig. 7).

A climate record of the last 2 ka from nearby Itilliq Lake (Thomas et al. 2011), located 5 km from KHL, shows few similarities to the most recent 2 ka of the KHL record. The distinct 1000 AD cold period described in Thomas et al. (2011) is not apparent in KHL. It is possible that our chronology and sample resolution does not properly resolve this event, although this should not change the fundamental structure and information contained in the proxy curves. Ultimately, the different records shown by these two lakes highlight the need to perform multiple studies

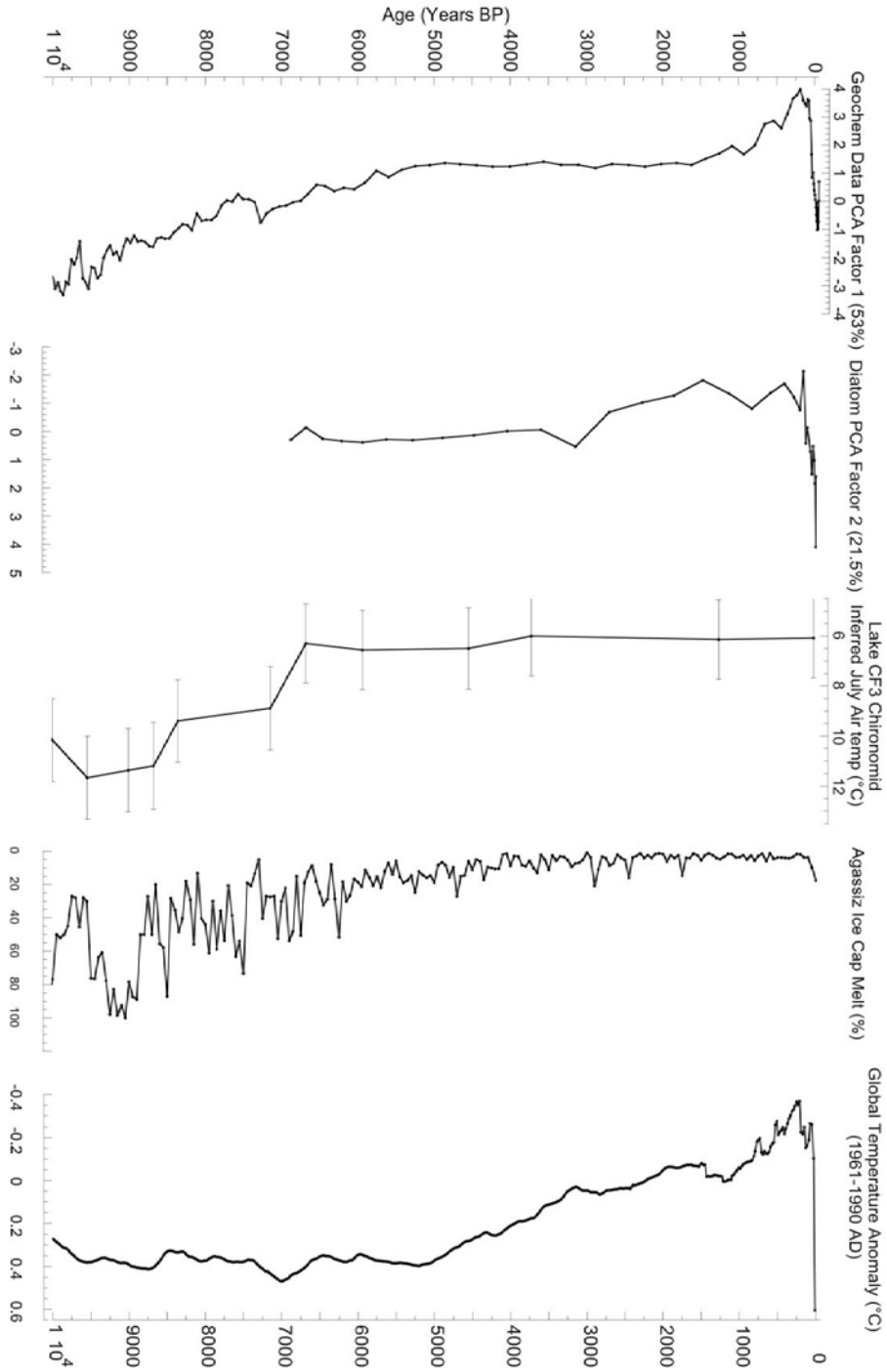

Figure 2.7. Summary of proxy data by PCA factor scores through time. Principal component 1 for the geochemical data set and principal component 2 for the diatom data set are interpreted as representing summer temperature at the site. These summary plots are compared to regional reconstructions of chironomid inferred July air temperature from nearby lake CF3 (Briner et al. 2006), Agassiz Ice Cap melt % (Fisher et al. 2012), and a proxy based reconstruction of global temperature anomalies (Marcott et al. 2013).

utilizing a variety of proxies in each region to account for the variability of natural systems in response to equivalent climatic events.

2.6. CONCLUSIONS

The multi-proxy reconstruction from KHL shows Holocene-scale changes in dominant primary producers and sediment organic matter provenance, as well as threshold changes of algal taxa during the HTM, Neoglacial, LIA, and 20th century. It is the first paleolimnological study in the region to integrate pigment-based reconstructions to a suite of more commonly measured proxies. The ratio of diagnostic carotenoids is shown to be a sensitive proxy for examining past abundances of photosynthetic organisms that cannot be differentiated by other methods. Dominant production shifted from chlorophytes, bryophytes, and higher plants in the early Holocene to diatoms in the mid- to late Holocene, reversing again following the LIA. This suggests that diatoms are less sensitive to summer cooling compared with higher plants and green algae. L:D provides a sensitive novel climatic indicator, particularly for periods of peak warmth in this environment, such as the HTM and 20th century.

The organic matter proxy values for the early Holocene require that considerable terrestrial biomass was established shortly after deglaciation. This is much earlier than the terrestrial floral development as indicated by pollen records, which suggest a modern flora was established only after 8 ka. We suggest that higher plant ecological dynamics and migration, rather than temperature limitations, were the dominant control on the appearance of pollen-producing plants in the watershed following deglaciation. The early Holocene vegetation must have comprised an abundant biomass dominated by few taxa. Terrestrial biomass became greatly

reduced by 3 ka, with sediments becoming almost completely comprised of autochthonous algal organic matter during the LIA.

The compilation of proxies by their PCA component scores enables a summary of regional Holocene climate evolution (Fig. 7). HTM conditions extended from 10 to 7 ka, with a transition to a cooler yet stable mid Holocene climate between 7 and 5 ka. Neoglacial cooling intensified from 3 to 1.5 ka and culminated in the LIA (beginning at ~1400 AD and peaking at 1870 AD), which is the coldest prolonged period of Holocene summers at this location. A dramatic return of some proxies to values similar to the HTM suggests that modern conditions are comparable those of the HTM. However, diatom species assemblages and several of the geochemical proxies have continued to evolve away from those of the HTM, possibly due to additional factors such as atmospheric nitrogen deposition, which indicates that the Anthropocene is truly unique in character

relative to the entirety of the Holocene (Wolfe et al. 2013).

2.7. ACKNOWLEDGEMENTS

Funding for this study was provided by the U.S. National Science Foundation ARCSS 8k project, Nonlinearities in the Arctic climate system during the Holocene. Algal pigment analyses received additional funding from a grant awarded to Áslaug Geirsdóttir from the University of Iceland Research Fund. Salary for C. Florian provided by the Doctoral Grant of the University of Iceland. We thank the Inuit of Qikiqtarjuaq as well as the Nunavut Research Institute for field work logistical support and assistance; Kurt Refsnider, Kate Zalzal and Alexis Ault for their help

in recovering the cores; Steve DeVogel and Roxane Bowden for excellent laboratory management and assistance with all things HPLC and IRMS related; Mark Graham for sharing algal pigment expertise and helping design the pigment lab at the University of Colorado; Amy Steiker, Sarah Crump and Darren Larsen for insightful discussion and reading drafts of the manuscript; the Limnological Research Center (LacCore) at the University of Minnesota for archiving sediments; and the Natural Sciences and Engineering Research Council of Canada (NSERC). This manuscript has been strengthened by the work of two anonymous reviewers who both provided diligent and detailed comments.

2.8 Addendum to Chapter 2:

Unpublished Baffin Island carbon and nitrogen elemental and isotopic data sets

In addition to the KHL record, five other sediment cores were subsampled and analyzed for C:N, $\delta^{13}C$, and $\delta^{15}N$. These records were deemed unsuitable for full multi-proxy analysis due to either lack of adequate chronology or to lack of apparent climate signal in the isotopic data.

2.8.1. Cores collected in the April 2009 field season

2.8.1.1 *Flat Lake (64°42'59" N, 70°48'43" W)*

Flat Lake is located in south central Baffin Island, on a peninsula that extends into the much larger Amadjuak Lake. This site was selected for its position on the carbonate bedrock that

extends from Foxe Basin across western central Baffin Island. While developing radiocarbon chronology is impossible due to reservoir age effects from dissolving bedrock, the carbonate composition of the sediment makes it easily dissolvable, and because of this, Flat Lake is well-suited to isolation of cryptotephra shards for the development of an age model. This portion of the Flat Lake study was led by Kate Zalzal, who successfully extracted and geochemically analyzed cryptotephra from the sediment. These tephra shards were identified as having Cascadian and Alaskan provenance, primarily a mixture of Mt. St. Helens, Newberry and White River. Unfortunately, distinct horizons of these tephra with consistent and diagnostic geochemistry were not found. Tephra of similar geochemistry was widely distributed throughout the sediment, suggesting that it was reworked and therefore unsuitable for use as a chronostratigraphic marker.

Despite challenges with sediment chronology, down-core analysis of C:N, $\delta^{13}C$, and $\delta^{15}N$ was carried out at the Carnegie Geophysical Lab in 2010 after removing sedimentary carbonate by acid fumigation. All elemental and isotopic parameters show strong, coherent trends through the length of the record. Total organic matter content gradually rises through the bottom two thirds of the core, stabilizing to around 16% in the upper 30 cm (Fig. 2.8). Organic matter content of the sediment is predominantly controlled by the balance between watershed productivity, and dilution by inorganic material. The monotonic increase in TOC suggests that dilution might be the driver of the changes seen. Aquatic productivity should develop relatively rapidly after initial lake formation, especially because the relatively late local deglaciation should lead to some of the warmest lake water temperatures directly after formation. The bottom, less organic-rich portion of the core likely represents a time of higher sedimentation rates and large amounts of mobile till present after deglaciation and before establishment of terrestrial plant

communities. A strong anticorrelation between $\delta^{13}C$ and $\delta^{15}N$ implies that a common factor may have been influencing the change of both proxies through the record (Fig. 2.8). This could be related to either the organic matter source or the productivity and nutrient dynamics of the lake. $\delta^{13}C$ reaches its highest value and $\delta^{15}N$ its lowest at around 48 to 55 cm, which should be less than 1000 years after local deglaciation based on a linear sediment-age assumption. Heavy carbon isotope values most likely indicate high aquatic productivity or aquatic macrophyte organic matter while decreases in $\delta^{13}C$ could have been caused by low aquatic productivity, a greater proportion of terrestrial or algal organic matter. Increasing C:N throughout the core suggests that the decrease in $\delta^{13}C$ is more likely driven by increasing terrestrial organic matter as opposed to algal material. The nitrogen isotopic record could either suggest a change in nutrient supply through time, a change in organic matter source, or changes in denitrification. Aquatic macrophyte samples measured from KHL (Table 2.2) are characterized by high $\delta^{13}C$ and relatively low $\delta^{15}N$, consistent with the proxy values of the early part of the Flat Lake record. Increasing $\delta^{15}N$ and C:N with decreasing $\delta^{13}C$ can be explained by a shift to a greater contribution of soil organic matter. Increasing organic matter content of the sediment should increase the activity of heterotrophic microbes and decrease pore water oxygen content. Rising $\delta^{15}N$ could also indicate increased denitrification and the resulting preferential removal of light nitrogen isotopes, which could also drive the slightly increasing C:N during this interval. A final mechanism that could be responsible for the change in $\delta^{15}N$ is a long-term shift from phosphorous to nitrogen limitation through the Holocene. In a nitrogen-limited environment, primary producers will not be able to discriminate against heavy nitrogen isotopes and they will be incorporated into aquatic organic matter.

The alkaline pH of Flat Lake water (resulting from the dissolution of carbonate bedrock) suggested that it may be a good place to look for alkenone biomarkers (Toney et al. 2010), which contain a paleotemperature signature (Prahl and Wakeham 1988) that has been widely utilized in marine (Brassell et al. 1986; Sachs and Lehman 1999; Bendle and Rosell-Mele 2007 and many others), and more recently, freshwater sediment records (Zink et al. 2001; D'Andrea and Huang 2005; Liu et al. 2006; D'Andrea et al. 2011). Produced by haptophyte algae that are not present in all environments, alkenones have been shown to be more common in freshwater environments than originally thought. After initial confirmation of clean and abundant alkenones in Flat Lake surface sediment by William D'Andrea in 2010, six samples at 10 cm increments from Flat Lake were selected for alkenone analysis at INSTAAR. These samples were extracted at high temperature and pressure using dicholomethane in an Accelerated Solvent Extractor, then separated and quantified by GC-FID analysis of the ketone fraction of the total lipid extract. The U^{k}_{37} index was calculated from each sample and converted to temperature using the Zink et al. (2001) calibration. Increasing alkenone-inferred temperatures occur from the base of the core to 40 cm, then decrease toward the top of the core, with the top two samples giving equivalent temperatures (Fig. 2.9). This temperature progression is what would be expected over this time interval, with an HTM shortly after deglaciation followed by late Holocene cooling. Further alkenone analysis of the Flat Lake sediment would be worthwhile if a secure chronology can be developed. The best hope for developing a chronology of this core is through compound specific radiocarbon dating of terrestrially derived organic molecules, which is not a trivial undertaking.

Absence of short-term variability in the Flat Lake record suggests that bioturbation may have led to mixing of the sediment. This is also supported by the lack of distinct cryptotephra

horizons. Future users of this core should be aware that this is likely a smoothed record not suited for high-resolution climate studies but may be acceptable on multi-centennial timescales.

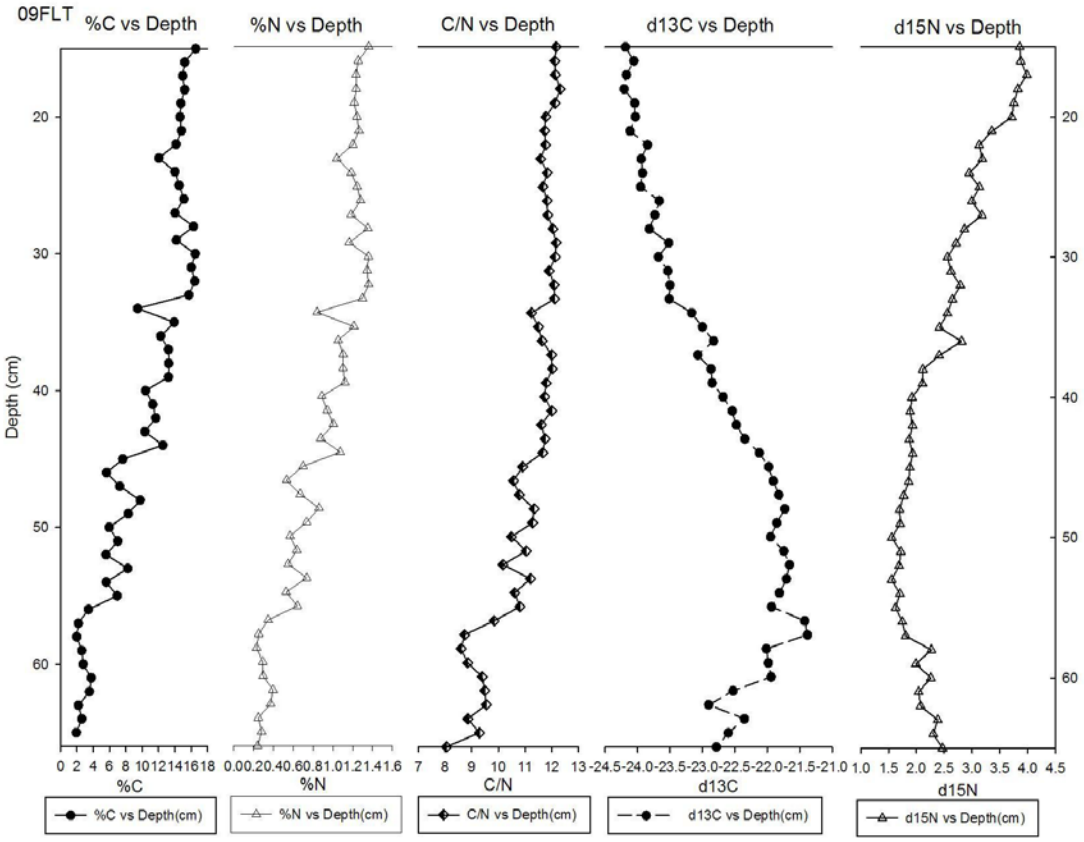

Figure 2.8. Proxy plots from Flat Lake, Baffin Island

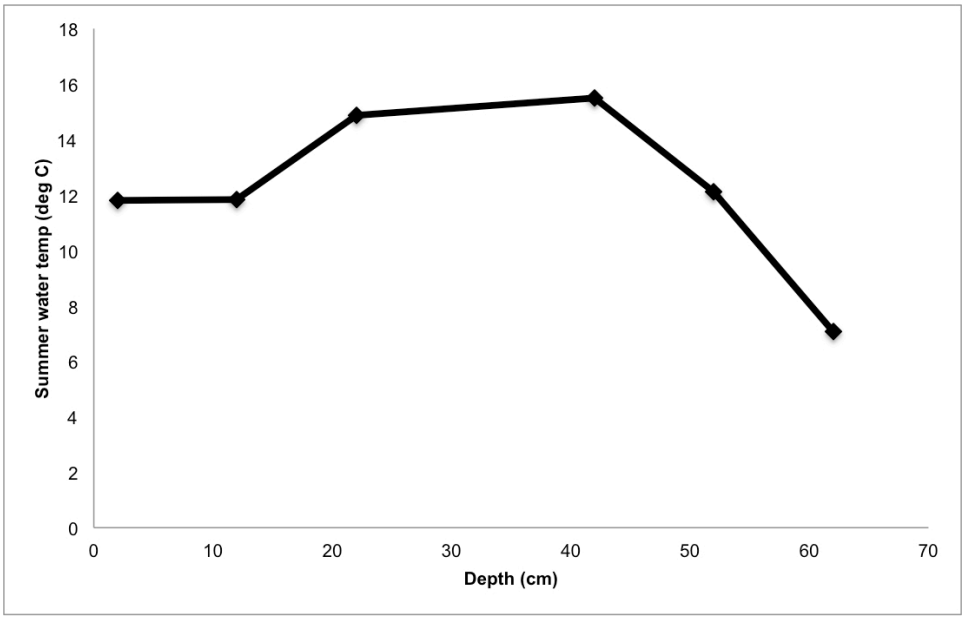

Figure 2.9. Alkenone-inferred summer water temperatures at Flat lake.

2.8.1.2. *Middle Lake (64°18'31" N, 69°51'39" W)*

Middle Lake, located 64 kilometers southwest of Flat Lake, is on the border between carbonate and crystalline bedrock and was selected in hope that the reservoir effect from the dissolved carbonate would not influence radiocarbon ages of aquatic macrofossils. A single macrofossil was submitted for dating from ~10 cm above the transition from glacial to lacustrine sediment. The radiocarbon date obtained from this macrofossil is ~7.5 ka, significantly older than the estimated local deglaciation of 6.3-6.8 ka (Dyke 2004) suggesting substantial reservoir effect and necessitating an alternate geochronological method. Clear changes in the isotopic

record (only the upper part of the core was analyzed) suggest that this record is not bioturbated like Flat Lake, and could be useful for future studies if a secure chronology can be developed.

2.8.1.3. *Ledge Lake*

Ledge Lake was selected for its proximity to Flat Lake and its position on crystalline bedrock, which allows a conventional radiocarbon age model to be developed. The ~90 cm of organic-rich sediment in this core (LDG09-02), which would have been deposited over approximately 6.5 thousand years, would allow for relatively high resolution sampling. This core was sampled and run at 1 cm resolution for C and N isotopes at the Carnegie Geophysical Laboratory. The proxy record lacks variability through the entire post-glacial portion interval, indicating low climate sensitivity of these proxies at this location (Fig. 2.10). Future analysis of other proxies, such as diatom species assemblages, may be more worthwhile. The surprising stability of isotopic values may suggest that the record is smoothed by bioturbation. An unchanging ^{210}Pb decay curve in the surface sediment would suggest bioturbation. This should be checked prior to conducting additional proxy analysis on this core. A basal radiocarbon date of this core, however, is worthwhile and would provide important age control, constraining the exact timing of local deglaciation.

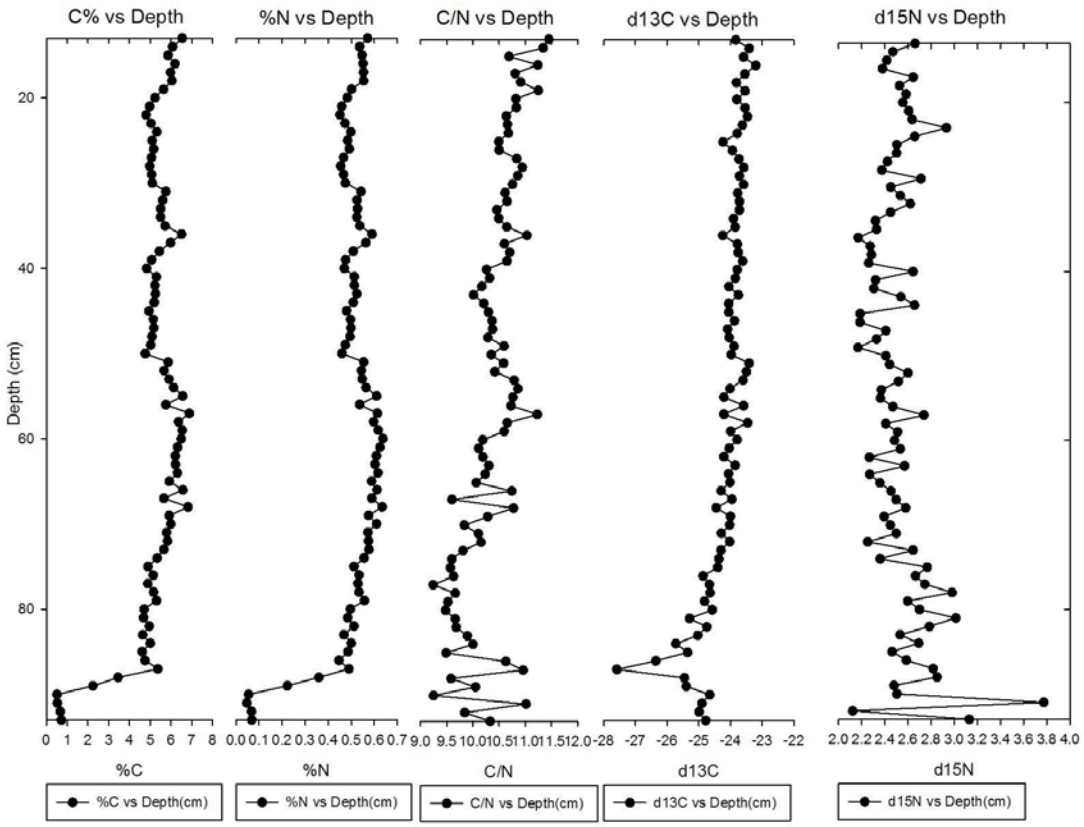

Figure 2.10. Carbon and nitrogen elemental and isotopic values from Ledge Lake

2.8.2. Cores from the August 2010 field season

2.8.2.1. *Kekerturnak Lake (67°51'26" N, 64°52'31" W)*

To complement the previous studies by Wolfe et al. (2001; 2002), an additional core of Kekerturnak Lake was taken in the 2010 field season due to its close proximity to KHL. This core was also subsampled and analyzed for carbon and nitrogen isotopes at the Carnegie Geophysical Laboratory. Although preliminary isotope data looked to provide interesting climate

information, the KHL record was selected for analysis due to constraints of time and funding. Due to the complete lack of macrofossils, developing a chronology for this core would require radiocarbon dating of humic acid, which is potentially hindered by a large reservoir effect (Wolfe et al. 2004).

2.8.3. Cores from previous field seasons

2.8.3.1. *Canso Lake (67°12'20"N, 63°34'12"W)*

The 98CAN-05 core was selected to examine an interval of laminated sediment, which suggests a period of anoxic bottom waters. Throughout this anoxic interval, labile biomarkers should be well preserved, making this core suitable for early Holocene organic geochemical studies. The timing of the anoxic interval itself could also have climate significance, as a period of high biological productivity or low wind stress. This core was subsampled and run for carbon and nitrogen isotopes at the Carnegie Geophysical Laboratory at high resolution (Fig. 2.11). The isotopic record shows coherent variability, although it seems that some of the major proxy excursions are driven by changes in organic matter dynamics at the transition between anoxic and oxygenated bottom waters. A multi-proxy approach would be necessary to contextualize the isotopic record. This is likely worthwhile due to the climate inferences that can be made from past lake stratification as well as the increased biomarker preservation potential of these sediments.

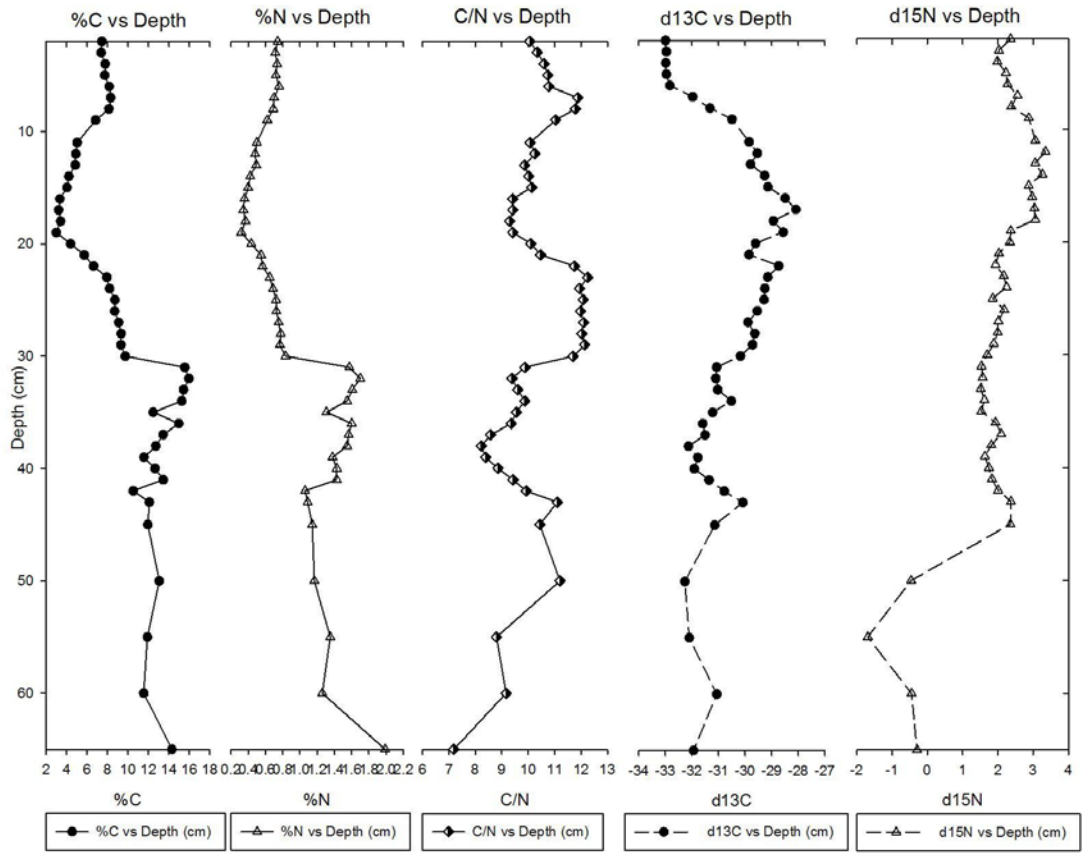

Figure 2.11. Carbon and nitrogen elemental and isotopic values from Ledge Lake

CHAPTER 3

Catchment geometry influences proxy response in late Holocene records from two proximal lakes located in north Iceland

Christopher Florian[1,2], Sarah Crump[1], Áslaug Geirsdóttir[2], Gifford Miller[1,2], Kate Zalzal[1,2]

[1]Institute of Arctic and Alpine Research and Department of Geological Sciences, University of Colorado, Boulder, CO 80309-0450, USA

[2] Department of Earth Sciences, University of Iceland, Sturlugata 7, Reykjavík 101, Iceland

3.1 ABSTRACT

Lake sediments are frequently utilized for reconstructing paleoclimate in the Arctic, particularly in Iceland, where high sedimentation rates and abundant tephra layers allow for the development of high-resolution, well-dated records. However, when developing climate records using biological proxies, catchment-specific processes must be understood and separated from the primary climate signal in order to develop accurate reconstructions. In this study, we compare proxy records (biogenic silica [BSi], C:N ratio, ∂^{13}C, and algal pigments) of the last 2 ka from two nearby lakes in northwest Iceland in order to elucidate how different catchments respond to similar climate history. Torfdalsvatn and Bæjarvötn are two coastal lakes located 60 km apart on either side of Húnaflói bay; mean summer temperatures are highly correlated between the two sites over the instrumental record, and likely for the past 2 ka as well. Consistent with other Icelandic lake records, both lakes record a first-order cooling as decreasing

aquatic productivity (BSi) over the last 2 ka. Both sediment cores also record the onset of landscape destabilization, reflected by increased terrestrial input (C:N and $\partial^{13}C$), which suggests an intensification of cooling. However, the timing and magnitude of this shift differ markedly between lakes. Biological proxies indicate gradual landscape destabilization beginning ~900 AD. This is more gradual at Torfdalsvatn than Bæjarvötn, where sharper, more intense landscape destabilization at ~1400 AD follows initial variability. Because temperatures at the two lakes are well correlated, different proxy responses are likely the result of catchment-specific thresholds and processes. Specifically, a steeper catchment and freeze-thaw processes due to higher precipitation at Bæjarvötn may allow for a more pronounced influx of terrestrial material as the critical shear stress for soil erosion is surpassed more readily.

3.2 INTRODUCTION

The chemical characteristics of lake sediment organic matter (OM) can be used to determine past total primary productivity and organic matter source (Meyers and Ishiwatari 1993; Meyers and Teranes 2001). Changes in climate modulate environmental parameters such as growing season length and availability of habitat and nutrients. This relationship allows temperature history to be inferred from changes in the biological and geochemical makeup of lake sediment (Douglas and Smol, 1999; Smol et al. 2005). Changes in the nature of sedimentary OM are driven by multiple factors in addition to temperature change; therefore, it is necessary to develop a local, watershed-scale interpretation relating proxy record trends to regional climate. Factors such as biological ontogeny, changes in precipitation, nutrient supply, human activity,

and the unique local-scale response of biological communities to environmental change may serve to amplify or obscure the signal of actual regional temperature changes.

The degree to which we are able to extract climate records from lake sediment archives depends on our ability to develop accurate interpretations of proxy records. Obtaining direct paleotemperature proxy records from lake sediment archives is often difficult, as quantitative proxies are only present in certain depositional environments or require local calibrations (Castañeda and Schouten 2011; Ho et al. 2014; D'Andrea et al. 2016). Because of this, qualitative biogeochemical proxies are frequently employed to infer past climate; this necessitates developing a best-possible interpretation of the relationship between proxy behavior and change in climate. Qualitative and quantitative calibration of climate state with proxy response is frequently accomplished utilizing high-resolution sediment records compared with instrumental temperature or precipitation data (Seppä and Birks, 2001; Bigler and Hall 2003; Autio and Hicks 2004; Mckay et al. 2008; Rühland et al. 2008; Geirsdóttir et al. 2009; and many others), but low sedimentation rates and a scarcity of meteorological data often render this impossible in the Arctic. Biogeochemical proxies have the potential to exhibit threshold behavior as specific tolerances of the catchment's biological system are met by changing environmental conditions (Tzedakis et al. 2004; Rühland et al. 2008; Dodds, et al. 2010; Willis et al. 2010). These threshold changes may not be observed in the limited range of variability represented in short-term comparisons with instrumental data and are difficult to deconvolve from rapid climate change events in proxy records. Additionally, parameters not measured in instrumental records, such as date of spring ice melt, may have significant influence on the translation between climate shift and biotic response. As the ability to develop accurate chronologies increases along with the technology to more accurately measure chemical proxies, improvements in understanding

proxy behavior are essential to the development of high quality paleoclimate records. When instrumental proxy calibration is not feasible, comparing proxy response in multiple proximal lakes is a means to examine which factors are driving proxy response in each basin, as well as to better understand regional climate history (Anderson et al. 2012).

Several previous studies have sought to address and quantify the way in which changes in climate are recorded in lake sediments and how this relationship is influenced by the local environment. Blenckner (2005) developed a conceptual model consisting of a 'landscape filter' and an 'internal lake filter' to better understand and explain why lakes respond uniquely to changes in climate. The landscape filter consists of variables such as the lake's geographic position, catchment characteristics, and lake morphometry. The internal lake filter consists of individual lake history and biotic-abiotic interactions (such as the changing ice cover altering phytoplankton blooms). This concept was further developed by Leavitt et al. (2009), who break down the way climate change alters lake systems as occurring through changes in the influx of either energy or mass to the lake (the 'Em flux approach'). Each of these parameters is filtered through either atmospheric or catchment processes before directly or indirectly affecting the lake. Anderson et al. (2012) examined paired lake records along a coastal-inland transect from southwest Greenland. The inland lake pair responded similarly to climate forcing but the costal records differed, likely due to catchment-specific factors filtering the climate signal. Although these studies provide a framework for assessing how different lake catchments variably incorporate climate information into sedimentary archives, local studies need to be carried out in order to properly address how catchment-specific factors in each study area influence what is observed in the proxy record.

In Iceland, where the high spatial density of lacustrine records allows for the compilation of detailed regional composite records, catchment-specific factors remain a key uncertainty. In this study we compare two 2-ka proxy records of sedimentary organic matter-inferred paleoenvironmental conditions from nearby lakes in north Iceland, which show different proxy response despite experiencing similar climatic histories. We hypothesize that differences in the morphology of each lake and catchment along with lake-specific biogeochemistry have led to variation in proxy response to late Holocene cooling.

3.2.1 Local climate history

A growing regional consensus from sediment archives shows the earliest onset of cooling in Iceland occurring between 5.5 and 4 ka, with evidence of initial ice cap regrowth at Langjökull (Larsen et al. 2011), reduced biological productivity at Haukadalsvatn (Geirsdóttir et al. 2013) and increasing drift ice on the North Iceland Shelf (Moros et al. 2006). The last 2 ka has been characterized by a period of widespread cooling temperatures in response to the long-term decrease in Northern Hemisphere summer insolation, as well as short-term perturbations such as increased sulfate aerosols from volcanic eruptions (Kaufman et al. 2009; Zhong et al. 2011; Miller et al, 2012). Each of these forcings is modulated by the internal dynamics of the climate system; therefore, the resulting cooling trend was not linear, but rather punctuated by relatively warm intervals and periods of rapid cooling. The strongest departure from the mean Holocene climate state occurs during the Little Ice Age (LIA, ca. 1250-1850 AD/CE) of the last millennium. Dramatically increasing sedimentation rates at glacial lake Hvítárvatn characterize the expansion of Langjökull, which reached its maximum extent at 1870 AD (Larsen et al. 2011).

The coldest diatom-inferred sea surface temperatures (SST) of the Holocene were observed off northern Iceland during this time (Jiang et al. 2015), which were also associated with maximum sea ice influence as recorded by elevated quartz and biomarker IP-25 in the same region (Andrews et al. 2009; Cabedo-Sanz et al. in review). An observed increase in terrestrial organic matter in multiple lake cores across Iceland suggests the onset of widespread landscape destabilization. This landscape destabilization is due to a reduction of overlying vegetation during the LIA, which lead to rapid erosion of soils (Wooller et al. 2008; Geirsdóttir et al. 2009; Larsen et al. 2011). At some sites, such as Vestra Gísholtsvatn in south Iceland, this is potentially overprinted by anthropogenic effects (Blair et al. 2015).

3.3 MATERIALS AND METHODS

3.3.1 Study Site

Lake sediment records from Icelandic lakes are characterized by relatively high sedimentation rates due to the easily eroded basaltic bedrock and contain abundant tephras that can be geochemically identified as chronostratigraphic markers. These tephra horizons can be dated using historical information and radiocarbon of soil, lacustrine and marine archives providing robust chronologies with minimal age uncertainties. These detailed chronologies allow for direct comparison of the records from nearby lakes to develop regional syntheses of climate history (Geirsdóttir et al. 2013). In addition to providing high-quality sediment records, Iceland is well-positioned to record past environmental changes. It is located at the interface between warm Atlantic and cold polar ocean currents; therefore, small shifts in these currents due to dynamical response to climate forcing should translate to significant changes in the mean

terrestrial climate state. Sea ice, both imported and locally formed off the north coast of Iceland during extreme cold events, provides a positive feedback for increasing the duration and severity of short-term perturbations such as volcanic eruptions (Miller et al. 2012).

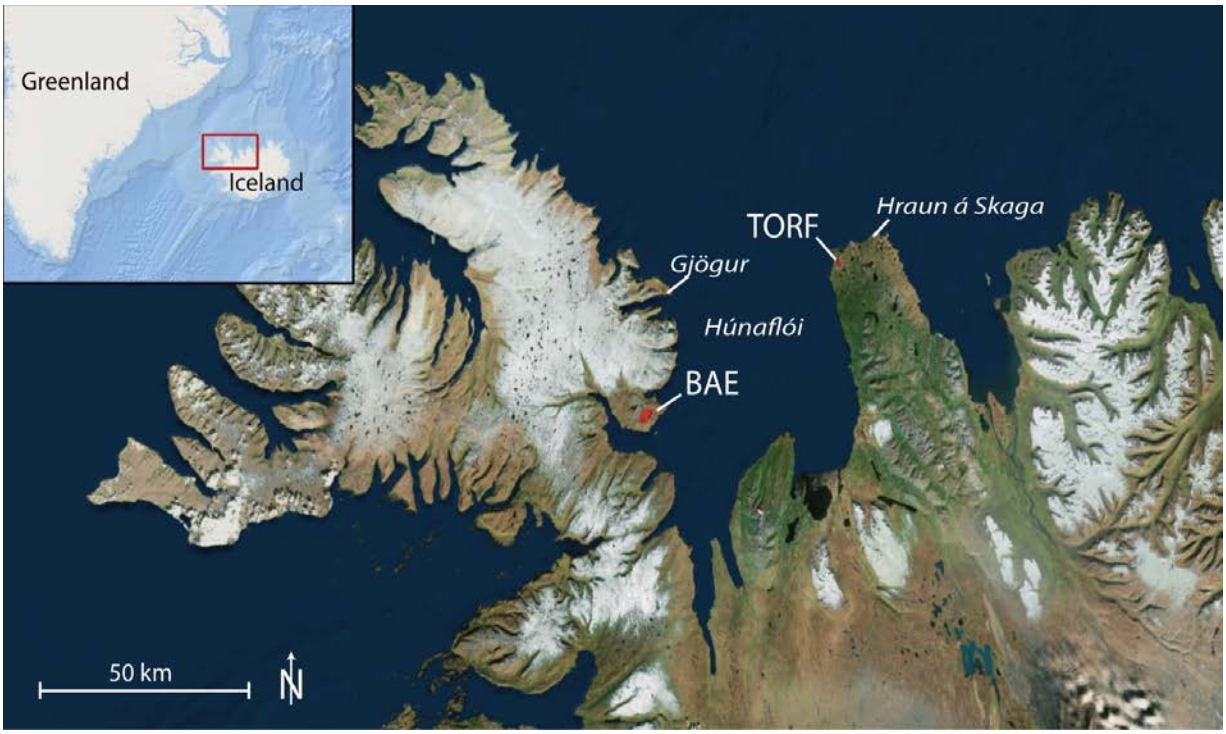

Figure 3.1. Map showing the location of each core along with proximal weather stations. The catchment of each lake is colored red.

3.3.1.1 *Torfdalsvatn (66° 13.56'N, 20° 122.81'W)*

Torfdalsvatn (Fig. 3.1) is located on the northwest tip of the Skagi peninsula of northern Iceland with a surface area of 0.4 km^2, maximum depth of 5.8 m, and elevation of 52 m above sea level (a.s.l.). The nearby weather station at Hraun á Skaga (~12 km to the northeast of Torfdalsvatn) reports mean annual air temperature from 1956-1990 of 2.5ºC, with 475 mm precipitation (http://en.vedur.is/Medaltalstoflur-txt/Hraun_352_med6190.txt). The catchment is

small (2.76 km^2), and the inlet stream had an estimated discharge of 0.25 m^3s^{-1} in July 2014. The landscape surrounding the lake has a relatively low gradient (average slope of 1.7º) with a vegetation cover of poor heathland (Fig. 2; Arnalds, 2015). An 8.2-m-long sediment core was retrieved in February 2012 using a hammer-driven piston corer from the lake ice in two drives, which were then sub-sectioned to 1.0-1.5 m in the field. This core was then split, imaged and measured for density and magnetic susceptibility using a GEOTEK MSCL-S at the University of Iceland. Modern water parameters as measured in July 2014 are listed in Table 3.1.

	Bæjarvötn	Torfdalsvatn
Latitude	65° 43.74'N	66° 13.56'N
Longitude	21° 25.74'W	20° 122.81'W
Altitude (m)	110	52
Catchment area (km^2)	10.35	2.76
Lake area (km^2)	0.65	0.4
Catchment: Lake area	15.9	6.9
Average catchment slope	2.53	1.68
Max depth (m)	23	5.8
Temperature (July 2014)	12.4	13.8
pH	7.4	7.6
Conductivity ($\mu S\ cm^{-1}$)	104	150
TDN ($mg\ L^{-1}$)	0.07	0.15
TDP ($mg\ L^{-1}$)	0.0065	0.0035
TDN:TDP	10.7	43.5

Table 3.1. Modern physical parameters and water chemistry from each lake.

Figure 3.2. Photographs of each lake taken in July 2014. The Torfdalsvatn catchment is less steep than that of Bæjarvötn, where there is significant visible erosion on steep slopes.

3.3.1.2 *Bæjarvötn (65° 43.74'N, 21° 25.74'W)*

Bæjarvötn (Fig. 3.1) is located 61 km to the southwest across Hunafloi (the inner N. Iceland shelf), with a surface area of 0.65 km^2, maximum depth of 23 m, and elevation of 110 m a.s.l (Fig. 1). The lake is separated into three distinct sub-basins, increasing in depth from north to south. The weather station at Gjögur (~30 km north of Bæjarvötn) records a 30-year mean annual air temperature of 2.7ºC and mean annual precipitation of 757 mm from 1956-1990 (http://www.vedur.is/Medaltalstoflur-txt/Stod_295_Gjogur.ArsMedal.txt). The catchment is 10.35 km^2 and has a higher average relief (2.5º) than the catchment of Torfdalsvatn (Table 3.1). Vegetation cover is similar between the sites. Evidence of soil erosion is apparent in the catchment, with eroded gullies occurring on the steep southeast shore of the lake (Fig. 3.2). A 1.38-meter-long sediment core with an undisturbed sediment-water interface was taken from the middle basin of the lake (10 meters water depth) in winter of 2010 using a hammer-driven piston corer. The core was split, imaged, and subsampled at the LacCore lab at the University of Minnesota.

Modern instrumental temperatures at the two sites are well correlated, and the two lakes are assumed to have experienced similar climate histories (Fig. 3.3).

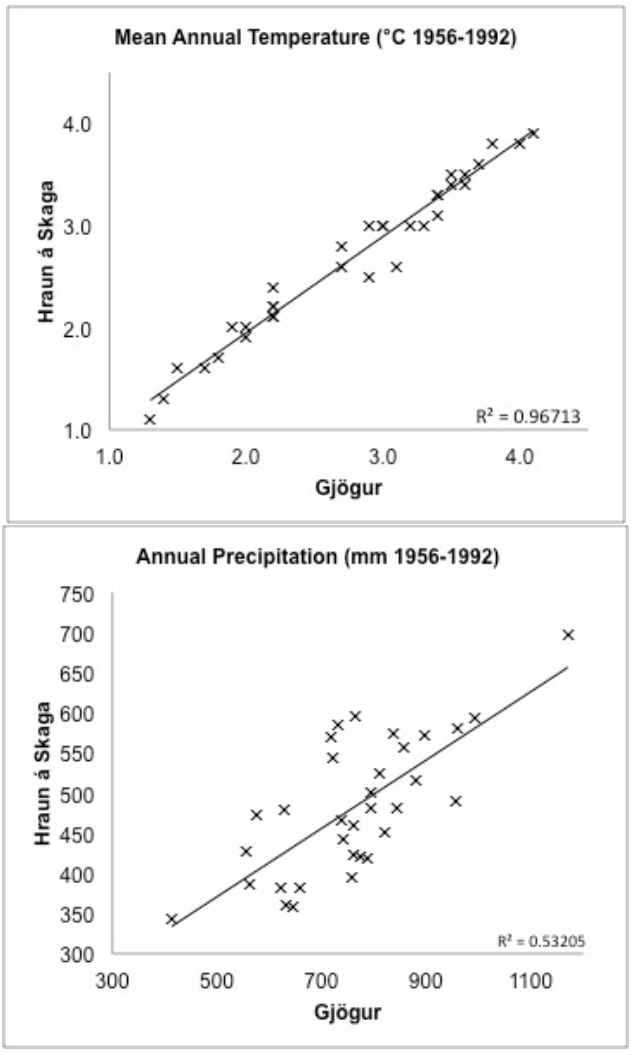

Figure 3.3. Correlation between instrumental mean annual temperature and annual precipitation records from Gjögur, located near Bæjarvötn, and Hraun á Skaga, near Torfdalsvatn. Modern temperatures between field sites are well correlated. Precipitation is higher at Gjögur and is not as strongly correlated between the sites.

3.3.2. Chronology

Chronologies for each sediment core were developed using a combination of radiocarbon dates on preserved aquatic macrofossils and tephrochronology, utilizing the wealth of chronostratagraphic markers left by historically documented Icelandic eruptions (Table 3.2). Tephra layers in each lake were visually and geochemically identified by comparing their

geochemical composition and stratigraphic position to that of known regional eruptions. Radiocarbon ages of aquatic macrofossils were calibrated using IntCal13 (Reimer et al. 2013) within the CLAM software package (Blaauw 2010).

Core	Depth (cm)	Material	^{14}C age (years BP)	Age Range (cal years BP)	AMS
BAE10-2C	29.1	Hekla 1477 AD		473±5	
BAE10-2C	53	Macrofossil	900 ± 25	741-908	
BAE10-2C	77.8	Settlement tephra		1079±2	
BAE10-2C	106.5	Macrofossil	2160 ± 25	2089-2305	
BAE10-2C	133	Hekla 3		2980±65	
TORF12-1A	17	Hekla 1766 AD*		184±2	
TORF12-1A	66	Hekla 1300 AD*		650±5	
TORF12-1A	84	Hekla 1104 AD		846±5	
TORF12-1A	125	Settlement tephra*		1079±10	
TORF12-1A	148	Macrofossil	1390 ± 15	1286-1331	
TORF12-1A	346	Macrofossil	3305 ± 15	3476-3570	

Table 3.2. Age control points from both cores. * denotes tephras that were identified visually

The Torfdalsvatn age model is comprised of a combination of visibly distinct tephra layers and radiocarbon dates of aquatic macrofossil plants (Table 3.2). Because radiocarbon ages of humic acid extracted from Icelandic lake sediment have been shown to be significantly older than their stratigraphic position suggests (e.g. Geirsdóttir et al. 2009), only aquatic macrofossils were used for dating. The uppermost part of the core is devoid of aquatic macrofossils and age control is provided solely by tephra in this interval. In the Bæjarvötn core, the age model is also comprised of tephra and radiocarbon control points; however, the macrofossils were not identifiable as aquatic or terrestrial. Tephras from both cores were sampled, cleaned, prepared for

geochemical analysis, and identified by comparison with regional eruptions. Age control points were entered into the CLAM software package (Blaauw 2010) operating in the R environment and an age-depth model was created using a smoothing spline curve fit (Fig. 3.4).

3.3.3. Sediment and modern sample isotope geochemistry

Carbon and nitrogen elemental and carbon isotopic analysis was performed on homogenized and freeze-dried modern and sediment core samples at the Carnegie Geophysical Laboratory, the University of California, Merced and the University of California, Davis. Sediment, soil, vegetation and epilithon samples were selected to characterize the primary organic matter sources to the sediment. An aliquot of material was weighed into a pre-combusted tin capsule that was crimped shut and run on an Elemental Analyzer Isotope Ratio Mass Spectrometer (Finnigan Delta V Plus with a CE NC 2500 Elemental Analyzer). Carbon isotopic values are expressed in standard delta notation in reference to the PDB.

3.3.4. Algal pigments

Algal pigments were solvent extracted from freeze dried sediment samples using 6 ml of 80:20 mixture of acetone:methanol overnight in amber vials under N_2 at -10°C. Samples were touch mixed and sonicated to disperse sediment and increase extraction efficiency, then filtered through a 0.2 µm PTFE syringe filter which was then rinsed with 2 ml of acetone to recover sample residue from the filter. The extract was then dried down and rehydrated with a known volume of acetone containing a known concentration of α-tocopherol standard. Samples were placed in the refrigerated autosampler of an Agilent 1200 series High Performance Liquid Chromatographer (HPLC) and derivitized to improve chromatographic behavior immediately

prior to injection with an equal volume of 28 mM tetrabutyl ammonium acetate in water. A binary mobile phase system was used with solvent A composed of a 70:30 mixture of methanol:28 mM tetrabutyl ammonium acetate in water and solvent B composed of pure methanol at a flow rate of 1 mL min^{-1}. An Agilent Eclipse XDB-C8 4.6 x 150 mm column was used to separate pigments whose absorbance of visible light was detected by an Agilent Diode Array Detector (DAD) scanning between 400 and 750 nm. Pigments were identified by comparing characteristic absorbance spectra with that stored in a library created from a suite of standards obtained from DHI Denmark.

3.3.5. FTIRS-Inferred biogenic silica

Subsamples of freeze-dried sediment were weighed and mixed with potassium bromide at a ratio of 0.02 to disperse and reduce the IR absorbance of the sample. The sediment and KBr mixture was then ground to a fine powder using a mortar and pestle, and analyzed by Diffuse Reflectance Fourier Transform Infrared Spectrometry (FTIRS) by a Bruker Vertex 70 with a Praying Mantis diffuse reflectivity accessory (Harrick). Samples were scanned 64 times at 4 cm^{-1} resolution over wavelengths ranging from 3750 to 450 cm^{-1}. Baseline shifts were removed by applying a linear baseline correction in the Opus software. Area under the absorbance curve was then integrated from 1000 to 1250 cm^{-1}, the region with the strongest correlation to biogenic silica (Meyer-Jacob et al. 2014). We chose to not calibrate the FTIRS areas to biogenic silica concentration for two reasons. First, we wished to avoid the additional sources of error associated with both the traditional wet-digestion measurement methods and the calibration transfer function itself. Additionally, because published calibration curves are linear, they would

only change the absolute BSi values and not the relative changes observed in downcore data. We do not interpret the absolute values of the FTIRS-inferred biogenic silica data, only relative changes over time, and therefore favor presenting the raw FTIR measurements.

3.4. RESULTS AND DISCUSSION

3.4.1. Chronology

At both sites radiocarbon ages correspond well with the ages derived from tephrochronology (Fig. 3.4, Table 3.2). Systematic age offsets between radiocarbon and tephrochronology, such as were found in nearby Haukadalsvatn (Geirsdóttir et al. 2009), were not observed in Torfdalsvatn. This lack of age offset is due to the sampling of aquatic remains in the cores, which, in contrast to terrestrial material, have a short residence time prior to deposition in the sediment. The radiocarbon ages of macrofossils at Bæjarvötn do show a slight offset from what would be expected based on tephra alone. This suggests that the macrofossils sampled from Bæjarvötn were terrestrial in origin, and the older ages reflect the longer residence time of the material on the landscape.

These age models show that the sediment records are continuous, without hiatuses or age reversals. The sedimentation rate at Torfdalsvatn is roughly twice that of Bæjarvötn, having an accumulation rate of approximately 100 cm per thousand years compared to just less than 50 cm per thousand years at Bæjarvötn. Because Torfdalsvatn has a smaller catchment with less relief, the higher sedimentation rate at this site is probably attributable to elevated aquatic productivity.

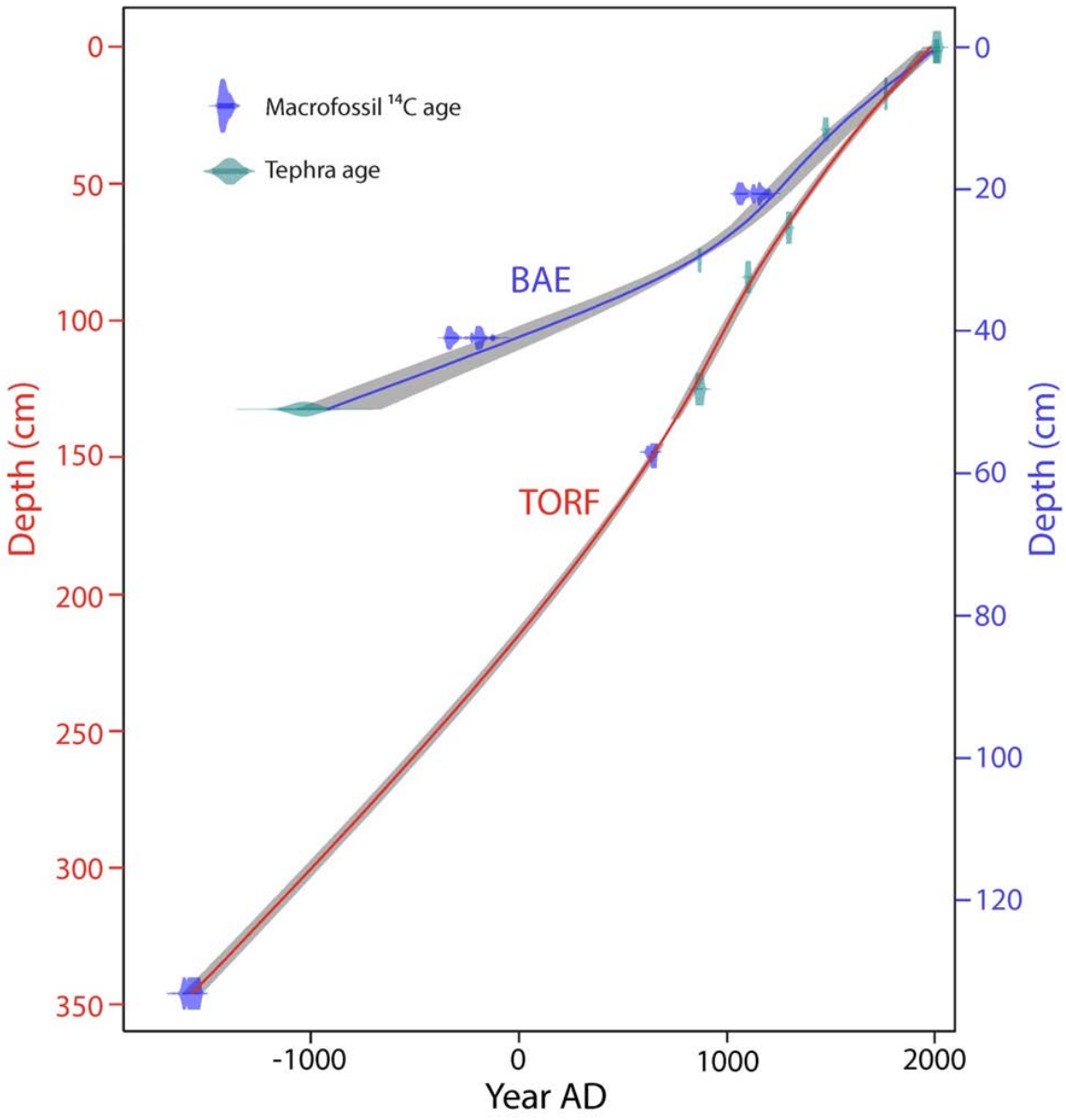

Figure 3.4. Age-depth model of both cores, Torfdalsvatn in red (left depth axis) and Bæjarvötn in blue (right axis).

This is expected, as Torfdalsvatn is much shallower with a greater proportion of the lake bottom in the photic zone and supporting the growth of aquatic macrophyte plants.

3.4.2. Modern samples

To characterize the modern environment and give local context to the proxy reconstruction, samples representing each source (algal, aquatic macrophyte plant, terrestrial vegetation, and soil) of sedimentary organic matter were collected from the lakes studied as well as other sites in northwest Iceland and analyzed for their carbon and nitrogen elemental and carbon isotopic ratios. End member values are presented in Table 3.3.

Organic matter source	$\delta^{13}C$ (‰)	C:N
Algae	-24.1 (±4.6)	13.2 (±5.7)
Aquatic vegetation	-15.5 (±5.1)	25.0 (± 11.6)
Soil	-26.1 (±0.97)	17.7 (±4.2)
Terrestrial Vegetation	-27.6 (±2.7)	46.2 (±17.7)

Table 3.3. Average C:N and carbon isotope values for each organic matter source. Complete data set in Appendix A.

3.4.3. Algal organic matter

The algal endmember was most difficult to collect as it is nearly impossible to sample by filtering or collecting epilithon without contamination from suspended or detrital terrestrial or aquatic macrophyte material. For this reason ‘algal’ values should be cautiously interpreted and assumed to be somewhat contaminated. Carbon isotopic composition of predominantly algal material varied widely from -6.7 to -30.1‰. Surprisingly enriched values were obtained from

Nostoc sp. dominated epilithon at Torfdalsvatn. These values were removed from the calculated averages of algal material because of their vastly different isotopic composition and because their low overall abundance renders them relatively unimportant as a source of sedimentary organic matter. Excluding the *Nostoc*-dominated material, carbon isotope values averaged -24‰ (±4.6), still somewhat more enriched than expected (Boutton 1991; Meyers and Lallier-Vergès 1999). This could be explained by contamination from other (likely aquatic macrophyte) sources or by the existence of a locally drawn down dissolved inorganic carbon (DIC) pool, which due to the preferential removal of light carbon atoms would lead to the successive enrichment of primary producer-derived organic matter.

Carbon-to-nitrogen ratios of many samples measured were higher than expected for purely algal material, ranging from 6.2 to 17.4 (avg. 13.2, ±5.7). The lower C:N samples likely represent the most purely algal material collected with the higher samples indicating contamination from other organic matter sources. High algal C:N values could also be due to nitrogen limitation at some of the sites; however, this is unlikely given the relatively depleted nitrogen isotope values of the samples.

3.4.4. Aquatic macrophyte organic matter

The aquatic macrophyte organic matter carbon isotopic composition averages -15.5‰, representing the most enriched organic matter source other than the much less abundant *Nostoc*-dominated epilithon. The range of values is from -10.5‰ to -24‰ and has minimal overlap with algal and terrestrial sources, allowing for robust identification of aquatic macrofossil material in the sediment by carbon isotopes.

Carbon-to-nitrogen ratios of aquatic macrophytes average 25 (±11.6) with a range of 8.0 to 47. The large range in C:N is likely attributable to the variable amount of nitrogen-poor structural material present in different species or leaf/stem material sampling bias. Overall the C:N of macrophyte material is higher than the algal values but not unique among all sources, indicating that isotopic composition is the best tracer of aquatic macrophyte material.

3.4.5 Soils

The soil end member is important to distinguish from terrestrial vegetation because it is hypothesized to be the most easily transported and therefore the most important allochthonous material contributing to lake sediment organic matter. Soils represent the least well-constrained end member other than algal material as previous studies focused terrestrial sampling on plant material (Wang and Wooller 2006).

The carbon isotopic composition of soils measured in this study has a relatively narrow range of -24.6 to -28‰, averaging 26.1‰ (±0.97). This is within the expected range of soils with organic matter derived from the decomposition of C3 plants (Staddon 2004). Discrimination against heavy isotopes during respiration and decomposition of parent material will lead to preferential removal of ^{12}C, leaving the remaining organic matter slightly enriched. Therefore, soil carbon isotopic composition is controlled by source material and degree of microbial decomposition. The efficiency of microbial decomposition is predominantly controlled by moisture, temperature and oxygen availability. Differences in these parameters most likely explain the variability in modern samples and it is possible that different past climate regimes would produce higher or lower isotopic values.

Soil C:N is between 13 and 36 (avg. 17.7, ±4.2). This value is somewhat higher than has been measured in soil pits near Hvítárvatn, where values remained consistent around 14 through the past 6 ka (Larsen et al. 2011). Variability in measured C:N values in modern soil samples probably results from variable vegetation cover and changes in environmental variables such as moisture content. Weintraub and Shimel (2003) measured higher C:N values in tussock tundra soil compared with wet meadow soil, in part attributed to the unfavorable conditions for decomposition in the wet sites and the difference in overlying vegetation.

3.4.6. Terrestrial Plants

Isotopic and elemental ratios of terrestrial plants and mosses in this study are within expected values of C3 plants with $\partial^{13}C$ ranging from -30.4 to -24.7‰ (avg. -27.6‰, ±2.7), and C:N ranging from 14 to 68 (avg. 46.2, ±17.7). Terrestrial plant material is a direct source of material contributing to the lake sediment and also the parent material for catchment soil organic matter. Low abundance of preserved terrestrial plant macrofossils in both cores suggest that soil, rather than intact plant material is the dominant terrestrial source to the sediment at both sites. For a larger dataset and detailed discussion of north Iceland terrestrial plant C:N and isotopic values, see Wang and Wooller (2006).

3.4.7. Sediment organic matter geochemistry

Total organic carbon content (TOC) in the Bæjarvötn core ranges from 2 to 15 percent, with consistently low values occurring earlier in the record, onset of variability occurring just before 900 AD, which is followed by a stepwise increase in TOC at ~1450 AD that persists for the remainder of the record. Consistent C:N values (~11.2) increase abruptly at ~1450 AD,

mirroring the stepwise change in TOC, to variable values between 14.5 and 21 (Fig. 3.5). Covariance in TOC and C:N suggests that the increase in TOC represents a change in OM source, with the additional carbon entering the sediment coming from high C:N terrestrial material. At Bæjarvötn, the most enriched carbon isotope values also occur in the older part of the record, with values around -22.5‰ sharply decreasing to values around -26.6‰ contemporaneous with the increase in TOC and C:N. This further indicates that the additional organic carbon entering the sediment represents a change in dominant organic matter source from aquatic to terrestrial. This shift in organic matter source is coincident with peak LIA conditions and can be attributed to increased erosion of soils after harsh climatic conditions led to a decrease in vegetation cover in the catchment.

Torfdalsvatn TOC is less variable, with a range of 5 to 10.5 percent. The Torfdalsvatn record has little first order change in TOC, with lower values corresponding to intervals of tephra deposition. In contrast, C:N increases throughout the last 2 ka as seen at Bæjarvötn, but the increase at Torfdalsvatn is gradual, from steady values around 7.9 until ~1000 AD, at which point values start to increase to 9.5 in the modern sediments (Fig. 3.5). The increase in C:N in the Torfdalsvatn core also represents a shift in organic matter source from aquatic to terrestrial, but the lack of covariance with TOC and lesser magnitude suggest a relatively subdued environmental shift compared to that at Bæjarvötn. Bulk sedimentary carbon isotopes at Torfdalsvatn show most enriched values of around -17‰ near 0 AD, steadily becoming more depleted to a value of -23‰ at 1700 AD, where the trend reverses and values rise to -21‰ at the top of the core. The heavier carbon isotope values at Torfdalsvatn imply a greater contribution of aquatic macrophytes to the sediment. This is consistent with modern observations of thick aquatic vegetation and abundant aquatic plant macrofossils observed in the sediment. While both

lakes show the sediment becoming terrestrial-like in composition, the transition at Torfdalsvatn is gradual with an earlier onset than the later-occurring stepwise shift seen at Bæjarvötn.

3.4.8. Sedimentary algal pigments and biogenic silica

Although a wide range of individual pigments were measured in each core, for simplicity of presentation the pigment data will be shown as total chlorin (the sum of chlorophyll and degradation products), and diatom-derived pigment (the sum of fucoxanthin, diadinoxanthin, and diatoxanthin). Because pigments are inherently unstable and are thus unlikely to survive transport from the landscape, they primarily reflect a within-lake source and represent aquatic productivity; this was confirmed by analyses of Icelandic soils and detrital leaves, which yielded only small concentrations of intact pigments (primarily degraded chlorins and lutein). Different climatic conditions may favor different algal groups through direct temperature influence, alteration of the duration of ice-free conditions, wind mixing, nutrient availability, and pH (Florian et al. 2015).

In Bæjarvötn, pigments show two periods of elevated inferred aquatic productivity based on total chlorins. The first interval is centered around 300 AD and the second ranges from ~950-1350 AD, potentially representing longer open-water season during the Medieval Warm Period (MWP). Between these intervals of high aquatic productivity is a slight decrease that could be associated with the Dark Ages Cold Period (DACP). After 1400 AD, coincident with regional intensification of LIA cooling, pigment concentration sharply decreases at a similar time as the major shift in organic matter source (Fig. 3.5). This is interpreted to be caused by a combination of decreasing aquatic productivity and the change in organic matter source. Pigment concentrations are normalized to TOC and a transition from pigment-rich aquatic material to

pigment-poor soil will appear as a reduction in total pigment concentration. Diatom carotenoid concentration shows a similar pattern as total chlorins, with a peak from 300-500 AD followed by a sharp trough between ~700 and 800 AD. This first decrease in diatom pigment likely represents the intensification of late Holocene cooling during the DACP. The highest diatom pigment concentration occurs between 1100 and 1300 AD, after which values decrease to a minimum value at 1700, broadly coincident with peak LIA conditions.

The BSi record also shows several strong negative departures at 300-500 AD, 900-1100 AD, and 1400-1500 AD (Fig. 3.5). The declines beginning at 300 and 1400 are associated with increases in C:N and decreases in $\partial^{13}C$, implying increased terrestrial organic matter washing into the lake at these times. This suggests that these were either cold intervals which lead to landscape destabilization, or that the BSi was diluted by a short-term influx of allochthonous material. This is difficult to test as the resolution of the age model does not allow accurate calculation of decadal-scale changes in sedimentation rate and associated BSi dilution. Regardless of the exact mechanism leading to the negative departures in the biogenic silica record, these suggest that there was a transition towards cooling temperatures at Baejarvotn before 900 AD. The diatom pigment record and BSi are not as well correlated as would be expected. Normalization of the pigments to organic carbon could reduce the influence of dilution by terrestrial organic matter. Algal pigment production is not constant and can change based on environmental conditions, such as light and nutrient availability (Goericke and Montoya 1998). Changing environmental conditions could potentially alter the amount of pigment produced by an algal community

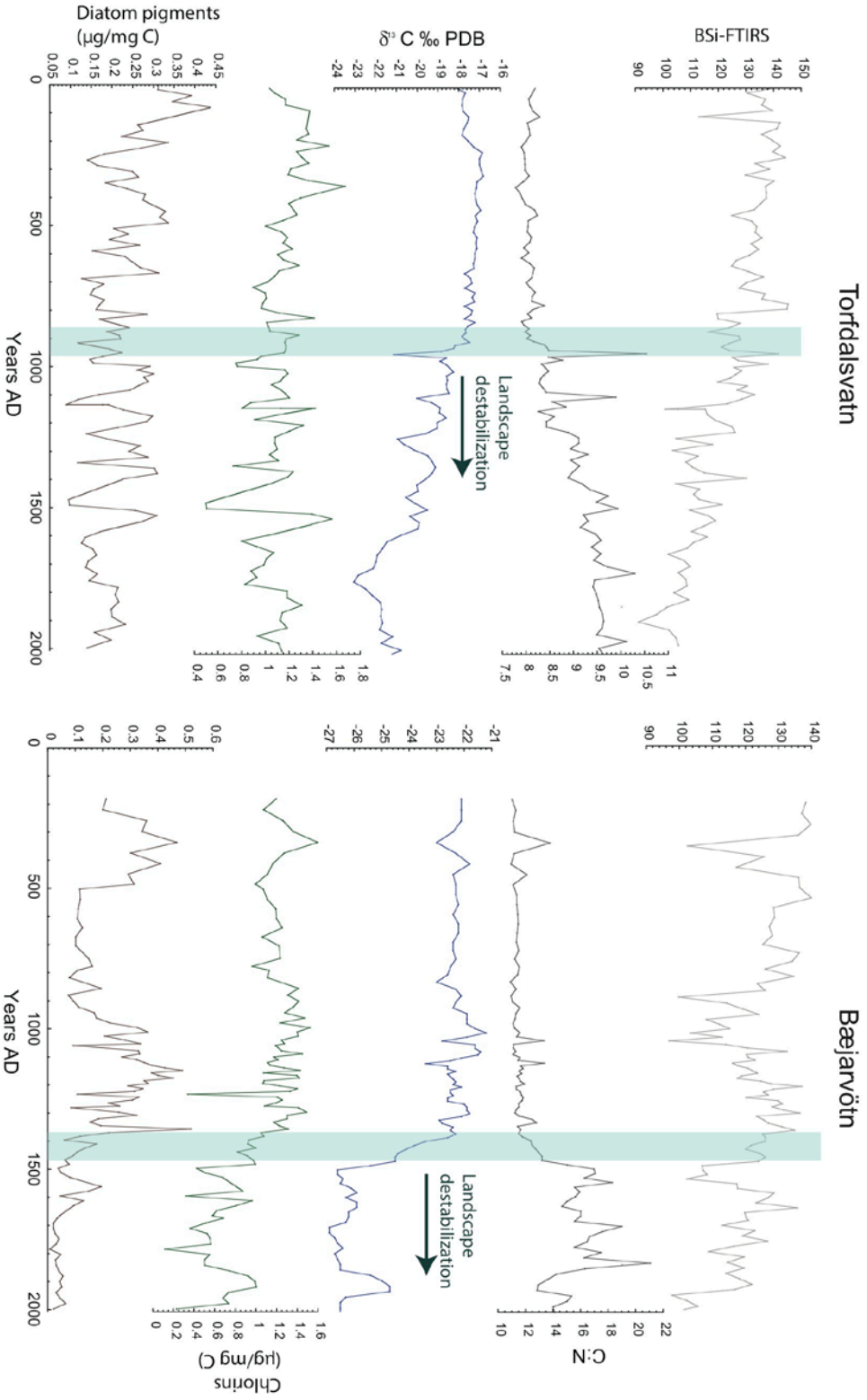

Figure 3.5. Biogenic silica, C:N, carbon isotopes, and pigment proxies from each core. Shading represents the onset of increased input of terrestrial organic matter.

of constant size, thereby changing the relationship between BSi and diatom pigment. Variable preservation of either diatom frustules or pigments in the sediment could also lead to a divergence in the proxy curves; however, this is not supported by any obvious changes in sediment character that would imply changes in redox conditions or depositional environment.

The pigment record from Torfdalsvatn shows less overall change (Fig. 3.5). Chlorin concentration, while showing short-term changes, is only slightly decreasing through time. This is consistent with what is expected from both decreasing total watershed productivity with cooling temperatures and dilution from pigment-poor terrestrial organic matter. Diatom pigments also show a subtle first-order decline, steepest between 0 and 1000 AD. The lack of significant changes in pigment abundance and composition in the last 2ka at Torfdalsvatn suggest that in this interval, aquatic productivity was relatively stable, responding to long-term cooling but not rapid climate change events.

BSi also shows a first-order decrease through the Torfdalsvatn record, exhibiting a greater overall change than the pigments (Fig. 3.5). As at Bæjarvötn there is an imperfect correspondence between diatom pigments and BSi, although they are more similar in this record than at Bæjarvötn. Dilution of the BSi by increased minerogenic and diatom-free terrestrial organic matter may play a stronger role at this site; however, the decrease in diatom abundance begins before the increase in organic matter, suggesting climate sensitivity at a time when the terrestrial biomass was still resilient to change. A change in diatom species assemblage in response to changing environmental conditions could also lead to decreasing abundance of biogenic silica if the assemblage shifts to a more lightly silicified species.

3.5. MECHANISMS DRIVING PROXY RESPONSE AT EACH SITE

The most notable feature of the 2 ka proxy records from Bæjarvötn and Torfdalsvatn is the increase in terrestrial organic matter entering the lake sediment after ~900 AD at Torfdalsvatn and ~1400 AD at Bæjarvötn shown by increasing sedimentary C:N and decreasing $\partial^{13}C$ (Fig. 5). While this same overall trend is seen at each site, we assume differences in timing and magnitude of this change are not related to differences in climate history between the sites, given their proximity and the tight correlation of their modern weather. Additionally, there is greater variability in pigment-inferred algal assemblages at Bæjarvötn compared to Torfdalsvatn. These differences in the proxy records can be explained by examining catchment-specific responses to late Holocene cooling, different biogeochemical status, and potential human disturbance of the landscape.

3.5.1 Climate sensitivity of soils and vegetation of Iceland

Increased input of terrestrial organic matter has been variably interpreted by many studies of Icelandic sediment cores as a proxy for local landscape destabilization and subsequent erosion due to deteriorating climate (Geirsdóttir et al. 2009) or as a result of clearing of Birch forests and development of agriculture by settlers after ~870 AD (Arnalds, 1987; Kristinsson 1995). Soils of Iceland are primarily volcanic andosols and are particularly susceptible to erosion due to their physical properties. There is widespread evidence of massive erosion of soils across Iceland during the last thousand years. This has been typically attributed to human activity (Arnalds 2015), but some lake records suggest that the onset of environmental change predated the settlement (Andrews et al. 2001; Geirsdóttir et al. 2009b). Historical accounts and pollen records

(Rundgren 1998; Hallsdóttir 1995; Hallsdóttir and Caseldine 2005; Eddudóttir et al. 2015) suggest that a large area of Iceland was covered by birch (*Betula*) forests prior to human settlement, which have since disappeared. It is known that settlers rapidly deforested the landscape for fuel wood (Thorarinsson 1974); however, some pollen records suggest that *Betula* was already in decline prior to the settlement (Andrews et al. 2001). In a century-long dendroclimatological study, Levanic and Eggertsson (2008) found that birch growth in north Iceland is negatively affected by dry winters and below average summer temperatures; these environmental conditions likely characterized the LIA. The late Holocene vegetation changes and soil erosion are likely due to a sum of these factors, and climate-induced reduction in woodland health due to decreased temperatures and possibly increasing aridity prior to settlement may have predisposed the landscape to disturbance from human settlement. Tephra deposition is also a mechanism for causing landscape destabilization and in wash of terrestrial material has been observed after eruptions in Icelandic lake records through the Holocene (Larsen et al. 2012; Blair et al. 2015). Frequent eruptions in the last 1.5 ka (Gudmundsdóttir et al. 2012; Larsen et al. 2014) most likely also contributed to degradation of terrestrial environments amplifying or predisposing the landscape to the impacts of cooling climate and anthropogenic disturbance.

Because andosols have little cohesion, once vegetation is removed due to an initial disturbance, the exposed soil is highly susceptible to rapid erosion and undercutting (Arnalds 2000). Subsequent collapse of the formerly stable land surface render these landscapes susceptible to threshold behavior, in which tipping point sensitivities may be dependent on watershed-specific factors, such as the resilience of local vegetation and steepness of the landscape. Andosols have a high capacity for storage of organic carbon of terrestrial origin

(Arnalds 2013), which is transported along with the minerogenic soil component during erosion. Both the minerogenic and organic components of the soil are deposited in lake sediment archives and this organic matter is chemically distinct from that produced within the lake (Meyers and Ishiwarti 1993; Meyers 1994). This allows the proportion of terrigenous organic matter contained in lake sediment to be used as a proxy for past erosion of soils (Noël et al. 2001; Geirsdóttir et al. 2009b).

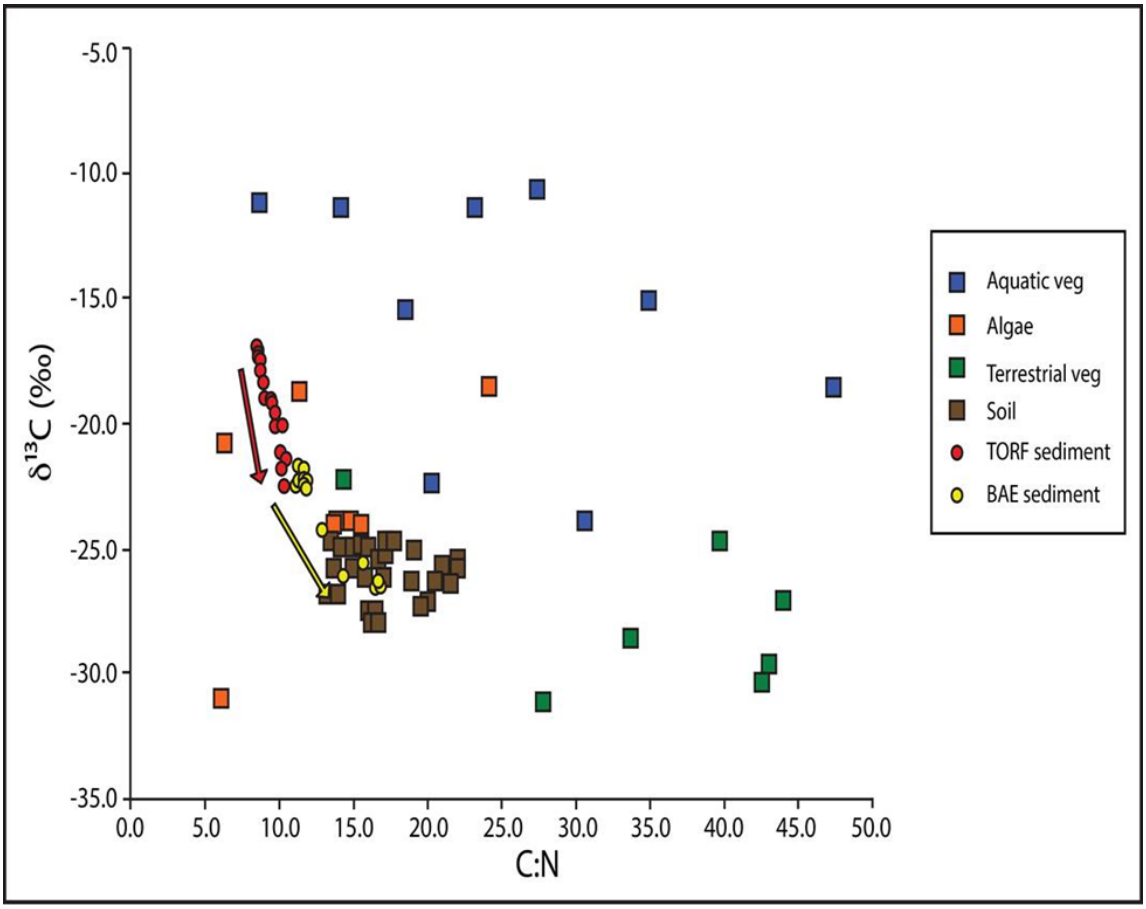

Figure 3.6. Carbon isotopes and C:N of modern samples from northwest Iceland of each major organic matter source. Circles represent lake sediment samples from each core, with arrows showing the increasing input of soil to the lake sediment through time.

The input of terrestrial material to a lake is in part controlled by climate (through terrestrial productivity, precipitation amount, weathering rates, etc.), but is also highly dependent

on catchment relief and vegetation cover (Rubensdotter and Rosqvist, 2003; Petterson et al., 2010; Anderson et al., 2012). Soil erosion in this region is likely driven by both aeolian and overland flow processes (Arnalds 2015). Wind, although relatively more important at Torfdalsvatn where there is less precipitation, likely impacts both catchments similarly, but catchment morphology is a primary control on overland flow erosion. Given that a significant amount of terrestrial erosion occurs via overland flow from rainfall and snowmelt, the non-climatic factors that influence overland flow sediment transport must be examined. Due to the higher precipitation near Bæjarvötn, overland flow processes may have a greater influence on erosion occurring in the Bæjarvötn catchment. Freeze-thaw processes and solifluction are common in northern Iceland, and were especially prevalent during colder intervals such as the LIA (Veit et al. 2011). Soil erosion occurs when the bed shear stress (τ) resulting from laminar flow exceeds some critical value, termed the critical shear stress (τ_c; Julien and Simons, 1985). Bed shear stress is defined as

$$\tau = \rho g h S$$

where ρ is the density of water, g is gravitational acceleration, h is the height of the flow, and S is the slope of the flow. Because shear stress is directly proportional to slope, a steeper catchment is more likely to meet the condition of $\tau > \tau_c$ and thus experience soil erosion given the same intensity of rainfall or snowmelt. We calculated the slope of each grid cell in a 50-m digital elevation model of each lake catchment to determine the relative relief of each site (Fig. 3.6). The median slope of Bæjarvötn is 1.9º, while the median slope at Torfdalsvatn is 1.1º, 42% less steep overall. The Bæjarvötn catchment is also characterized by steeper terrain directly adjacent to the lake (Fig. 3.7), which likely plays an important role in determining the efficiency with which eroded soil is deposited in the lake basin. Erosion due to freeze-thaw processes, which are

not accounted for in the above equation, is assumed to be directly proportional to precipitation and slope, both of which are higher at Bæjarvötn. This difference in catchment relief may in part explain the greater magnitude, and stepwise proxy response at Bæjarvötn (Fig. 3.5), which points to increased soil input during LIA cooling (Fig. 3.6).

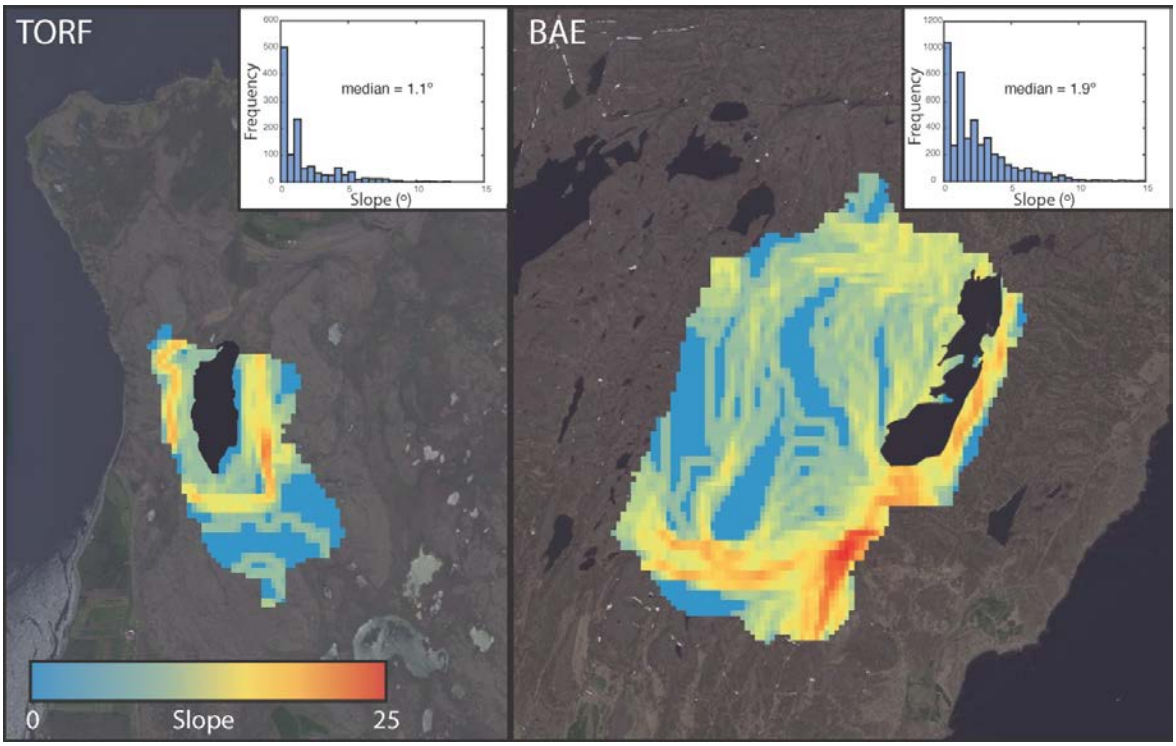

Figure 3.7. Slope calculated from a 50 m digital elevation model for each watershed. The number of pixels representing each slope value is shown in the insets. The Torfdalsvatn catchment has a lower median steepness, with the majority of the area having a slope of less than 2º.

3.5.2. Algal response to environmental change

Proxies of past aquatic productivity are complementary indicators of climatic conditions, serving as independent recorders of past conditions when used along with landscape stability proxies. Aquatic productivity can be reconstructed and characterized in two ways: through the total magnitude of productivity, and through the assemblage of primary producers occurring in

the lake. The total magnitude of aquatic productivity is determined by a combination of the length of growing season and the availability of light, a carbon source, and nutrients. Because length of the ice-free season and the degree of thermal stratification exert significant control on aquatic productivity, aquatic communities are sensitive to changes in summer temperatures (Smol et al. 2005). The exact response of lacustrine biological communities to warmer summers is not linear in all environments and can vary based on what the controlling environmental variable at each location is (Adrian et al. 2009). Algal microfossil abundance, measured as the amount of primarily diatom-derived biogenic silica (Conley and Schelske 2002), has been shown to covary with regional temperature records at decadal timescales (Blaas et al. 2007; McKay et al. 2008). Biogenic silica, however, only records one portion of total lacustrine primary productivity, and other methods such as analysis of sedimentary algal pigments can be employed to gain a more comprehensive understanding of changes in aquatic primary productivity through time. Lake sediment contains both universally-produced pigments (by all algae and higher plants), such as chlorophyll *a*, along with algal group specific xanthophyll carotenoids, which serve as biomarker molecules of algal type and overall abundance. The concentration of chlorin (all chlorophylls and their degradation products) has been employed as a total productivity measure while individual diagnostic carotenoids are used as a way to reconstruct past abundance of various algal groups, whose prevalence is potentially linked to certain climate states.

Nutrients are a predominant control on the overall nature and magnitude of primary productivity. The availability of phosphorous is often correlated to phytoplankton abundance, as it is the limiting nutrient in many lacustrine environments. Ratios of major nutrients are a control on abundances of major algal groups, with nitrogen-fixing cyanobacteria more likely to have a competitive advantage in lakes with TN:TP ratio below 30 (Pick and Lean 1987).

Seasonal succession of algal groups typically begins with a diatom bloom in the spring, followed by cyanobacteria and chlorophytes in the summer and fall (Lin 1972), although other studies have shown that this progression may be regionally variable (Zhang and Prepas 1996). Short summers associated with cold climate intervals may not allow for this complete succession, therefore making late-succession algal groups (cyanobacteria and chlorophytes) stronger climate indicators. Longer, warmer summers increase lake stratification, which changes nutrient dynamics and reduces bottom water oxygen concentration.–Warmer summers also result in increased weathering of bedrock and increased leaching of soil nutrients (Adrian et al. 2009). Both of these factors should lead to increased availability of nutrients during warm times, allowing for higher productivity.

Differences in nutrient availability between the lakes may play a large role in algal groups varying response to past climate events. Torfdalsvatn is phosphorus limited (TN:TP 43.5, well above the Redfield ratio of 16:1; Table 3.1) and therefore likely has a relatively sparse phytoplankton community and is rich in aquatic macrophytes (Sondergaard 2007). If algal communities are strongly phosphorus limited, temperature response may be muted because populations run out of nutrients before the end of the ice-free season. The aquatic macrophytes that thrive in P-limited environments are also poor climate indicators because they are able to maintain their biomass through the winter, therefore maintaining a more stable population through time. Bæjarvötn, which is more N-limited (TN:TP 10.7, which is below, but closer to Redfield ratio values), is likely to contain a greater algal biomass which is not as severely nutrient limited as a Torfdalsvatn. This may allow temperature to influence algal communities and abundance to a greater degree. Differences in lake morphology help to explain the difference in nutrient status between the two sites. The primary source of phosphorous to the water column

is from the sediment. Deeper lakes like Bæjarvötn are more stratified more of the time, allowing accumulation of phosphorous in the bottom waters where it is out of the photic zone and inaccessible to primary producers. Well-mixed, shallow lakes like Torfdalsvatn will not have this period of re-accumulation to reset their nutrient balances.

3.5.3. Human activity or climate?

One factor that may influence proxy response and is not well addressed by this study is the influence of human arrival in each watershed. While modern populations are very sparse locally, sheep are present at both sites and must have been brought there at some point between settlement and present day. The arrival of sheep and associated physical disturbance of grazing on the landscape, along with potential human-caused deforestation, is likely to influence what is seen in the sediment record. Without a proxy for anthropogenic activity, it is impossible to determine the exact sedimentary horizon where humans begin to alter the local biological system. Organic biomarker molecules specific to humans and livestock are a promising tool, making possible a watershed-scale history of anthropogenic impact and therefore deconvolving the human and climate signals (D'Anjou et al., 2012; Pansu et al. 2015).

3.6. CONCLUSIONS

Sediment core records from proximal Torfdalsvatn and Bæjarvötn provide the opportunity to examine how proxy records can potentially be influenced by differences in lake and catchment morphology—in this case a deep lake in a steep catchment versus a shallower lake in a catchment with low relief. Both records show general cooling over the last 2ka, in

agreement with other regional lake and marine core records, with peak cold conditions inferred from both records during the LIA. The contrasting sensitivity of algal groups to environmental change at each site suggests that biological thresholds in environmental tolerance were not crossed during the LIA at Torfdalsvatn, but were in Bæjarvötn, resulting in a marked increase in pigment-inferred productivity during the MWP relative to the DACP and the LIA.

As seen in other Icelandic lake sediment records, there is an increase in the proportion of terrestrial material entering the sediment of both lakes during the last 2 ka, representing the widespread late Holocene destabilization of soils (Fig. 3.6). We interpret the difference in timing of the destabilization between sites to reflect threshold-type response of the steep catchment at Bæjarvötn to late Holocene cooling as opposed to the more gradual response of lesser magnitude at Torfdalsvatn (Fig. 3.5, Fig. 3.7). Additionally, freeze-thaw processes may be a significant driver of the nature of soil erosion at Bæjarvötn, as this site has significantly higher precipitation than Torfdalsvatn. This highlights the potential for differences in apparent climate reconstructions from various sites due to catchment-specific processes. Both sites give climatic information but must be interpreted within the context of their specific catchment and lake morphologies. The organic matter proxies at Bæjarvötn do not consistently reflect climate changes linearly. Minor fluctuations begin in all proxies before 900 AD, but this early variability is followed by the simultaneous and permanent shift in proxies that occurs at ~1450 AD likely reflects a significant climate change toward colder temperatures. The signal was insensitive to climate events before the threshold response, then nearly saturated afterward, with a sediment C:N and $\delta^{13}C$ indistinguishable from the soils of the catchment (Fig. 6). Algal pigments and BSi at Bæjarvötn show similar response to changes at the site and allow for the development of a continuous local record of aquatic productivity. The Torfdalsvatn record of terrestrial

destabilization is much more gradual, beginning in ~900 AD and indicating a lower overall magnitude of change. The aquatic proxies show less change through time, and there appears to be little climate sensitivity of algal assemblages over the late Holocene. This suggests that while overall aquatic productivity declined due to cooling, algal assemblages were controlled by other factors such as nutrient dynamics.

When selecting lakes as study sites for past climate change, it should be considered that steep catchments are potentially more likely to exhibit threshold behavior, but may give a larger overall signal than lakes with a gradual catchment. Shallower, warmer lakes may require a greater climate shift to change the assemblage of aquatic primary producers. Because of this, proxies such as sedimentary algal pigments may be more successful in colder environments, as these colder environments will have greater variability in length of ice-free conditions between warm and cold times. Biogeochemical proxies are inherently sensitive to complex landscape processes—which may have variable response to changing climate between locations. Additionally, human activity often completely restructures multiple aspects of watershed biogeochemistry, overprinting the proxy record. Even in Iceland, where there are excellent records of settlement history, the precise timing and magnitude of human influence is difficult to determine. Future studies will employ biomarker molecules to better quantify past human influence on sediment records. Additionally, quantitative temperature proxies not subject to catchment-specific factors will be the focus of future Icelandic terrestrial climate reconstructions.

3.7. DISCUSSION OF NITROGEN ISOTOPES IN MODERN SAMPLES OMITTED FROM THE PUBLICATION (Data in Appendix A)

Nitrogen isotopic composition of algal material ranges from -1.6 to 4.4‰, with an average value of 0.7‰. The range of values could be due to different overall catchment DIN values between sites as a result of differences in nitrogen fixation or nutrient limitation. The 4.4‰ sample could also be potentiality contaminated by invertebrate heterotroph material, which is consistently more enriched than algae.

Nitrogen isotopes of aquatic macrophyte plants are the most depleted of all sources measured, with an average value of -3.8‰ and a range of -15.5 to +3.2‰. These values fall in the expected range due to the greater availability of isotopically lighter ammonium in sediments, and the ability of rooted macrophytes to access a larger sedimentary nitrogen pool and more effectively discriminate against heavy isotopes (Barko et al. 1991; Talbot 2001).

Soil ∂^{15}N averages 1.8‰, ranging from a high value of 4.9‰ and a low of -1.6‰. Soil nitrogen isotope abundance is controlled the balance of N-fixation and atmospheric deposition (N-inputs), with losses from microbial metabolism (denitrification), plant uptake, and leaching. The compilation of global soil nitrogen isotope values by Amundson et al. (2003) shows a trend toward lower ∂^{15}N with increasing latitude, as a result of the strong temperature and moisture dependence of processes controlling the soil nitrogen cycle. The measured values from this study are in good agreement, although slightly lighter, than the estimated range for Icelandic soils of 2.1-4.8‰ from Amundson et al. (2003). As a result of the influence of temperature and precipitation on soil ∂^{15}N, the isotopic composition of Icelandic soil may have changed with Holocene climate variability.

CHAPTER 4

A 12 ka record of aquatic productivity and landscape stability from Torfdalsvatn, North Iceland

Christopher Florian[1,2], Gifford Miller[1,2], Áslaug Geirsdóttir[2]

[1] Institute of Arctic and Alpine Research and Department of Geological Sciences, University of Colorado, Boulder, CO 80309-0450, USA

[2] Department of Earth Sciences, University of Iceland, Sturlugata 7, Reykjavík 101, Iceland

4.1. ABSTRACT

Icelandic climate is controlled by processes that are globally significant. Biological communities are directly affected by changes in climate; therefore the regional climate history can be inferred by examining evidence of past biogeochemical change preserved in lake sediment. Building on past studies at the site, we develop a high-resolution, multiproxy lake record of Torfdalsvatn, North Iceland. The proxies used in this study provide a history of landscape stability along with the magnitude and characteristics of past aquatic productivity. This study is the first to generate a complete Holocene record of sedimentary algal pigments from an Icelandic lake. Prior to the Saksunarvatn tephra, most proxies reflect the establishment of a Holocene-like environment. The Holocene Thermal Maximum is evident after 8 ka, characterized by increased cyanobacterial abundance and denitrification which occur as a result of longer ice-free season, lower wind stress, and greater aquatic productivity. Soil stability lags regional peak warmth, with proxies for erosion reaching the lowest Holocene values after 6ka. C:N reflects increasing input of terrestrial organic matter after 4.5 ka with the onset of late Holocene cooling. A transition to increased erosion after 1.8 ka indicates landscape

destabilization as a result of cooling temperatures, which occurs in two steps. An increase in minerogenic material, likely due to increased Aeolian transport, precedes an abrupt increase in terrestrial organic matter derived from the destabilization of soils. Aquatic productivity also declines at this time, with peak erosion and lowest productivity occurring during Little Ice Age (ca. 1250-1850 AD/CE). Diatom and green algal pigments do not track regional climate events, therefore other factors such as nutrient availability may control the relative abundance of these groups. The cyanobacterial pigment record, however, corresponds well to sea surface temperatures from MD99-2275 and nearby lake sediment records, suggesting temperature sensitivity of cyanobacterial populations. Because of this, algal pigments may become an important part of Icelandic paleoclimate studies. Additionally, this study suggests that future warming may lead to an increase in cyanobacterial populations in Icelandic lakes.

4.2. INTRODUCTION

A wealth of recent studies indicate North Atlantic Holocene climate evolution has been nonlinear, despite being controlled on millennial timescales by the long-term monotonic change in Northern Hemisphere summer insolation (Berger and Loutre 1991). Changes in complex regional oceanic and atmospheric circulations, as well as ice-albedo feedbacks, are a mechanism for these rapid, non-linear climate events (Mayewski et al. 2004; Wanner et al. 2011; Geirsdóttir et al. 2013). As the North Atlantic is the site of the largest equator to pole heat flux of the Northern Hemisphere (Wunsch 1980), and the location of deep water formation that drives the global Thermohaline Circulation, changes in local climate have widespread global influence (Denton and Broecker 2008). A better understanding of past changes in North Atlantic climate

history is vital to our understanding of how these global heat transport systems may respond to Anthropogenic warming and the potential for future rapid climate change events.

Iceland is located in a region of strong temperature gradients, from the warm Atlantic currents to the south to the cold, Arctic waters to the north (Einarsson 1984; Orvik and Niiler 2002; Rudels et al. 2002, 2005). Small changes in ocean and atmospheric dynamics can have a profound influence on local sea surface temperatures, which are a predominant control on terrestrial air temperatures. When reconstructing climate history, marine records are often limited by difficulty in developing accurate chronologies due to uncertainty of past reservoir age of dissolved carbon in ocean water (Reimer et al. 2002; Ascough et al. 2005). Complex stratification of ocean water also hinders proxy interpretations, as the water column source of the proxy must be well characterized, and a temperature change at one depth, while still giving important climatic information, may not be representative of boundary layer conditions. Lake sediment records provide an alternative continuous archive of past environmental change that directly reflects local air temperature due to smaller volume and less complex hydrology. In this study, we utilize a high-resolution lake sediment record from Torfdalsvatn to better constrain the Holocene climate history of north Iceland.

Biological primary productivity is a good indicator of paleoenvironmental conditions. This is especially true in high-latitude environments where the length of ice-free season determines the length of the growing season. Changes in climate will alter the length of ice-free season, which has direct and indirect implications on multiple aspects of catchment biogeochemistry (Smol and Cumming 2000; Wolfe 2002; Smol et al. 2005; Schindler and Smol 2006). Sedimentary algal pigments, primarily derived from within-lake algae and macrophyte plants, provide a record of past algal group assemblages (Leavitt and Hodgson 2001). Change in

algal group assemblages over time holds additional climate information that is not contained in records of total productivity, as changing environmental conditions alter the succession of algal types through the summer. In particular, it is hypothesized that algal groups such as green algae and cyanobacteria, that tend to dominate during warm conditions and the second half of the growing season, will be most sensitive to change (Lin 1972; Zhang and Prepas 1996; De Senerpont Domis et al. 2007). In addition to climate reconstruction, understanding the past nature of aquatic productivity is important in making predictions of how freshwater ecosystems may change with anthropogenic warming and nutrient inputs (Smol and Cumming 2000). The goal of this study is to develop an additional high-quality, multi-proxy, lake sediment record from north Iceland which incorporates algal pigments to track changes in the climate history and nature of aquatic productivity. This will fill in a spatial gap in Holocene terrestrial climate records from Iceland as well as test the how each organic matter proxy responds to climate variability at this site.

4.3. STUDY SITE

4.3.1. Geological setting

Torfdalsvatn (Figure 4.1, 6613.5670N, 20122.8150W) is a relatively small (0.4 km^2) and shallow (Z=5.8 m) lake on the Skagi peninsula of northern Iceland. It is located approximately 0.5 km from the modern coastline at 52 m a.s.l., just above the Holocene marine limit (Rundgren et al. 1997). Because of its temporally-long lacustrine sediment record, along with its proximity to marine core records and high sedimentation rate, Torfdalsvatn has been the site of several previous studies. These past studies examined tephrochronology, pollen assemblages (Bjorck et al. 1992; Rundgren 1995, 1998; Rundgren et al. 1997), chironomid inferred summer

temperatures (Axford et al. 2007), and isotopic composition of lake sediment and landscape plants (Wang and Wooller 2006; Axford et al. 2007).

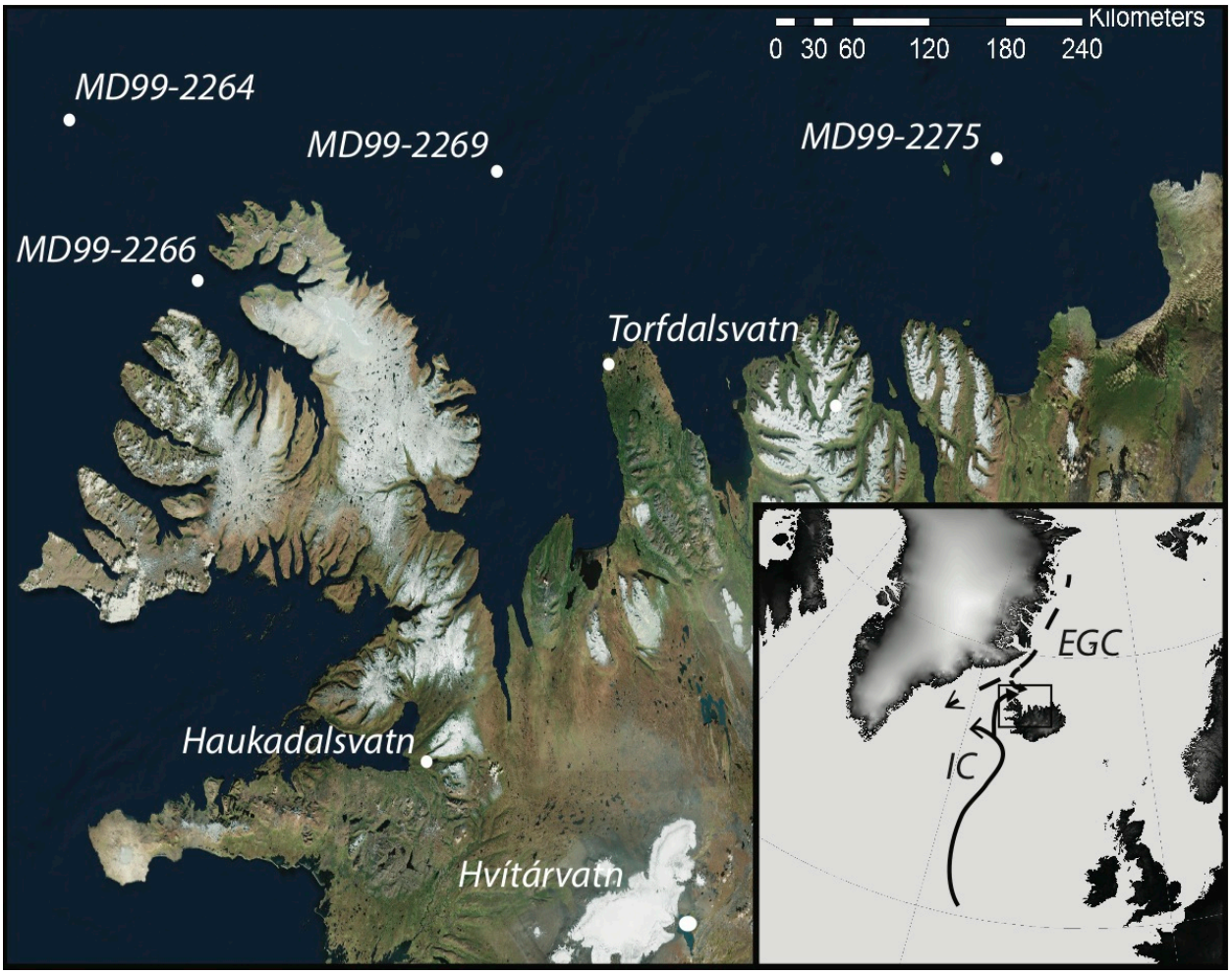

Figure 4.1. Map of Torfdalsvatn relative to other sediment records mentioned in the chapter. Approximate location of the cold East Green Current (EGC) and warm Irminger Current (IC) are marked with dashed and solid lines.

4.3.2. Controls on regional climate

Present day air temperature at Torfdalsvatn is strongly correlated to sea surface temperatures off the coast over the instrumental record (Fig. 4.2). Regional ocean temperatures are largely determined by the

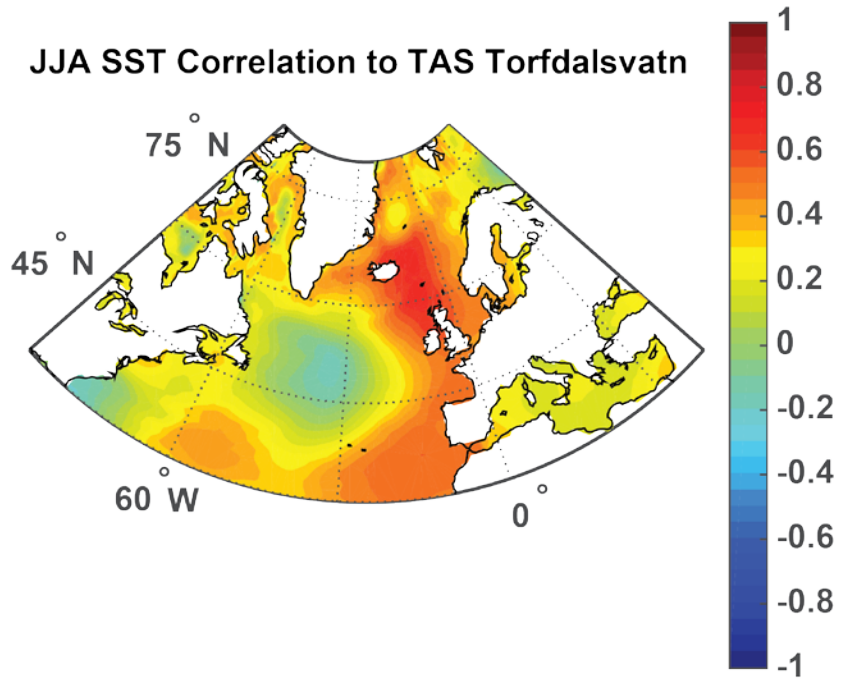

Figure 4.2. Co-variance of detrended summer (JJA average) 2-meter air temperature over Torfdalsvatn with JJA averaged sea-surface temperatures from 1950 to 2010. The figure was produced by Leif Anderson using Air temperature data from Legates and Willmott (1990) and SSTs from http://www.esrl.noaa.gov/psd/data/gridded/data.cobe.html. The strongest correlation of summer air temperature with SST occurs just east of Torfdalsvatn, near the marine sediment core MD99-2275. Therefore we compare the Torfdalsvatn record to reconstructed summer SSTs this core (Jiang et al. 2015) rather than the more proximal but less well-correlated MD99-2269.

relative dominance of the cold East Greenland Current (EGC) and the Warm Irminger Current (IC). The EGC is made up of cold Arctic Ocean water of relatively low salinity, and is the main conduit of polar waters and exported sea ice from the Arctic Ocean to the North Atlantic through the Fram Strait. Southward migration, or increases in the strength of the ECG, will lead to regional cooling and increased presence of sea ice off North Iceland (Moros et al. 2006). The IC is a branch of the North Atlantic Current, both of which comprise a significant proportion of oceanic poleward heat transport (Orvik and Niiler 2002). The IC splits from NAC at the North Atlantic Subpolar Gyre, and changes in the size and location of the gyre will change the

trajectory of the IC (Hátún et al. 2005). As the IC reaches Iceland, it branches to form the North Iceland Irminger Current (NIIC), which directly influences the north coast of Iceland (Stefansson 1962). The strength and northward extent of the IC is in part controlled by the vigor of the Atlantic Meridional Overturning Circulation (AMOC), which is a global-scale control on climate (Thornalley et al. 2009). North Iceland is the closest landmass to the interface of the IC and the EGC, therefore small changes in the strength and extent of these currents have a large influence over regional temperature; terrestrial records from North Iceland should reflect the oceanographic history of the region.

On shorter timescales, changes in atmospheric circulation patterns such as the North Atlantic Oscillation (NAO), which describes the pressure gradient between the Azores High and the Icelandic Low and subsequent northward or southward displacement of the westerlies (Hurrel 1995; Hurrel et al. 2003), can also lead to a change in predominant climate conditions over Iceland. While the NAO is always variable on inter-annual to decadal timescales, different extended mean states can occur, and have contributed to multi-centennial climate events such MWP and LIA (Trouet et al. 2009; Larsen et al. 2013). Long term positive or negative NAO states can influence ocean currents due to the variable trajectory of the westerlies, with an associated contraction or expansion of the North Atlantic Subpolar Gyre (Hátún et al. 2005; Lohmann et al. 2008), which in turn leads to variable extent and strength of the NIIC (Blindheim and Malmberg 2005; Miettinen et al. 2011).

4.4. MATERIALS AND METHODS

An 8.2-meter-long sediment core (TORF12-1A/2A-1N) was recovered in February 2012 using a hammer driven piston corer from the lake-ice platform. The entire sediment package was

recovered in two successive drives where re-entry of the previous coring hole was made possible by shallow water. The first drive was 2.6 meters and the second was 5.8 m, reaching dense, deglacial sediment. The two drives are assumed to be continuous, with no evidence of missing or reworked sediment. The core was then sub-sectioned in the field into 1.5-meter sections which were transported back to the University of Iceland and stored in a refrigerated cold room. The cores were then split, imaged, and measured for density and magnetic susceptibility by a GEOTEK (MSCL-S) core scanner. The core was sampled continuously at 2-cm-resolution and the subsamples were placed in pre-combusted glass vials, which were freeze-dried for geochemical analysis and frozen under nitrogen for algal pigment analysis.

A chronology for this core was developed using tephra and radiocarbon dating of aquatic macrofossils (Table 4.1). Only identifiably aquatic macrofossils were used to avoid the potential age offsets that can occur from long residence time of terrestrial organic matter and humic acids, resulting in dates that are too old for their stratigraphic position (e.g. Geirsdóttir et al. 2009b). Tephras were identified visibly and geochemically by comparing with those from other nearby Icelandic sites. The age control points were entered into the CLAM software (Blaauw 2010), where radiocarbon ages were calibrated using the IntCal13 calibration curve (Reimer et al. 2013). An age-depth model was also developed in CLAM using a smoothing spline, where the sediment contribution of visible tephras was removed by assigning values of equal age over intervals with thick, visible ash layers.

Core	Depth (cm)	Material	^{14}C age (years BP)	Age Range (cal years BP)	AMS result number
TORF12-1A	17	Hekla 1766 AD*		184±2	
TORF12-1A	66	Hekla 1300 AD*		650±5	
TORF12-1A	84	Hekla 1104 AD		846±5	
TORF12-1A	125	Settlement tephra*		1079±10	
TORF12-1A	148	Macrofossil	1390 ± 15	1286-1331	CURL-15806
TORF12-1A	346	Macrofossil	3305 ± 15	3476-3570	CURL-15814
TORF12-2A	391	Hekla 4		4198-4317	
TORF12-2A	489.5	Macrofossil	4785 ± 20	5474-5588	CURL-15812
TORF12-2A	557	TV-5 tephra		6502-6697	
TORF12-2A	642	Macrofossil	6660±20	7499-7578	CURL-15794
TORF12-2A	754	Saksunarvatn tephra		10251-10348	

Table 4.1. Age control points used to develop an age-depth model for the TORF12-1A/2A core. Pre-historical tephra ages from Björck et al. (1992), Dugmore et al. 1995 and Rasmussen et al. (2006) Tephras marked with an * have been visually identified.

4.4.1. Sediment isotope geochemistry

Sub-samples of carbon and nitrogen isotopes and elemental ratios were measured at the Carnegie Geophysical Laboratory using a Finnigan Delta V isotope ratio mass spectrometer with a CE NC 2500 Elemental Analyzer. Isotopic ratios were corrected for drift using an acetanilide standard and are reported in standard delta notation relative to the standards V-PDB for carbon and Air for nitrogen. Duplicate analyses show a precision of less than 0.2‰ for each isotope ratio.

4.4.2. Algal pigments (Methodology is identical to that reported in Chapter 3 and is repeated here for completeness)

Algal pigments were solvent extracted from freeze dried sediment samples using 6 ml of 80:20 mixture of acetone:methanol overnight in amber vials under N2 at -10°C. Samples were touch mixed and sonicated to disperse sediment and increase extraction efficiency, then filtered

through a 0.2 µm PTFE syringe filter which was then rinsed with 2 ml of acetone to recover sample residue from the filter. The extract was then dried down and rehydrated with a known volume of acetone containing a known concentration of α-tocopherol standard. Samples were placed in the refrigerated autosampler of an Agilent 1200 series HPLC and derivitized to improve chromatographic behavior immediately prior to injection with an equal volume of 28 mM tetrabutyl ammonium acetate in water. A binary mobile phase system was used with solvent A composed of a 70:30 mixture of methanol:28 mM tetrabutyl ammonium acetate in water and solvent B composed of pure methanol at a flow rate of 1 mL min-1. An Agilent Eclipse XDB-C8 4.6 x 150mm column was used to separate pigments whose absorbance of visible light was detected by an Agilent Diode Array Detector (DAD) scanning between 400 and 750 nm. Pigments were identified by comparing characteristic absorbance spectra with that stored in a library created from a suite of standards obtained from DHI Denmark.

4.4.3. FTIRS-Inferred biogenic silica (Methodology is identical to that reported in Chapter 3 and is repeated here for completeness)

Subsamples of freeze-dried sediment were weighed and mixed with potassium bromide at a ratio of 0.02 to disperse and reduce the IR absorbance of the sample. The sediment and KBr mixture was then ground to a fine powder using a mortar and pestle, and analyzed by diffuse reflectance FTIRS by a Bruker Vertex 70 with a Praying Mantis diffuse reflectivity accessory (Harrick). Samples were scanned 64 times at 4 cm^{-1} resolution over wavelengths ranging from 3750 to 450 cm^{-1}. Baseline shifts were removed by applying a linear baseline correction in the Opus software. Area under the absorbance curve was then integrated from 1000 to 1250 cm^{-1}, the region with the strongest correlation to biogenic silica (Meyer-Jacob et al. 2014). The measured

values are expressed in FTIR absorbance rather than mass (BSi) in order to avoid error associated with the calibration. Published calibrations are linear, and therefore the calibration does not change the structure of the proxy curve derived from the measurements.

4.5. RESULTS AND DISCUSSION

4.5.1. Chronology

The age-depth model for TORF12-1A/2A core integrates four radiocarbon dates and eight geochemically and/or visibly identified tephra layers (Fig. 4.3). The tephra and radiocarbon derived age control points agree without significant offset. Despite the assumed presence of unconsolidated minerogenic material upon deglaciation, sedimentation rates prior to the Saksunarvatn tephra are the lowest of the record. This may indicate very short ice-free season for at least some of this time, which would reduce import of material to the lake as well as limit productivity. Sedimentation rates steadily increase from ~10 to ~7 ka, associated with an increase in organic matter content, suggesting that material derived from aquatic productivity is a major contributor to the sediment at Torfdalsvatn. The age-depth relationship remains nearly linear for the remainder of the record, supported by all subsequent age control points. The lack of variability in sedimentation rate leads to relatively low age uncertainties for the most recent 7 ka of the record.

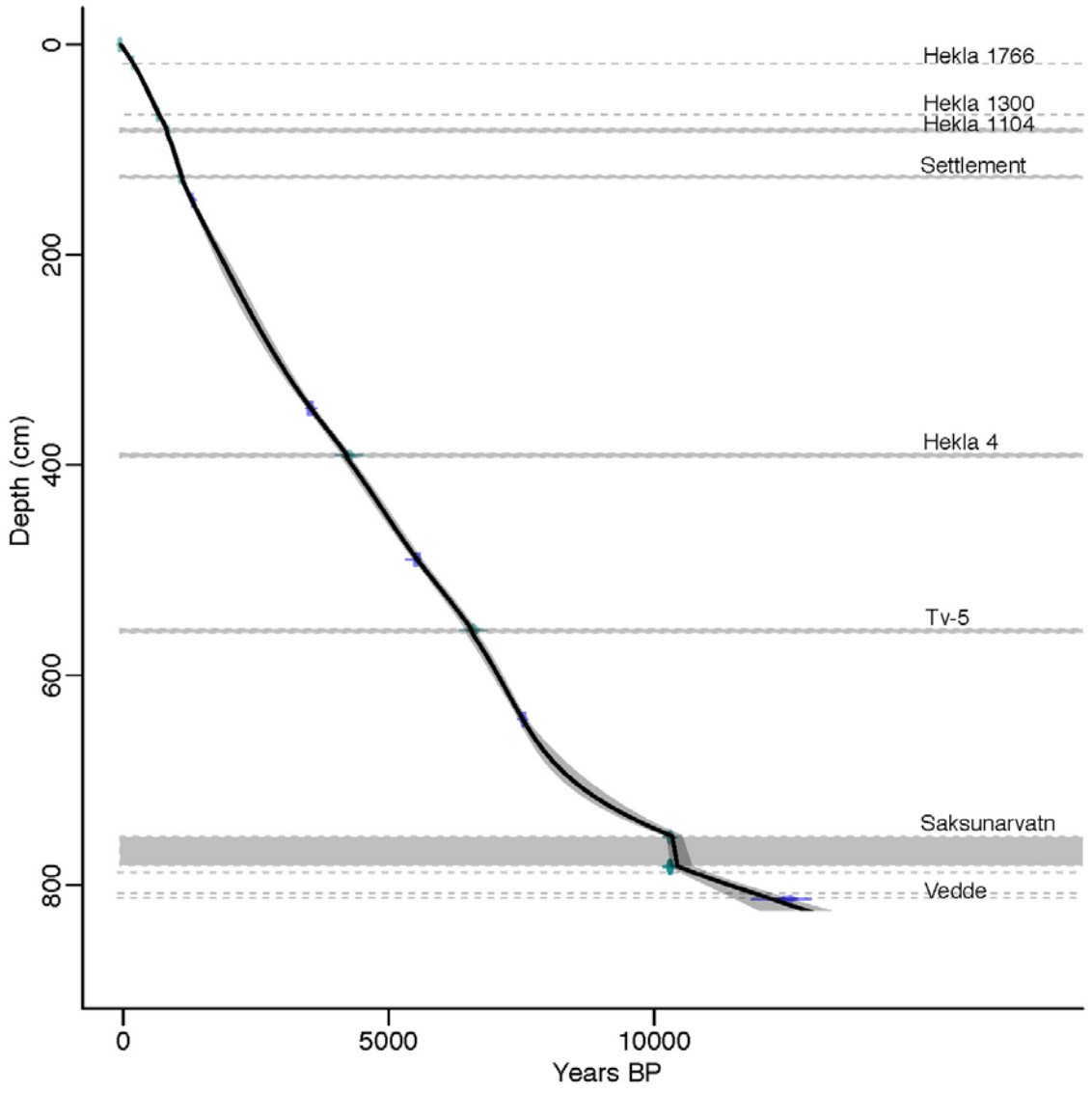

Figure 4.3. Age-depth model of the TORF12-1A/2A core, grey shading represents tephra horizons over which an equivalent age has been assigned

4.5.2 Landscape stability record

A record of past landscape stability and erosion can be developed by comparing proxies for minerogenic flux (magnetic susceptibility) and terrestrial versus aquatic organic matter source (C:N). The controlling factors on the quantity of magnetic material that enters the lake are

the amount fine-grained inorganic material available (from receding glaciers or tephra deposition), how well stabilized this material is by vegetation, and the strength of a transport mechanism (erosion by wind or water). Organic matter source can be easily distinguished as either terrestrial or aquatic by carbon to nitrogen ratio and isotopic composition (Meyers and Teranes 2001). This reflects the relative biomass in each environment, as well as efficiency of the transport of stored terrestrial material by soil erosion, which in Iceland, is easily accomplished by both wind and water due to the lack of cohesion of andosol soil (Arnalds 2015). An increase in magnetic material without associated increase in C:N represents either an increase in available source material (such as tephra), stable terrestrial vegetation that is resistant to wind, or a relatively small carbon-producing biomass that reduces dilution of minerogenic material.

Shortly after deglaciation there was abundant, easily erodible material deposited by the receding Pleistocene glaciers. Terrestrial vegetation cover had not yet developed, and this interval is characterized by the highest values of MS seen in the record (Figure 4.4). MS decreases as the quantity of easily erodible material was depleted and vegetation cover began to develop. The pollen record from Torfdalsvatn indicates that the first pioneer grass and herb species were present in the catchment as early as ~13ka, with dwarf shrubs appearing at approximately 12.7 BP, likely associated with Bølling-Allerød warmth (Rundgren 1995). Although Rundgren (1995) sees a decrease in shrubs during the Younger Dryas at Torfdalsvatn, the MS continues to decrease along with increasing

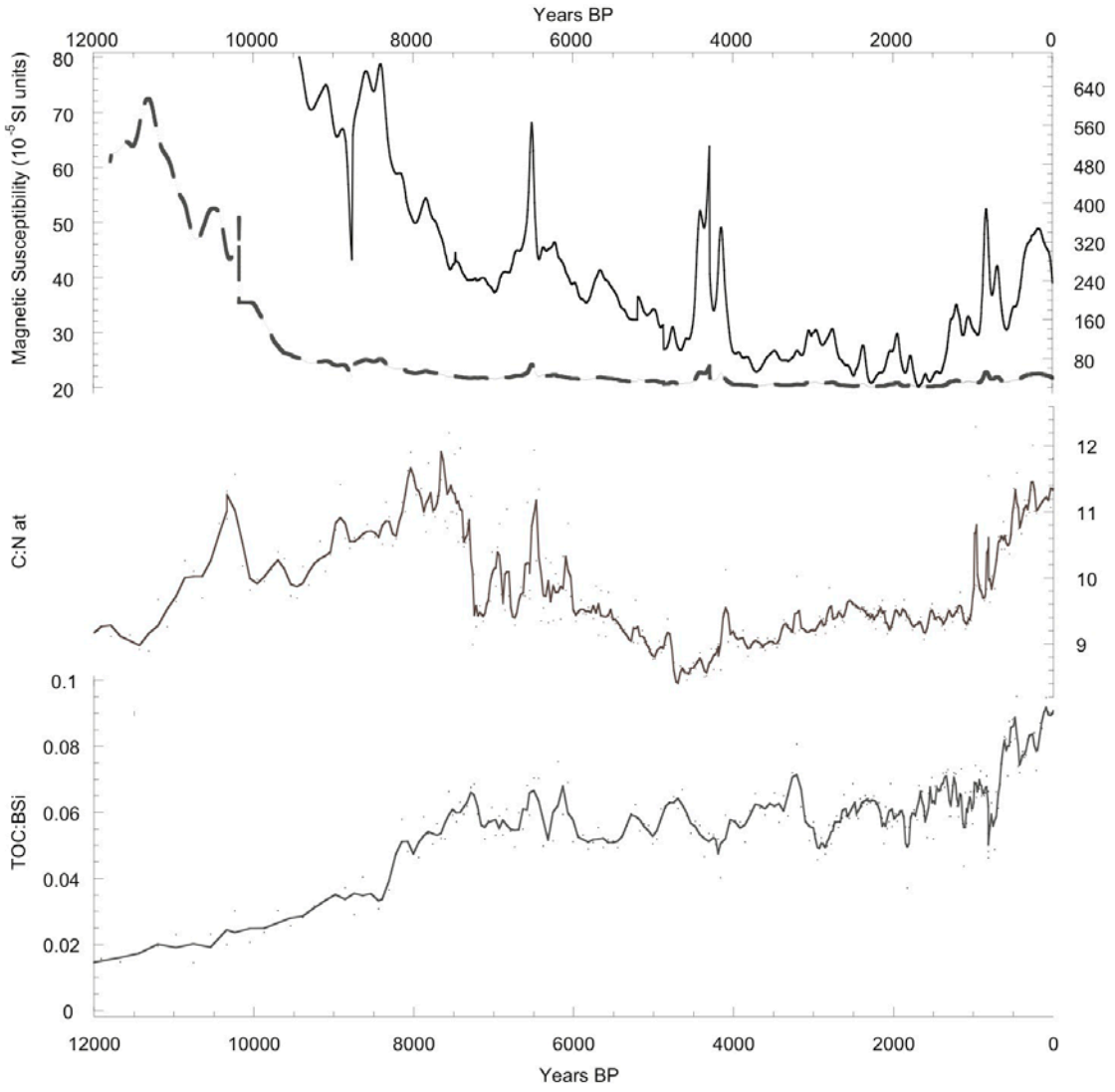

Figure 4.4. Proxies reflecting organic matter source and catchment erosion, elevated values in each proxy indicate a greater flux of allochthonous material to the lake sediment.

C:N, indicating further development of terrestrial biomass and stability of catchment soils. MS sharply increases at ~10.3 ka associated with the Saksunarvatn tephra, decreases rapidly until ~7 ka, and more gradually until 2 ka when the lowest MS values occur (Fig. 4.4). Spikes of MS through the mid Holocene represent major tephra horizons, and therefore are not interpreted to be related to climate-induced landscape change.

The ratio of BSi to TOC is a relative measure of proportion of aquatic to overall watershed productivity (Fig. 4.5). As expected in the earliest part of the record, this ratio is at its lowest, with watershed productivity being predominantly aquatic prior to the colonization and expansion terrestrial plants. The steady increase until ~7.5 ka suggests the maturation of the terrestrial environment, at which point the ratio remains stable until just after 1 ka. This period of stability indicates that there was no dramatic change to either the terrestrial or aquatic ecosystems at this time.

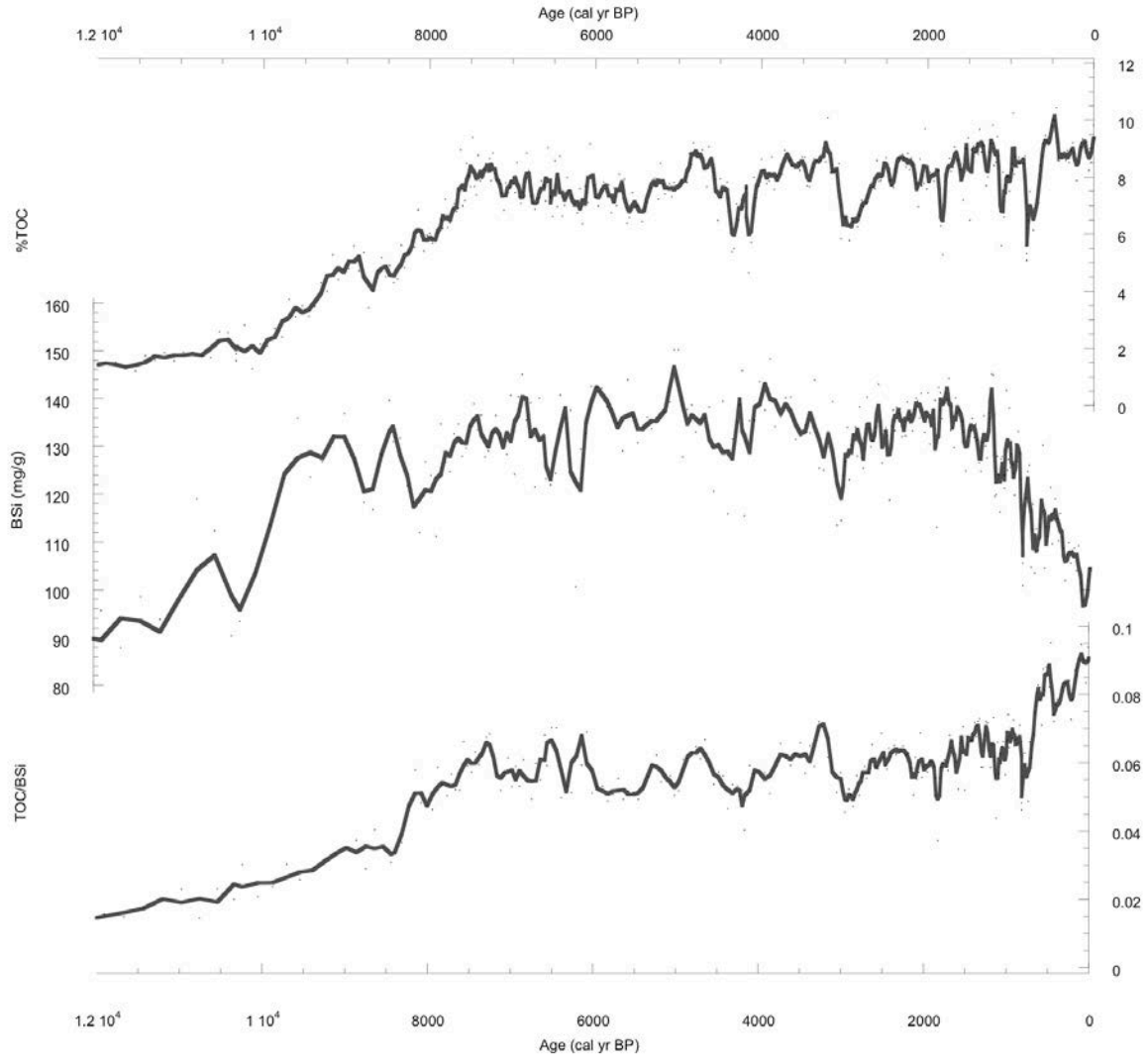

Figure 4.5. Total organic carbon, biogenic silica and the ratio of the two values. This ratio provides an alternate measure of terrestrial vs. aquatic organic matter source.

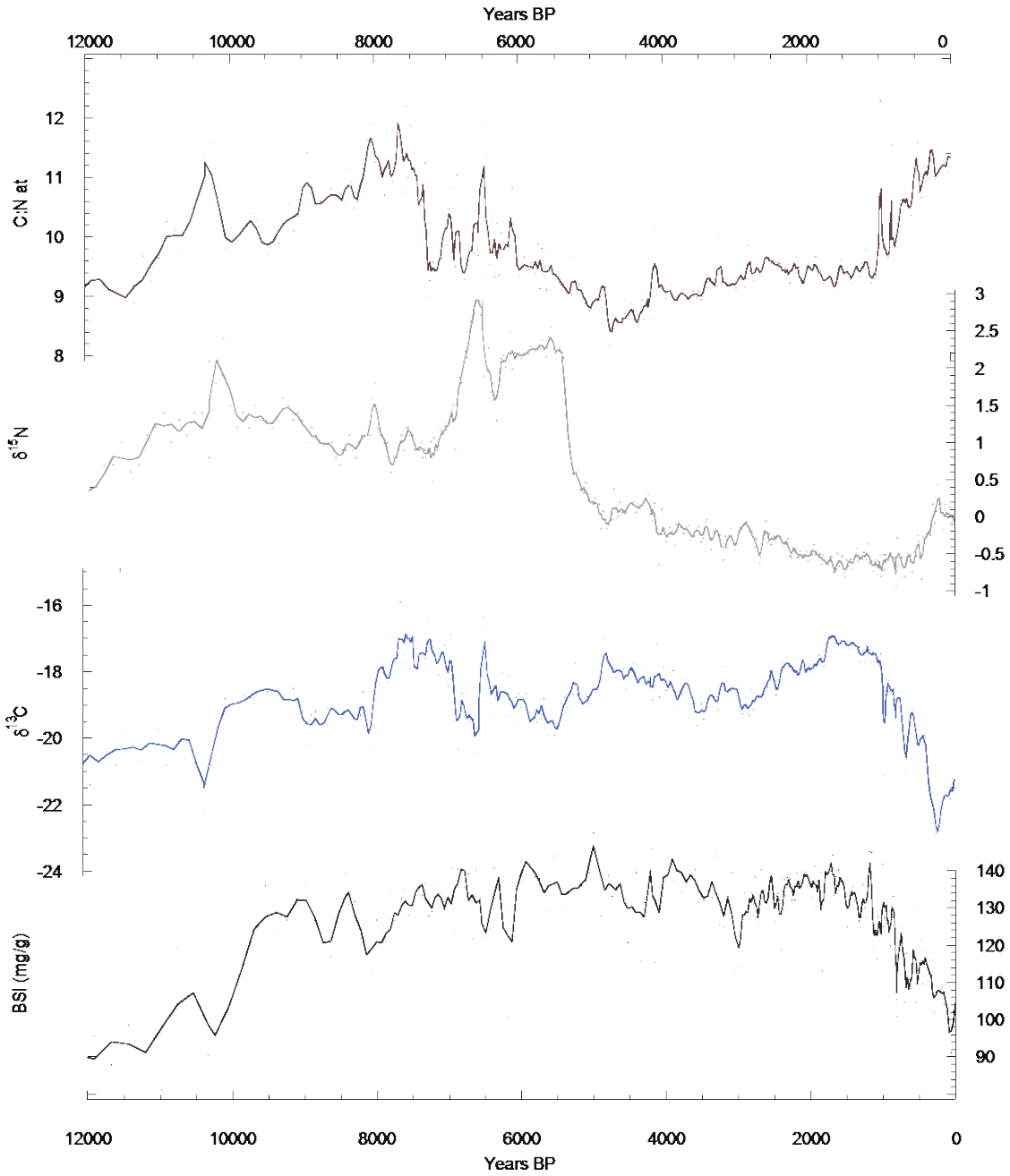

Figure 4.6. Carbon to nitrogen ratio, nitrogen isotopes, carbon isotopes, and biogenic silica from Torfdalsvatn

C:N rises steadily from 12 to 8 ka, possibly representing increased terrestrial biomass which did not accumulate in soils. Carbon isotopes, however, become increasingly enriched, indicating that abundant aquatic macrophyte plants (high C:N and $\delta^{13}C$) may have been the dominant control over C:N at this time. C:N then decreases, reaching a minimum value of ~8.5 just after 5 ka. This decrease in C:N is most likely driven by a reduction of the influx of terrestrial material because $\delta^{13}C$ remains high (Fig. 4.6), suggesting that aquatic macrophyte abundance was unchanging. A reduction in the influx of terrestrial organic matter, when it is known that regional terrestrial productivity was high from pollen records (Rundgren 1998; Hallsdóttir and Caseldine 2005; Eddudóttir et al. 2015), may indicate a reduction in the transport of terrestrial material which would have led to organic matter accumulation in soils.

A pronounced increase in erosion is evident in MS and organic matter source proxies beginning at 1.8 ka. At this time, the decreasing trend of MS is reversed, suggesting that late Holocene cooling became severe enough to both decrease vegetation cover, and increase wind transport of minerogenic material to the sediment. Several eruptions occur within several hundred years on either side of 1 ka (Grönvald et al. 1995; Stothers 1998; Thordarson and Larsen 2007) and the associated tephra also contributes to the elevated MS during this time. Unlike earlier tephra deposition events, which appear as short-lived spikes, MS never returns to its baseline state after 1.5 ka. This suggests that cooling climate may have increased the susceptibility of soils to damage from tephra deposition. At 1 ka, shortly after the increase in MS, C:N begins to rise along with the TOC to BSi ratio, also associated with a decrease in $\delta^{13}C$ (Fig. 4.6). This change in proxy values unanimously suggests a shift to increasing flux of terrestrial organic matter to the sediment. The initial increase in MS precedes the change in organic matter source as well as major tephra layers, which suggests increased wind and surface

shear stress could be the primary driver. The import of terrestrial material to the sediment is interpreted as the destabilization and erosion of soils in the catchment, as has been seen in lake records across Iceland (Wooller et al. 2008; Geirsdóttir et al. 2009b; Larsen et al. 2011). This increase in soil erosion could be derived from the combined influence of cooling climate, human colonization, and disturbance from tephra deposition.

4.5.3. Algal and aquatic productivity proxy record

The second focus of this study develops a comprehensive history of past lacustrine productivity at Torfdalsvatn, utilizing algal pigments and FTIR-inferred BSi. Using this approach, both the total magnitude and aquatic primary producer composition can be deduced. Through changing length of summer ice-free season, and subsequent alteration of total productivity and algal group succession, paleoenvironmental reconstructions can be developed from the nature and magnitude of aquatic productivity.

BSi, reflecting the relative amount of siliceous material produced by lake algae (mostly diatoms), is a commonly used measure for reconstructing total aquatic productivity (Conley and Schelske 2001). At the beginning of the record BSi is at its lowest value, indicating low overall aquatic productivity (Fig. 4.5). Low abundance is also attributable to dilution by the large amount of minerogenic material entering the lake at this time. BSi steadily rises until ~9.5 ka due to increased aquatic productivity and decreasing dilution by minerogenic material. Warming temperatures through this interval would have led to longer ice-free season and increasing terrestrial vegetation cover and landscape stability, which would have reduced the flux of inorganic material. BSi reaches its highest value at 5 ka, after which there is a general trend towards decreasing values, punctuated by increases at around 4 and 2 ka. This trend toward

decreasing aquatic productivity could indicate the onset of late Holocene cooling. After 1.8 ka, biogenic silica concentration begins a sharp decline that continues to the top of the core. This time period has been identified as the onset intensified cooling (Massé et al. 2008; Sicre et al. 2008; Larsen et al. 2011; Geirsdóttir et al. 2009b), therefore we interpret this decrease in BSi to reflect reduced aquatic productivity as a result of decreasing ice free season and reduced maximum summer lake water temperature. There is also increased dilution of BSi by minerogenic material and terrestrial organic matter due to increased erosion as inferred from MS and C:N, however this is probably not the main driver of the BSi signal, as there is no discernable increase in sedimentation rate.

Algal pigments provide a more comprehensive view of past aquatic productivity as they record all groups, rather than just those that produce silicified structures (Leavitt and Hodgson 2001). Here, algal pigment results are presented as total chlorin (chlorophyll + degradation products), diatom pigments (fucoxanthin + diatoxanthin + diadinoxanthin), lutein to diatoxanthin ratio (L:D; ratio of green algae and higher plants to diatoms and chrysophytes), and the cyanobacterial pigment canthaxanthin (Figure 4.7). These pigment concentrations and ratios can be used to characterize both total aquatic productivity and the relative contribution of the three major algal groups. Additionally, the majority of pigments used are relatively stable (with the exception of fucoxanthin and diadinoxanthin), reducing the bias of variable pigment preservation through time. Pigments are expressed as normalized to sedimentary organic matter content, as percent of total pigments, or as a ratio of two pigments. Each way of expressing the pigment data gives slightly different information about past conditions and each requires making particular assumptions about pigment production, deposition, and preservation. The standard way to express pigment data from sediment cores is to normalize to organic matter, usually measured by

loss on ignition (Leavitt and Hodgson 2001). This method assumes that the primary control on pigment concentration is the total organic content of the sediment, and that meaningful information about past algal productivity can best be obtained by removing the influence of variable overall organic matter content. Although the proportion of pigment to total organic matter depends on the amount of aquatic productivity, dilution by pigment-poor organic matter, such as soil, can also be a mechanism for changing proxy values. Expressing pigment data as percent of total pigment helps remove the influence of dilution and poor preservation. These curves cannot be interpreted as total productivity records, as they only show how pigment composition, and therefore algal assemblages, have changed over time. Similarly, ratios of pigments diagnostic to a particular algal group are used to track relative abundance. This assumes that pigments used to calculate the ratio are similarly stable and a change in the depositional environment will affect both equally. Specifically, the ratio of lutein to diatoxanthin (L:D) is used to track the relative proportion of green algae to diatoms as they are similarly stable. Using these methods of data presentation, a comprehensive reconstruction of past overall aquatic productivity, algal group relative abundance and organic matter source can be developed.

Primary factors influencing the total magnitude of aquatic productivity and biological community structure on Holocene timescales are changes in climate and nutrients (Smith 1979; Smol and Cumming 2000). Additional factors influencing the pigment records are assumed to be changes in preservation, dilution, and variable pigment production per amount of algal biomass. The greatest pigment preservation will occur in material with the least transport distance and associated exposure to oxidative and heterotrophic degradation (Leavitt and Hodgson 2001). Interpretation of total pigment concentration history is based on using a multi-proxy approach to determine which of these processes were most dominant through time.

In all samples measured, chlorins are the most abundant pigment, making up between ~65 and 95 % of total pigments detected (Fig. 4.7). This reflects their ubiquity in all photosynthetic organisms and their function as dominant light harvesting pigment. In the earliest part of the record, chlorin concentration is at its highest value, peaking at ~11.5 ka, rapidly decreasing until ~9.8 ka. Directly after deglaciation and before development of terrestrial biomass, the majority of organic matter was autochthonous and therefore pigment rich. The decrease in chlorin values between 11.5 and 9.8 ka is interpreted as the development of terrestrial biomass and associated import of pigment-poor material, not as reduction in overall aquatic productivity. This interpretation is supported by the TOC:BSi and C:N, which indicate increased proportion of non-aquatic carbon through this interval (Fig. 4.4; 4.5). Chlorin concentration remains low until increasing again, remaining elevated between 5.5 and 3.5 ka. These higher chlorin values are associated with the lowest C:N of the record, suggesting that a shift of organic matter source towards more aquatic might be again responsible for the higher pigment concentrations. From pollen records (Rundgren 1998; Hallsdóttir and Caseldine 2005; Eddudóttir et al. 2015) we know that terrestrial vegetation communities were well-developed at the time, which, to explain observed proxy values, would require either elevated aquatic productivity or very stable terrestrial conditions reducing the export of organic matter to the lake. After this broad peak centered around 4.5 ka, chlorins steadily decline, reaching their lowest values during the LIA at around 1500 AD. The mechanism for this is again interpreted as a shift towards greater influx of pigment-poor terrestrial organic matter as a result of the late Holocene landscape destabilization and erosion discussed in the previous section.

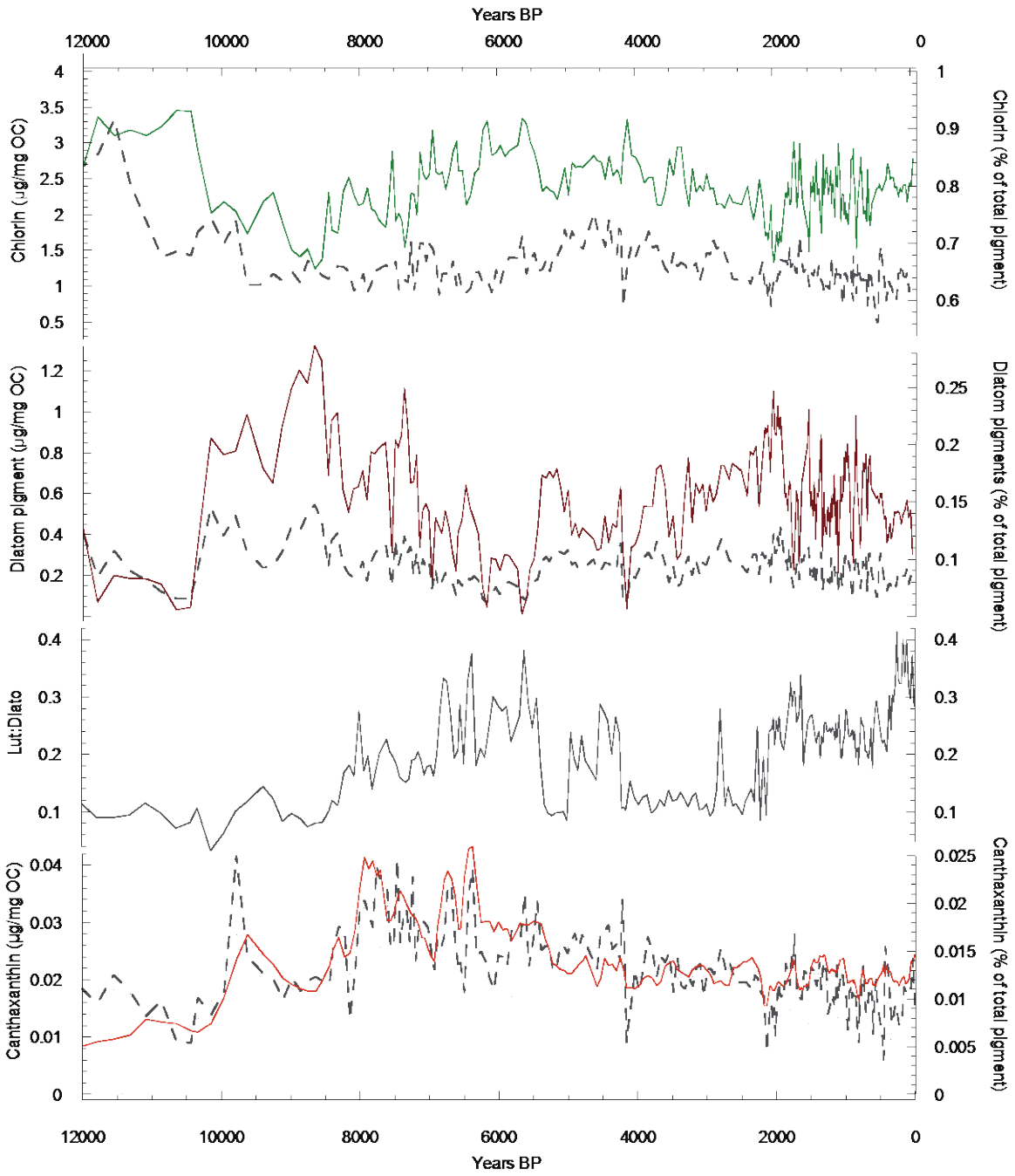

Figure 4.7. Pigments from Torfdalsvatn representing total productivity (chlorins), diatom pigments, relative abundance of green algae and plants vs. diatoms (lut:diato), and cyanobacteria (canthaxanthin). Values expressed as normalized to organic carbon (left axis, dashed line) and as fraction of total pigment (right axis, solid line).

The proportion of diatom pigments is variable, ranging from ~1 to 27% of total pigment with the lowest relative abundance of diatom pigments occuring in the beginning of the record. This is unexpected as diagnostic accessory pigments from other algal groups are also low, which suggests low overall algal abundance despite elevated sedimentary chlorins, which show high aquatic productivity. Although a mechanism for this is difficult to assign, it is possible that different depositional environment characteristics may have favored preservation of chlorins over carotenoids, or accessory pigment production in algae was suppressed due to environmental conditions. Diatom pigments become more abundant after the deposition of the Saksunarvatn tephra and an increase in BSi during this interval suggests that an increase in overall diatom abundance occurred during this time (Fig. 4.6; 4.7). After peaking at 8.5 ka, diatom pigment abundance begins to decrease, anticorrelated with the ratio of lutein to diatoxanthin. This, along with a decrease in C:N, suggests that green algae became more abundant. Lutein-producing (green) species remain dominant and the relative proportion of diatom pigments is low until 4 ka. Between 4 and 2.5 ka, diatom pigments steadily increase and L:D stays low, suggesting elevated diatom relative abundance through this interval. Interestingly, BSi does not track diatom pigment abundance for much of the record, making it difficult to conclusively derive past diatom abundance. While siliceous tephra could potentially contaminate the BSi record, elevated BSi is not observed in samples adjacent to tephra layers and this is assumed to not be a significant factor influencing FTIRS-BSi values. The best explanation for this is that there are several complicating factors using both organic and inorganic microfossils to reconstruct past algal biomass. Both these proxies can be influenced by differences in amount of each compound per unit of algal biomass, varying species assemblage, and environmental conditions (Alberte et al. 1981; Lavaud et al. 2002; Rousseau et al. 2002; Stramski et al. 2002; Finkel et al. 2010). Also,

pigment relative abundance and ratios are not indicators of total productivity, only of the proportion of productivity attributable to each group. An increase in green algae during the mid Holocene could help reconcile the pigment and BSi records by driving the decrease in relative abundance of diatom pigments.

Both diatom proxies change coherently during the last 2 ka, with a decrease in total pigment concentration, relative abundance, and BSi all pointing towards reduced diatom productivity. The combined increase of C:N and L:D, with associated decrease in $\delta^{13}C$, suggest that even though pigment concentration in soils is low, it may have been enough to increase the lutein content of the sediment during the vigorous soil erosion of the last 2 ka. The first increase of L:D precedes the change in other diatom proxies and may reflect a shift in aquatic productivity towards more macrophytes as it immediately precedes an interval of elevated $\delta^{13}C$ (Fig. 4.6, 4.7). Shallowing of the lake could lead to a threshold-like increase in aquatic macrophytes as the bottom of the lake enters the photic zone. Further increase in L:D is associated with decreasing $\delta^{13}C$ and therefore cannot be attributed to aquatic macrophyte organic matter, most likely this is lutein from terrestrial vegetation washed into the lake.

Cyanobacterial populations have been shown to quickly increase in response to temperature and nutrients, and may prove to be an important indicator species for past lake conditions (De Senerpont Domis et al. 2007; Paerl and Paul 2012). The only detectable pigment biomarker of cyanobacteria in Torfdalsvatn is canthaxanthin, present throughout the core at low relative abundance between ~0.5 and 2.5% of total pigment. *Nostoc* sp. were commonly observed on shoreline rocks while sampling epilithon in July 2014, and are the most likely source of canthaxanthin. Cyanobacterial relative abundance and total concentration track each other more closely than is seen with other pigments, implying that increasing cyanobacterial

relative abundance is consistently due to an increase in overall biomass, not driven by a decrease in other algal groups.

Cyanobacterial pigments are low between 12 and 10 ka, then steadily increase until 8 ka. Both relative abundance and concentration remain high until ~5.5 ka, with relative abundance reaching its maximum value at ~6.5 ka. Relative abundance then decreases until becoming stable at 4 ka, while total concentration continues to decrease, reaching a minimum value during the LIA. The pattern of change in canthaxanthin, mirrors other regional temperature records (Fig. 4.8), suggesting that the abundance of cyanobacteria may controlled by more closely by temperature and length of summer than the other algal groups.

Together, the pigment records show a complex history of algal group abundance, with each group having a different response to past environmental change. The lack of coherent trend between all pigments implies that each algal group may be responding to a different environmental variable. Organic matter source may play an equally dominant role in the signal seen in pigment proxy records as changing algal group abundance. The Holocene algal group ontogeny at Torfdalsvatn progressed from dominantly diatoms shortly after the Saksunarvatn tephra, transitioning to predominantly green algae, aquatic macrophytes and cyanobacteria. This is assumed to have been driven by increased temperatures and length of summer during the HTM; the time of peak cyanobacterial abundance may represent the warmest Holocene temperatures at Torfdalsvatn. After the HTM, diatom abundance increases again in the late Holocene, although the import of terrestrial organic matter begins to influence the pigment record after 2 ka, making information about algal groups difficult to infer. The lowest cyanobacterial abundance occurs during the LIA and this is presumed to be a direct result of cooling temperatures and decreased length of ice-free season.

4.5.4. Nitrogen isotope record

The relative complexity of the nitrogen cycle often makes unique interpretations of sedimentary nitrogen isotope records difficult, as multiple processes may have the same influence on sedimentary values (Talbot 2001). Nitrogen isotopic composition, as with the other organic matter proxies, can be influenced by both changes in lacustrine biogeochemistry and organic matter source. A best-possible interpretation of nitrogen isotope records needs to take into account both local values of material contributing to the sediment, along with the biogeochemical information contained in other proxies.

The nitrogen isotope record at Torfdalsvatn begins with increasing values from 12 to 10 ka. Pioneer species are often N-fixers (Lawrence et al 1967; Crittenden 1975) as this offers a competitive advantage in freshly deglaciated environments, which, in some cases, have very little available N (Hobbie et al. 1998). Nitrogen that is biologically fixed undergoes little fractionation, and the subsequent organic matter produced will have a signature of around 0‰ (fractionation factor of -3 to +1‰ from Fogel and Cifuentes 1993; or negligible fractionation factor in fixation by cyanobacteria as reviewed by Talbot 2001). Through biological fractionation, light isotopes are removed preferentially and may be exported from the catchment. The remaining nitrogen will become more enriched until a balance between the light nitrogen isotopes from fixation and heavier residual nitrogen is reached (Talbot 2001).

At ~9.5 ka, nitrogen isotope values begin to decrease, associated with an increase in $\delta^{13}C$ and C:N (Fig. 4.6). As discussed previously, the increase in $\delta^{13}C$ and C:N is attributed to increasing aquatic macrophyte plants. Aquatic macrophytes have the most depleted nitrogen isotopes of all modern organic matter sources (see discussion in Chapter 3). The decrease in

nitrogen isotopes is consistent with this, and supports increasing macrophyte abundance in the early Holocene. The interval of decreasing values abruptly transitions to a broad peak, containing the highest $\delta^{15}N$ recorded in the sediment (Fig. 4.6). This excursion begins with a sharp peak to ~3‰ at 6.5 ka, which then levels off, with values remaining between 2 and 2.5‰ until decreasing sharply at 5.4 ka. This abrupt increase in $\delta^{15}N$ is not mirrored by any of the other organic matter proxies and is not likely to be due to a shift in organic matter source, which would also influence C:N and $\delta^{13}C$. Changes in the local nitrogen cycle are the most probable mechanism for the increase in values.

Decreased sediment oxygen content can increase denitrification by heterotrophic bacteria that utilize mineralized nitrogen as an electron acceptor (Knowles 1982), which strongly fractionates against heavy isotopes (Blackmer and Bremner 1977). The product of this denitrification is N_2 gas, which then diffuses into the atmosphere (Knowles 1982). This process efficiently removes light nitrogen isotopes from the sediment, leaving the remaining nitrogen enriched (Mariotti et al. 1981). Denitrifiers require low oxygen content along with organic carbon to break down for energy. Periods of reduced bottom water oxygen concentration and high organic carbon will both increase this process (Knowles 1982). High productivity will reduce bottom water oxygen concentration by increasing populations of heterotrophic bacteria as well as increase the organic content of the sediment, creating ideal conditions for denitrification to occur. Lower wind stress will also reduce mixing and lead to increased summer stratification of the lake (Imboden and Wüest 1995), resulting in reduced oxygen content and increased denitrification (Meissner et al. 2005). If the cause of the increase in sedimentary $\delta^{15}N$ is assumed to be from denitrification, then it can be deduced that environmental conditions from 6.5 to 5.4

ka at Torfdalsvatn were characterized by high productivity, low wind stress, or the combination of the two factors as a result of the HTM.

After 5 ka, $\delta^{15}N$ continues to gradually decline before reaching its most negative values between 2 and 1 ka. Increasing $\delta^{13}C$ and C:N again point to this being driven by changes in organic matter source (Fig. 4.6). Abundant aquatic macrophyte populations could be the cause for this as they were earlier in the record. Steady shallowing of the lake throughout the Holocene would have reduced the water depth by more than half, increasing the amount of available light at the sediment surface and likely favoring the growth of macrophyte plants. During the LIA, $\delta^{15}N$ becomes sharply higher at the same time as terrestrial landscape destabilization occurs and the sediment becomes increasingly comprised of terrestrial organic matter. Soils measured regionally have higher $\delta^{15}N$ than macrophyte plants (see organic matter sources in Chapter 3), further supporting the interpretation that unstable catchment soils were mobilized during the LIA.

The first-order trend in nitrogen isotopes through the Holocene is toward increasingly depleted values due to the consistent shallowing of the lake and subsequent increase in aquatic macrophyte plants. The mid Holocene departure from this trend suggests increased denitrification due to high productivity and stratification of the water column. Late Holocene increases in $\delta^{15}N$ are attributed to the widespread erosion of terrestrial soil, and subsequent change in dominant sedimentary organic matter source. In this location, the departures from the long-term trend provide important paleoenvironmental information and help characterize both the HTM and the LIA.

4.6. COMPARISON WITH REGIONAL RECORDS

4.6.1. Deglaciation to Saksunarvatn (before 12 ka to 10.2 ka)

As the only known Icelandic lake record with non-marine sediments extending to beyond 12 ka, Torfdalsvatn provides some of the only terrestrial climate information available regionally over this interval. In marine sediment cores from the Icelandic Shelf, foraminiferal assemblages at this time are characterized by decreasing abundance of arctic species, with boreal species appearing just after 11 ka, rapidly increasing in abundance. This change in assemblage indicates a shift from the dominance of cold, polar water masses to establishment of the IC bringing warm North Atlantic water north of Iceland and resulting northward migration of the Polar Front. Bottom water temperatures off northwest Iceland increased by nearly 4 degrees between 11.5 ka and 10.5 ka, but foraminiferal assemblages indicate a stratified water column with surface waters influenced by cold, fresh water from melting ice (Ólafsdóttir et al. 2010). Pollen records from Torfdalsvatn show a transient appearance of shrubs at 12.5 ka, which then disappeared during the Younger Dryas before permanently becoming established at ~10.5 (Rundgren 1995), contemporaneous with the northward extension of the IC bringing warm Atlantic water (Ólafsdóttir et al. 2010). Diatom-inferred SSTs at MD99-2269 also indicate that the IC had strong influence on the North Iceland Shelf at this time, with diatom species assemblages showing a strong warming to HTM conditions occurring between 10.5 and 10.2 ka (Justwan et al. 2008). The proxies measured at Torfdalsvatn are consistent with these previous studies, indicating warming during this time. Increasing aquatic productivity (BSi, diatom pigments), along with the establishment of terrestrial plants (C:N), suggest longer growing seasons. The predominantly aquatic OM source however, suggests that terrestrial biomass remained relatively suppressed. As this was a period of lake and landscape ontogeny, the proxy signal likely

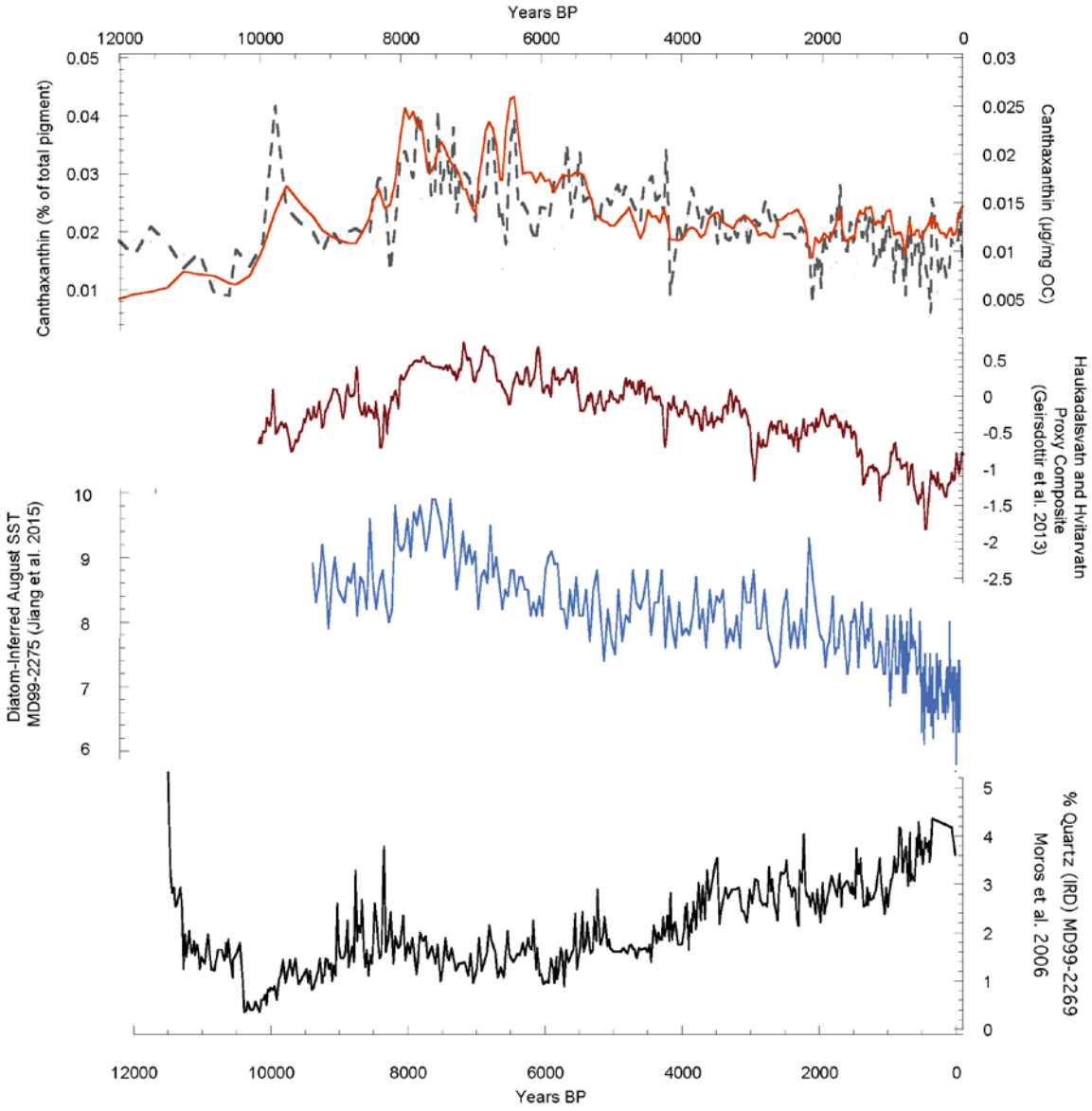

Figure 4.8. The Torfdalsvatn canthaxanthin record compared to regional climate proxies from Icelandic lake sediments (Geirsdóttir et al. 2013), Diatom-inferred SSTs from the marine core MD99-2275 (Jiang et al. 2015) and sea ice derived quartz from MD99-2269 (Moros et al. 2006)

represents the combined influence of warming temperatures and early succession of biological communities.

4.6.2. Early Holocene (10.2 to 8 ka)

Although the deposition of the locally up to 28-cm-thick Saksunarvatn ash was a setback to the development of terrestrial biological communities, pollen indicates that this was only temporary, with limited lasting effect on terrestrial plant species assemblages (Rundgren 1998). Reflecting this, terrestrial OM in the Torfdalsvatn core (Fig. 4.4; 4.6) continues to increase, with reduced erosion indicating a stabilizing landscape. In regional lacustrine records, this time period was characterized by increasing productivity (Geirsdóttir et al. 2013). A temperature record from terrestrial soil derived biomarkers derived from a ratio of the cyclization to methylation of branched tetraethers (CBT/MBT) by Moossen et al. (2015), suggests that this was the insolation-forced terrestrial HTM in northwest Iceland, however this is not supported by regional lake records (Larsen et al. 2012; Geirsdóttir et al. 2013). Diatom-inferred marine SSTs (which directly influence terrestrial air temperatures) from core MD99-2275 also shows temperatures below peak Holocene values (Jiang et al. 2015). An HTM at this time is supported by a multiproxy record from MD99-2269 (Kristjánsdóttir 2005). A potential explanation for these discrepancies is increased marine stratification, with cold Polar surface waters existing off north Iceland and locally suppressing early Holocene temperatures (Axford et al. 2007; Ólafsdóttir et al. 2010). Cyanobacterial pigments, which appear to track summer temperatures at Torfdalsvatn, are low but increasing; further suggesting that peak warmth did not occur in north Iceland until after 8ka, despite this being the time of peak summer insolation (Berger and Loutre 1991). The regionally significant 8.2 ka event (Alley and Ágústsdóttir 2005) is not as well

characterized in the Torfdalsvatn record as in other nearby lakes (Larsen et al. 2012), indicating that biological temperature thresholds may not have been crossed at Torfdalsvatn during this time.

4.6.3. Holocene Thermal Maximum (8 ka to 5.5 ka)

Both marine and lake proxy records indicate that the maximum temperatures of the Holocene in and around Iceland occurred shortly after 8 ka (Eiríksson et al., 2000; Castañeda et al., 2004; Kristjánsdóttir, 2005; Justwan et al., 2008; Knudsen et al., 2008; Ran et al., 2008; Quillmann et al., 2010; Geirsdottir et al. 2013; Jiang et al. 2015). This is slightly later than the early Holocene insolation maximum, likely due to residual fresh surface water in the North Atlantic from glacial melt suppressing AMOC-driven northward heat transport to the central North Atlantic (Kaufman et al. 2004). The time period shortly after 8 ka is characterized by maximum northward heat transport by the IC (Olafsdottir et al. 2010), which was also expressed in surface water proxy records (Jiang et al. 2015). The Torfdalsvatn proxies agree with the regional consensus of HTM timing. Shortly after 8 ka, there is a decrease in erosion and import of terrestrial organic matter to the lake (decreasing C:N and MS), indicating stability and accumulation of soils. During this time, diatoms become less abundant, and evidence of increased denitrification ($\delta^{15}N$) suggests increased bottom water anoxia from either lower wind stress, or increased aquatic productivity. The period of highest cyanobacterial pigment relative abundance and concentration coincides with the highest August SST at MD99-2275 (Fig. 4.6; Jiang et al. 2015) and the highest inferred temperatures from the lake sediment proxy composite of Geirsdóttir et al. (2013). This contrasts somewhat with the biomarker temperature record from Moossen et al. (2015), which suggests that the terrestrial HTM occurred contemporaneous with

the summer insolation maximum between 10 and 8 ka (similar to what was observed on Baffin Island, Chapter 2) and preceded the local marine thermal maximum. The tight coupling of terrestrial air temperatures with SSTs in Iceland requires that the timing of maximum marine and terrestrial temperatures be concurrent (Figure 4.2). This study utilized terrestrially derived branched Glycerol Dialkyl Glycerol Tetraether (brGDGT) that were transported to fjord sediment (MD99-2266). Changes in inferred soil pH during this time are attributed by Moossen et al. (2015) to be due to decreasing aridity, however we prefer an alternate interpretation: increasing organic matter storage in soils would decrease pH due to leaching of organic acids. The soil pH reconstructed by Moossen et al. (2015) mirrors the record of inferred soil stability at Torfdalsvatn, suggesting that the timing of soil development may have followed a similar pattern across northwest Iceland. Changes in brGDGT source as soil organic matter increased through the early Holocene could have led to a warm bias in the earliest part of the Moossen et al. (2015) record, when the soil-derived GDGTs are at their lowest concentration. Additionally, this record is constructed utilizing reworked terrestrial material extracted from a fjord core (MD99-2266) which introduces uncertainties about the exact source of the organic matter, which may have changed through time. Chironomid-inferred temperature records from north Iceland (including Torfdalsvatn) contrastingly point to a delayed HTM (Axford et al. 2007). While it is possible that the chironomid records are sensitive to temperature change in a different part of the summer than the other proxy records, lack of a strong temperature indicator species in north Iceland could allow for other environmental factors to influence the reconstructed temperatures. Canonical Correspondence Analysis (CCA) of the northwest Iceland chironomid temperature training set shows some of the dominant species at Torfdalsvatn plotting along CCA Axis 1, which appears to be additionally controlled by sediment organic matter content (Langdon et al. 2008). This

would suggest that the low sedimentary TOC concentrations in early Holocene might have led to a cold bias in the chironomid record. Because of these discrepancies, additional biomarker temperature records should be developed from multiple depositional environments in north Iceland to determine whether this early terrestrial HTM seen in the fjord record, or the late HTM seen in the chironomid record, can be replicated. The qualitative proxies from the Torfdalsvatn record add to the regional consensus of peak Holocene summer temperatures after 8 ka.

4.6.4. Mid Holocene Transition to Neoglacial (5.5 to 2 ka)

With the onset of late Holocene glacier growth (Gudmundsson, 1997; Geirsdóttir et al. 2009a; Larsen et al. 2012; Striberger et al. 2012), increasing IRD in marine sediment cores (Moros et al. 2006; Fig. 8), and the incremental cooling in response to decreasing summer insolation as recorded by multiple proxies in other Icelandic lakes (Striberger et al. 2012; Geirsdóttir et al. 2013; Fig. 4.8), the Torfdalsvatn record begins to show a transition toward cooling temperatures at 4.5 ka although this signal is not as strong as in other regional records. MS decreases throughout this time, and C:N reaches its lowest values indicating stable soils in the catchment until the trend in C:N reverses and begins to increase after ~4.5 ka. Canthaxanthin concentration begins to slowly decline at a similar time, suggesting shorter growing seasons. Diatom pigment relative abundance increases, as conditions may have become more favorable to diatoms over to other algal groups. Shorter summers, or environmental parameters such as increasing wind speed, may have led to a comparative advantage of diatoms. Analysis of diatom species assemblage change through this interval could elucidate which environmental variable led to the increase in diatom relative abundance and allow a more complete paleoenvironmental interpretation.

4.6.5. Neoglacial to LIA (2 ka to 1850 AD)

While proxies at Torfdalsvatn show variable response to climate events during most of the record, coherent shifts occur at 1.8 ka and 1 ka, which strongly suggest cooling. These changes in proxy values are persistent, and represent a fundamental environmental change at Torfdalsvatn. Intensified cooling at approximately 1.8 ka is well-represented in other regional records as a prominent non-linear response to decreasing summer insolation. A reduction in Icelandic lake productivity and increased deposition of glacial sediment occurs at the start of the DACP (Larsen et al. 2011; Geirsdóttir et al. 2013). This is contemporaneous with the disappearance of *Betula* pollen from a fjord core at Reykjarfjördur, just west of Torfdalsvatn (Andrews et al. 2001). Decreasing SSTs are seen in multiple records, particularly in the last millennium during the LIA (Massé et al. 2008; Sicre et al. 2008; Jiang et al. 2015). Icelandic terrestrial records show increased erosion over the last 1 ka as is seen at Torfdalsvatn. This landscape destabilization is nearly ubiquitous in all Icelandic lake sediment proxy records (Wooller et al. 2008; Geirsdóttir et al. 2009b; Larsen et al. 2011), although the anthropogenic impacts of the settlement of Iceland may confound the temperature information held by these proxies in some locations (Blair et al. 2015).

4.7. CONCLUSIONS

The multiple biogeochemical proxy record at Torfdalsvatn provides a novel view of Holocene environmental conditions in north Iceland. After deglaciation, organic matter source proxies indicate the gradual establishment of terrestrial biological communities along with a general increase in productivity, which is only briefly impacted by the deposition of the

Saksunarvatn tephra. There is little evidence for the 8.2 ka event in this record, despite being observed in other Icelandic lakes. The HTM occurred just after 8 ka, characterized by elevated cyanobacterial productivity and increased bottom water anoxia due to high productivity or low wind stress. Despite this warmth, proxies for erosion (MS, C:N) show some degree of soil instability in the catchment until 6 ka. By 4 ka, several of the proxies begin suggest the onset of gradual cooling. The late Holocene is characterized by a two-staged cooling, with abrupt transitions beginning just after 1.8 ka and 1 ka reflecting decreased aquatic productivity and increased erosion, followed by a complete destabilization of catchment soils and further decreased aquatic productivity. The coldest inferred temperatures occur during the LIA, in agreement with the regional consensus. There is no coherent shift between 'green' (chlorophyte and higher plant) and diatom primary productivity (lutein:diatoxanthin) during regional warm/cold times as was seen on Baffin Island, suggesting an aclimatic (nutrient or ontogeny) control on green/diatom algal group abundance. The cyanobacterial pigment canthaxanthin tracks regional records of summer temperature, which indicates that it may be a useful proxy for reconstructing temperature history in future studies of Icelandic lake records. There remain discrepancies about the timing of the north Iceland HTM, which suggests the need for quantitative temperature proxies, such as alkenones, from Icelandic lakes. Quantitative temperature records allow for more consistent regional inter-comparison and additionally will provide insight into how past changes in temperature have induced changes in watershed biogeochemistry.

CHAPTER 5

5.1. CONCLUSIONS

This dissertation presents records of biogeochemical change from a suite of multi-proxy studies of lake sediment records from three lakes, two Icelandic and one from Baffin Island. The motivating questions of this study were: *What was the nature, timing and spatiotemporal variability of Holocene climate events in Baffin Island and Iceland? How did these changes in climate influence watershed biogeochemistry? How do catchment characteristics influence lake sediment records?* To better answer these questions, this study incorporated algal pigments along with a suite of biological and geochemical proxies to constrain the local climate history and the different biogeochemical regimes characterizing periods of long and short ice-free season.

This research effort is the first to utilize sedimentary algal pigments in reconstructing past algal group abundance in both regions. Comparison of the algal pigment record with other proxies has increased knowledge about the response of algal communities in Arctic lakes to Holocene climate evolution. There is a shift from green algal and higher plant pigments to those derived from diatoms and chrysophytes in the Baffin Island record. This shift in algal group abundance does not occur in the Iceland record, where most algal groups do not show a coherent response to changing climate. Cyanobacterial pigments from Torfdalsvatn do show elevated abundances during the HTM, indicating that summer temperature may be a control on Icelandic cyanobacterial populations.

The variable response of algal communities between locations suggests the need for developing a regional understanding of proxy behavior prior to making climate interpretations. Many lake sediment climate records rely heavily on past abundance of diatoms because their siliceous microfossils are easily quantified. However, the results of the algal pigment analysis

suggests that diatom relative abundance does not always tell the whole story of lacustrine productivity, this should be considered when interpreting climate information from biogenic silica records. Biological proxies can show differing response to equivalent climate history due to catchment-specific factors such as landscape steepness and nutrient availability. Additionally, each proxy has its own specific response threshold, sensitive to a particular range of environmental variability. In the KHL record, pigments distinctly characterize the HTM and Anthropocene warmth, but show little variability during the Neoglacial. The environmental conditions dictating algal group change had already shifted to favor a predominantly diatom algal assemblage by ~7 ka. Diatom species assemblages at KHL undergo most of their change after 3 ka, associated with intensified Neoglacial cooling. This highlights the need for using multiple biological proxies as the whole range of Holocene variability is not recorded in each. In addition to the need for the use of multiple proxies, results from this dissertation suggest that, due to catchment-specific factors influencing proxy response, multiple lakes from the same region must be studied before developing a climatic interpretation of the proxy record. If either the Torfdalsvatn or Bæjarvötn core had been the only regional record of late Holocene climate history, a different climate interpretation would have been developed about the region. Only with multiple proxies from multiple lakes can a complete regional environmental history be developed from biological proxies in sediment cores.

One motivating question of this study that is not well addressed by the results is that of the nature of rapid, non-linear climate events during the Holocene. Using biological proxies, it is difficult to distinguish periods of rapid environmental change from those where a certain biological threshold was reached. While periods of rapid change in biological communities most likely signify a significant climate event, it is impossible to apply a linear climate interpretation

to qualitative biological proxies. Because of this, quantitative proxies or non-biological systems such as glaciers are more likely to consistently and faithfully record times of rapid climate change.

5.2 IMPLICATIONS OF FUTURE ANTHROPOGENIC CHANGE ON ARCTIC LAKE BIOGEOCHEMISTRY

By studying changes in how biological communities and carbon and nitrogen dynamics of Arctic lakes have changed from the HTM to the LIA, we can begin to make predictions of how future warming and anthropogenic nutrient inputs will impact these lakes. The various biogeochemical proxies used in this study have distinct responses to Holocene environmental change between the western and central North Atlantic regions. Examining environmental conditions during the HTM provides a possible analogue for those that may exist as the warming projected to occur in the Anthropocene proceeds.

Early Holocene warmth in eastern Baffin Island is characterized by elevated accumulation rates of organic carbon, lower sedimentary oxygen content, and increased relative abundance of chlorophyte algae and higher plants. Longer summers, with potentially elevated temperatures, favored greater total productivity and the increased length of summer allowing for longer seasonal succession of algal groups and increased abundance of chlorophytes. Recent changes back to similar conditions are observed in the KHL core, with increasing carbon accumulation rate and chlorophyte/higher plant abundance. This indicates that elevated productivity will increase the flux and sequestration of atmospheric carbon in lake sediments of Baffin Island in the Anthropocene. As all proxies do not return to HTM values, it is clear that there is no exact analogue for current conditions. Despite this, the proxies that have returned to

an HTM-like state show that there has been significant environmental change in Baffin Island during the 20th century due to anthropogenic warming.

In Iceland, HTM conditions led to increasing stability of soils, elevated cyanobacterial abundance and elevated denitrification due to inferred reduced bottom water oxygen content. There is no clear carbon cycle signal between warm times, when organic matter accumulates in soil, and cold times when there is an increased flux of organic matter from the previously accumulated soils to the lake sediment. The aquatic conditions that typified the HTM at Torfdalsvatn suggest the potential for decreased water quality in Iceland with future warming. Decreased oxygen content could negatively impact fisheries and increased predominance of cyanobacteria indicates the potential for future toxic algal blooms (Paerl and Paul 2012).

Greater proxy response to anthropogenic warming at KHL suggests that regions with lower mean annual air temperature may undergo more biogeochemical changes in response to increasing temperature. The lesser response of proxies to modern warming in Icelandic lakes could be due to lesser magnitude of recent temperature change in Iceland, or because human settlement has altered the environment, and in some cases, changed proxy-climate relationship.

5.3. FUTURE RESEARCH

The questions addressed by this dissertation still remain open for future study and likely will be for years to come, as analytical techniques make possible continued proxy development. Directly following this dissertation, there are several avenues of study that stand out. Additional pigment records are needed from Arctic lakes to determine the relationship between algal assemblages and climate change. Lack of a consistent relationship between climate event and algal group response across Baffin Island and Iceland indicates that each region, or even each

lake, may respond differently. Larger changes in algal group assemblage may occur in cold environments, which undergo greater change in duration of ice-free season between warm and cold times. The relationship between pigments and climate at KHL has not been replicated in Iceland. Additional pigment records from Baffin Island lakes should be developed to evaluate Holocene scale changes in algal groups. Additionally, higher elevation lakes from Iceland that experience shorter summers should be examined to see if Holocene changes are more similar to those of Baffin Island. Additionally, a modern study of algal pigment composition of lakes in different Icelandic environments would contextualize the pigment record from Torfdalsvatn. Records of cyanobacterial abundance in low elevation lakes across Iceland should be developed to assess potential water quality issues that may arise with future warming.

Improved characterization of modern organic matter sources to lakes in Iceland will better constrain organic matter source history, which has proven to be one of the better proxies for Icelandic paleoenvironmental reconstructions. It remains unknown if isotopic compositions of terrestrial and aquatic organic matter vary from north to south across Iceland or are different between high and low elevation sites. It is also unknown if these end member values changed over the Holocene. It would be possible to estimate this by sampling both freshly deglaciated and mature landscapes. Additionally, the algal end member remains poorly characterized due to contamination by suspended particulate organic matter from aquatic macrophytes and soil.

Lipid biomarkers have great potential to improve Icelandic paleoclimate and paleoenvironmental reconstructions. Quantitative temperature proxies will be necessary to determine whether there was spatial heterogeneity in early Holocene warmth in north Iceland. Preliminary analysis of lipid extracts from Torfdalsvatn sediment indicate the presence of alkenones, which would allow the development of a quantitative temperature record at the site

that could be compared to the chironomid record and the diatom-inferred temperatures from MD99-2269 and MD99-2275. Quantitative temperature history at Torfdalsvatn will make possible studying the link between surface water and terrestrial summer temperatures. Another potentially valuable organic geochemical proxy at Torfdalsvatn is using the chain length composition of *n*-alkanes and *n*-alkanoic acids to refine organic matter source history, especially to confirm past changes in aquatic macrophyte abundance (e.g. Ficken et al. 2000).

One of the greatest challenges to developing records of recent climate change in Iceland is deconvolving the signal from human activity and landscape degradation from that of LIA cooling. Measurement of fecal sterol biomarkers produced by livestock and humans would make possible answering the long standing question of what component of the late Holocene landscape destabilization seen in the sediment core records is due to humans and what is a result of deteriorating climate (e.g. D'Anjou et al. 2013).

References

Abbott MB, Stafford Jr. TW (1996) Radiocarbon Geochemistry of Modern and Ancient Arctic Lake Systems, Baffin Island, Canada. Quat Res 45:300–311

Adrian R, Reilly CMO, Zagarese H, et al (2009) Lakes as sentinels of climate change. Limnol Oceanogr 54:2283–2297.

Alberte RS, Friedman AL, Gustafson DL, et al (1981) Light-harvesting systems of brown algae and diatoms. Isolation and characterization of chlorophyll a c and chlorophyll a fucoxanthin pigment-protein complexes. Biochem Biophisica Acta 635:304–316. doi: 10.1016/0005-2728(81)90029-3

Alley RB, Ágústsdóttir AM (2005) The 8k event: Cause and consequences of a major Holocene abrupt climate change. Quat Sci Rev 24:1123–1149. doi: 10.1016/j.quascirev.2004.12.004

Amundson R, Austin AT, Schuur EAG, et al (2003) Global patterns of the isotopic composition of soil and plant nitrogen. Global Biogeochem Cycles 17:1031. doi: 10.1029/2002GB001903

Anderson NJ, Liversidge AC, McGowan S, Jones MD (2012) Lake and catchment response to Holocene environmental change: Spatial variability along a climate gradient in southwest Greenland. J Paleolimnol 48:209–222. doi: 10.1007/s10933-012-9616-3

Andrews JT, Barry RG, Bradley RS, Miller GH, Williams LD (1972) Past and Present Glaciological Responses to Climate in Eastern Baffin Island. Quat Res 2:303–314

Andrews JT, Caseldine C, Weiner NJ, Hatton J (2001) Late Holocene (ca. 4 ka) marine and Reykjarfjordur, north Iceland: climate and / or settlement ? J Quat Sci 16:133–143.

Andrews JT, Belt ST, Olafsdottir S, et al (2009) Sea ice and marine climate variability for NW Iceland/Denmark Strait over the last 2000 cal. yr BP. The Holocene 19:775–784. doi: 10.1177/0959683609105302

Antoniades D, Douglas MS V., Smol JP (2005) Quantitative estimates of recent environmental changes in the Canadian High Arctic inferred from diatoms in lake and pond sediments. J Paleolimnol 33:349–360

Appleby PG, Oldfield F (1978) The calculation of lead-210 dates assuming a constant rate of supply of unsupported< sup> 210</sup> Pb to the sediment. Catena 5:1-8.

Arnalds A (1987) Ecosystem Disturbance in Iceland. Arct Alp Res 19:508–513.

Arnalds O (2000) The Icelandic “Rofabard” soil erosion features. Earth Surf Process Landforms 25:17–28. doi: 10.1002/(SICI)1096-9837(200001)25:1<17::AID-ESP33>3.0.CO;2-M

Arnalds O, Orradottir B, Aradottir AL (2013) Carbon accumulation in Icelandic desert Andosols during early stages of restoration. Geoderma 193-194:172–179. doi: 10.1016/j.geoderma.2012.10.018

Arnalds, O. (2015) The soils of Iceland. Springer.

Ascough P, Cook G, Dugmore A (2005) Methodological approaches to determining the marine radiocarbon reservoir effect. Prog Phys Geogr 29:532–547. doi: 10.1191/0309133305pp461ra

Autio J, Hicks S (2004) Annual variations in pollen deposition and meteorological conditions on the fell Aakenustunturi in northern Finland: Potential for using fossil pollen as a climate proxy. Grana 43:31–47. doi: 10.1080/00173130310017409

Axford Y, Miller GH, Geirsdóttir Á, Langdon PG (2007) Holocene temperature history of northern Iceland inferred from subfossil midges. Quat Sci Rev 26:3344–3358. doi: 10.1016/j.quascirev.2007.09.003

Axford Y, Briner JP, Cooke C a, Francis DR, Michelutti N, Miller GH, Smol JP, Thomas EK, Wilson CR, Wolfe AP (2009) Recent changes in a remote Arctic lake are unique within the past 200,000 years. Proc Nat Acad Sci USA 106

Barko JW, Gunnison D, Carpenter SR (1991) Sediment interactions with submersed macrophyte growth and community dynamics. Aquat Bot 41:41–65. doi: 10.1016/0304-3770(91)90038-7

Bendle, J. a. P., Rosell-Mele, a., 2007. High-resolution alkenone sea surface temperature variability on the North Icelandic Shelf: implications for Nordic Seas palaeoclimatic development during the Holocene. The Holocene 17, 9–24. doi:10.1177/0959683607073269

Berger A, Loutre MF (1991) Insolation values for the climate of the last 10 million years. Quat Sci Rev 10:297–317. doi: 10.1016/0277-3791(91)90033-Q

Berkes F, Jolly D (2001) Adapting to climate change: Social-ecological resilience in a Canadian western arctic community. Conserv Ecol. 5(2)

Besonen MR, Patridge W, Bradley RS, Francus P, Stoner JS, Abbott MB (2008) A record of climate over the last millennium based on varved lake sediments from the Canadian High Arctic. The Holocene 18:169–180

Bianchi, TS, Findlay S (1990) Plant pigments as tracers of emergent and submergent macrophytes from the Hudson River. Can. J. Fish. aquat. Sci. 47: 492–494

Bianchi, T.S., Dibb, J.E., Findlay, S., 1993. Early Diagenesis of Plant Pigments in Hudson River Sediments. Estuar. Coast. Shelf Sci. 36, 517–527.

Bigler C, Hall RI (2003) Diatoms as quantitative indicators of July temperature: A validation attempt at century-scale with meteorological data from northern Sweden. Palaeogeogr Palaeoclimatol Palaeoecol 189:147–160. doi: 10.1016/S0031-0182(02)00638-7

Björck S, Ingólfsson Ó, Haflidason H, et al (1992) Lake Torfadalsvatn: a high resolution record of the North Atlantic ash zone I and the last glacial-interglacial environmental changes in Iceland. Boreas 21:15–22. doi: 10.1111/j.1502-3885.1992.tb00009.x

Blaauw M (2010) Methods and code for “classical” age-modelling of radiocarbon sequences. Quat Geochronol 5:512–518

Blackmer AM, Bremner JM (1977) Nitrogen isotope discrimination in denitrification of nitrate in soils. Soil Biol Biochem 9:73–77. doi: 10.1016/0038-0717(77)90040-2

Blair CL, Geirsdóttir Á, Miller GH (2015) A high-resolution multi-proxy lake record of Holocene environmental change in southern Iceland. J Quat Sci 30:281–292. doi: 10.1002/jqs.2780

Blass A, Bigler C, Grosjean M, Sturm M (2007) Decadal-scale autumn temperature reconstruction back to AD 1580 inferred from the varved sediments of Lake Silvaplana (southeastern Swiss Alps). Quat Res 68:184–195. doi: 10.1016/j.yqres.2007.05.004

Blenckner T (2005) A conceptual model of climate-related effects on lake ecosystems. Hydrobiologia 533:1–14. doi: 10.1007/s10750-004-1463-4

Blindheim J, Malmberg SA (2005) The mean sea level pressure gradient across the Denmark Strait as an indicator of conditions in the North Icelandic Irminger Current. The Nordic Seas: An Integrated Perspective 14:65-71.

Blois JL, Zarnetske PL, Fitzpatrick MC, Finnegan S (2013) Climate Change and the Past, Present, and Future of Biotic Interactions. Science (80-) 341:499–504. doi: 10.1126/science.1237184

Boutton TW (1991) Stable carbon isotope ratios of natural materials: II. Atmospheric, terrestrial, marine, and freshwater environments. Carbon isotope techniques.1:173.

Bradshaw EG, Anderson NJ (2001) Validation of a diatom - phosphorus calibration set for Sweden. Freshw Biol 46:1035–1048.

Brassel, S.C., Eglinton, G., Marlowe, I.T., Pflaumann, U., Sarnthein, M., 1986. Molecular stratigraphy: a new tool for climate assessment. Nature 320, 129–133.

Brenner M, Whitmore TJ, Curtis JH, et al (1999) Stable isotope (delta 13C and delta 15N) signature of sedimented organis matter as indicators of historic lake trophic state. J Paleolimnol 22:205–211. doi: 10.1023/A:1008078222806

Briner JP, Michelutti N, Francis DR, Miller GH, Axford Y, Wooller MJ, Wolfe AP (2006) A multi-proxy lacustrine record of Holocene climate change on northeastern Baffin Island, Arctic Canada. Quat Res 65:431–442

Briner JP, Overeem I, Miller G, Finkel R (2007) The deglaciation of Clyde Inlet, northeastern Baffin Island, Arctic Canada. J of Quat Sci 22:223–232

Buntgen U, Tegel W, Nicolussi K, et al (2011) 2500 Years of European Climate Variability and Human Susceptibility. Science 331:578–582.

Castañeda IS, Smith LM, Kristjánsdóttir GB, Andrews JT (2004) Temporal changes in Holoceneδ18O records from the northwest and central North Iceland Shelf. J Quat Sci 19:321–334. doi: 10.1002/jqs.841

Castañeda IS, Schouten S (2011) A review of molecular organic proxies for examining modern and ancient lacustrine environments. Quat Sci Rev 30:2851–2891. doi: 10.1016/j.quascirev.2011.07.009

Conley DJ, Schelske CL (2001) Biogenic Silica. Track Environ Chang Using Lake Sediments 3:281–293.

Crittenden PD (1975) Nitrogen fixation by lichens on Glacial Drift in Iceland. New Phytol 74:41–49.

D'Andrea, W.J., Huang, Y., 2005. Long chain alkenones in Greenland lake sediments: Low d13C values and exceptional abundance. Org. Geochem. 36, 1234–1241. doi:10.1016/j.orggeochem.2005.05.001

D'Andrea, W.J., Lage, M., Martiny, J.B.H., Laatsch, A.D., Amaral-Zettler, L.A., Sogin, M.L., Huang, Y., 2006. Alkenone producers inferred from well-preserved 18S rDNA in Greenland lake sediments. J. Geophys. Res. Biogeosciences 111, 1–8. doi:10.1029/2005JG000121

D'Andrea WJ, Huang Y, Fritz SC, Anderson NJ (2011) Abrupt Holocene climate change as an important factor for human migration in West Greenland. Proc Natl Acad Sci U S A 108:9765–9. doi: 10.1073/pnas.1101708108

D'Andrea WJ, Theroux S, Bradley RS, Huang X (2016) Does phylogeny control UK 37-temperature sensitivity? Implications for lacustrine alkenone paleothermometry. Geochim Cosmochim Acta 175:168–180. doi: 10.1016/j.gca.2015.10.031

D'Anjou RM, Bradley RS, Balascio NL, Finkelstein DB (2012) Climate impacts on human settlement and agricultural activities in northern Norway revealed through sediment biogeochemistry. Proc Natl Acad Sci U S A 109:20332–7. doi: 10.1073/pnas.1212730109

De Senerpont Domis LN, Mooij WM, Huisman J (2007) Climate-induced shifts in an experimental phytoplankton community: A mechanistic approach. Hydrobiologia 584:403–413. doi: 10.1007/s10750-007-0609-6

Denton GH, Broecker WS (2008) Wobbly ocean conveyor circulation during the Holocene? Quat Sci Rev 27:1939–1950. doi: 10.1016/j.quascirev.2008.08.008

Dodds WK, Clements WH, Gido K, et al (2010) Thresholds, breakpoints, and nonlinearity in freshwaters as related to management. J North Am Benthol Soc 29:988–997. doi: 10.1899/09-148.1

Douglas MS, Smol JP. (1999) Freshwater diatoms as indicators of environmental change in the High Arctic. In: Stoermer EF, Smol JP (eds.) The diatoms: applications for the environmental and earth sciences. 19:227

Dugmore AJ, Cook GT, Shore JS, Newton AJ (1995) Radiocarbon dating tephra layers in britain and Iceland. Radiocarbon 37:379–388.

Dyke AS, Andrews JT, Clark PU, England JH, Miller GH, Shaw J, Veillette JJ (2002) The Laurentide and Innuitian ice sheets during the Last Glacial Maximum. Quat Sci Rev 21:9–31

Eddudóttir SD, Erlendsson E, Gísladóttir G (2015) Life on the periphery is tough: Vegetation in Northwest Iceland and its responses to early-Holocene warmth and later climate fluctuations. The Holocene 25:1437–1453. doi: 10.1177/0959683615585839

M.A. Einarsson (1984) Climate of Iceland In: H. Van Loon (Ed.), World Survey of Climatology, vol. 45 Elsevier, Amsterdam, pp. 673–697

M.A. Einarsson (1993) Temperature conditions in Iceland and the Eastern North Atlantic Region, based on observations 1901-1990. Jokull 43:1-13

Eiriksson J, Knudsen KL, Haflidason H, Henriksen P (2000) Late-glacial and Holocene palaeoceanography of the North Icelandic shelf. J Quat Sci 15:23–42. doi: 10.1002/(SICI)1099-1417(200001)15:1<23::AID-JQS476>3.0.CO;2-8

Environment Canada (2016) National climate archive. http://climate.weatheroffice.ec.gc.ca

Ficken KJ, Li B, Swain DL, Eglinton G (2000) An n -alkane proxy for the sedimentary input of submerged/Floating freshwater aquatic macrophytes. Or 31:745–749.

Finkel Z V., Matheson KA, Regan KS, Irwin AJ (2010) Genotypic and phenotypic variation in diatom silicification under paleo-oceanographic conditions. Geobiology 8:433–445. doi: 10.1111/j.1472-4669.2010.00250.x

Fisher D, Zheng J, Burgess D, Zdanowicz C, Kinnard C, Sharp M, Bourgeois J (2012) Recent melt rates of Canadian arctic ice caps are the highest in four millennia. Global Planet Change 84-85:3–7

Florian CR, Miller GH, Fogel ML, et al (2015) Algal pigments in Arctic lake sediments record biogeochemical changes due to Holocene climate variability and anthropogenic global change. J Paleolimnol 53–69. doi: 10.1007/s10933-015-9835-5

Fogel ML, Cifuentes LA (1993) Isotope fractionation during primary productivity. In: Engel MH, Macko SA (eds) Organic Geochemistry. Plenum Press, New York, pp 73–98

Geirsdóttir Á, Miller GH, Axford Y (2009a) Holocene and latest Pleistocene climate and glacier fluctuations in Iceland. Quat Sci Rev 28:2107–2118. doi: 10.1016/j.quascirev.2009.03.013

Geirsdóttir Á, Miller GH, Thordarson T, Ólafsdóttir KB (2009b) A 2000 year record of climate variations reconstructed from Haukadalsvatn, West Iceland. J Paleolimnol 41:95–115. doi: 10.1007/s10933-008-9253-z

Geirsdóttir Á, Miller GH, Larsen DJ, Ólafsdóttir S (2013) Abrupt Holocene climate transitions in the northern North Atlantic region recorded by synchronized lacustrine records in Iceland. Quat Sci Rev 70:48–62. doi: 10.1016/j.quascirev.2013.03.010

Goericke R, Montoya JP (1998) Estimating the contribution of microalgal taxa to chlorophyll a in the field - Variations of pigment ratios under nutrient- and light-limited growth. Mar Ecol Prog Ser 169:97–112. doi: 10.3354/meps169097

Gronvold K, Oskarsson N, Johnsen SJ, et al (1995) Ash layers from Iceland in the Greenland GRIP ice core correlated with oceanic and land sediments. Earth Planet Sci Lett 135:149–155. doi: 10.1016/0012-821X(95)00145-3

Gu B, Schelske CL, Hoyer MV (1996) Stable isotopes of carbon and nitrogen as indicators of diet and trophic structure of the fish community in a shallow hypereutrophic lake. Journal of fish biology. 49(6):1233-43.

Gudmundsdóttir ER, Larsen G, Eiriksson J (2012) Tephra stratigraphy on the north Icelandic shelf: Extending tephrochronology into marine sediments off north iceland. Boreas 41:719–734. doi: 10.1111/j.1502-3885.2012.00258.x

Gudmundsson HJ (1997) A review of the Holocene environmental history of Iceland. Quat Sci Rev 16:81–92. doi: 10.1016/S0277-3791(96)00043-1

Hallsdóttir M, Caseldine CJ. (2005) The Holocene vegetation history of Iceland, state-of-the-art and future. In: Caseldine C, Russell A, Hardardóttir J, Knudsen O (eds.) Iceland-Modern Processes and Past Environments. 5:319.

Hassan K, Swinehart JB, Spaulding RF (1997) Evidence for holocene environmental change from C/N ratios, and d13C and d15N values in Swan Lake sediments, western Sand Hills, Nebraska. J Paleolimnol 18:121–130. doi: 10.1023/A:1007993329040

Hátún H (2005) Circulation Influence of the Atlantic Subpolar Gyre on the Thermohaline Circulation. 309:1841–1844. doi: 10.1126/science.1114777

Heathcote AJ, Anderson NJ, Prairie YT, et al (2015) Large increases in carbon burial in northern lakes during the Anthropocene. Nat Commun 6:1–6. doi: 10.1038/ncomms10016

Hede MU, Rasmussen P, Noe-Nygaard N, Clarke AL, Vinebrooke RD, Olsen J (2010) Multiproxy evidence for terrestrial and aquatic ecosystem responses during the 8.2 ka cold event as recorded at Højby Sø, Denmark. Quat Res 37:485-496.

Hendry GAF, Houghton JD, Brown SB (1987) The degradation of chlorophyll — a biological enigma. New Phytol 107:255–302.

Ho SL, Mollenhauer G, Fietz S, et al (2014) Appraisal of TEX86 and TEX86L thermometries in subpolar and polar regions. Geochim Cosmochim Acta 131:213–226. doi: 10.1016/j.gca.2014.01.001

Hobbie EA, MacKo SA, Shugart HH (1998) Patterns in N dynamics and N isotopes during primary succession in Glacier Bay, Alaska. Chem Geol 152:3–11. doi: 10.1016/S0009-2541(98)00092-8

Hodell DA, Schelske CL (1998) Production, sedimentation, and isotopic composition of organic matter in Lake Ontario. Limnol Oceanogr 43:200–214. doi: 10.4319/lo.1998.43.2.0200

Hodgson D, Vyverman W, Verleyen E, Sabbe K, Leavitt P, Taton A, Squier A, Keely B (2004) Environmental factors influencing the pigment composition of in situ benthic microbial communities in east Antarctic lakes. Aquat Microb Ecol 37:247–263

Hollander DJ, McKenzie JA (1991) CO2 control on carbon-isotope fractionation during aqueous photosynthesis: A paleo-pCO2 barometer. Geology 19:929–932.

Holtgrieve GW, Schindler DE, Hobbs WO, Leavitt PR, Ward EJ, Bunting L, Chen G, Finney BP, Gregory-Eaves I, Holmgren S, Lisac MJ, Lisi PJ, Nydick K, Rogers L a, Saros JE, Selbie DT, Shapley MD, Walsh PB, Wolfe AP (2011) A coherent signature of anthropogenic nitrogen deposition to remote watersheds of the Northern Hemisphere. Science 334

Hu FS, Ito E, Brown T a, et al (2001) Pronounced climatic variations in Alaska during the last two millennia. Proc Natl Acad Sci U S A 98:10552–10556. doi: 10.1073/pnas.181333798

Hughen KA, Overpeck JT, Anderson, RF (2000) Recent warming in a 500-year palaeotemperature record from varved sediments, Upper Soper Lake, Baffin Island, Canada. The Holocene 10:9-19

Hurrell JW (1995) Decadal trends in the north atlantic oscillation: regional temperatures and precipitation. Science 269:676–9. doi: 10.1126/science.269.5224.676

Hurrell JW, Kushnir Y, Ottersen G, Visbeck M. (2003) An overview of the North Atlantic oscillation. American Geophysical Union.

Imboden DM, Wüest a (1995) Mixing Mechanisms in Lakes. Phys Chem Lakes SE - 4 83–138. doi: 10.1007/978-3-642-85132-2_4

Japan Meteorological Agency (2006) Characteristics of Global Sea Surface Temperature Analysis Data (COBE-SST) for Climate Use. Monthly Report on Climate System Separated Volume, 12, 116pp.

Jeffery SW, Mantoura SFC, Wright SW eds. (1997) Phytoplankton pigments in oceanography. UNESCO, Paris

Jiang H, Muscheler R, Bjorck S, et al (2015) Solar forcing of Holocene summer sea-surface temperatures in the northern North Atlantic. Geology 43:2–5. doi: 10.1130/G36377.1

Jones DL, Shannon D, Murphy D V., Farrar J (2004) Role of dissolved organic nitrogen (DON) in soil N cycling in grassland soils. Soil Biol Biochem 36:749–756. doi: 10.1016/j.soilbio.2004.01.003

Joynt III EH, Wolfe AP (2001) Paleoenvironmental inference models from sediment diatom assemblages in Baffin Island lakes (Nunavut, Canada) and reconstruction of summer water temperature. Can J Fish Aquat Sci 58:1222–1243

Juggins S (2011) C2 Version 1.7: Software for ecological and paleoecological data analysis and visualisation. University of Newcastle, Newcastle upon Tyne

Julien PY, Simons DB (1985) Sediment Trasnport Capacity of Overland Flow. Trans. ASAE 28:755–762.

Justwan A, Koç N, Jennings AE (2008) Evolution of the Irminger and East Icelandic Current systems through the Holocene, revealed by diatom-based sea surface temperature reconstructions. Quat Sci Rev 27:1571–1582. doi: 10.1016/j.quascirev.2008.05.006

Kaufman D, Ager TA, Anderson NJ, Anderson PM, Andrews JT, Bartlein PJ, Brubraker LB, Coats LL, Cwynar LC, Duvall ML, Dyke AA, Edwards ME, Eisner WR, Gajewski K, Geirsdóttir Á, Hu FS, Jennings AE, Kaplan MR, Kerwin MW, Lozhkin GM, MacDonald GM, Miller GH, Mock CJ, Oswald WW, Otto-Bliesner BL, Porinchu DF, Ruhland K, Smol JP, Steig EJ, Wolfe BB (2004) Holocene thermal maximum in the western Arctic (0–180°W). Quat Sci Rev 23:529–560

Kaufman DS, Schneider DP, McKay NP, et al (2009) Recent warming reverses long-term arctic cooling. Science 325:1236–9. doi: 10.1126/science.1173983

Kaushal S, Binford MW (1999) Relationship between C:N ratios of lake sediments, organic matter sources, and historical deforestation in Lake Pleasant, Massachusetts, USA. J Paleolimnol 22:439–442. doi: 10.1023/A:1008027028029

Knowles R (1982) Denitrification. Microbiol Rev 46:43–70.

Knudsen KL, Søndergaard MKB, Eiríksson J, Jiang H (2008) Holocene thermal maximum off North Iceland: Evidence from benthic and planktonic foraminifera in the 8600–5200 cal year BP time slice. Mar Micropaleontol 67:120–142. doi: 10.1016/j.marmicro.2007.11.003

Kristinsson H (1995) Post-settlement history of Icelandic forests. Icelandic Agric. Sci. 9:31–35.

Kristjansdottir GB. (2005) Holocene climatic and environmental changes on the Iceland shelf: d18O, Mg/Ca, and tephrochronology of core MD99-2269 (Doctoral dissertation, Dept. of Geological Sciences, University of Colorado, Boulder).

Lamb AL, Leng MJ, Mohammed MU, Lamb HF (2004) Holocene climate and vegetation change in the Main Ethiopian Rift Valley, inferred from the composition (C/N and d13C) of lacustrine organic matter. Quat Sci Rev 23:881–891. doi: 10.1016/j.quascirev.2003.06.010

Langdon PG, Holmes N, Caseldine CJ (2008) Environmental controls on modern chironomid faunas from NW Iceland and implications for reconstructing climate change. J Paleolimnol 40:273–293. doi: 10.1007/s10933-007-9157-3

Larsen DJ, Miller GH, Geirsdóttir Á, Thordarson T (2011) A 3000-year varved record of glacier activity and climate change from the proglacial lake Hvítárvatn, Iceland. Quat Sci Rev 30:2715–2731. doi: 10.1016/j.quascirev.2011.05.026

Larsen DJ, Miller GH, Geirsdóttir Á, Ólafsdóttir S (2012) Non-linear Holocene climate evolution in the North Atlantic: a high-resolution, multi-proxy record of glacier activity and environmental change from Hvítárvatn, central Iceland. Quat Sci Rev 39:14–25. doi: 10.1016/j.quascirev.2012.02.006

Larsen DJ, Miller GH, Geirsdóttir Á (2013) Asynchronous Little Ice Age glacier fluctuations in Iceland and European Alps linked to shifts in subpolar North Atlantic circulation. Earth Planet Sci Lett 380:52–59. doi: 10.1016/j.epsl.2013.07.028

Larsen G, Eiriksson J, Gudmundsdottir ER (2014) Last millennium dispersal of air-fall tephra and ocean-rafted pumice towards the north Icelandic shelf and the Nordic seas. Geol Soc London, Spec Publ 398:113–140. doi: 10.1144/SP398.4

Lavaud J, Rousseau B, van Gorkom HJ, Etienne A-L (2002) Influence of the diadinoxanthin pool size on photoprotection in the marine planktonic diatom Phaeodactylum tricornutum. Plant Physiol 129:1398–1406. doi: 10.1104/pp.002014

Lawrence ADB, Schoenike RE, Quispel A, Bond G (1967) The Role of Dryas Drummondii in Vegetation Development Following Ice Recession at Glacier Bay , Alaska , with Special Reference to Its Nitrogen Fixation by Root Nodules Published by : British Ecological Society Stable URL : http://www.jstor.org/stable/225. 55:793–813.

Leavitt PR (1993) A review of factors that regulate carotenoid and chlorophyll deposition and fossil pigment abundance. J Paleolimnol 9:109–127. doi: 10.1007/BF00677513

Leavitt PR, Vinebrooke RD, Donald DB, Smol JP, Schindler DW (1997) Past Ultraviolet Radiation Environments in Lakes Derived From Fossil Pigments. Nature 338:457–459

Leavitt PR, Hodgson DA (2001) Sedimentary pigments. In: Smol, J.P., H.J.B. Birks and W.M. Last (eds.), Tracking Environmental Change using Lake Sediments. Volume 3: Terrestrial, Algal and Siliceous Indicators. Kluwer Academic Publishers, Dordrcht. The Netherlands, 295-325

Leavitt, P.R.; Hodgson, D.A.; Pienitz, R. (2003) Past UVR environments and impacts in lakes. In: Helbling, E.W.; Zagarese, H., (eds.) UV effects in aquatic organisms and ecosystems. Cambridge, Royal Society of Chemistry, 509-545

Leavitt PR, Fritz SC, Anderson NJ, et al (2009) Paleolimnological evidence of the effects on lakes of energy and mass transfer from climate and humans. Limnol Oceanogr 54:2330–2348. doi: 10.4319/lo.2009.54.6_part_2.2330

Legates, D. R., and C. J. Willmott, (1990) Mean seasonal and spatial variability in global surface air temperature. Theor. Appl. Climatol., 41, 11-21.

Leng M, Anderson NJ (2014) The influence of Holocene climate and catchment ontogeny on organic carbon cycling in low-Arctic lakes of SW Greenland. InEGU General Assembly Conference Abstracts Vol. 16: 2929

Levanič T, Eggertsson O (2008) Climatic effects on birch (Betula pubescens Ehrh.) growth in Fnjoskadalur valley, northern Iceland. Dendrochronologia 25:135–143. doi: 10.1016/j.dendro.2006.12.001

Lewin J. C. (1961) The dissolution of silica from diatom walls. Geochim. Cosmochim. Acta 21, 182–198.

Lin CK (1972) Phytoplankton succession in a Eutrophic lake with special reference to blue-green algal blooms. Hydrobiologia 39:321–334. doi: 10.1007/BF00046648

Liu, Z., Henderson, A.C.G., Huang, Y., 2006. Alkenone-based reconstruction of late-Holocene surface temperature and salinity changes in Lake Qinghai, China. Geophys. Res. Lett. 33, 2–5. doi:10.1029/2006GL026151

Lohmann K, Drange H, Bentsen M (2009) Response of the North Atlantic subpolar gyre to persistent North Atlantic oscillation like forcing. Clim Dyn 32:273–285. doi: 10.1007/s00382-008-0467-6

Marcott SA, Shakun JD, Clark PU, Mix AC (2013) A Reconstruction of Regional and Global Temperature for the Past 11,300 Years. Science 339:1198–1201

Mariotti A, Germon JC, Hubert P, et al (1981) Experimental determination of nitrogen kinetic isotope fractionation: Some principles; illustration for the denitrification and nitrification processes. Plant Soil 62:413–430. doi: 10.1007/BF02374138

Massé G, Rowland SJ, Sicre MA, et al (2008) Abrupt climate changes for Iceland during the last millennium: Evidence from high resolution sea ice reconstructions. Earth Planet Sci Lett 269:564–568. doi: 10.1016/j.epsl.2008.03.017

Mayewski P a., Rohling EE, Curt Stager J, et al (2004) Holocene climate variability. Quat Res 62:243–255. doi: 10.1016/j.yqres.2004.07.001

McKay NP, Kaufman DS, Michelutti N (2008) Biogenic silica concentration as a high-resolution, quantitative temperature proxy at Hallet Lake, south-central Alaska. Geophys Res Lett 35:4–9. doi: 10.1029/2007GL032876

Meissner KJ, Galbraith ED, Völker C (2005) Denitrification under glacial and interglacial conditions: A physical approach. Paleoceanography 20:1–13. doi: 10.1029/2004PA001083

Meyer-Jacob C, Vogel H, Boxberg F, et al (2014) Independent measurement of biogenic silica in sediments by FTIR spectroscopy and PLS regression. J Paleolimnol 52:245–255. doi: 10.1007/s10933-014-9791-5

Meyers PA, Ishiwatari R (1993) Lacustrine organic geochemistry-an overview of indicators of organic matter sources and diagenesis in lake sediments. Org Geochem 20:867–900. doi: 10.1016/0146-6380(93)90100-P

Meyers PA (1994) Preservation of elemental and isotopic source identification of sedimentary organic matter. Chem Geol 114:289–302. doi: 10.1016/0009-2541(94)90059-0

Meyers PA, Lallier-Verges E (1999) Lacustrine sedimentary organic matter records of Late Quaternary paleoclimates. J Paleolimnol 21:345–372. doi: 10.1023/A:1008073732192

Meyers PA, Teranes JL (2001) Sediment organic matter. In: Last, W.M., Smol, J.P., eds., Tracking Environmental Change Using Lake Sediments, Volume 2. Physical and Geochemical Methods. Kluwer Academic Publishers, Dordrcht. The Netherlands, 239-269.

Michelutti N (2005) Recent primary production increases in arctic lakes. Geophys Res Lett 32

Michelutti N, Wolfe AP, Briner JP, Miller GH (2007) Climatically controlled chemical and biological development in Arctic lakes. J Geophys Res 112

Michelutti N, Keatley BE, Brimble S, et al (2009) Seabird-driven shifts in Arctic pond ecosystems. Proc Biol Sci 276:591–596. doi: 10.1098/rspb.2008.1103

Miettinen A, Koç N, Hall IR, et al (2011) North Atlantic sea surface temperatures and their relation to the North Atlantic Oscillation during the last 230 years. Clim Dyn 36:533–543. doi: 10.1007/s00382-010-0791-5

Miller GH, Mode WN, Wolfe AP, Sauer PE, Bennike O, Forman SL, Short SK, Stafford TW (1999) Stratified interglacial lacustrine sediments from Baffin Island, Arctic Canada: chronology and paleoenvironmental implications. Quat Sci Rev 18:789–810

Miller GH, Wolfe AP, Briner JP, Sauer PE, Nesje A (2005) Holocene glaciation and climate evolution of Baffin Island, Arctic Canada. Quat Sci Rev 24:1703–1721

Miller GH, Brigham-Grette J, Alley RB, Anderson L, Bauch HA, Douglas MSV, Edwards ME, Elias SA, Finney BP, Fitzpatrick JJ, Funder SV, Herbert TD, Hinzman LD, Kaufman DS, MacDonald GM, Polyak L, Robock A, Serreze MC, Smol JP, Spielhagen R, White JWC, Wolfe AP, Wolff EW (2010) Temperature and precipitation history of the Arctic. Quat Sci Rev 29:1679–1715

Miller GH, Geirsdóttir Á, Zhong Y, Larsen DJ, Otto-Bliesner BL, Holland MM, Bailey D a., Refsnider K a., Lehman SJ, Southon JR, Anderson C, Björnsson H, Thordarson T (2012) Abrupt onset of the Little Ice Age triggered by volcanism and sustained by sea-ice/ocean feedbacks. Geophys Res Lett 39

Miller, G.H., Lehman, S.J., Refsnider, K. a., Southon, J.R., Zhong, Y., 2013. Unprecedented recent summer warmth in Arctic Canada. Geophys. Res. Lett. 40, 5745–5751.

Moore JJ, Hughen KA, Miller GH, Overpeck JT (2001) Little Ice Age recorded in summer temperature reconstruction from varved sediments of Donard Lake , Baffin Island , Canada. J Paleolimnol 25:503–517

Moossen H, Bendle J, Seki O, et al (2015) North Atlantic Holocene climate evolution recorded by high-resolution terrestrial and marine biomarker records. Quat Sci Rev 129:111–127. doi: 10.1016/j.quascirev.2015.10.013

Moros M, Andrews JT, Eberl DD, Jansen E (2006) Holocene history of drift ice in the northern North Atlantic: Evidence for different spatial and temporal modes. Paleoceanography 21:PA2017. doi: 10.1029/2005PA001214

Nichols, BW. 1973. Lipid composition and metabolism. In: The Biology of Blue-Green Algae, Eds. Carr, NG and Whitton, BA. Oxford, UK: Blackwell Scientific Publications 144–161.

Noel H, Garbolino E, Brauer A, et al (2001) Human impact and soil erosion during the last 5000 yrs as recorded in lacustrine sedimentary organic matter at Lac d'Annecy, the French Alps. J Paleolimnol 25:229–244. doi: 10.1023/A:1008134517923

Ólafsdóttir S, Jennings AE, Geirsdóttir Á, et al (2010) Holocene variability of the North Atlantic Irminger current on the south- and northwest shelf of Iceland. Mar Micropaleontol 77:101–118. doi: 10.1016/j.marmicro.2010.08.002

Orvik KA (2002) Major pathways of Atlantic water in the northern North Atlantic and Nordic Seas toward Arctic. Geophys Res Lett 29:1–4. doi: 10.1029/2002GL015002

Overpeck JT, Cole JE (2006) Abrupt change in Earth's climate system. Annu Rev Environ Resour 31:1–31.

Paerl HW, Paul VJ (2012) Climate change: Links to global expansion of harmful cyanobacteria. Water Res 46:1349–1363. doi: 10.1016/j.watres.2011.08.002

Pansu J, Giguet-Covex C, Ficetola GF, et al (2015) Reconstructing long-term human impacts on plant communities: An ecological approach based on lake sediment DNA. Mol Ecol 24:1485–1498. doi: 10.1111/mec.13136

Patoine A, Graham MD, Leavitt PR (2006) Spatial variation of nitrogen fixation in lakes of the northern Great Plains. 51:1665–1677.

Petterson G, Renberg I, Sjostedt-de Luna S, Arnqvist P, Anderson NJ (2010) Climatic influence on the inter-annual variability of late-Holocene minerogenic sediment supply in a boreal forest catchment. Earth Surf Proc Landforms 35:390–398

Pick FR, Lean DRS (1987) The role of macronutrients (C, N, P) in controlling cyanobacterial dominance in temperate lakes. New Zeal J Mar Freshw Res 21:425–434. doi: 10.1080/00288330.1987.9516238

Podritske B, Gajewski K (2007) Diatom community response to multiple scales of Holocene climate variability in a small lake on Victoria Island, NWT, Canada. Quat Sci Rev 26:3179–3196

Prach, K., Rachlewicz, G., 2012. Succession of vascular plants in front of retreating glaciers. Pol. Polar Res. 33, 319–328.

Prahl, F.G., Muehlhausen, L.A., Zahnle, D.L., 1988. Further evaluation of long-chain alkenones as indicators of paleoceanographic conditions. Geochim. Cosmochim. Acta 52, 2303–2310. doi:10.1016/0016-7037(88)90132-9

R Development Core Team (2010) R: a language and environment for statistical computing. R Foundation for Statistical Computing, Vienna, Austria. Available from http://www.R-project.org.

Ran L, Jiang H, Knudsen KL, Eiríksson J (2008) A high-resolution Holocene diatom record on the North Icelandic shelf. Boreas 37:399–413. doi: 10.1111/j.1502-3885.2008.00032.x

Rasmussen SO, Andersen KK, Svensson AM, et al (2006) A new Greenland ice core chronology for the last glacial termination. J Geophys Res Atmos 111:1–16. doi: 10.1029/2005JD006079

Redfield AC (1958) The Biological Control of Chemical Factors in the Environment. Am. Sci. 205–221.

Reimer PJ, McCormac FG, Moore J, et al (2002) Marine radiocarbon reservoir corrections for the mid- to late Holocene in the eastern subpolar North Atlantic. Holocene 12:129–135. doi: 10.1191/0959683602h1528rp

Reimer PJ, Baille MGL, Bard E, Bayliss A et al (2009) INTCAL09 and MARINE09 radiocarbon age calibration curves, 0-50,000 years cal BP. Radiocarbon 51:1111–1150

Reimer P, Bard E, Bayless A, et al (2013) IntCal13 and Marine13 Radiocarbon Age Calibration Curves 0–50,000 Years cal BP. Radiocarbon 55:1869–1887. doi: 10.2458/azu_js_rc.55.16947

Reuss N, Conley DJ (2005) Effects of sediment storage conditions on pigment analyses. Oceanography:methods 3:477–487.

Rosén P, Hall R, Korsman T, Renberg I (2000) Diatom transfer-functions for quantifying past air temperature, pH and total organic carbon concentration from lakes in northern Sweden. J Paleolimnol 24:109–123. doi: 10.1023/A:1008128014721

Rubensdotter L, Rosqvist G (2003) The effect of geomorphological setting on Holocene lake sediment variability, northern Swedish Lapland. J Quat Sci 18:757–767. doi: 10.1002/jqs.800

Rousseau V, Leynaert a, Daoud N, Lancelot C (2002) Diatom sucession, silicification and silicic acid availability in Belgian coastal waters (Southern North Sea). Mar Ecol Prog Ser 236:61–73. doi: 10.3354/meps236061

Rowan KS, (1989) Photosynthetic pigments of algae. Cambridge, UK, New York, NY, USA: Cambridge University Press.

Rudels B, Fahrbach E, Meincke J, et al (2002) The East Greenland Current and its contribution to the Denmark Strait overflow, ICES J. Mar Sci 59:101006/jmsc20021284. doi: 10.1006/jmsc.2002.1284

Rudels B, Björk G, Nilsson J, et al (2005) The interaction between waters from the Arctic Ocean and the Nordic Seas north of Fram Strait and along the East Greenland Current: Results from the Arctic Ocean-02 Oden expedition. J Mar Syst 55:1–30. doi: 10.1016/j.jmarsys.2004.06.008

Ruhland K, Paterson AM, Smol JP (2008) Hemispheric-scale patterns of climate-related shifts in planktonic diatoms from North American and European lakes. Glob Chang Biol 14:2740–2754. doi: 10.1111/j.1365-2486.2008.01670.x

Rundgren M (1995) Biostratigraphic Evidence of the Allerod-Younger Dryas-Preboreal Oscillation in Northern Iceland. Quat Res 44:405–416.

Rundgren M, Ingolfsson O, Bjorck S, et al (1997) Dynamic sea-level change during the last deglaciation of northern Iceland. Boreas 26:201–215.

Rundgren M (1998) Early-Holocene vegetation of northern Iceland: pollen and plant macrofossil evidence from the Skagi peninsula. The Holocene 8:553–564. doi: 10.1191/095968398669995117

Ryves, D.B., Juggins, S., Fritz, S.C., Battarbee, R.W., 2001. Experimental diatom dissolution and the quantification of microfossil preservation in sediments. Palaeogeogr. Palaeoclimatol. Palaeoecol. 172, 99–113.

Sachs, J.P., Lehman, S.J., 1999. Subtropical North Atlantic Temperatures 60,000 to 30,000 Years Ago. Science 286, 756–759. doi:10.1126/science.286.5440.756

Scheer H (1991) Structure and occurence of chlorophylls. Chlorophylls 3–23.

Schindler DW, Smol JP, Schindler DW, et al (2006) Cumulative effects of climate warming and other human activities on freshwaters of Arctic and subarctic North America. Ambio 35:160–168. doi: 10.1579/0044-7447(2006)35[160:CEOCWA]2.0.CO;2

Seppa H, Birks H (2001) July mean temperature and annual precipitation trends during the Holocene in the Fennoscandian tree-line area: pollen-based climate reconstructions. The Holocene 11:527–539. doi: 10.1191/095968301680223486

Serreze MC, Carse F, Barry RG, Rogers JC (1997) Icelandic low cyclone activity: Climatological features, linkages with the NAO, and relationships with recent changes in the Northern Hemisphere circulation. J Clim 10:453–464. doi: 10.1175/1520-0442(1997)010<0453:ILCACF>2.0.CO;2

Serreze MC, Francis JA (2006) The Arctic Amplification Debate. Clim Chang 76:241–264

Serreze MC, Barry RG (2011) Processes and impacts of Arctic amplification: A research synthesis. Glob Planet Change 77:85–96. doi: 10.1016/j.gloplacha.2011.03.004

Sicre M-A, Jacob J, Ezat U, et al (2008) Decadal variability of sea surface temperatures off North Iceland over the last 2000 years. Earth Planet Sci Lett 268:137–142. doi: 10.1016/j.epsl.2008.01.011

Smith VH (1979) Nutrient dependence of primary productivity in lakes. Limnol Oceanogr 24:1051–1064.

Smol JP, Cumming BF (2000) Tracking Long-Term Changes in Climate Using Algal Indicators In Lake Sediments. J Phycol 1011:986–1011

Smol JP, Wolfe AP, Birks HJB, Douglas MS V, et al (2005) Climate-driven regime shifts in the biological communities of arctic lakes. Proc Nat Acad Sci USA 102:4397–402

Smol JP, Douglas MS V (2007) From controversy to consensus: making the case for recent climate using lake sediments. Front Ecol Environ 5:466–474. doi: 10.1890/060162

Smol, J.P (2008) Pollution of lakes and rivers: A paleoenvironmental perspective. 2nd ed. Oxford: Wiley-Blackwell

Sobek S, Anderson NJ, Bernasconi SM, Del Sontro T (2014) Low organic carbon burial efficiency in arctic lake sediments. J Geophys Res Biogeosciences 119:1231–1243. doi: 10.1002/2014JG002612

Søndergaard M (2007) Nutrient dynamics in lakes. Doctoral Dissertation, University of Aarhus, Denmark

Staddon PL (2004) Carbon isotopes in functional soil ecology. Trends Ecol Evol 19:148–154. doi: 10.1016/j.tree.2003.12.003

Stauber JL, Jeffrey SW (1988) Photosynthetic pigments in fifty-one species of marine diatoms. J Phycol. 24:158-72.

Stothers RB (1998) Far reach of the Tenth century Eldgja eruption, Iceland. Clim Change 39:715–726. doi: 10.1023/A:1005323724072

Stramski D, Sciandra A, Claustre H (2002) Effects of temperature, nitrogen, and light limitation on the optical properties of the marine diatom Thalassiosira pseudonana. Limnol Oceanogr 47:392–403. doi: 10.4319/lo.2002.47.2.0392

Striberger J, Björck S, Holmgren S, Hamerlík L (2012) The sediments of Lake Lögurinn - A unique proxy record of Holocene glacial meltwater variability in eastern Iceland. Quat Sci Rev 38:76–88. doi: 10.1016/j.quascirev.2012.02.001

Talbot MR (2001) Nitrogen isotopes in paleolimnology. In: Last WM, Smol JP (eds) Tracking Environmental Change Using Lake Sediments. Volume 2: Physical and Geochemical Methods, Volume 2. . Kluwer Academic Publishers, Dordrcht. The Netherlands, pp 401–439

Tang CCL, Ross CK, Yao T, et al (2004) The circulation, water masses and sea-ice of Baffin Bay. Prog Oceanogr 63:183–228. doi: 10.1016/j.pocean.2004.09.005

Tani Y, Matsumoto GI, Soma M, Soma Y, Hashimoto S, Kawai T (2009) Photosynthetic pigments in sediment core HDP-04 from Lake Hovsgol, Mongolia, and their implication for changes in algal productivity and lake environment for the last 1Ma. Quatern Int 205:74–83

Teranes JL, Bernasconi SM (2000) The record of nitrate utilization and productivity limitation provided by d15N values in lake organic matter—. A study of sediment trap and core sediments from Baldeggersee, Switzerland. Limnol Oceanogr 45:801–813. doi: 10.4319/lo.2000.45.4.0801

Thomas EK, Briner JP (2008) Climate of the past millennium inferred from varved proglacial lake sediments on northeast Baffin Island, Arctic Canada. J Paleolimnol 41:209–224

Thomas EK, Briner JP, Axford Y, Francis DR, Miller GH, Walker IR (2011) A 2000-yr-long multi-proxy lacustrine record from eastern Baffin Island, Arctic Canada reveals first millennium AD cold period.

Thorarinsson T, (1974). þjóðin lifði en skógurinn dó [The people survived but the woods perished]. Ársrit Skógræktarfélags Íslands, 1974, 16–29. [In Icelandic, English summary].

Thordarson T, Larsen G (2007) Volcanism in Iceland in historical time: Volcano types, eruption styles and eruptive history. J Geodyn 43:118–152. doi: 10.1016/j.jog.2006.09.005

Thornalley DJR, Elderfield H, McCave IN (2009) Holocene oscillations in temperature and salinity of the surface subpolar North Atlantic. Nature 457:711–4. doi: 10.1038/nature07717

Trouet V, Esper J, Graham NE, et al (2009) Persistent positive North Atlantic oscillation mode dominated the Medieval Climate Anomaly. Science 324:78–80. doi: 10.1126/science.1166349

Tzedakis PC, Frogley MR, Lawson IT, et al (2004) Ecological thresholds and patterns of millennial-scale climate variability: the response of vegetation in Greece during the last glacial period. Geology. 32(2):109-12.

Veit, H., Marti, T., Winiger, L., 2011. Environmental changes in Northern Iceland since the Younger Dryas inferred from periglacial slope deposits. The Holocene 22, 325–335. doi:10.1177/0959683611423695

Wang Y, Wooller MJ (2006) The stable isotopic (C and N) composition of modern plants and lichens from northern Iceland : with ecological and paleoenvironmental implications. Jokull:27–37

Wanner H, Solomina O, Grosjean M, et al (2011) Structure and origin of Holocene cold events. Quat Sci Rev 30:3109–3123. doi: 10.1016/j.quascirev.2011.07.010

Warthmann R, Lith Y Van, Mckenzie JA (2000) Bacterially induced dolomite precipitation in anoxic culture experiments. Geology 28:1091–1094

Weintraub MN, Schimel JP (2003) Interactions between Carbon and Nitrogen Mineralization and Soil Organic Matter Chemistry in Arctic Tundra Soils. Ecosystems 6:129–143. doi: 10.1007/s10021-002-0124-6

Whitehead PG, Wilby RL, Battarbee RW, et al (2009) A review of the potential impacts of climate change on surface water quality. Hydrol Sci 54:101–123. doi: 10.1623/hysj.54.1.101

Willis KJ, Bailey RM, Bhagwat SA, Birks HJB (2010) Biodiversity baselines, thresholds and resilience: Testing predictions and assumptions using palaeoecological data. Trends Ecol Evol 25:583–591. doi: 10.1016/j.tree.2010.07.006

Wilson CR, Michelutti N, Cooke CA, Briner JP, Wolfe AP, Smol JP (2012) Arctic lake ontogeny across multiple interglaciations. Quat Sci Rev 31:112–126

Wolfe AP (1994) Late Wisconsinan and Holocene diatom stratigraphy from Amarok Lake , Baffin Island, N.W.T., Canada. J Paleolimnol 10:129–139

Wolfe AP, Hartling JW (1996) The late Quaternary development of three ancient tarns on southwestern Cumberland Peninsula, Baffin Island, Arctic Canada: paleolimnological evidence from diatoms and sediment chemistry. J Paleolimnol 15:1–18

Wolfe AP, Baron JS, Cornett RJ (2001) Anthropogenic nitrogen deposition induces rapid ecological changes in alpine lakes of the Colorado Front Range (USA). J Paleolimnol 25:1–7. doi: 10.1023/A:1008129509322

Wolfe AP (2002) Climate modulates the acidity of Arctic lakes on millennial time scales. Geology 30:215–218

Wolfe AP (2003) Diatom community responses to late-Holocene climatic variability, Baffin Island, Canada: a comparison of numerical approaches. The Holocene 13:29–37

Wolfe AP, Miller GH, Olsen CA, Forman SL, Doran PT, Holmgren SU (2004) Geochronology of high latitude lake sediments. In Long-Term Environmental Change in Arctic and Antarctic Lakes. Springer Netherlands pp. 19-52

Wolfe AP, Hobbs WO, Birks HH, Briner JP, Holmgren SU, Ingólfsson Ó, Kaushal SS, Miller GH, Pagani M, Saros JE, Vinebrooke RD (2013) Stratigraphic expressions of the Holocene–Anthropocene transition revealed in sediments from remote lakes. Earth Sci Rev 116:17–34

Wolfe BB, Edwards TWD, Aravena R (1999) Changes in carbon and nitrogen cyclingduring tree-line retreat recorded in the isotopic content of lacustrine organic matter, western Taimyr Peninsula, Russia. The Holocene 9:215–222. doi: 10.1191/095968399669823431

Wolin JA, Duthie HC. (1999) Diatoms as indicators of water level change in freshwater lakes. The diatoms: Applications for the environmental and earth sciences. 183-202.

Wooller M, Wang Y, Axford Y (2008) A multiple stable isotope record of Late Quaternary limnological changes and chironomid paleoecology from northeastern Iceland. J Paleolimnol 40:63–77. doi: 10.1007/s10933-007-9144-8

Wunsch C (1980) Meridional heat flux of the North Atlantic Ocean. Proc Natl Acad Sci 77:5043–5047.

Zalasiewicz J, Williams M, Haywood A, Ellis M (2011) The Anthropocene: a new epoch of geological time? Philos Trans A Math Phys Eng Sci 369:835–41. doi: 10.1098/rsta.2010.0339

Zhang Y, Prepas EE (1996) Regulation of the dominance of planktonic diatoms and cyanobacteria in four eutrophic hardwater lakes by nutrients, water column stability, and temperature. Can J Fish Aquat Sci 53:621–633. doi: 10.1139/f95-205

Zhong Y, Miller GH, Otto-Bliesner BL, et al (2011) Centennial-scale climate change from decadally-paced explosive volcanism: A coupled sea ice-ocean mechanism. Clim Dyn 37:2373–2387. doi: 10.1007/s00382-010-0967-z

Zink, K.G., Leythaeuser, D., Melkonian, M., Schwark, L., 2001. Temperature dependency of long-chain alkenone distributions in Recent to fossil limnic sediments and in lake waters. Geochim. Cosmochim. Acta 65, 253–265. doi:10.1016/S0016-7037(00)00509-3

Appendix A.

Isotopic composition of modern samples from Iceland.

Type	SID	Collected by	13C	15N	C:N
Algae	GDD10-Aq algae	Zalzal	-18.73	-1.6	11.3
Algae	GDD10-Plankton	Zalzal	-31.11	4.4	
Algae	SVG10-Plankton	Zalzal	-31.1	1.1	6.2
Algae	BAE10-Plankton	Zalzal	-20.86	0.9	6.3
Algae	TORF algae	Florian	-18.54	-1.0	24.2
Algae	TORF epilithon	Florian	-8.12	-0.4	14.5
Algae	TORF epilithon 2	Florian	-6.67	-0.5	17.4
Algae	TORF epilithon 1-2	Florian	-7.16	-0.6	15.0
Algae	TORF epilithon 2-2	Florian	-8.41	-0.4	15.7
Algae	BAE-1 epilithon	Florian	-24.02	2.4	15.3
Algae	BAE-1 epilithon-2	Florian	-24.02	2.2	14.9
Algae	BAE-3 epilithon	Florian	-23.92	1.1	13.8
Algae	BAE 3 epilithon 2	Florian	-24.14	1.1	13.6
Aquatic Veg	LakeB-Aq-1	Zalzal	-18.53	-2.8	47.3
Aquatic Veg	SVG10-Aq-2	Zalzal	-23.99	-3.0	30.7
Aquatic Veg	SVG10-Aq-4	Zalzal	-22.40	-1.9	20.3
Aquatic Veg	BAE10-Aq-5	Zalzal	-11.27	3.2	23.2
Aquatic Veg	BAE10-Aq-1	Zalzal	-15.05	0.7	34.9
Aquatic Veg	BAE10-Aq-2	Zalzal	-10.54	-1.5	27.5
Aquatic Veg	GJG10-Aq-1	Zalzal	-15.48	1.5	18.5
Aquatic Veg	TORF Aq. 1	Florian	-11.26	-14.5	14.2
Aquatic Veg	TORF Aq. 2	Florian	-11.09	-15.5	8.7
Soil	BAE-1 Soil	Florian	-24.66	4.2	13.6
Soil	BAE-1-2 Soil	Florian	-25.12	2.9	16.2
Soil	BAE-3 Soil a	Florian	-26.25	1.5	15.7
Soil	TORF-1-2 Soil	Florian	-26.17	2.8	17.0
Soil	TORF-2 Soil	Florian	-25.17	4.3	17.3
Soil	BAE-3 Soil b	Florian	-25.89	4.3	13.6
Soil	TORF-1 Soil	Florian	-25.39	4.9	16.7
Soil	BAE-2 Soil	Florian	-26.28	3.2	18.9
Soil	BAE-3-2 Soil	Florian	N/A	-1.1	36.2
Soil	M13-I 01-1	Miller	-24.93	2.7	14.3
Soil	M13-01-2	Miller	-24.99	2.6	14.5
Soil	M13-02-1	Miller	-25.77	0.3	21.0
Soil	M13-02-2	Miller	-25.87	0.2	22.0
Soil	M13-03-1	Miller	-24.74	2.3	17.2
Soil	M13-03-2	Miller	-24.84	2.1	17.8
Soil	M13-04-1	Miller	-24.90	-0.7	15.7
Soil	M13-04-2	Miller	-24.98	0.1	15.0
Soil	M13-05-1	Miller	-26.31	-0.4	20.6
Soil	M13-05-2	Miller	-26.50	-1.6	21.7
Soil	M13-06-1	Miller	-26.39	0.6	20.6

Soil	M13-06-2	Miller	-26.45	0.4	21.4
Soil	M13-07-1	Miller	-25.19	-0.8	19.1
Soil	M13-07-2	Miller	-25.61	-1.2	22.1
Soil	M13-08-1	Miller	-25.93	3.6	15.1
Soil	M13-08-2	Miller	-25.98	3.4	15.6
Soil	M13-09-1	Miller	-27.29	1.4	19.6
Soil	M13-09-2	Miller	-27.15	1.3	20.0
Soil	M13-10-1	Miller	-28.00	1.0	16.6
Soil	M13-10-2	Miller	-28.03	1.0	16.2
Soil	M13-11-1	Miller	-26.86	3.1	14.0
Soil	M13-11-2	Miller	-26.90	3.0	14.1
Soil	M13-12-1	Miller	-26.92	4.1	13.1
Soil	M13-12-2	Miller	-26.86	4.2	13.1
Soil	M13-13-1	Miller	-27.56	2.0	16.5
Soil	M13-13-2	Miller	-27.57	2.2	16.1
Terrestrial Veg	GDD10-Grass-1	Zalzal	-28.62	-0.8	33.7
Terrestrial Veg	GDD10-Moss-1	Zalzal	-27.10	-3.9	44.0
Terrestrial Veg	SVG10-Moss-2	Zalzal	-26.15	-3.7	65.4
Terrestrial Veg	SVG10-Grass-2	Zalzal	-28.78	-2.0	62.7
Terrestrial Veg	SVG10-Moss3	Zalzal	-24.72	-3.2	39.8
Terrestrial Veg	BAE-1 Moss	Florian	-26.13	-2.1	67.0
Terrestrial Veg	BAE-1 Leaf	Florian	-31.15	-1.2	27.8
Terrestrial Veg	BAE-1 Grass	Florian	-29.17	-1.8	67.9
Terrestrial Veg	BAE-1-2 Moss	Florian	-22.27	0.9	14.3
Terrestrial Veg	TORF-1 Leaf	Florian	-30.36	0.8	42.6
Terrestrial Veg	TORF-1 Moss	Florian	-29.62	-1.3	43.1

Appendix B.

Modern water chemistry and isotopic composition from July 2014

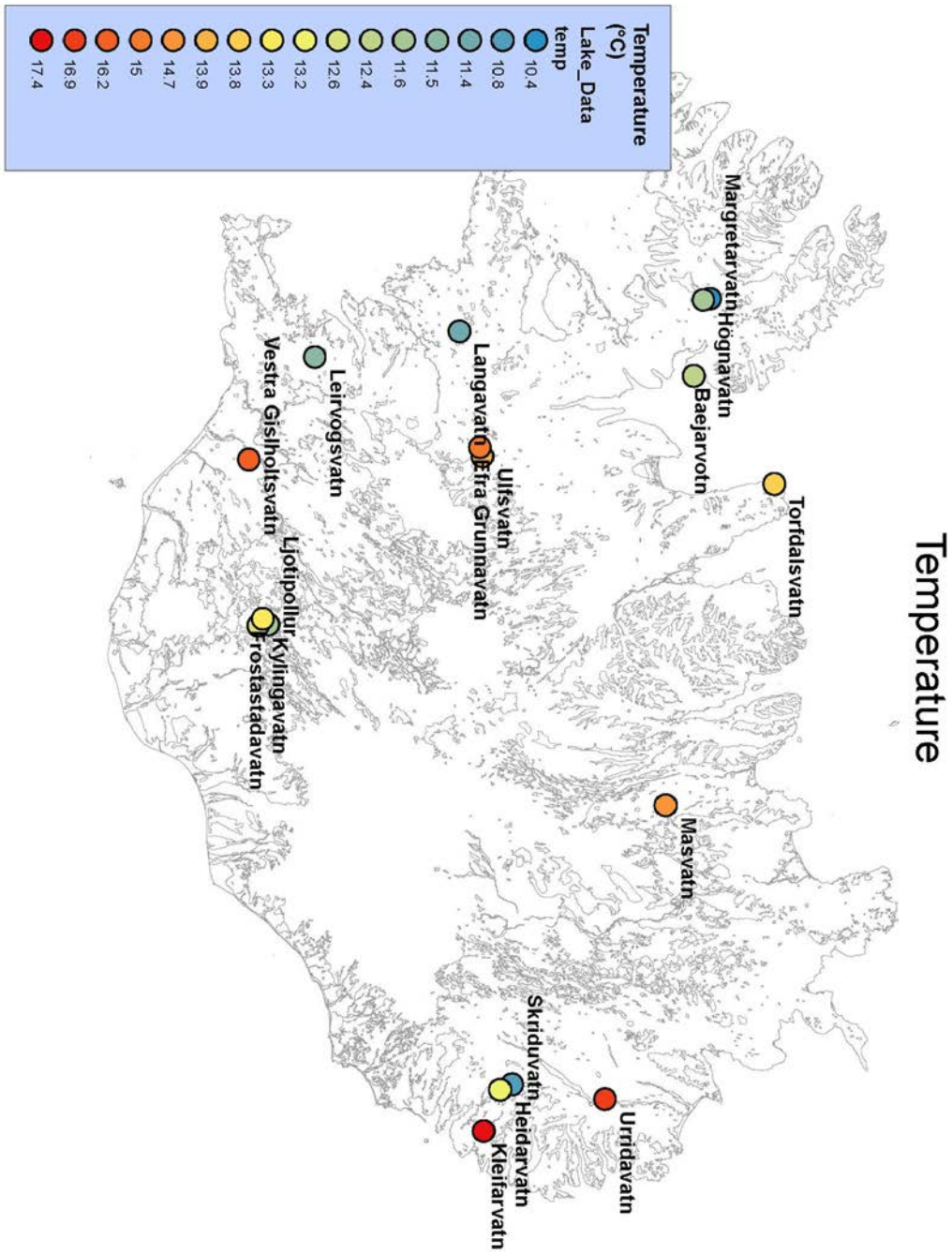

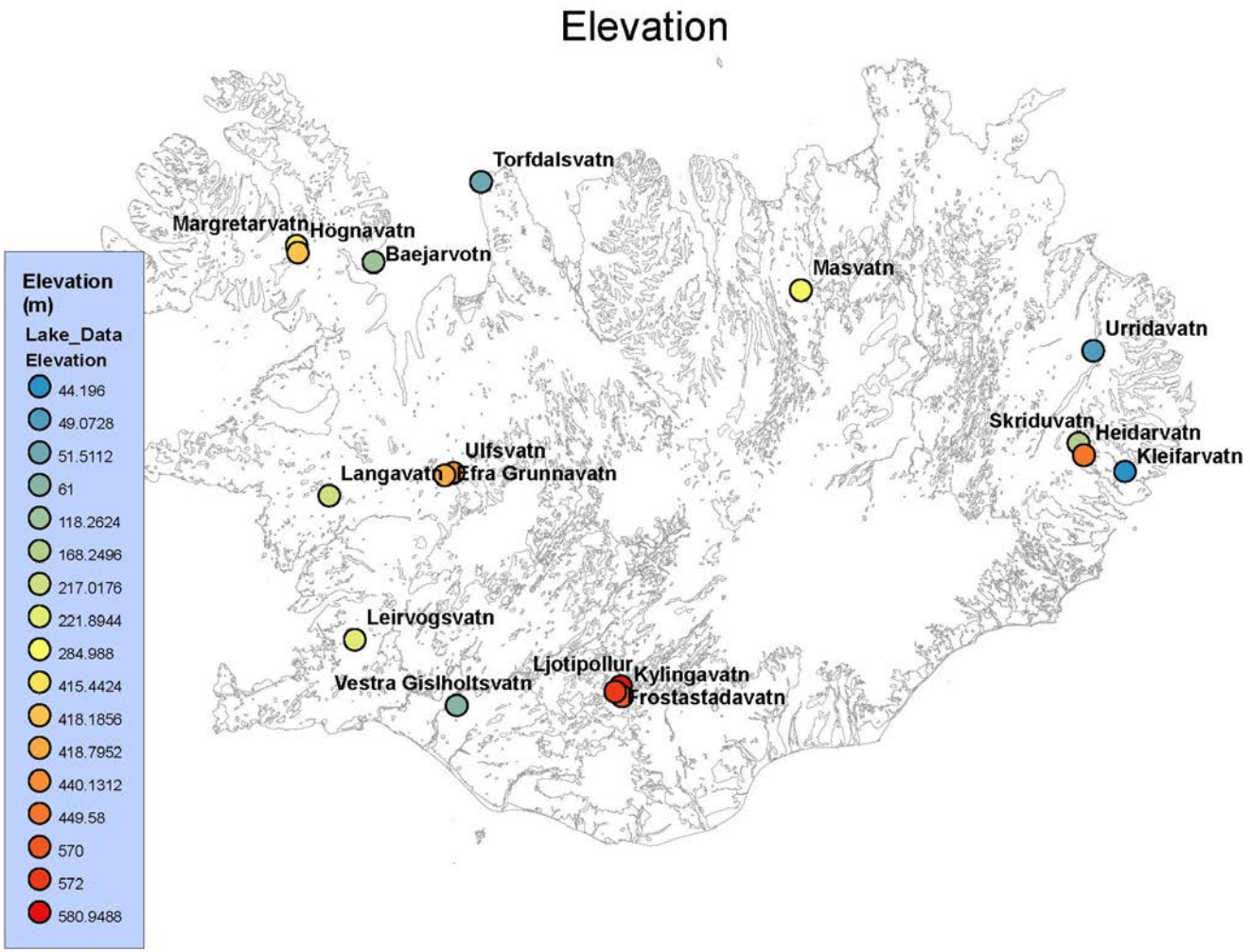
Elevation
Elevation (m)
Lake_Data Elevation
44.196
49.0728
51.5112
61
118.2624
168.2496
217.0176
221.8944
284.988
415.4424
418.1856
418.7952
440.1312
449.58
570
572
580.9488
Torfdalsvatn
Margretarvatn
Högnavatn
Baejarvotn
Masvatn
Urridavatn
Skriduvatn
Heidarvatn
Kleifarvatn
Ulfsvatn
Langavatn
Efra Grunnavatn
Leirvogsvatn
Ljotipollur
Kylingavatn
Frostastadavatn
Vestra Gislholtsvatn

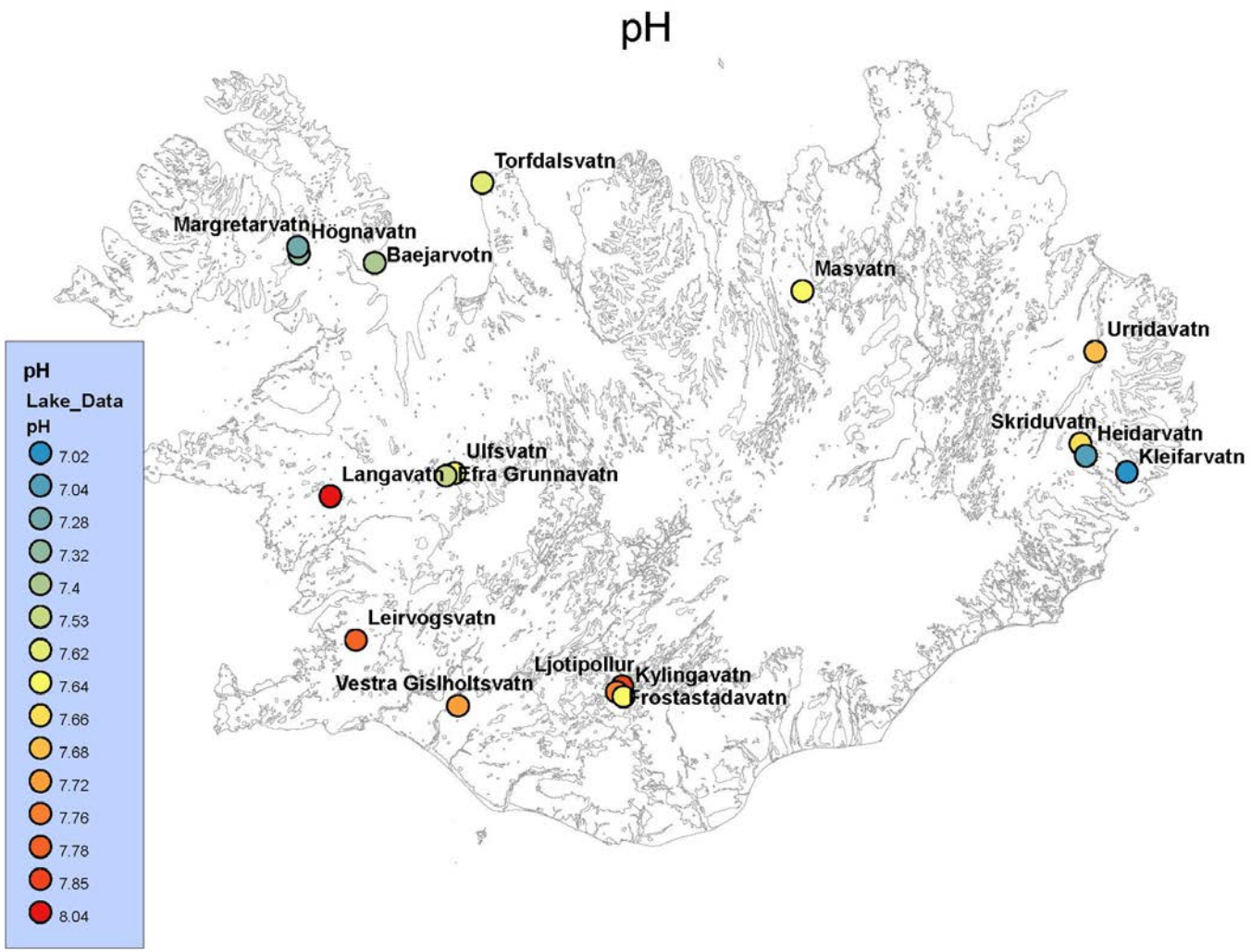
pH
Torfdalsvatn
Margretarvatn
Högnavatn
Baejarvotn
Masvatn
Urridavatn
Skriduvatn
Heidarvatn
Kleifarvatn
Ulfsvatn
Langavatn
Efra Grunnavatn
Leirvogsvatn
Ljotipollur
Kylingavatn
Vestra Gislholtsvatn
Frostastadavatn
pH
Lake_Data
pH
7.02
7.04
7.28
7.32
7.4
7.53
7.62
7.64
7.66
7.68
7.72
7.76
7.78
7.85
8.04

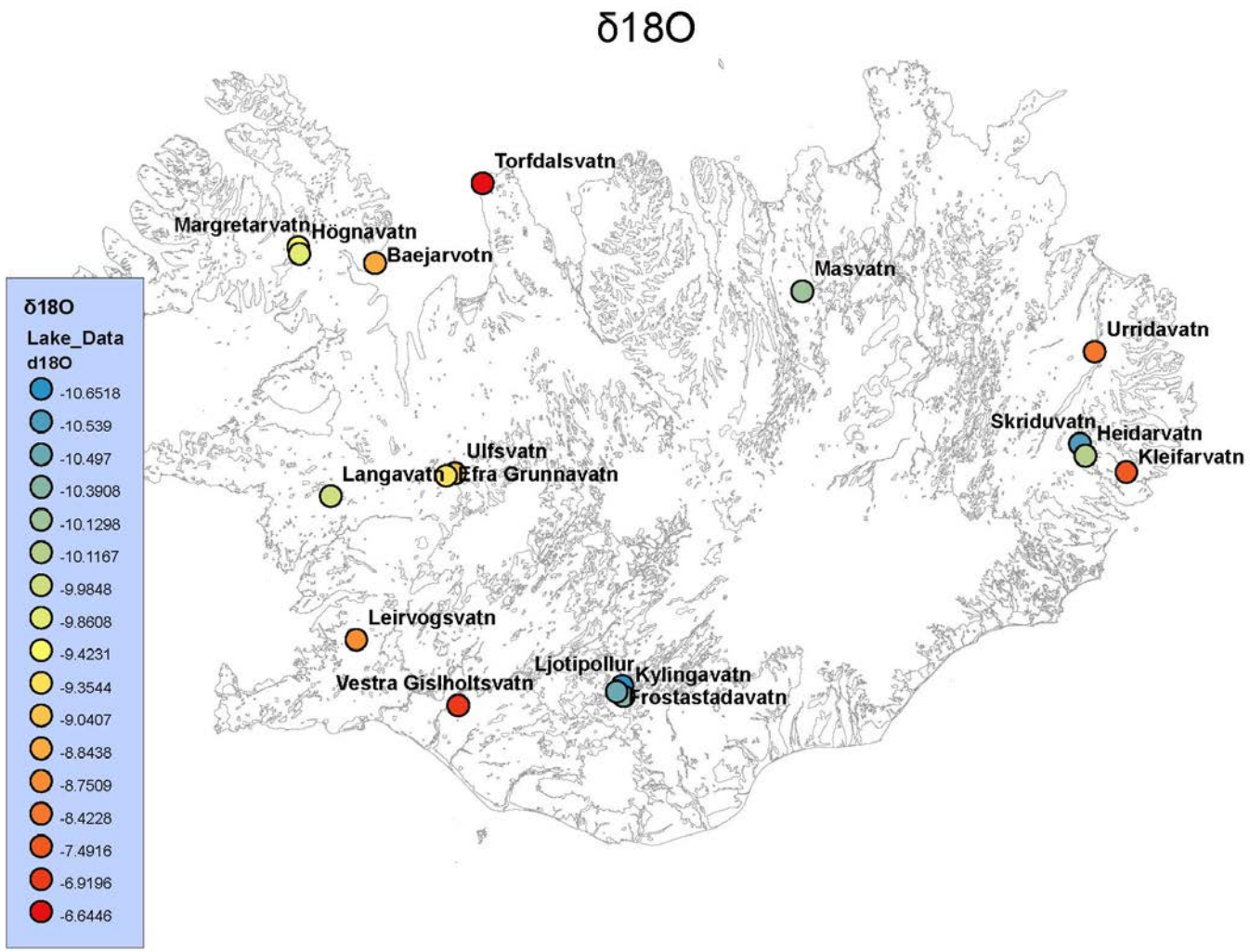
δ18O
δ18O
Lake_Data
d18O
-10.6518
-10.539
-10.497
-10.3908
-10.1298
-10.1167
-9.9848
-9.8608
-9.4231
-9.3544
-9.0407
-8.8438
-8.7509
-8.4228
-7.4916
-6.9196
-6.6446
Torfdalsvatn
Margretarvatn
Högnavatn
Baejarvotn
Masvatn
Urridavatn
Skriduvatn
Heidarvatn
Kleifarvatn
Ulfsvatn
Langavatn
Efra Grunnavatn
Leirvogsvatn
Ljotipollur
Kylingavatn
Frostastadavatn
Vestra Gislholtsvatn

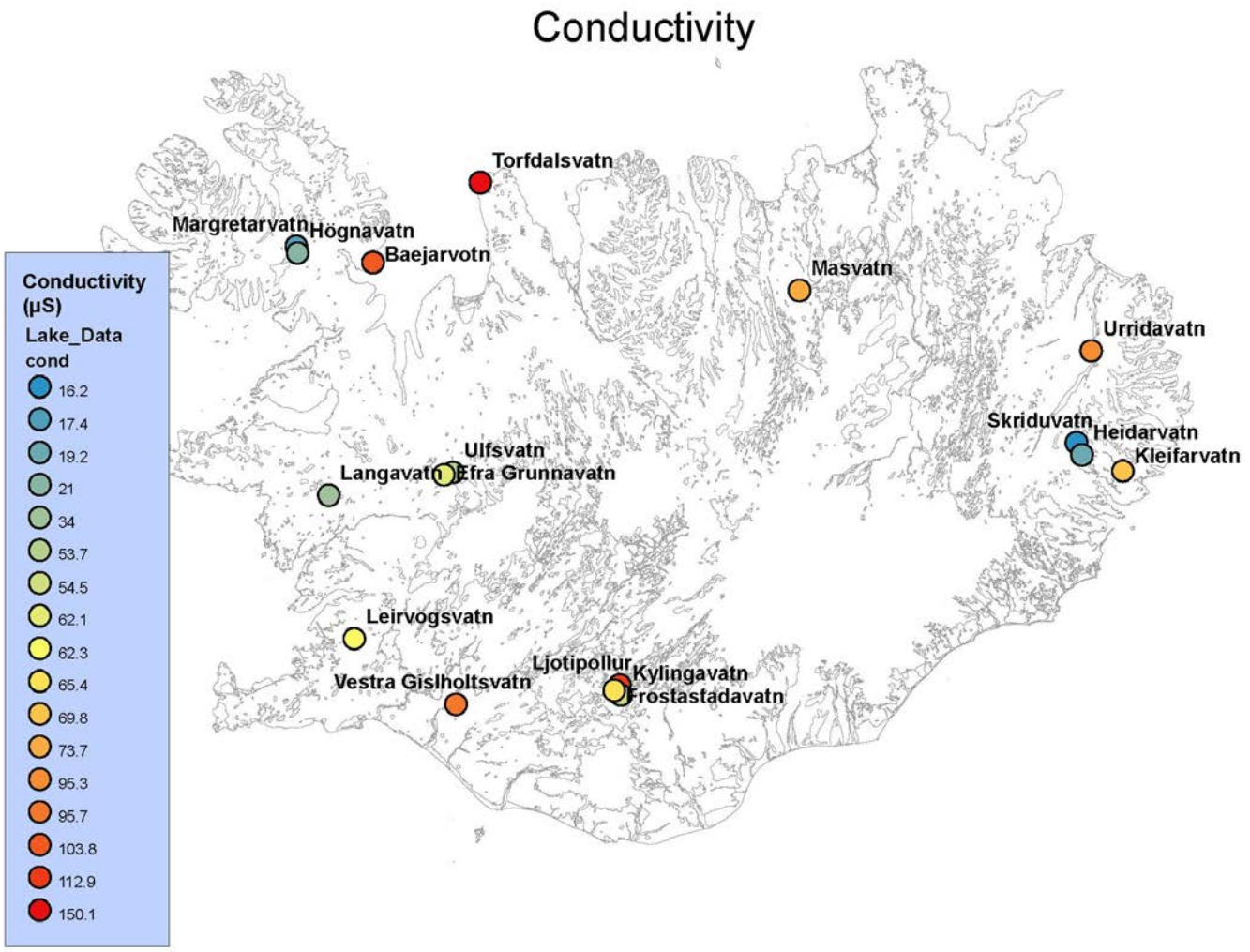
Conductivity
Conductivity (µS)
Lake_Data
cond
16.2
17.4
19.2
21
34
53.7
54.5
62.1
62.3
65.4
69.8
73.7
95.3
95.7
103.8
112.9
150.1
Torfdalsvatn
Margretarvatn
Högnavatn
Baejarvotn
Masvatn
Urridavatn
Skriduvatn
Heidarvatn
Kleifarvatn
Ulfsvatn
Langavatn
Efra Grunnavatn
Leirvogsvatn
Ljotipollur
Kylingavatn
Frostastadavatn
Vestra Gislholtsvatn

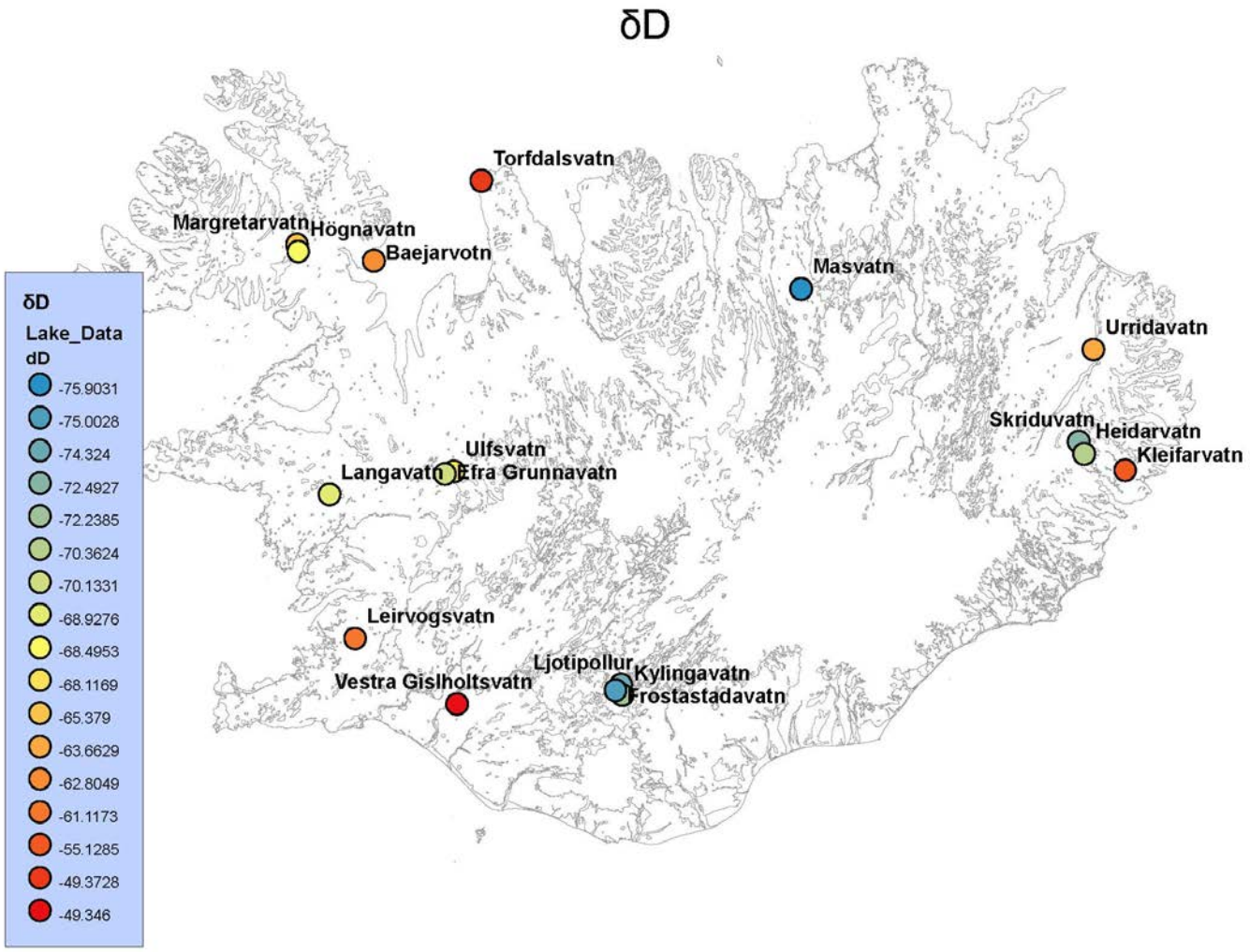
δD
Torfdalsvatn
Margretarvatn
Högnavatn
Baejarvotn
Masvatn
Urridavatn
Skriduvatn
Heidarvatn
Kleifarvatn
Ulfsvatn
Langavatn
Efra Grunnavatn
Leirvogsvatn
Ljotipollur
Kylingavatn
Vestra Gislholtsvatn
Frostastadavatn
δD
Lake_Data
dD
-75.9031
-75.0028
-74.324
-72.4927
-72.2385
-70.3624
-70.1331
-68.9276
-68.4953
-68.1169
-65.379
-63.6629
-62.8049
-61.1173
-55.1285
-49.3728
-49.346

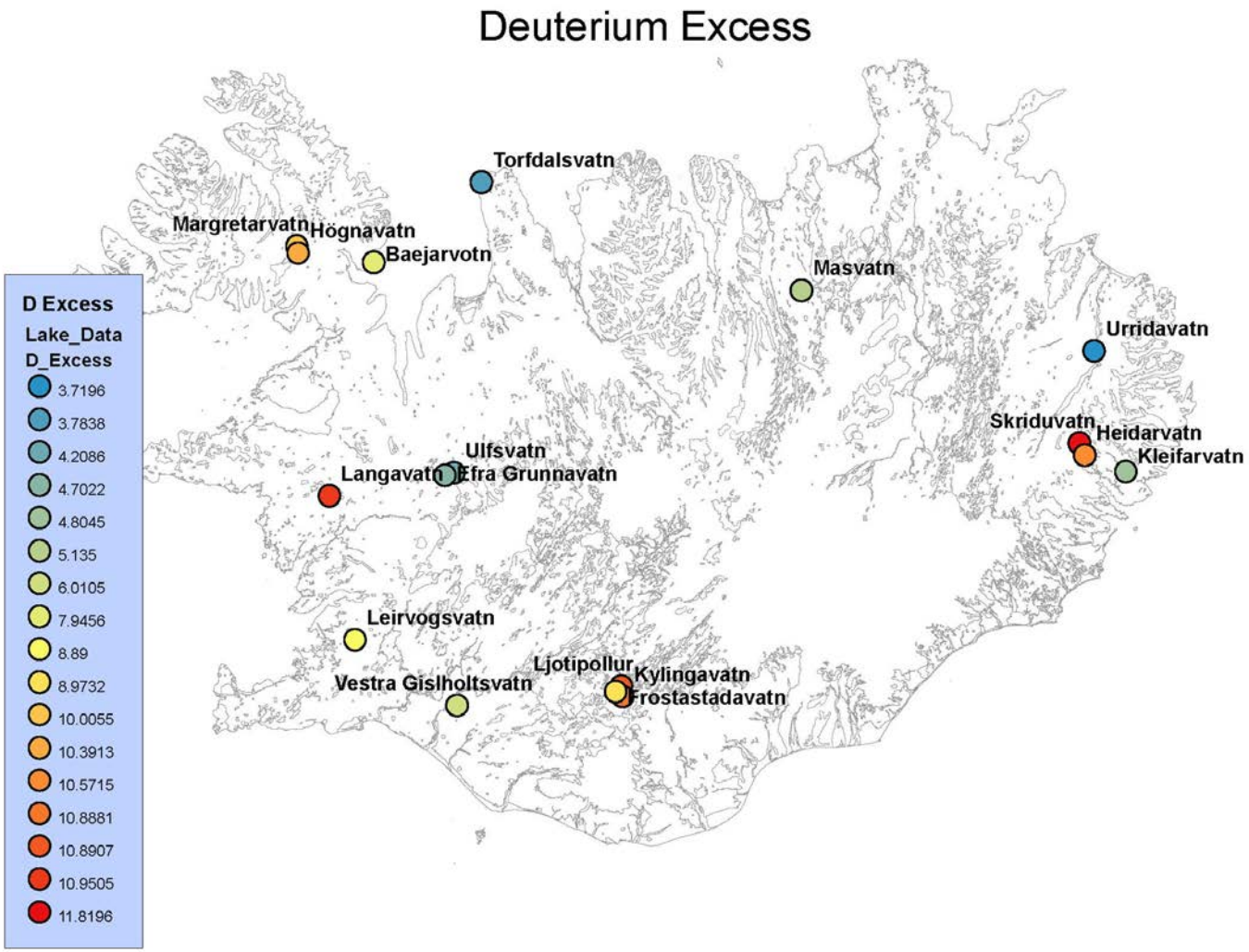
Deuterium Excess
D Excess
Lake_Data
D_Excess
3.7196
3.7838
4.2086
4.7022
4.8045
5.135
6.0105
7.9456
8.89
8.9732
10.0055
10.3913
10.5715
10.8881
10.8907
10.9505
11.8196
Torfdalsvatn
Margretarvatn
Högnavatn
Baejarvotn
Masvatn
Urridavatn
Skriduvatn
Heidarvatn
Kleifarvatn
Ulfsvatn
Langavatn
Efra Grunnavatn
Leirvogsvatn
Ljotipollur
Kylingavatn
Frostastadavatn
Vestra Gislholtsvatn

Lake name	lat	long	Elevation	temp	pH	cond	temp corr. cond	salinity
Margaretarvatn	N65 46.543	W22 11.192	415	10.4	7.28	17.4	24	0
Skriduvatn	N64 57.056	W14 38.199	168	10.8	7.66	16.2	22.2	0
Langavatn	N64 46.721	W21 45.476	217	11.4	8.04	34	45	0
Leirvogsvatn	N64 12.114	W21 27.809	222	11.5	7.78	62.3	83.5	0
By Soleyjardalur	N65 44.875	W22 10.254	418	11.6	7.32	21	28.1	0
Ljotipollur	N64 02.192	W19 00.038	581	11.6	7.85	112.9	151.3	0.1
Baejarvotn	N65 43.476	W21 25.528	118	12.4	7.4	103.8	136.7	0.1
Kylingavatn	N63 59.723	W18 59.378	570	12.6	7.64	54.5	71.3	0
Heidarvatn	N64 54.136	W14 35.591	450	13.2	7.04	19.2	24.8	0
Frostastadavatn	N64 00.877	W19 02.980	572	13.3	7.76	65.4	84.2	0
Torfdalsvatn	N66 03.696	W20 23.238	52	13.8	7.62	150.1	191	0.1
Ulfsvatn	N64 53.265	W20 35.458	440	13.9	7.64	53.7	68.1	0
Masvatn	N65 37.313	W17 14.438	285	14.7	7.64	73.7	91.6	0
Efra Grunnavatn	N64 52.610	W20 40.315	419	15	7.53	62.1	74.3	0
Vestra Gislholtsvatn	N63 57.017	W20 30.481	61	16.2	7.72	95.7	115.2	0.1
Urridavatn	N65 19.008	W14 25.782	49	16.9	7.68	95.3	112.8	0.1
Kleifarvatn	N64 49.458	W14 12.689	44	17.4	7.02	69.8	81.3	0

Surface water isotopes July 2014

Sample Identi	d18O	dD	d-excess
LAN-1	-9.99354146	-69.1542938	10.79403787
MAR-1	-9.42459404	-65.4049127	9.991839621
SOL-1	-9.81336048	-68.5590045	9.947879293
BAE-1	-8.83803261	-62.6852585	8.01900244
SHL-1	-9.41430746	-70.066015	5.248444635
ULF-1	-9.02016831	-68.1177869	4.043559576
TORF-1	-6.69780779	-50.2527423	3.329719965
MAS-1	-10.1152633	-75.9396013	4.982505294
URR-1	-8.38524466	-63.8262351	3.25572217
EST-1	-10.560892	-72.5458313	11.94130469
FOG-1	-10.0963819	-70.3957183	10.37533672
BGY-1	-7.45474199	-55.0276929	4.610243051
KYL-1	-10.5076478	-72.2122402	11.84894196
FRO-1	-10.4928091	-75.2192504	8.723222302
LJO-1	-10.598566	-74.4645155	10.32401278
VGHV-1	-7.0153909	-49.6526076	6.470519569
LEI-1	-8.77164006	-61.3913618	8.781758702
LAN-1-2	-9.9759824	-68.7008953	11.10696394
MAR-1-2	-9.42153374	-65.353088	10.01918194
SOL-1-2	-9.90830255	-68.4316532	10.83476721
BAE-1-2	-8.84959355	-62.9246335	7.872114937
SHL-1-2	-9.29451432	-70.200213	4.15590157
ULF-1-2	-9.06120671	-68.1160456	4.373607993
TORF-1-2	-6.68982142	-49.9151748	3.603396551
MAS-1-2	-10.1442615	-75.8666308	5.287460987
URR-1-2	-8.46036961	-63.4995519	4.183404943
EST-1-2	-10.5171731	-72.4395157	11.69786686
FOG-1-2	-10.1371102	-70.3291342	10.76774708
BGY-1-2	-7.52852082	-55.2294024	4.998764111
KYL-1-2	-10.2740117	-72.2648348	9.927258603
FRO-1-2	-10.501181	-74.7862525	9.223195768
LJO-1-2	-10.7051066	-74.1835305	11.45732212
VGHV-1-2	-6.82373505	-49.039367	5.550513417
LEI-1-2	-8.73018651	-60.8431681	8.998323969
TORF-1-3	-6.68143533	-49.2626221	4.188860552
TORF-1-4	-6.71764514	-49.2723995	4.468761621
TORF-1-5	-6.57763039	-49.1238496	3.497193544
TORF-1-6	-6.55176795	-48.9485085	3.465635143
TORF-1-7	-6.62953421	-49.0298201	4.006453554
TORF-1-8	-6.61097217	-49.1770628	3.710714599

Appendix C. Sediment core data

Age (Years BF	TOC%	C/N	13C	15N	%C flux	Chlorophyll F	Bsi Flux (g/cr	Lutein Flux (ι	Diatoxanthin
-60	11.609	10.481	-23.792	0.837	0.058733	0.13872	0.038553	0.00059584	0.00015012
-56	12.423	10.893	-23.77	0.736	0.07672	0.17325		0.00077222	0.00017915
-53	12.37	10.915	-23.439	0.49	0.1375	0.25218	0.090924	0.0014096	0.0003802
-49	11.14	10.619	-23.464	0.514	0.1236	0.32084		0.0016712	0.00038892
-45	13.233	10.786	-23.449	0.562	0.15376	0.25027	0.070645	0.0012819	0.00034276
-41	12.543	10.974	-23.301	0.55	0.10789	0.21159		0.0010777	0.00028788
-36	11.977	10.819	-23.314	0.638	0.20758	0.39209	0.087696	0.0021856	0.00056965
-32	12.889	10.689	-23.255	0.567	0.14778	0.27172		0.0013491	0.00037543
-27	12.241	10.711	-23.393	0.575	0.17756	0.34215	0.11721	0.0017004	0.00036629
-21	12.111	10.756	-23.095	0.655	0.16142	0.32949		0.0015466	0.00033318
-16	12.501	10.749	-22.816	0.638	0.18531	0.17295	0.12377	0.00078844	0.00019011
-9	11.408	10.625	-22.979	0.779	0.15667	0.19374		0.00080777	0.00019016
-3	12.085	10.723	-22.739	0.828	0.14241	0.22148	0.19537	0.00099134	0.00025803
5	11.458	10.603	-22.822	0.975	0.1515	0.25986		0.0010533	0.0002861
13	8.3295	10.589	-22.669	1.061	0.11898	0.31326	0.10085	0.0012347	0.00037778
21	11.291	10.4	-22.848	1.213	0.12695	0.24114		0.00094303	0.00030253
30	10.727	10.43	-22.822	1.2	0.10054	0.17679	0.06523	0.0011425	0.00025344
40	9.6363	10.1	-23.176	1.526	0.077417	0.15123		0.0006467	0.00017624
51	8.5685	10.03	-23.241	1.616	0.06397	0.16678	0.042853	0.00061414	0.00042976
62	4.6582	9.9075	-23.498	1.873	0.062789	0.18247		0.00072662	0.00049071
74	6.499	9.4328	-24.617	2.146	0.091024	0.26104	0.13866	0.00040174	0.00044673
88	5.0705	9.7765	-24.394	2.113	0.053723	0.21221		0.00084297	0.00071538
104	5.1211	10.028	-24.032	1.87	0.046081	0.12877	0.13938	0.00062382	0.0005294
125	4.5667	10.148	-23.956	2.151	0.028543	0.081424		0.00077579	0.00047002
151	5.088	10.103	-23.872	1.992	0.033215	0.062731	0.091264	0.00060311	0.00052992
186	4.6704	10.051	-23.997	2.208	0.019098	0.059693		0.00047717	0.00054277
230	4.2995	10.166	-23.902	2.014	0.01454	0.070682	0.043491	0.00057486	0.00059457
286	4.0508	10.432	-23.767	2.064	0.015164	0.065596		0.00055974	0.00058887
355	4.0242	10.597	-23.631	1.411	0.010601	0.032495	0.021416	0.00028762	0.00024191
438	3.8191	11.092	-22.62	1.26	0.012909	0.040855		0.00049214	0.00042657
538	4.207	10.729	-22.644	1.181	0.012478	0.038292	0.019013	0.00058992	0.00079056
654	4.8585	10.813	-22.423	1.257	0.0127	0.044319	0.013514	0.00072445	0.00072498
784	4.6033	11.133	-22.578	1.186	0.035615	0.098941		0.0031878	0.0024575
927	6.2204	11.405	-22.174	0.93	0.043969	0.064846	0.04439	0.0023981	0.0017566
1083	5.59	11.393	-22.528	1.272	0.035946	0.06933		0.0026632	0.0020724
1251	6.25	11.54	-22.289	0.894	0.037572	0.057822	0.03613	0.0019478	0.0017577
1429	8.4	11.615	-21.538	0.728	0.048517	0.06233		0.0011315	0.0010912
1616	8.8086	11.547	-21.484	0.582	0.048785	0.068198	0.035058	0.0010981	0.00084182
1812	9.2267	11.574	-21.218	0.57	0.048221	0.075322		0.0009771	0.00097826
2015	7.9957	11.498	-21.244	0.505	0.041738	0.077325	0.025108	0.0010852	0.0010886
2225	9.1388	11.696	-20.973	0.525	0.045592	0.059033		0.0010545	0.0011936
2440	8.8753	11.564	-20.766	0.513	0.043653	0.078422	0.028822	0.0011834	0.0013856
2659	9.3232	11.419	-20.564	0.462	0.043918	0.076982		0.00096396	0.00091007
2881	9.972	11.373	-20.599	0.283	0.048224	0.060442	0.023116	0.00083076	0.00066356
3105	9.4439	11.267	-20.378	0.376	0.045241	0.058132		0.0010445	0.0007797
3331	8.8963	11.343	-21.577	0.117	0.042071	0.057682	0.022747	0.0011661	0.00099702
3557	8.9654	11.254	-21.151	0.356	0.041601	0.064382		0.0011137	0.0008731
3781	9.8172	11.253	-20.992	0.302	0.047891	0.063467	0.024147	0.0010812	0.00083036
4004	9.0375	11.371	-21.093	0.415	0.044308	0.070494		0.0014602	0.00095867
4224	9.3653	11.422	-21.022	0.383	0.04641	0.049608	0.022052	0.0014499	0.00092823
4440	9.1194	11.327	-21.145	0.444	0.047351	0.059511		0.0016235	0.0010459
4651	8.9643	11.215	-21.201	0.441	0.045967	0.062755	0.01928	0.0017584	0.0010781
4855	8.8103	11.191	-21.172	0.53	0.04668	0.080414		0.0015564	0.00097172
5053	8.8201	11.17	-21.263	0.473	0.051229	0	0.021955	0.0017609	0.0012035
5242	9.2762	11.096	-21.115	0.406	0.05392	0.076111		0.0015424	0.0010976
5423	8.9547	11.158	-21.185	0.313	0.056194	0.082468	0.020207	0.001769	0.0011734

KHL10 proxy data

5593	8.8398	11.512	-21.637	0.257	0.060137	0.10972		0.002555	0.0016056
5754	9.5629	11.07	-21.394	0.328	0.069064	0.1226	0.028311	0.0023833	0.0014633
5905	9.4389	11.07	-21.401	0.124	0.071405	0.15935		0.0024084	0.0011329
6048	9.2716	11.096	-21.317	0.074	0.075138	0.15093	0.029904	0.0032247	0.0013769
6182	9.6038	10.901	-21.383	0.124	0.082784	0.12967		0.0036664	0.0015909
6309	8.846	11.008	-21.389	-0.064	0.080062	0.13338	0.043805	0.0043565	0.0022372
6429	10.229	11.003	-21.289	0.035	0.097415	0.11048		0.0035043	0.0020717
6542	9.6439	11.074	-21.286	0.078	0.094919	0.16715	0.029921	0.0039686	0.0019093
6650	9.7893	11.06	-21.15	0.039	0.10218	0.13585		0.0042471	0.0018135
6751	9.7112	11.075	-21.158	0.009	0.10943	0.15902	0.041353	0.0033946	0.0013455
6848	9.6173	10.774	-21.411	0.042	0.11221	0.20026		0.0047002	0.0017493
6940	9.7241	10.917	-21.68	-0.256	0.12124	0.32032	0.03279	0.004618	0.0018536
7028	10.343	11.026	-21.846	-0.14	0.12888	0.20448		0.0041002	0.0016525
7113	10.163	10.97	-21.906	-0.277	0.13674	0.38258	0.04669	0.0039929	0.0017386
7195	9.7553	10.988	-21.854	-0.13	0.13378	0.11737		0.0037976	0.0018337
7274	9.3905	11.385	-22.146	-0.5	0.12952	0.13247		0.0040247	0.0021382
7351	9.7807	11.329	-21.808	-0.135	0.13865	0.092715		0.0047811	0.0023526
7427	9.7566	11.228	-21.816	-0.201	0.143	0.10873		0.003857	0.0022462
7502	9.1362	11.856	-22.104	-0.116	0.13965	0.11378	0.050135	0.0015755	0.0015197
7575	8.1832	12.133	-20.406	0.478	0.12311	0.13315		0.0014706	0.0012258
7647	9.0392	11.849	-20.325	0.693	0.14187	0.18294	0.043006	0.0023688	0.0012914
7717	8.8784	11.535	-20.676	0.34	0.14181	0.14057		0.0031419	0.0014655
7787	8.7631	11.436	-21.387	0.072	0.13885	0.14277	0.045157	0.0035979	0.0015254
7855	9.4682	11.252	-21.994	-0.348	0.15335	0.16206		0.0041783	0.0014264
7921	10.819	11.122	-22.024	-0.427	0.17583	0.11578	0.059482	0.0039898	0.001213
7987	9.043	11.083	-21.925	-0.404	0.15089	0.17546		0.0050839	0.0014517
8051	8.9147	11.094	-21.967	-0.479	0.15204	0.12871	0.04963	0.0052975	0.0014947
8114	8.4955	11.285	-21.954	0.25	0.14967	0.18621		0.0055006	0.0015432
8176	8.5523	11.314	-21.864	-0.469	0.15484	0.23715	0.080565	0.0058637	0.0016269
8237	8.959	11.387	-21.745	-0.536	0.16289	0.24523		0.0049435	0.0016257
8297	8.3794	11.218	-21.961	-0.496	0.1527	0.31769	0.05066	0.0057401	0.0017512
8356	9.0215	11.25	-21.955	-0.279	0.17267	0.30703		0.0051525	0.0016581
8413	8.9175	11.425	-22	-0.373	0.17094	0.27046	0.045815	0.0057706	0.0017843
8470	8.7523	11.492	-22.114	-0.43	0.16708	0.24283		0.0068711	0.0019551
8526	8.8763	11.44	-22.089	-0.265	0.18157	0.203	0.047254	0.0065578	0.0018352
8580	8.7818	11.653	-21.952	-0.193	0.17533	0.25191		0.0066541	0.0019528
8634	9.0249	11.76	-21.895	-0.141	0.19016	0.32257	0.052466	0.0057742	0.0017713
8686	8.9623	11.842	-21.682	-0.081	0.19339	0.35278		0.0073817	0.0018338
8738	8.1794	11.989	-22.459	-0.045	0.18231	0.53385		0.0087502	0.0020345
8789	8.0727	11.65	-22.018	0.011	0.18355	0.21062	0.0598	0.0085064	0.0019923
8839	7.5709	11.617	-21.951	0.084	0.17531	0.29436		0.009966	0.0023147
8888	7.4694	11.816	-22.12	0.271	0.1764	0.3747	0.057625	0.0094215	0.0022185
8936	6.7987	11.964	-22.078	0.186	0.16613	0.42602		0.010907	0.0028624
8984	6.7115	12.343	-22.559	0.321	0.16323	0.29116	0.088043	0.01037	0.0026447
9031	6.8689	11.883	-22.146	0.223	0.17296	0.21459		0.0058781	0.0017163
9076	7.0357	12.11	-21.985	0.202	0.18147	0.25123		0.011959	0.0032289
9122	6.5916	12.483	-22.442	0.078	0.17175	0.35024	0.050287	0.011388	0.0030986
9166	6.3227	12.291	-22.584	0.313	0.1657	0.35254	0.056083	0.011368	0.0029092
9210	6.4845	12.01	-22	0.297	0.17111	0.60546		0.0098087	0.0024105
9253	6.6092	11.929	-22.19	0.56	0.17619	0.45713	0.060515	0.011176	0.0027841
9295	6.2859	11.754	-22.307	0.529	0.17379	0.42541		0.010967	0.0026239
9337	6.3826	11.8	-22.295	0.516	0.18264	0.68975		0.011545	0.0030316
9378	5.8193	12.002	-22.457	0.546	0.1675	0.5169		0.012899	0.0032499
9419	6.3227	12.291	-22.584	0.313	0.18284	0.60024	0.068247	0.012632	0.0033672
9459	6.4204	11.772	-22.154	0.376	0.18582	0.40632		0.01258	0.0032602
9498	6.5173	11.682	-22.094	0.453	0.18818	0.55359	0.061211	0.012048	0.0030434
9537	8.2809	12.145	-21.825	0.604	0.24621	0.24983		0.0094485	0.0022605

KHL10 proxy data

9576	7.5133	12.092	-21.841	0.544	0.23084	0.29589	0.053152	0.0083725	0.0021378
9614	7.8006	12.117	-22.126	0.704	0.23496	0.57263		0.0081937	0.0019727
9651	6.6457	12.07	-22.819	0.477	0.20796	0.42801	0.056013	0.012914	0.0029402
9688	7.709	11.985	-22.728	0.391	0.24305	0.36327		0.0094224	0.0023824
9725	7.7072	12.563	-22.398	0.44	0.24347	0.52134	0.072026	0.0063463	0.00164
9761	7.2052	11.779	-23.181	0.514	0.22871	0.45387		0.0039872	0.00092522
9797	7.8484	12.981	-23.31	0.115	0.25499	0.46074	0.063029	0.011263	0.002545
9833	6.9525	13.104	-23.097	0.379	0.22094	0.58083		0.013699	0.0029735
9868	8.2818	12.266	-22.297	0.261	0.27049	0.5901	0.064342	0.0079356	0.0015731
9903	8.6155	12.634	-22.086	0.105	0.28725	0.50847		0.0029763	0.00083973
9938	6.8975	12.079	-22.741	-0.23	0.23462	0.57264	0.070751	0.0073615	0.0019305
9972	8.0914	12.547	-22.793	0.023	0.2737	0.88043		0.0056937	0.0012917
10007	7.6816	11.03	-22.308	0.252	0.2672	1.1568	0.054264	0.0081117	0.0018464

KHL10 proxy data

C:N at	Lutein	Diato	Total Chlorin	Lutein/Diato	Norm. Proxy	Sediment Ac	PCA AGE	GEO PCA 1	GEO PCA 2
12.231	0.17286	0.070875	27.419	3.9691	0.38838	0.50594	-60	-0.2776	0.471
12.712	0.18354	0.069294	28.054	4.3105	0.45144	0.61755	-56	-0.44755	0.45183
12.738	0.18613	0.081703	22.688	3.7074	0.50193	1.1115	-53	-0.5448	0.4879
12.392	0.22108	0.083729	28.917	4.297	0.49795	1.1095	-49	-0.53423	0.5306
12.587	0.16193	0.070464	21.54	3.74	0.50145	1.1619	-45	-0.66613	0.60183
12.807	0.18389	0.079945	24.598	3.7434	0.48794	0.86016	-41	-0.51898	0.43578
12.626	0.1851	0.078512	22.623	3.8367	0.54764	1.7331	-36	-0.7808	0.76443
12.474	0.1727	0.078215	23.699	3.5935	0.49289	1.1465	-32	-0.60349	0.56174
12.5	0.17206	0.060318	23.588	4.6423	0.55759	1.4506	-27	-0.77825	0.6623
12.552	0.1703	0.059707	24.719	4.6419	0.55672	1.3329	-21	-0.70009	0.5617
12.544	0.07807	0.030635	11.668	4.1473	0.56468	1.4823	-16	-0.67639	0.52761
12.399	0.086329	0.033075	14.107	4.2478	0.52308	1.3734	-9	-0.50355	0.49461
12.514	0.12348	0.052305	18.796	3.8419	0.50757	1.1784	-3	-0.4298	0.39582
12.374	0.11692	0.051685	19.653	3.6816	0.48461	1.3222	5	-0.34355	0.44238
12.357	0.12687	0.063174	21.93	3.2682	0.44181	1.4284	13	-0.03429	0.35821
12.137	0.12311	0.064275	21.448	3.1172	0.40935	1.1243	21	-0.15318	0.44378
12.172	0.17893	0.064593	18.864	4.5081	0.45903	0.93722	30	-0.29391	0.43092
11.787	0.11815	0.0524	18.824	3.6695	0.34251	0.80338	40	-0.00511	0.519
11.705	0.12074	0.1375	22.34	1.429	0.21462	0.74657	51	0.45504	0.44408
11.562	0.079122	0.086959	13.537	1.4807	0.17784	1.3479	62	0.71563	0.53049
11.008	0.042101	0.076189	18.638	0.89929	0.069783	1.4006	74	0.76846	0.79607
11.409	0.11678	0.16128	20.029	1.1783	0.090016	1.0595	88	0.81699	0.68825
11.703	0.10175	0.14053	14.311	1.1783	0.1347	0.89983	104	0.77244	0.55391
11.843	0.18218	0.17963	13.027	1.6505	0.13454	0.62503	125	0.77038	0.58401
11.79	0.1356	0.1939	9.6092	1.1381	0.12674	0.65282	151	0.78628	0.54662
11.73	0.17128	0.31706	14.598	0.87914	0.079669	0.40891	186	0.89491	0.58952
11.864	0.24949	0.41995	20.9	0.96684	0.10618	0.33819	230	0.86763	0.53083
12.174	0.21947	0.37576	17.523	0.95054	0.12512	0.37434	286	0.86229	0.50168
12.367	0.16026	0.21936	12.336	1.189	0.19716	0.26342	355	0.74968	0.33268
12.944	0.2137	0.30144	12.087	1.1537	0.28594	0.33802	438	0.70887	0.09577
12.521	0.49796	0.59361	12.91	0.74621	0.24863	0.29661	538	0.66531	0.13038
12.619	0.60789	0.76981	16.955	0.99927	0.27056	0.2614	654	0.64671	0.09777
12.992	0.47558	0.69842	12.788	1.2971	0.31895	0.77368	784	0.67351	0.05805
13.31	0.28755	0.45128	9.1739	1.3652	0.38254	0.70685	927	0.54066	-0.07803
13.296	0.29101	0.36308	10.782	1.2851	0.33091	0.64304	1083	0.58931	0.04167
13.467	0.27441	0.44711	9.6185	1.1082	0.37166	0.60116	1251	0.54139	-0.08976
13.555	0.30515	0.49813	10.792	1.037	0.42784	0.57758	1429	0.38153	-0.23279
13.475	0.31026	0.5715	12.314	1.3044	0.44942	0.55383	1616	0.36036	-0.26333
13.507	0.35315	0.67289	14.412	0.99881	0.44964	0.52263	1812	0.33564	-0.30911
13.418	0.30036	0.46149	14.813	0.99693	0.44368	0.522	2015	0.36925	-0.30563
13.649	0.25215	0.32776	11.833	0.88349	0.46467	0.49888	2225	0.2642	-0.3562
13.495	0.32003	0.38879	15.944	0.8541	0.46411	0.49185	2440	0.26656	-0.37145
13.326	0.35912	0.49972	16.342	1.0592	0.47783	0.47106	2659	0.26513	-0.39866
13.272	0.32173	0.41045	12.499	1.252	0.49852	0.48359	2881	0.19	-0.41473
13.149	0.35338	0.44167	12.135	1.3396	0.49724	0.47904	3105	0.22912	-0.41844
13.237	0.42185	0.45073	12.197	1.1696	0.45509	0.47291	3331	0.22683	-0.29996
13.133	0.44103	0.45949	13.875	1.2756	0.45646	0.46402	3557	0.16864	-0.32935
13.132	0.46686	0.48947	13.01	1.3021	0.47349	0.48783	3781	0.21163	-0.3071
13.27	0.51213	0.51098	14.379	1.5232	0.47561	0.49027	4004	0.18925	-0.32874
13.329	0.43067	0.43759	10.011	1.562	0.48776	0.49555	4224	0.23746	-0.29205
13.219	0.42311	0.47059	11.461	1.5522	0.47194	0.51924	4440	0.26064	-0.27328
13.088	0.40347	0.46724	12.238	1.6311	0.4652	0.51278	4651	0.26387	-0.2538
13.06	0.38745	0.41825	15.177	1.6017	0.4577	0.52984	4855	0.24127	-0.24171
13.035	0.51625	0.52798		1.4632	0.45316	0.58083	5053	0.19933	-0.26246
12.949	0.49959	0.49918	13.094	1.4053	0.45958	0.58126	5242	0.12275	-0.2577
13.021	0.49861	0.38168	13.142	1.5076	0.47336	0.62754	5423	0.06335	-0.20011

KHL10 proxy data

13.435	0.52937	0.36785	16.128	1.5913	0.48534	0.6803	5593	0.09894	-0.24768
12.919	0.6217	0.43902	16.975	1.6288	0.47204	0.72221	5754	0.13737	-0.27929
12.919	0.63841	0.53354	21.064	2.126	0.51138	0.7565	5905	0.07018	-0.21983
12.949	0.5689	0.54734	18.623	2.342	0.53332	0.81042	6048	0.04315	-0.25979
12.721	0.59345	0.46465	15.043	2.3046	0.51823	0.86199	6182	-0.05949	-0.23874
12.846	0.60122	0.41779	14.737	1.9473	0.51972	0.90507	6309	-0.04905	-0.23642
12.841	0.41516	0.26781	11.601	1.6915	0.5175	0.95234	6429	-0.03714	-0.26437
12.923	0.55955	0.33891	16.982	2.0786	0.53515	0.98424	6542	-0.04004	-0.26666
12.907	0.54191	0.35399	13.015	2.3419	0.56093	1.0438	6650	0.014	-0.19233
12.925	0.51078	0.33502	14.113	2.5229	0.57734	1.1268	6751	-0.00266	-0.22611
12.573	0.4537	0.32149	17.164	2.6869	0.55405	1.1667	6848	0.00118	-0.19417
12.74	0.48456	0.38076	25.691	2.4914	0.56962	1.2468	6940	-0.03297	-0.19308
12.867	0.44493	0.38468	16.411	2.4812	0.56535	1.246	7028	0.05672	-0.18723
12.802	0.54534	0.4367	28.434	2.2967	0.56616	1.3455	7113	0.11305	-0.24547
12.823	0.43004	0.40758	8.559	2.071	0.54635	1.3713	7195	0.00503	-0.21769
13.286	0.14598	0.22917	9.6043	1.8823	0.5727	1.3793	7274	0.04314	-0.40038
13.221	0.10852	0.14721	6.5402	2.0323	0.57186	1.4176	7351	-0.06985	-0.30411
13.103	0.22142	0.19646	7.4185	1.7171	0.55845	1.4656	7427	-0.14601	-0.26626
13.836	0.28755	0.21828	7.4437	1.0367	0.54405	1.5285	7502	-0.1913	-0.19259
14.159	0.34379	0.2372	8.8501	1.1997	0.59243	1.5045	7575	-0.28525	-0.14455
13.828	0.41921	0.23289	11.656	1.8342	0.60584	1.5695	7647	-0.38454	-0.11973
13.461	0.43514	0.2153	8.8008	2.1439	0.61007	1.5972	7717	-0.27235	-0.14344
13.346	0.48262	0.22427	9.0105	2.3587	0.59833	1.5845	7787	-0.18729	-0.17041
13.131	0.45051	0.20686	10.006	2.9294	0.62634	1.6196	7855	-0.11314	-0.05565
12.979	0.43657	0.19932	7.1239	3.2892	0.65558	1.6252	7921	-0.18896	-0.20682
12.934	0.46452	0.20974	10.516	3.5021	0.64791	1.6686	7987	-0.24961	-0.23617
12.947	0.4028	0.21557	7.5466	3.5442	0.6549	1.7055	8051	-0.23634	-0.17745
13.17	0.44115	0.21903	10.569	3.5645	0.61357	1.7618	8114	-0.26602	-0.12785
13.203	0.39498	0.20685	13.099	3.6042	0.67748	1.8104	8176	-0.24889	-0.16926
13.289	0.43963	0.22123	13.488	3.0409	0.67206	1.8182	8237	-0.21879	-0.18223
13.091	0.57278	0.26523	17.433	3.2778	0.65227	1.8223	8297	-0.32847	-0.11781
13.129	0.55166	0.25125	16.042	3.1075	0.6452	1.9139	8356	-0.36021	-0.14919
13.333	0.57515	0.27469	14.109	3.234	0.66555	1.917	8413	-0.37184	-0.15719
13.411	0.53393	0.26655	12.72	3.5144	0.67889	1.909	8470	-0.37004	-0.1893
13.35	0.65511	0.26485	9.9237	3.5733	0.67798	2.0456	8526	-0.20155	-0.13335
13.599	0.66986	0.25347	12.618	3.4075	0.68016	1.9965	8580	-0.17245	-0.13167
13.724	0.6836	0.26057	15.309	3.2599	0.68954	2.1071	8634	-0.06808	-0.11509
13.82	0.72362	0.27352	16.348	4.0254	0.7381	2.1579	8686	-0.0881	-0.15089
13.991	0.69578	0.26663	23.951	4.3009	0.71347	2.2289	8738	-0.11652	-0.11546
13.596	0.69787	0.29806	9.2632	4.2696	0.70808	2.2738	8789	-0.16983	-0.16102
13.557	0.72176	0.29957	12.712	4.3055	0.69954	2.3156	8839	-0.07522	-0.14513
13.789	0.36657	0.17419	15.866	4.2468	0.68857	2.3617	8888	-0.06818	-0.05191
13.962	0.7347	0.32281	17.435	3.8104	0.67824	2.4435	8936	-0.00927	-0.02885
14.404	0.51064	0.22612	11.971	3.921	0.67284	2.4321	8984	-0.03885	-0.03128
13.867	0.53578	0.22314	8.522	3.4248	0.65428	2.518	9031	-0.01876	-0.02997
14.132	0.45354	0.18139	9.7403	3.7039	0.69664	2.5793	9076	-0.06947	-0.07228
14.568	0.61193	0.24809	13.442	3.6752	0.6994	2.6055	9122	-0.09979	-0.04758
14.344	0.55071	0.21442	13.452	3.9075	0.67018	2.6207	9166	-0.26386	-0.08017
14.016	0.64949	0.27756	22.944	4.0691	0.69228	2.6388	9210	-0.15128	-0.10486
13.921	0.59617	0.24444	17.147	4.0142	0.66031	2.6659	9253	-0.1304	-0.0379
13.717	0.63142	0.2739	15.387	4.1797	0.65223	2.7647	9295	-0.1404	0.03022
13.771	0.63795	0.26907	24.104	3.8081	0.64572	2.8615	9337	-0.24072	0.03057
14.006	0.51171	0.21036	17.958	3.9691	0.64518	2.8784	9378	-0.27143	0.15815
14.344	0.49516	0.19279	20.757	3.7516	0.67532	2.8918	9419	-0.31631	-0.07975
13.738	0.38525	0.16009	14.039	3.8585	0.66533	2.8942	9459	-0.37395	-0.18141
13.633	0.46865	0.18363	19.173	3.9588	0.66324	2.8873	9498	-0.24695	-0.10707
14.173	0.52218	0.19348	8.4027	4.1799	0.74587	2.9732	9537	-0.29873	-0.09279

KHL10 proxy data

14.111	0.43864	0.18049	9.6305	3.9163	0.7228	3.0724	9576	-0.03066	0.02047
14.141	0.31541	0.13265	19.011	4.1535	0.71354	3.0121	9614	-0.11787	-0.05379
14.086	0.18437	0.069624	13.678	4.3921	0.68659	3.1292	9651	0.12909	0.01313
13.986	0.48218	0.17732	11.522	3.955	0.69678	3.1529	9688	0.37115	-0.16871
14.661	0.53115	0.18763	16.503	3.8696	0.74099	3.159	9725	-0.61755	-0.18379
13.746	0.34281	0.11059	14.298	4.3095	0.6601	3.1742	9761	-0.57899	-0.04039
15.149	0.16366	0.075146	14.181	4.4253	0.78268	3.2489	9797	-0.47725	-0.07702
15.292	0.27078	0.11556	18.277	4.6071	0.76488	3.1779	9833	0.00329	-0.15941
14.314	0.26023	0.096077	18.067	5.0447	0.81434	3.2661	9868	-0.3042	-0.07061
14.744	0.33797	0.12519	15.25	3.5443	0.80078	3.3341	9903		
14.096	0.29984	0.11451	16.835	3.8133	0.73463	3.4015	9938		
14.642	0.47929	0.18842	26.028	4.408	0.79894	3.3827	9972		
12.872	0.4259	0.21944	33.257	4.3933	0.70458	3.4785	10007		
	0.2721	0.13047							
	0.3663	0.18458	29.327						
	0.77218	0.4228	21.808						
	0.53817	0.43929							
	0.55496	0.41994	39.08						
	0.31377	0.1939	22.71						
	0.6275	0.36588	18.706						
	0.71645	0.44593	16.765						
	0.5533	0.43942	22.126						
	0.77178	0.52661							
	0.94477	0.38751	16.861						
	1.2344	0.40856	25.913						
	1.2309	0.41436	25.312						
	0.14341	0.11541	11.88						
	0.2146	0.098517	3.9019						

KHL10 proxy data

DIAT PCA AG	DIAT PCA 1	DIAT PCA 2
-60	-0.784	0.471
-53	-0.784	1.081
-45	-0.517	0.519
-36	-0.609	0.337
-16	-0.369	0.159
-3	-0.486	0.406
13	-0.468	0.211
51	-0.48	0.01
74	-0.485	0.122
104	-0.644	-0.534
151	-0.676	-0.183
230	-0.618	-0.35
355	-0.656	-0.43
538	-0.604	-0.387
784	-0.685	-0.199
1083	-0.539	-0.362
1429	-0.736	-0.409
1812	-0.569	-0.263
2225	-0.249	-0.206
2659	0.363	-0.182
3105	0.607	0.089
3557	0.912	-0.059
4004	0.894	-0.045
4440	0.966	-0.032
4855	1.01	-0.005
5242	0.98	0.019
5593	1.016	0.011
5905	0.971	0.06
6182	0.976	0.055
6429	1.033	0.059
6650	0.701	-0.035
6848	0.53	0.074

KHL10 proxy data

KHL10 raw diatom counts samples labeled as cm depth in core

0.0-0.25 cm		1.0-1.25 cm	
Achnanthes helveticum	2	Achnanthes helveticum	
Achnanthes levanderi	1	Achnanthes levanderi	9
Aulacoseira distans A1	24	Aulacoseira distans A1	23
Aulacoseira perglabra A2	8	Aulacoseira perglabra A2	12
Aulacoseira perglabra var florinaeA3	26	Aulacoseira perglabra var florinaeA3	10
Brachysira brebisonii	16	Brachysira brebisonii	18
Brachysira brebisonii long	3	Brachysira brebisonii long	8
Encyonema gaeumanii	4	Encyonema gaeumanii	8
Encyonema hebredicum	5	Encyonema hebredicum	9
Encyonema ventricosa or minuta var. groenlandica (J		Encyonema ventricosa or minuta var. groenlandica (J	
Cyclotella stelligera	5	Cyclotella stelligera	9
Cavinula pseudoscutiformis		Cavinula pseudoscutiformis	
Cymbopleura incerta/incertiformis		Cymbopleura incerta/incertiformis	
Eunotia bigibba		Eunotia bigibba	
Eunotia monodon		Eunotia monodon	
Eunotia diodon		Eunotia diodon	
Eunotia, short fat, rhomboidia	5	Eunotia, short fat, rhomboidia	5
Eunotia, long thin straightish		Eunotia, long thin straightish	2
Eunotia exigua like	2	Eunotia exigua like	3
Eunotia pectinalis var. minor		Eunotia pectinalis var. minor	1
Eunotia triodon	1	Eunotia triodon	
Eunotia vanheurckii		Eunotia vanheurckii	1
Fragillariaforma		Fragillariaforma	
Frustulia rhomboidies var. saxonica	28	Frustulia rhomboidies var. saxonica	30
Gomphonema parvulum		Gomphonema parvulum	3
Neidium bisulcatum	3	Neidium bisulcatum	3
Neidium iridus	3	Neidium iridus	2
Nitzschia fonticola	6	Nitzschia fonticola	9
Nitzschia perminuta	6	Nitzschia perminuta	4
Pinnularia biceps	32	Pinnularia biceps	29
Pinnularia mesolepta?		Pinnularia mesolepta?	
Pinnularia cf. brebisonii	7	Pinnularia cf. brebisonii	4
Pinnularia.. Big	5	Pinnularia.. Big	2
Pseudostaurosiera elliptica		Pseudostaurosiera elliptica	
Surirella sp large	1	Surirella sp large	
Surirella sp smallish		Surirella sp smallish	1
Stauroforma exiguiformis, bent	3	Stauroforma exiguiformis, bent	2
Stauroforma exiguiformis	24	Stauroforma exiguiformis	34
Stauroneus anceps	1	Stauroneus anceps	
Stauroneus phoenicenteron	1	Stauroneus phoenicenteron	
Staurosiera construens	1	Staurosiera construens	
Tabellaria flocculosa	14	Tabellaria flocculosa	14
Chrysophyte cysts	14	Chrysophyte cysts	13
Chrysophyte cysts bumpy	4	Chrysophyte cysts bumpy	2
Total	255	Total	270

KHL10 raw diatom counts samples labeled as cm depth in core

2.0-2.25 cm		3.0-3.25	
Achnanthes helveticum	2	Achnanthes helveticum	3
Achnanthes levanderi	8	Achnanthes levanderi	6
Aulacoseira distans A1	22	Aulacoseira distans A1	20
Aulacoseira perglabra A2	13	Aulacoseira perglabra A2	18
Aulacoseira perglabra var florinaeA3	9	Aulacoseira perglabra var florinaeA3	16
Brachysira brebisonii	19	Brachysira brebisonii	20
Brachysira brebisonii long	5	Brachysira brebisonii long	4
Encyonema gaeumanii	3	Encyonema gaeumanii	6
Encyonema hebredicum	7	Encyonema hebredicum	4
Encyonema ventricosa or minuta var. gr	1	Encyonema ventricosa or minuta var. groenlandica (J	
Cyclotella stelligera	4	Cyclotella stelligera	4
Cavinula pseudoscutiformis		Cavinula pseudoscutiformis	1
Cymbopleura incerta/incertiformis		Cymbopleura incerta/incertiformis	
Eunotia bigibba	2	Eunotia bigibba	1
Eunotia monodon		Eunotia monodon	1
Eunotia diodon		Eunotia diodon	
Eunotia, short fat, rhomboidia	1	Eunotia, short fat, rhomboidia	7
Eunotia, long thin straightish	1	Eunotia, long thin straightish	1
Eunotia exigua like	2	Eunotia exigua like	1
Eunotia pectinalis var. minor		Eunotia pectinalis var. minor	
Eunotia triodon		Eunotia triodon	
Eunotia vanheurckii		Eunotia vanheurckii	2
Fragillariaforma		Fragillariaforma	
Frustulia rhomboidies var. saxonica	30	Frustulia rhomboidies var. saxonica	38
Gomphonema parvulum		Gomphonema parvulum	
Neidium bisulcatum		Neidium bisulcatum	1
Neidium iridus	5	Neidium iridus	3
Nitzschia fonticola	5	Nitzschia fonticola	12
Nitzschia perminuta	4	Nitzschia perminuta	1
Pinnularia biceps	27	Pinnularia biceps	38
Pinnularia mesolepta?		Pinnularia mesolepta?	
Pinnularia cf. brebisonii	6	Pinnularia cf. brebisonii	
Pinnularia.. Big	9	Pinnularia.. Big	4
Pseudostaurosiera elliptica		Pseudostaurosiera elliptica	
Surirella sp large		Surirella sp large	1
Surirella sp smallish		Surirella sp smallish	1
Stauroforma exiguiformis, bent	2	Stauroforma exiguiformis, bent	
Stauroforma exiguiformis	37	Stauroforma exiguiformis	53
Stauroneus anceps		Stauroneus anceps	
Stauroneus phoenicenteron		Stauroneus phoenicenteron	
Staurosiera construens		Staurosiera construens	
Tabellaria flocculosa	27	Tabellaria flocculosa	22
Chrysophyte cysts	16	Chrysophyte cysts	22
Chrysophyte cysts bumpy	1	Chrysophyte cysts bumpy	
Total	268	Total	311

KHL10 raw diatom counts samples labeled as cm depth in core

5.0-5.5	
Achnanthes helveticum	3
Achnanthes levanderi	3
Aulacoseira distans A1	29
Aulacoseira perglabra A2	14
Aulacoseira perglabra var florinaeA3	15
Brachysira brebisonii	19
Brachysira brebisonii long	1
Encyonema gaeumanii	3
Encyonema hebredicum	8
Encyonema ventricosa or minuta var. gr	2
Cyclotella stelligera	1
Cavinula pseudoscutiformis	
Cymbopleura incerta/incertiformis	
Eunotia bigibba	
Eunotia monodon	
Eunotia diodon	
Eunotia, short fat, rhomboidia	4
Eunotia, long thin straightish	
Eunotia exigua like	1
Eunotia pectinalis var. minor	
Eunotia triodon	1
Eunotia vanheurckii	1
Fragillariaforma	
Frustulia rhomboidies var. saxonica	37
Gomphonema parvulum	
Neidium bisulcatum	
Neidium iridus	5
Nitzschia fonticola	5
Nitzschia perminuta	4
Pinnularia biceps	34
Pinnularia mesolepta?	
Pinnularia cf. brebisonii	3
Pinnularia.. Big	11
Pseudostaurosiera elliptica	
Surirella sp large	
Surirella sp smallish	
Stauroforma exiguiformis, bent	
Stauroforma exiguiformis	73
Stauroneus anceps	
Stauroneus phoenicenteron	
Staurosiera construens	1
Tabellaria flocculosa	21
Chrysophyte cysts	12
Chrysophyte cysts bumpy	
Total	311

6.0-6.5	
Achnanthes helveticum	4
Achnanthes levanderi	2
Aulacoseira distans A1	26
Aulacoseira perglabra A2	21
Aulacoseira perglabra var florinaeA3	19
Brachysira brebisonii	40
Brachysira brebisonii long	1
Encyonema gaeumanii	3
Encyonema hebredicum	4
Encyonema ventricosa or minuta var. groenlandica (J Cramer)	
Cyclotella stelligera	7
Cavinula pseudoscutiformis	
Cymbopleura incerta/incertiformis	1
Eunotia bigibba	1
Eunotia monodon	
Eunotia diodon	
Eunotia, short fat, rhomboidia	2
Eunotia, long thin straightish	1
Eunotia exigua like	1
Eunotia pectinalis var. minor	
Eunotia triodon	
Eunotia vanheurckii	3
Fragillariaforma	
Frustulia rhomboidies var. saxonica	38
Gomphonema parvulum	
Neidium bisulcatum	2
Neidium iridus	
Nitzschia fonticola	4
Nitzschia perminuta	4
Pinnularia biceps	43
Pinnularia mesolepta?	
Pinnularia cf. brebisonii	5
Pinnularia.. Big	3
Pseudostaurosiera elliptica	
Surirella sp large	1
Surirella sp smallish	
Stauroforma exiguiformis, bent	1
Stauroforma exiguiformis	62
Stauroneus anceps	
Stauroneus phoenicenteron	1
Staurosiera construens	
Tabellaria flocculosa	25
Chrysophyte cysts	18
Chrysophyte cysts bumpy	
Total	343

KHL10 raw diatom counts samples labeled as cm depth in core

7.0-7.5		8.0-8.5	
Achnanthes helveticum	5	Achnanthes helveticum	3
Achnanthes levanderi	2	Achnanthes levanderi	
Aulacoseira distans A1	31	Aulacoseira distans A1	28
Aulacoseira perglabra A2	24	Aulacoseira perglabra A2	18
Aulacoseira perglabra var florinaeA3	9	Aulacoseira perglabra var	11
Brachysira brebisonii	28	Brachysira brebisonii	29
Brachysira brebisonii long		Brachysira brebisonii long	2
Encyonema gaeumanii	3	Encyonema gaeumanii	3
Encyonema hebredicum	9	Encyonema hebredicum	1
Encyonema ventricosa or minuta var. gr	2	Encyonema ventricosa or minuta var. gr	
Cyclotella stelligera	1	Cyclotella stelligera	3
Cavinula pseudoscutiformis		Cavinula pseudoscutiformis	
Cymbopleura incerta/incertiformis		Cymbopleura incerta/incertiformis	
Eunotia bigibba		Eunotia bigibba	
Eunotia monodon	1	Eunotia monodon	
Eunotia diodon		Eunotia diodon	
Eunotia, short fat, rhomboidia	3	Eunotia, short fat, rhombc	2
Eunotia, long thin straightish	1	Eunotia, long thin straightish	
Eunotia exigua like	1	Eunotia exigua like	3
Eunotia pectinalis var. minor		Eunotia pectinalis var. minor	
Eunotia triodon	1	Eunotia triodon	2
Eunotia vanheurckii		Eunotia vanheurckii	2
Fragillariaforma		Fragillariaforma	
Frustulia rhomboidies var. saxonica	39	Frustulia rhomboidies var.	29
Gomphonema parvulum	2	Gomphonema parvulum	2
Neidium bisulcatum		Neidium bisulcatum	
Neidium iridus	5	Neidium iridus	6
Nitzschia fonticola	2	Nitzschia fonticola	4
Nitzschia perminuta	2	Nitzschia perminuta	3
Pinnularia biceps	32	Pinnularia biceps	68
Pinnularia mesolepta?		Pinnularia mesolepta?	
Pinnularia cf. brebisonii		Pinnularia cf. brebisonii	
Pinnularia.. Big	10	Pinnularia.. Big	6
Pseudostaurosiera elliptica		Pseudostaurosiera elliptica	
Surirella sp large	1	Surirella sp large	1
Surirella sp smallish		Surirella sp smallish	
Stauroforma exiguiformis, bent	1	Stauroforma exiguiformis, bent	
Stauroforma exiguiformis	64	Stauroforma exiguiformis	59
Stauroneus anceps		Stauroneus anceps	1
Stauroneus phoenicenteron		Stauroneus phoenicenteron	
Staurosiera construens		Staurosiera construens	
Tabellaria flocculosa	9	Tabellaria flocculosa	9
Chrysophyte cysts	13	Chrysophyte cysts	16
Chrysophyte cysts bumpy		Chrysophyte cysts bumpy	1
Total	301	Total	312

KHL10 raw diatom counts samples labeled as cm depth in core

9.0-9.5		10.0-10.5		11.0-11.5	
Achnanthes helveticum	4	Achnanthes helveticum	1	Achnanthes helveticum	9
Achnanthes levanderi	2	Achnanthes levanderi		Achnanthes levanderi	5
Aulacoseira distans A1	29	Aulacoseira distans A1	17	Aulacoseira distans A1	22
Aulacoseira perglabra A2	21	Aulacoseira perglabra A2	71	Aulacoseira perglabra A2	84
Aulacoseira perglabra var	13	Aulacoseira perglabra var	18	Aulacoseira perglabra var	32
Brachysira brebisonii	18	Brachysira brebisonii	11	Brachysira brebisonii	11
Brachysira brebisonii long	1	Brachysira brebisonii long		Brachysira brebisonii long	1
Encyonema gaeumanii	3	Encyonema gaeumanii	1	Encyonema gaeumanii	7
Encyonema hebredicum	5	Encyonema hebredicum	2	Encyonema hebredicum	4
Encyonema ventricosa or r	1	Encyonema ventricosa or minuta var. gr		Encyonema ventricosa or minuta var. gr	
Cyclotella stelligera	4	Cyclotella stelligera		Cyclotella stelligera	1
Cavinula pseudoscutiformis		Cavinula pseudoscutiformis		Cavinula pseudoscutiform	12
Cymbopleura incerta/incertiformis		Cymbopleura incerta/incertiformis		Cymbopleura incerta/incertiformis	
Eunotia bigibba	1	Eunotia bigibba		Eunotia bigibba	
Eunotia monodon		Eunotia monodon	2	Eunotia monodon	3
Eunotia diodon		Eunotia diodon		Eunotia diodon	
Eunotia, short fat, rhombc	2	Eunotia, short fat, rhomboidia		Eunotia, short fat, rhombc	5
Eunotia, long thin straight	2	Eunotia, long thin straightish		Eunotia, long thin straightish	
Eunotia exigua like		Eunotia exigua like	1	Eunotia exigua like	
Eunotia pectinalis var. minor		Eunotia pectinalis var. minor		Eunotia pectinalis var. minor	
Eunotia triodon		Eunotia triodon		Eunotia triodon	
Eunotia vanheurckii	1	Eunotia vanheurckii	3	Eunotia vanheurckii	
Fragillariaforma		Fragillariaforma		Fragillariaforma	
Frustulia rhomboidies var.	32	Frustulia rhomboidies var.	18	Frustulia rhomboidies var.	38
Gomphonema parvulum		Gomphonema parvulum		Gomphonema parvulum	
Neidium bisulcatum		Neidium bisulcatum		Neidium bisulcatum	
Neidium iridus	7	Neidium iridus	2	Neidium iridus	7
Nitzschia fonticola	2	Nitzschia fonticola		Nitzschia fonticola	
Nitzschia perminuta	3	Nitzschia perminuta	2	Nitzschia perminuta	
Pinnularia biceps	79	Pinnularia biceps	105	Pinnularia biceps	89
Pinnularia mesolepta?		Pinnularia mesolepta?		Pinnularia mesolepta?	
Pinnularia cf. brebisonii	3	Pinnularia cf. brebisonii		Pinnularia cf. brebisonii	
Pinnularia.. Big	5	Pinnularia.. Big	1	Pinnularia.. Big	3
Pseudostaurosiera elliptica		Pseudostaurosiera elliptica		Pseudostaurosiera elliptic	2
Surirella sp large		Surirella sp large		Surirella sp large	
Surirella sp smallish		Surirella sp smallish		Surirella sp smallish	1
Stauroforma exiguiformis,	1	Stauroforma exiguiformis,	1	Stauroforma exiguiformis, bent	
Stauroforma exiguiformis	59	Stauroforma exiguiformis	46	Stauroforma exiguiformis	53
Stauroneus anceps		Stauroneus anceps		Stauroneus anceps	
Stauroneus phoenicenteron		Stauroneus phoenicenteron		Stauroneus phoenicenteron	
Staurosiera construens	1	Staurosiera construens	2	Staurosiera construens	3
Tabellaria flocculosa	4	Tabellaria flocculosa	1	Tabellaria flocculosa	2
Chrysophyte cysts	14	Chrysophyte cysts	2	Chrysophyte cysts	7
Chrysophyte cysts bumpy	1	Chrysophyte cysts bumpy	1	Chrysophyte cysts bumpy	
Total	318	Total	308	Total	401

KHL10 raw diatom counts samples labeled as cm depth in core

12.0-12.5		13.0-13.5		14.0-14.5	
Achnanthes helveticum	1	Achnanthes helveticum	1	Achnanthes helveticum	
Achnanthes levanderi	4	Achnanthes levanderi	1	Achnanthes levanderi	
Aulacoseira distans A1	28	Aulacoseira distans A1	15	Aulacoseira distans A1	16
Aulacoseira perglabra A2	99	Aulacoseira perglabra A2	95	Aulacoseira perglabra A2	98
Aulacoseira perglabra var	17	Aulacoseira perglabra var	11	Aulacoseira perglabra var	12
Brachysira brebisonii	10	Brachysira brebisonii	8	Brachysira brebisonii	11
Brachysira brebisonii long		Brachysira brebisonii long		Brachysira brebisonii long	
Encyonema gaeumanii	2	Encyonema gaeumanii	1	Encyonema gaeumanii	
Encyonema hebredicum	4	Encyonema hebredicum	3	Encyonema hebredicum	5
Encyonema ventricosa or minuta var. gr		Encyonema ventricosa or minuta var. gr		Encyonema ventricosa or minuta var. gr	
Cyclotella stelligera		Cyclotella stelligera		Cyclotella stelligera	
Cavinula pseudoscutiform	1	Cavinula pseudoscutiform	5	Cavinula pseudoscutiform	2
Cymbopleura incerta/incertiformis		Cymbopleura incerta/incertiformis		Cymbopleura incerta/incertiformis	
Eunotia bigibba		Eunotia bigibba		Eunotia bigibba	
Eunotia monodon		Eunotia monodon		Eunotia monodon	
Eunotia diodon		Eunotia diodon		Eunotia diodon	
Eunotia, short fat, rhombc	2	Eunotia, short fat, rhombc	6	Eunotia, short fat, rhomboidia	
Eunotia, long thin straight	1	Eunotia, long thin straightish		Eunotia, long thin straightish	
Eunotia exigua like		Eunotia exigua like		Eunotia exigua like	
Eunotia pectinalis var. minor		Eunotia pectinalis var. minor		Eunotia pectinalis var. minor	
Eunotia triodon		Eunotia triodon		Eunotia triodon	
Eunotia vanheurckii	3	Eunotia vanheurckii	2	Eunotia vanheurckii	4
Fragillariaforma		Fragillariaforma		Fragillariaforma	
Frustulia rhomboidies var.	38	Frustulia rhomboidies var.	33	Frustulia rhomboidies var.	32
Gomphonema parvulum		Gomphonema parvulum		Gomphonema parvulum	
Neidium bisulcatum		Neidium bisulcatum		Neidium bisulcatum	
Neidium iridus	4	Neidium iridus	3	Neidium iridus	4
Nitzschia fonticola		Nitzschia fonticola	1	Nitzschia fonticola	
Nitzschia perminuta	1	Nitzschia perminuta	1	Nitzschia perminuta	3
Pinnularia biceps	66	Pinnularia biceps	67	Pinnularia biceps	65
Pinnularia mesolepta?		Pinnularia mesolepta?		Pinnularia mesolepta?	
Pinnularia cf. brebisonii		Pinnularia cf. brebisonii	4	Pinnularia cf. brebisonii	
Pinnularia.. Big	3	Pinnularia.. Big	3	Pinnularia.. Big	3
Pseudostaurosiera elliptica		Pseudostaurosiera elliptica		Pseudostaurosiera elliptica	
Surirella sp large		Surirella sp large		Surirella sp large	
Surirella sp smallish		Surirella sp smallish		Surirella sp smallish	
Stauroforma exiguiformis, bent		Stauroforma exiguiformis,	1	Stauroforma exiguiformis, bent	
Stauroforma exiguiformis	53	Stauroforma exiguiformis	41	Stauroforma exiguiformis	41
Stauroneus anceps		Stauroneus anceps	1	Stauroneus anceps	1
Stauroneus phoenicenteron		Stauroneus phoenicenteron		Stauroneus phoenicenteron	
Staurosiera construens	8	Staurosiera construens	1	Staurosiera construens	
Tabellaria flocculosa	3	Tabellaria flocculosa	2	Tabellaria flocculosa	4
Chrysophyte cysts	2	Chrysophyte cysts	2	Chrysophyte cysts	6
Chrysophyte cysts bumpy		Chrysophyte cysts bumpy		Chrysophyte cysts bumpy	
Total	350	Total	308	Total	307

KHL10 raw diatom counts samples labeled as cm depth in core

2A 11-11.5		2A 12-12.5		2A 13.0-13.5	
Achnanthes helveticum	2	Achnanthes helveticum	1	Achnanthes helveticum	1
Achnanthes levanderi	4	Achnanthes levanderi		Achnanthes levanderi	1
Aulacoseira distans A1	16	Aulacoseira distans A1	16	Aulacoseira distans A1	15
Aulacoseira perglabra A2	75	Aulacoseira perglabra A2	76	Aulacoseira perglabra A2	61
Aulacoseira perglabra var florinaeA3	20	Aulacoseira perglabra var	14	Aulacoseira perglabra var	25
Brachysira brebisonii	12	Brachysira brebisonii	19	Brachysira brebisonii	8
Brachysira brebisonii long	1	Brachysira brebisonii long	3	Brachysira brebisonii long	
Encyonema gaeumanii	5	Encyonema gaeumanii		Encyonema gaeumanii	1
Encyonema hebredicum	6	Encyonema hebredicum	1	Encyonema hebredicum	2
Encyonema ventricosa or minuta var. groenlandica (J		Encyonema ventricosa or	1	Encyonema ventricosa or minuta var. gr	
Cyclotella stelligera		Cyclotella stelligera	1	Cyclotella stelligera	
Cavinula pseudoscutiformis	5	Cavinula pseudoscutiformi	1	Cavinula pseudoscutiform	3
Cymbopleura incerta/incertiformis		Cymbopleura incerta/incertiformis		Cymbopleura incerta/incertiformis	
Eunotia bigibba		Eunotia bigibba		Eunotia bigibba	
Eunotia monodon	1	Eunotia monodon		Eunotia monodon	
Eunotia diodon		Eunotia diodon		Eunotia diodon	
Eunotia, short fat, rhomboidia	1	Eunotia, short fat, rhombc	3	Eunotia, short fat, rhombc	3
Eunotia, long thin straightish		Eunotia, long thin straightish		Eunotia, long thin straightish	
Eunotia exigua like		Eunotia exigua like		Eunotia exigua like	
Eunotia pectinalis var. minor		Eunotia pectinalis var. minor		Eunotia pectinalis var. minor	
Eunotia triodon		Eunotia triodon		Eunotia triodon	
Eunotia vanheurckii	2	Eunotia vanheurckii	1	Eunotia vanheurckii	9
Fragillariaforma		Fragillariaforma		Fragillariaforma	
Frustulia rhomboidies var. saxonica	35	Frustulia rhomboidies var.	31	Frustulia rhomboidies var.	32
Gomphonema parvulum		Gomphonema parvulum	1	Gomphonema parvulum	
Neidium bisulcatum	6	Neidium bisulcatum	1	Neidium bisulcatum	
Neidium iridus	3	Neidium iridus	3	Neidium iridus	3
Nitzschia fonticola		Nitzschia fonticola	1	Nitzschia fonticola	
Nitzschia perminuta	1	Nitzschia perminuta		Nitzschia perminuta	
Pinnularia biceps	76	Pinnularia biceps	66	Pinnularia biceps	65
Pinnularia mesolepta?		Pinnularia mesolepta?		Pinnularia mesolepta?	1
Pinnularia cf. brebisonii	2	Pinnularia cf. brebisonii	1	Pinnularia cf. brebisonii	
Pinnularia.. Big	1	Pinnularia.. Big	2	Pinnularia.. Big	4
Pseudostaurosiera elliptica		Pseudostaurosiera elliptica		Pseudostaurosiera elliptica	
Surirella sp large		Surirella sp large		Surirella sp large	
Surirella sp smallish		Surirella sp smallish		Surirella sp smallish	
Stauroforma exiguiformis, bent	1	Stauroforma exiguiformis,	2	Stauroforma exiguiformis, bent	
Stauroforma exiguiformis	32	Stauroforma exiguiformis	37	Stauroforma exiguiformis	44
Stauroneus anceps		Stauroneus anceps		Stauroneus anceps	
Stauroneus phoenicenteron		Stauroneus phoenicenteron		Stauroneus phoenicenteron	
Staurosiera construens	3	Staurosiera construens	4	Staurosiera construens	3
Tabellaria flocculosa	1	Tabellaria flocculosa	4	Tabellaria flocculosa	6
Chrysophyte cysts	5	Chrysophyte cysts	3	Chrysophyte cysts	3
Chrysophyte cysts bumpy		Chrysophyte cysts bumpy	2	Chrysophyte cysts bumpy	3
Total	1	Total	13	Total	32
Total	317	Total	308	Total	325
Total diatoms	316	Total diatoms	295	Total diatoms	293

KHL10 raw diatom counts samples labeled as cm depth in core

2A 14.0-14.5		15-15.5	
Achnanthes helveticum	2	Achnanthes helveticum	
Achnanthes levanderi	1	Achnanthes levanderi	
Aulacoseira distans A1	10	Aulacoseira distans A1	14
Aulacoseira perglabra A2	58	Aulacoseira perglabra A2	35
Aulacoseira perglabra var	12	Aulacoseira perglabra var florinaeA3	10
Brachysira brebisonii	6	Brachysira brebisonii	9
Brachysira brebisonii long	1	Brachysira brebisonii long	2
Encyonema gaeumanii		Encyonema gaeumanii	
Encyonema hebredicum	4	Encyonema hebredicum	3
Encyonema ventricosa or minuta var. gr		Encyonema ventricosa or minuta var. groenlandica (J	
Cyclotella stelligera		Cyclotella stelligera	
Cavinula pseudoscutiform	6	Cavinula pseudoscutiformis	2
Cymbopleura incerta/incertiformis		Cymbopleura incerta/incertiformis	
Eunotia bigibba		Eunotia bigibba	
Eunotia monodon		Eunotia monodon	2
Eunotia diodon		Eunotia diodon	
Eunotia, short fat, rhombc	6	Eunotia, short fat, rhomboidia	3
Eunotia, long thin straightish		Eunotia, long thin straightish	
Eunotia exigua like		Eunotia exigua like	
Eunotia pectinalis var. minor		Eunotia pectinalis var. minor	
Eunotia triodon		Eunotia triodon	
Eunotia vanheurckii	7	Eunotia vanheurckii	4
Fragillariaforma		Fragillariaforma	2
Frustulia rhomboidies var.	27	Frustulia rhomboidies var. saxonica	24
Gomphonema parvulum	1	Gomphonema parvulum	
Neidium bisulcatum	2	Neidium bisulcatum	
Neidium iridus		Neidium iridus	2
Nitzschia fonticola		Nitzschia fonticola	1
Nitzschia perminuta	2	Nitzschia perminuta	
Pinnularia biceps	47	Pinnularia biceps	47
Pinnularia mesolepta?	1	Pinnularia mesolepta?	10
Pinnularia cf. brebisonii	2	Pinnularia cf. brebisonii	6
Pinnularia.. Big	3	Pinnularia.. Big	2
Pseudostaurosiera elliptic	1	Pseudostaurosiera elliptica	7
Surirella sp large	1	Surirella sp large	
Surirella sp smallish		Surirella sp smallish	1
Stauroforma exiguiformis,	2	Stauroforma exiguiformis, bent	3
Stauroforma exiguiformis	51	Stauroforma exiguiformis	76
Stauroneus anceps		Stauroneus anceps	
Stauroneus phoenicenteron		Stauroneus phoenicenteron	
Staurosiera construens	5	Staurosiera construens	7
Tabellaria flocculosa	3	Tabellaria flocculosa	7
Chrysophyte cysts	3	Chrysophyte cysts	8
Chrysophyte cysts bumpy		Chrysophyte cysts bumpy	
Total	33	Total	50
Total	297	Total	337
Total diatoms	264	Total diatoms	287

KHL10 raw diatom counts samples labeled as cm depth in core

16-16.5		17-17.5	
Achnanthes helveticum		Achnanthes helveticum	
Achnanthes levanderi		Achnanthes levanderi	
Aulacoseira distans A1	10	Aulacoseira distans A1	6
Aulacoseira perglabra A2	8	Aulacoseira perglabra A2	2
Aulacoseira perglabra var florinaeA3	5	Aulacoseira perglabra var	1
Brachysira brebisonii	8	Brachysira brebisonii	
Brachysira brebisonii long	2	Brachysira brebisonii long	1
Encyonema gaeumanii		Encyonema gaeumanii	1
Encyonema hebredicum		Encyonema hebredicum	1
Encyonema ventricosa or minuta var. gr	1	Encyonema ventricosa or minuta var. gr	
Cyclotella stelligera		Cyclotella stelligera	2
Cavinula pseudoscutiformis	1	Cavinula pseudoscutiformis	
Cymbopleura incerta/incertiformis		Cymbopleura incerta/incertiformis	
Eunotia bigibba		Eunotia bigibba	
Eunotia monodon		Eunotia monodon	1
Eunotia diodon		Eunotia diodon	
Eunotia, short fat, rhomboidia		Eunotia, short fat, rhomboidia	
Eunotia, long thin straightish		Eunotia, long thin straightish	
Eunotia exigua like	1	Eunotia exigua like	
Eunotia pectinalis var. minor		Eunotia pectinalis var. minor	
Eunotia triodon		Eunotia triodon	
Eunotia vanheurckii	2	Eunotia vanheurckii	1
Fragillariaforma		Fragillariaforma	
Frustulia rhomboidies var. saxonica	16	Frustulia rhomboidies var.	12
Gomphonema parvulum		Gomphonema parvulum	
Neidium bisulcatum		Neidium bisulcatum	
Neidium iridus	1	Neidium iridus	2
Nitzschia fonticola		Nitzschia fonticola	
Nitzschia perminuta		Nitzschia perminuta	
Pinnularia biceps	28	Pinnularia biceps	15
Pinnularia mesolepta?	7	Pinnularia mesolepta?	11
Pinnularia cf. brebisonii	3	Pinnularia cf. brebisonii	2
Pinnularia.. Big	5	Pinnularia.. Big	4
Pseudostaurosiera elliptica	23	Pseudostaurosiera elliptic	23
Surirella sp large		Surirella sp large	
Surirella sp smallish		Surirella sp smallish	
Stauroforma exiguiformis, bent		Stauroforma exiguiformis,	1
Stauroforma exiguiformis	116	Stauroforma exiguiformis	143
Stauroneus anceps		Stauroneus anceps	
Stauroneus phoenicenteron		Stauroneus phoenicenteron	
Staurosiera construens	6	Staurosiera construens	4
Tabellaria flocculosa	5	Tabellaria flocculosa	4
Chrysophyte cysts	5	Chrysophyte cysts	5
Chrysophyte cysts bumpy	1	Chrysophyte cysts bumpy	1
Total	57	Total	75
Total	311	Total	318
Total diatoms	254	Total diatoms	243

KHL10 raw diatom counts samples labeled as cm depth in core

18-18.5		19-19.5		20-20.5	
Achnanthes helveticum		Achnanthes helveticum		Achnanthes helveticum	
Achnanthes levanderi		Achnanthes levanderi		Achnanthes levanderi	
Aulacoseira distans A1	3	Aulacoseira distans A1	5	Aulacoseira distans A1	6
Aulacoseira perglabra A2		Aulacoseira perglabra A2		Aulacoseira perglabra A2	
Aulacoseira perglabra var	1	Aulacoseira perglabra var florinaeA3		Aulacoseira perglabra var florinaeA3	
Brachysira brebisonii	1	Brachysira brebisonii	2	Brachysira brebisonii	5
Brachysira brebisonii long		Brachysira brebisonii long		Brachysira brebisonii long	
Encyonema gaeumanii		Encyonema gaeumanii	1	Encyonema gaeumanii	
Encyonema hebredicum		Encyonema hebredicum		Encyonema hebredicum	
Encyonema ventricosa or minuta var. gr		Encyonema ventricosa or minuta var. gr		Encyonema ventricosa or minuta var. gr	
Cyclotella stelligera		Cyclotella stelligera		Cyclotella stelligera	
Cavinula pseudoscutiformis		Cavinula pseudoscutiformis		Cavinula pseudoscutiformis	
Cymbopleura incerta/incertiformis		Cymbopleura incerta/incertiformis		Cymbopleura incerta/incertiformis	
Eunotia bigibba		Eunotia bigibba		Eunotia bigibba	
Eunotia monodon		Eunotia monodon	1	Eunotia monodon	
Eunotia diodon		Eunotia diodon		Eunotia diodon	
Eunotia, short fat, rhomboidia		Eunotia, short fat, rhomboidia		Eunotia, short fat, rhomboidia	
Eunotia, long thin straightish		Eunotia, long thin straightish		Eunotia, long thin straightish	
Eunotia exigua like		Eunotia exigua like		Eunotia exigua like	
Eunotia pectinalis var. minor		Eunotia pectinalis var. minor		Eunotia pectinalis var. minor	
Eunotia triodon		Eunotia triodon		Eunotia triodon	
Eunotia vanheurckii		Eunotia vanheurckii		Eunotia vanheurckii	
Fragillariaforma		Fragillariaforma		Fragillariaforma	
Frustulia rhomboidies var.	12	Frustulia rhomboidies var.	6	Frustulia rhomboidies var.	5
Gomphonema parvulum		Gomphonema parvulum		Gomphonema parvulum	
Neidium bisulcatum		Neidium bisulcatum		Neidium bisulcatum	
Neidium iridus		Neidium iridus		Neidium iridus	
Nitzschia fonticola		Nitzschia fonticola		Nitzschia fonticola	
Nitzschia perminuta		Nitzschia perminuta		Nitzschia perminuta	
Pinnularia biceps	17	Pinnularia biceps	12	Pinnularia biceps	3
Pinnularia mesolepta?	7	Pinnularia mesolepta?	13	Pinnularia mesolepta?	6
Pinnularia cf. brebisonii	1	Pinnularia cf. brebisonii	2	Pinnularia cf. brebisonii	4
Pinnularia.. Big	2	Pinnularia.. Big	4	Pinnularia.. Big	3
Pseudostaurosiera elliptic	16	Pseudostaurosiera elliptic	20	Pseudostaurosiera elliptic	19
Surirella sp large		Surirella sp large		Surirella sp large	
Surirella sp smallish		Surirella sp smallish		Surirella sp smallish	
Stauroforma exiguiformis,	1	Stauroforma exiguiformis,	2	Stauroforma exiguiformis,	1
Stauroforma exiguiformis	173	Stauroforma exiguiformis	198	Stauroforma exiguiformis	182
Stauroneus anceps		Stauroneus anceps		Stauroneus anceps	
Stauroneus phoenicenteron		Stauroneus phoenicenteron		Stauroneus phoenicenteron	
Staurosiera construens	4	Staurosiera construens	3	Staurosiera construens	3
Tabellaria flocculosa	6	Tabellaria flocculosa	5	Tabellaria flocculosa	10
Chrysophyte cysts	9	Chrysophyte cysts	6	Chrysophyte cysts	4
Chrysophyte cysts bumpy	1	Chrysophyte cysts bumpy		Chrysophyte cysts bumpy	1
Total	75	Total	56	Total	70
Total	329	Total	336	Total	322
Total diatoms	254	Total diatoms	280	Total diatoms	252

KHL10 raw diatom counts samples labeled as cm depth in core

21-21.5		22-22.5		23-23.5	
Achnanthes helveticum		Achnanthes helveticum		Achnanthes helveticum	
Achnanthes levanderi		Achnanthes levanderi		Achnanthes levanderi	
Aulacoseira distans A1	2	Aulacoseira distans A1	4	Aulacoseira distans A1	2
Aulacoseira perglabra A2		Aulacoseira perglabra A2	1	Aulacoseira perglabra A2	2
Aulacoseira perglabra var florinaeA3		Aulacoseira perglabra var florinaeA3		Aulacoseira perglabra var florinaeA3	
Brachysira brebisonii	1	Brachysira brebisonii		Brachysira brebisonii	1
Brachysira brebisonii long		Brachysira brebisonii long		Brachysira brebisonii long	1
Encyonema gaeumanii		Encyonema gaeumanii		Encyonema gaeumanii	
Encyonema hebredicum		Encyonema hebredicum		Encyonema hebredicum	
Encyonema ventricosa or minuta var. gr		Encyonema ventricosa or r	1	Encyonema ventricosa or minuta var. gr	
Cyclotella stelligera		Cyclotella stelligera		Cyclotella stelligera	
Cavinula pseudoscutiformis		Cavinula pseudoscutiformis		Cavinula pseudoscutiformis	
Cymbopleura incerta/incertiformis		Cymbopleura incerta/incertiformis		Cymbopleura incerta/incertiformis	
Eunotia bigibba		Eunotia bigibba		Eunotia bigibba	
Eunotia monodon		Eunotia monodon		Eunotia monodon	
Eunotia diodon		Eunotia diodon		Eunotia diodon	
Eunotia, short fat, rhomboidia		Eunotia, short fat, rhomboidia		Eunotia, short fat, rhomboidia	
Eunotia, long thin straightish		Eunotia, long thin straightish		Eunotia, long thin straightish	
Eunotia exigua like		Eunotia exigua like		Eunotia exigua like	
Eunotia pectinalis var. minor		Eunotia pectinalis var. minor		Eunotia pectinalis var. minor	
Eunotia triodon		Eunotia triodon		Eunotia triodon	
Eunotia vanheurckii		Eunotia vanheurckii		Eunotia vanheurckii	
Fragillariaforma		Fragillariaforma		Fragillariaforma	
Frustulia rhomboidies var.	9	Frustulia rhomboidies var.	11	Frustulia rhomboidies var.	10
Gomphonema parvulum		Gomphonema parvulum		Gomphonema parvulum	
Neidium bisulcatum		Neidium bisulcatum		Neidium bisulcatum	
Neidium iridus		Neidium iridus		Neidium iridus	
Nitzschia fonticola		Nitzschia fonticola		Nitzschia fonticola	
Nitzschia perminuta		Nitzschia perminuta		Nitzschia perminuta	1
Pinnularia biceps	4	Pinnularia biceps	3	Pinnularia biceps	2
Pinnularia mesolepta?	6	Pinnularia mesolepta?	10	Pinnularia mesolepta?	3
Pinnularia cf. brebisonii		Pinnularia cf. brebisonii	1	Pinnularia cf. brebisonii	1
Pinnularia.. Big	3	Pinnularia.. Big	5	Pinnularia.. Big	3
Pseudostaurosiera elliptic:	22	Pseudostaurosiera elliptic:	25	Pseudostaurosiera elliptic:	27
Surirella sp large		Surirella sp large		Surirella sp large	
Surirella sp smallish		Surirella sp smallish		Surirella sp smallish	
Stauroforma exiguiformis, bent		Stauroforma exiguiformis, bent		Stauroforma exiguiformis, bent	
Stauroforma exiguiformis	178	Stauroforma exiguiformis	163	Stauroforma exiguiformis	166
Stauroneus anceps		Stauroneus anceps		Stauroneus anceps	
Stauroneus phoenicenteron		Stauroneus phoenicenteron		Stauroneus phoenicenteron	
Staurosiera construens	5	Staurosiera construens	8	Staurosiera construens	6
Tabellaria flocculosa	12	Tabellaria flocculosa	12	Tabellaria flocculosa	10
Chrysophyte cysts	8	Chrysophyte cysts	14	Chrysophyte cysts	6
Chrysophyte cysts bumpy	2	Chrysophyte cysts bumpy		Chrysophyte cysts bumpy	2
Total	79	Total	99	Total	89
Total	331	Total	357	Total	332
Total diatoms	252	Total diatoms	258	Total diatoms	243

KHL10 raw diatom counts samples labeled as cm depth in core

24-24.5		25-25.5		26-26.5	
Achnanthes helveticum		Achnanthes helveticum		Achnanthes helveticum	
Achnanthes levanderi		Achnanthes levanderi		Achnanthes levanderi	
Aulacoseira distans A1		Aulacoseira distans A1		Aulacoseira distans A1	
Aulacoseira perglabra A2	1	Aulacoseira perglabra A2	1	Aulacoseira perglabra A2	1
Aulacoseira perglabra var florinaeA3		Aulacoseira perglabra var	2	Aulacoseira perglabra var florinaeA3	
Brachysira brebisonii	3	Brachysira brebisonii		Brachysira brebisonii	1
Brachysira brebisonii long		Brachysira brebisonii long	1	Brachysira brebisonii long	
Encyonema gaeumanii	1	Encyonema gaeumanii	1	Encyonema gaeumanii	
Encyonema hebredicum		Encyonema hebredicum		Encyonema hebredicum	
Encyonema ventricosa or minuta var. gr		Encyonema ventricosa or minuta var. gr		Encyonema ventricosa or minuta var. gr	
Cyclotella stelligera		Cyclotella stelligera		Cyclotella stelligera	
Cavinula pseudoscutiformis		Cavinula pseudoscutiformis		Cavinula pseudoscutiformis	
Cymbopleura incerta/incertiformis		Cymbopleura incerta/incertiformis		Cymbopleura incerta/incertiformis	
Eunotia bigibba		Eunotia bigibba		Eunotia bigibba	
Eunotia monodon		Eunotia monodon	1	Eunotia monodon	2
Eunotia diodon		Eunotia diodon		Eunotia diodon	
Eunotia, short fat, rhomboidia		Eunotia, short fat, rhomboidia		Eunotia, short fat, rhomboidia	
Eunotia, long thin straightish		Eunotia, long thin straightish		Eunotia, long thin straightish	
Eunotia exigua like		Eunotia exigua like		Eunotia exigua like	
Eunotia pectinalis var. minor		Eunotia pectinalis var. minor		Eunotia pectinalis var. minor	
Eunotia triodon		Eunotia triodon		Eunotia triodon	
Eunotia vanheurckii		Eunotia vanheurckii		Eunotia vanheurckii	
Fragillariaforma		Fragillariaforma		Fragillariaforma	
Frustulia rhomboidies var.	9	Frustulia rhomboidies var.	7	Frustulia rhomboidies var.	8
Gomphonema parvulum		Gomphonema parvulum		Gomphonema parvulum	
Neidium bisulcatum		Neidium bisulcatum		Neidium bisulcatum	
Neidium iridus		Neidium iridus		Neidium iridus	
Nitzschia fonticola		Nitzschia fonticola		Nitzschia fonticola	
Nitzschia perminuta		Nitzschia perminuta		Nitzschia perminuta	
Pinnularia biceps	4	Pinnularia biceps	4	Pinnularia biceps	3
Pinnularia mesolepta?	4	Pinnularia mesolepta?	2	Pinnularia mesolepta?	
Pinnularia cf. brebisonii		Pinnularia cf. brebisonii		Pinnularia cf. brebisonii	
Pinnularia.. Big	2	Pinnularia.. Big	4	Pinnularia.. Big	6
Pseudostaurosiera elliptic	47	Pseudostaurosiera elliptic	54	Pseudostaurosiera elliptic	54
Surirella sp large		Surirella sp large		Surirella sp large	
Surirella sp smallish		Surirella sp smallish		Surirella sp smallish	
Stauroforma exiguiformis,	1	Stauroforma exiguiformis, bent		Stauroforma exiguiformis,	4
Stauroforma exiguiformis	152	Stauroforma exiguiformis	136	Stauroforma exiguiformis	130
Stauroneus anceps		Stauroneus anceps		Stauroneus anceps	
Stauroneus phoenicenteron		Stauroneus phoenicenteron		Stauroneus phoenicenteron	
Staurosiera construens	9	Staurosiera construens	9	Staurosiera construens	11
Tabellaria flocculosa	13	Tabellaria flocculosa	4	Tabellaria flocculosa	6
Chrysophyte cysts	12	Chrysophyte cysts	7	Chrysophyte cysts	5
Chrysophyte cysts bumpy	1	Chrysophyte cysts bumpy		Chrysophyte cysts bumpy	
Total	97	Total	93	Total	98
		S. pinnata	8	S. pinnata	5
Total	356	Total	334	Total	334
Total diatoms	259	Total diatoms	233	Total diatoms	231

KHL10 raw diatom counts samples labeled as cm depth in core

27-27.5		28-28.5	
Achnanthes helveticum		Achnanthes helveticum	1 marginulatum
Achnanthes levanderi		Achnanthes levanderi	
Aulacoseira distans A1	4	Aulacoseira distans A1	7
Aulacoseira perglabra A2	3	Aulacoseira perglabra A2	7
Aulacoseira perglabra var	1	Aulacoseira perglabra var	2
Brachysira brebisonii	3	Brachysira brebisonii	1
Brachysira brebisonii long		Brachysira brebisonii long	
Encyonema gaeumanii		Encyonema gaeumanii	1
Encyonema hebredicum		Encyonema hebredicum	
Encyonema ventricosa or minuta var. gr		Encyonema ventricosa or minuta var. groenlandica (J Cramer)	
Cyclotella stelligera		Cyclotella stelligera	1 maybe stephanodiscus
Cavinula pseudoscutiform	1	Cavinula pseudoscutiformis	
Cymbopleura incerta/incertiformis		Cymbopleura incerta/incertiformis	
Eunotia bigibba		Eunotia bigibba	
Eunotia monodon	1	Eunotia monodon	1
Eunotia diodon		Eunotia diodon	
Eunotia, short fat, rhombc	1	Eunotia, short fat, rhomboidia	
Eunotia, long thin straightish		Eunotia, long thin straightish	
Eunotia exigua like		Eunotia exigua like	
Eunotia pectinalis var. minor		Eunotia pectinalis var. minor	
Eunotia triodon		Eunotia triodon	
Eunotia vanheurckii		Eunotia vanheurckii	2
Fragillariaforma		Fragillariaforma	
Frustulia rhomboidies var.	12	Frustulia rhomboidies var.	19
Gomphonema parvulum		Gomphonema parvulum	
Neidium bisulcatum		Neidium bisulcatum	
Neidium iridus		Neidium iridus	2
Nitzschia fonticola		Nitzschia fonticola	2
Nitzschia perminuta		Nitzschia perminuta	
Pinnularia biceps	11	Pinnularia biceps	7
Pinnularia mesolepta?	3	Pinnularia mesolepta?	4
Pinnularia cf. brebisonii		Pinnularia cf. brebisonii	1
Pinnularia.. Big	9	Pinnularia.. Big	3
Pseudostaurosiera elliptic	29	Pseudostaurosiera elliptic	24
Surirella sp large		Surirella sp large	
Surirella sp smallish		Surirella sp smallish	
Stauroforma exiguiformis,	1	Stauroforma exiguiformis, bent	
Stauroforma exiguiformis	101	Stauroforma exiguiformis	82
Stauroneus anceps		Stauroneus anceps	
Stauroneus phoenicenteron		Stauroneus phoenicenteron	
Staurosiera construens	5	Staurosiera construens	5
Tabellaria flocculosa	9	Tabellaria flocculosa	7
Chrysophyte cysts	12	Chrysophyte cysts	15
Chrysophyte cysts bumpy		Chrysophyte cysts bumpy	2
Total	120	Total	133
S. pinnata	1	S. pinnata	8
Total	327	Total	337
Total diatoms	206	Total diatoms	196

FLT09 proxy data

Depth(cm)	%C	%N	C/N	d13C	d15N
15	16.5616894	1.3613341	12.1657787	-24.184	3.854
16	15.2019869	1.2545838	12.11715543	-24.056	3.871
17	14.9633615	1.2329132	12.13658958	-24.169	3.983
18	15.200828	1.233953	12.31880631	-24.204	3.822
19	14.7406372	1.2157921	12.12430744	-24.042	3.75
20	14.6308444	1.2414827	11.78497646	-24.033	3.713
21	14.8200471	1.2623886	11.73968705	-24.113	3.354
22	14.1515202	1.2018383	11.77489534	-23.842	3.127
23	12.0484816	1.0396325	11.58917367	-23.94	3.185
24	14.0254328	1.1850576	11.83523299	-23.92	2.948
25	14.5222864	1.2441596	11.67236615	-23.95	3.131
26	15.1162377	1.2774981	11.83268899	-23.662	2.996
27	14.0327722	1.1841256	11.85074641	-23.73	3.176
28	16.288076	1.3520265	12.04715736	-23.817	2.863
29	14.1684721	1.1646003	12.16595264	-23.516	2.714
30	16.4958274	1.359467	12.13404033	-23.678	2.558
31	16.0159338	1.3445879	11.91140706	-23.532	2.621
32	16.4502094	1.3598035	12.09749012	-23.499	2.788
33	15.7250032	1.2984637	12.11046809	-23.509	2.648
34	9.4422792	0.8402244	11.23780647	-23.163	2.556
35	13.9250999	1.2112865	11.49612408	-22.999	2.414
36	12.2710735	1.0540086	11.64228973	-22.826	2.812
37	13.2284084	1.1026216	11.99723314	-23.07	2.409
38	13.2464247	1.1016809	12.02383077	-22.866	2.115
39	13.2181294	1.1207691	11.79380249	-22.85	2.108
40	10.4156907	0.8876652	11.73380538	-22.68	1.92
41	11.300938	0.9419735	11.99708697	-22.541	1.888
42	11.67108	1.0052839	11.60973532	-22.476	1.931
43	10.3226854	0.8782089	11.75424822	-22.346	1.87
44	12.5296699	1.0740001	11.66635822	-22.123	1.932
45	7.6299572	0.6993348	10.91030677	-21.977	1.882
46	5.6367593	0.5336024	10.56359435	-21.907	1.861
47	7.2423399	0.6712509	10.78931872	-21.823	1.772
48	9.7551468	0.8602043	11.34049993	-21.729	1.698
49	8.2918695	0.7346307	11.28712631	-21.851	1.707
50	5.9554884	0.5680072	10.48488188	-21.948	1.557
51	7.0183099	0.6354119	11.04529188	-21.745	1.721
52	5.5754424	0.548286	10.16885786	-21.657	1.689
53	8.2453589	0.7361834	11.20014238	-21.705	1.556
54	5.6001143	0.5276632	10.61304692	-21.812	1.703
55	6.9393953	0.6420734	10.80779129	-21.935	1.626
56	3.4159838	0.3470476	9.842983499	-21.423	1.746
57	2.1973771	0.2515707	8.734630464	-21.38	1.807
58	1.985049	0.2308039	8.600586905	-22.014	2.269
59	2.596559	0.2933404	8.851692437	-21.983	1.991
60	2.7778794	0.2956969	9.394347387	-21.941	2.259
61	3.7493073	0.3950337	9.491107468	-22.525	2.04
62	3.5501058	0.3718357	9.547511979	-22.902	2.074
63	2.1926127	0.2475061	8.858822873	-22.35	2.383
64	2.6117875	0.2812927	9.284945894	-22.599	2.302
65	1.9414644	0.2411441	8.05105495	-22.783	2.467

LDG09 proxy data

Depth(cm)	%C	%N	C/N	d13C	d15N
13	6.5406162	0.5710351	11.45396526	-23.83	2.662
14	6.0786354	0.5358491	11.34393134	-23.403	2.469
15	5.855001	0.5476094	10.69192932	-23.584	2.418
16	6.1973858	0.5512696	11.2420235	-23.201	2.38
17	5.9796534	0.5534443	10.80443579	-23.544	2.646
18	6.0440654	0.5537991	10.91382308	-23.811	2.528
19	5.6459917	0.5017672	11.25221358	-23.534	2.584
20	5.2282656	0.4831011	10.82230117	-23.795	2.555
21	4.970749	0.4590226	10.82898533	-23.532	2.607
22	4.8020013	0.4513549	10.63908091	-23.463	2.636
23	5.0429671	0.4730913	10.65960651	-23.62	2.933
24	5.3196918	0.498137	10.6791742	-23.786	2.659
25	5.0927349	0.4852208	10.49570608	-24.236	2.504
26	5.1656555	0.4918539	10.5024185	-23.937	2.503
27	5.0661349	0.4673547	10.84002129	-23.728	2.423
28	4.9762722	0.454697	10.94415006	-23.577	2.376
29	5.0685295	0.4668325	10.85727643	-23.718	2.713
30	5.1048722	0.4744694	10.75911787	-23.584	2.452
31	5.7540437	0.5420805	10.61474025	-23.77	2.535
32	5.6026253	0.5259028	10.65334754	-23.712	2.621
33	5.515025	0.5273369	10.45825733	-23.717	2.45
34	5.5041945	0.5245087	10.49400039	-23.903	2.319
35	5.723042	0.537593	10.64567805	-23.848	2.329
36	6.5139342	0.5903126	11.03471991	-24.242	2.17
37	5.9847915	0.5644951	10.6020256	-23.777	2.273
38	5.4458718	0.5088443	10.70243255	-23.751	2.284
39	5.0687378	0.4758211	10.6526125	-23.615	2.261
40	4.8272527	0.4705358	10.2590551	-23.784	2.644
41	5.2999887	0.5135158	10.32098467	-23.843	2.32
42	5.2285263	0.514013	10.17197289	-24.048	2.304
43	5.253432	0.5248458	10.00947707	-23.745	2.539
44	5.193454	0.5088416	10.20642573	-24.053	2.657
45	4.9386335	0.4796615	10.29608067	-24.049	2.186
46	5.1535629	0.4970692	10.36789827	-23.87	2.185
47	5.1767441	0.498945	10.37538025	-24.086	2.409
48	5.0904412	0.4949012	10.28577259	-24.038	2.329
49	5.0268817	0.4744351	10.59550969	-23.889	2.167
50	4.7590903	0.4598213	10.34986918	-23.975	2.409
51	5.8690801	0.5543235	10.5878248	-23.41	2.442
52	5.6721479	0.5443221	10.42057249	-23.493	2.6
53	5.9132842	0.5480788	10.78911317	-23.6	2.518
54	6.1345095	0.5647579	10.86219334	-24.014	2.37
55	6.568256	0.6101588	10.7648304	-24.203	2.362
56	5.754345	0.5363593	10.72852657	-23.585	2.469
57	6.890902	0.6134714	11.23263774	-24.205	2.739
58	6.3666863	0.5974311	10.6567708	-23.453	2.408
59	6.540181	0.6171781	10.59691036	-23.995	2.511
60	6.4992285	0.637917	10.18820395	-23.788	2.484
61	6.3188586	0.6250675	10.10908198	-24.035	2.534
62	6.2103594	0.6094579	10.18997276	-24.206	2.267
63	6.2222416	0.6037739	10.30558227	-23.848	2.572
64	6.3077122	0.6161135	10.23790617	-24.058	2.27

LDG09 proxy data

65	5.9220564	0.5884529	10.06377299	-24.014	2.357
66	6.5768067	0.6120263	10.74595438	-24.295	2.454
67	5.6612859	0.5896789	9.600624849	-23.951	2.498
68	6.8290112	0.6337009	10.77639498	-24.449	2.581
69	5.9161909	0.5752634	10.28431654	-24.001	2.394
70	6.001055	0.6100589	9.836845262	-24.027	2.449
71	5.7862719	0.5725533	10.10608427	-24.287	2.499
72	5.8322006	0.574278	10.1557096	-24.024	2.252
73	5.6562279	0.5765149	9.811069757	-24.297	2.644
74	5.3354766	0.5558669	9.598478701	-24.364	2.36
75	4.8977643	0.5118301	9.569121277	-24.4	2.767
76	5.1474104	0.5345701	9.629065299	-24.866	2.665
77	4.8888261	0.5291082	9.239747371	-24.663	2.747
78	5.158483	0.5338332	9.663098886	-24.643	2.982
79	5.3053942	0.5570544	9.524014531	-24.816	2.598
80	4.7063232	0.496635	9.476422725	-24.57	2.701
81	4.685954	0.4849627	9.662503941	-25.291	3.015
82	4.9569275	0.5120881	9.679833411	-24.743	2.785
83	4.6393517	0.4688553	9.8950608	-25.028	2.532
84	5.0027207	0.5001414	10.00261266	-25.727	2.693
85	4.6184975	0.4868353	9.486776123	-25.353	2.463
86	4.7496275	0.4468662	10.62874637	-26.354	2.586
87	5.3722527	0.4901511	10.96040119	-27.587	2.819
88	3.4512995	0.3601565	9.582777209	-25.45	2.852
89	2.2390803	0.2227979	10.04982677	-25.39	2.479
90	0.5152228	0.05572	9.246640345	-24.647	2.505
91	0.5240092	0.0475614	11.01753102	-24.903	3.775
92	0.6672637	0.0677786	9.844754834	-24.987	2.122
93	0.7142205	0.0691385	10.33028631	-24.777	3.131

KEK10 proxy data

Depth (cm)	%C	C/N	d13C	d15N
11	5.60	13.5373389	-27.7	4.2
11.5	5.85	13.4897848	-28.0	4.0
12	5.71	13.4915844	-28.2	4.2
12.5	5.79	13.4516685	-28.0	4.2
13	5.64	13.4962421	-28.0	4.3
13.5	5.53	13.4606815	-27.8	4.2
14.5	4.14	13.3194361	-27.8	4.5
15	5.17	13.3560145	-27.7	4.3
15.5	6.60	13.3187773	-27.8	4.2
16	4.82	13.109502	-28.3	4.1
16.5	5.39	13.1010057	-28.2	3.9
17	5.03	13.5930067	-28.0	4.1
17.5	5.25	13.4283407	-27.9	4.6
18	3.49	13.3392329	-27.8	4.6
18.5	3.67	13.0970969	-27.6	4.7
19	3.70	13.2029372	-27.5	4.6
19.5	3.73	13.1011679	-27.5	4.8
20	4.01	13.058467	-27.8	4.6
20.5	4.24	13.1067408	-28.1	4.6
21	4.08	13.2409338	-27.8	4.5
21.5	4.21	13.1762329	-27.8	4.4
22	3.98	13.0820669	-27.5	4.6
22.5	3.79	13.0311974	-27.5	4.6
23	3.59	13.0386016	-27.3	4.6
23.5	3.39	12.6358872	-26.9	4.8
24	3.36	12.5982938	-26.7	4.8
24.5	3.11	12.4527751	-26.7	4.9
25	3.20	12.4223379	-26.6	4.8
25.5	3.25	12.5167507	-26.3	4.6
26	3.16	12.5889683	-26.2	4.7
26.5	3.29	12.604404	-26.5	4.8
27	3.23	12.6343327	-26.6	4.8
27.5	3.02	12.5683956	-25.9	4.6
28	2.85	12.2672981	-25.8	4.8
28.5	2.80	12.3819756	-25.5	4.7
29	2.56	12.1227103	-25.6	4.7
29.5	2.43	12.1753692	-25.6	4.8
30	2.33	11.7815635	-25.9	4.6
30.5	2.27	11.972779	-25.8	4.5
31	2.27	11.9730984	-25.9	4.6
31.5	2.41	12.1292306	-25.6	4.8
32	2.09	12.0944877	-25.6	4.5

KEK10 proxy data

32.5	2.13	12.3313972	-25.6	4.2
33	2.04	12.3662264	-25.6	4.0
33.5	1.82	12.271533	-25.5	4.0
34	1.73	11.764693	-25.6	4.1
34.5	1.70	11.8858977	-25.6	4.0
35	1.56	11.7971999	-25.4	3.8
35.5	1.48	11.7052772	-25.4	4.3
36	1.33	11.9759487	-25.3	4.1
36.5	1.29	11.9021645	-25.3	4.3
37	1.45	12.4100091	-25.4	3.9
37.5	1.62	12.0473776	-25.6	4.0
38	1.26	12.111504	-25.3	4.2
38.5	1.35	12.3972013	-25.4	4.0
39	1.39	12.8960433	-25.5	3.8
39.5	1.28	12.6024236	-25.5	4.1
40	1.21	12.2237151	-25.4	4.5
40.5	1.13	12.6317598	-25.2	4.4
41	1.04	12.4038646	-25.1	4.3
41.5	1.06	12.0167817	-25.8	4.3
42	1.08	11.9685078	-26.2	3.9
42.5	1.09	12.3739245	-26.4	4.1
43	1.22	13.0815156	-26.5	4.2
43.5	1.24	12.9466161	-26.7	4.5
44	1.26	13.0274427	-26.6	4.4
44.5	1.29	12.508531	-25.7	3.9
45	1.29	12.7240947	-25.4	3.9
45.5	1.17	12.8294924	-26.5	4.5
46	1.18	12.9074427	-26.9	4.6
46.5	1.07	13.1049139	-26.3	4.2
47	1.11	13.621146	-26.0	4.3
47.5	1.18	14.0474666	-26.1	4.2
48	1.34	16.6318053	-26.3	4.2
48.5	1.38	18.9693757	-26.5	3.5
49	1.31	19.7595248	-26.6	3.7
49.5	1.08	16.7010514	-26.3	3.8
50	1.12	13.5063742	-26.7	3.9
50.5	1.05	13.5152936	-26.5	3.7
51	0.94	12.963122	-26.5	3.5
51.5	0.93	12.6732732	-26.6	3.8
52	0.86	10.580105	-26.57	3.47
52.5	0.87	11.3361725	-26.75	3.26
53	0.83	11.8666382	-26.97	3.24
53.5	0.53	17.5349017	-26.82	

KEK10 proxy data

54	1.69	19.8428385	-27.26	3.51
54.5	1.28	19.9442976	-27.09	3.45
55	1.51	18.6362876	-26.87	3.49
55.5	1.39	15.8243571	-26.94	3.90
56	1.31	14.4416749	-26.68	3.71
56.5	1.27	15.1963558	-26.49	3.65
57	1.59	16.2407036	-26.30	4.46
57.5	1.46	16.0673234	-26.44	4.11
58	1.46	16.3620846	-26.23	3.88
58.5	1.29	15.5545118	-25.99	3.67
59	0.81	13.7513656	-25.31	3.15
59.5	0.71	13.285372	-24.69	3.08
60	1.20	13.3825148	-25.48	3.40
60.5	0.92	12.0450452	-25.38	3.48
61	0.71	10.63244	-24.88	3.49
61.5	0.67	10.4712659	-24.70	3.96
62	0.71	10.7215862	-24.75	3.97
62.5	0.65	10.3543562	-24.08	4.61
63	0.61	10.8125169	-23.94	4.04
63.5	0.65	10.442915	-24.08	4.41
64	0.66	10.5979179	-23.95	3.96
64.5	0.56	11.0696104	-23.58	3.78
65	0.58	10.7827606	-24.00	4.38
65.5	0.66	10.7540466	-23.86	4.83
66	0.65	10.506342	-22.96	5.18
66.5	0.62	10.4387574	-22.04	4.47
67	0.35	10.1788416	-22.55	2.86

CAN98 proxy data

Depth (cm)	%C	%N	C/N	d13C	d15N
2	7.4661918	0.741641	10.067124	-32.991	2.361
3	7.3916416	0.7147395	10.341728	-32.959	2.03
4	7.7910271	0.7347189	10.604092	-32.98	1.988
5	7.7473674	0.7210231	10.744964	-32.959	2.225
6	8.1802716	0.758472	10.785199	-32.833	2.273
7	8.3150284	0.7005527	11.86924	-31.973	2.556
8	8.1634125	0.6926412	11.785918	-31.324	2.382
9	6.85423	0.6210414	11.036672	-30.494	2.875
11	5.0474272	0.5009165	10.076384	-29.845	3.062
12	4.9189396	0.479652	10.255226	-29.539	3.349
13	4.8676927	0.4930865	9.8718839	-29.797	3.062
14	4.2437838	0.4235285	10.020067	-29.268	3.26
15	4.0533141	0.3998856	10.136184	-29.145	2.874
16	3.3641226	0.3572768	9.4160119	-28.496	2.973
17	3.2430498	0.3442254	9.4212972	-28.093	3.034
18	3.4328488	0.3686867	9.3110188	-28.938	3.064
19	3.0168963	0.3200302	9.4269113	-28.562	2.365
20	4.3943453	0.4347274	10.108278	-29.608	2.339
21	5.7455976	0.54891	10.467285	-29.85	2.03
22	6.6447171	0.5651847	11.756718	-28.741	1.936
23	7.9521429	0.6492476	12.248244	-29.146	2.165
24	8.2167288	0.6879172	11.944357	-29.259	2.247
25	8.7373621	0.7229487	12.085729	-29.285	1.853
26	8.7079373	0.7267765	11.981589	-29.543	2.181
27	9.1097022	0.7528602	12.100125	-29.89	2.015
28	9.350013	0.7773904	12.027436	-29.636	1.996
29	9.3178315	0.7676323	12.138405	-29.718	1.883
30	9.7485813	0.8330268	11.702602	-30.177	1.697
31	15.556274	1.5741461	9.8823569	-31.07	1.536
32	15.963578	1.7001705	9.3893984	-31.1	1.567
33	15.440729	1.608076	9.6019898	-31.029	1.513
34	15.275274	1.5474818	9.8710523	-30.518	1.62
35	12.482785	1.3066468	9.5532972	-31.225	1.531
36	14.971736	1.6005923	9.3538721	-31.596	1.935
37	13.442273	1.5651109	8.588703	-31.504	2.093
38	12.736866	1.5479879	8.2280139	-32.125	1.814
39	11.568695	1.3781574	8.3943205	-31.774	1.632
40	12.65354	1.4279127	8.8615644	-31.909	1.746
41	13.453822	1.4267235	9.4298732	-31.353	1.835
42	10.522899	1.060334	9.9241361	-30.786	2.006
43	12.100748	1.0901164	11.100418	-30.082	2.37
45	11.947428	1.1440968	10.442672	-31.144	2.355
50	13.075451	1.1672576	11.201855	-32.265	-0.458
55	11.908857	1.3524976	8.8050856	-32.098	-1.688
60	11.550308	1.2602877	9.1648184	-31.067	-0.448
65	14.303542	1.9897449	7.1886309	-31.937	-0.29

BAE10 proxy data

SID	DEPTH	AGE	AD YEARS	15N	%N	13C	TOC%	C:N
BAE10-2C-5.!	0	-7	2007	2.3	0.86	-26.5	10.44	14.12
6.5-7	1	12	1988	2.5	0.85	-26.5	10.15	14.01
7.5-8	2	32	1968	2.6	0.78	-26.5	10.04	15.02
8.5-9	3	51	1949	2.6	0.78	-26.3	10.29	15.35
9.5-10	4	71	1929	2.2	0.62	-24.7	6.86	12.85
10.5-11	5	90	1910	1.9	0.69	-24.7	7.64	12.92
11.5-12	6	110	1890	1.8	0.69	-25	8.06	13.62
12.5-13	7	129	1871	1.9	0.67	-25.4	8.24	14.28
13.5-14	8	148	1852	1.7	0.77	-26.5	10.77	16.34
14.5-15	9	168	1832	1.5	0.86	-26.5	15.45	21.08
15.5-16	10	187	1813	1.6	0.73	-26.6	10.25	16.27
16.5-17	11	206	1794	1.5	0.8	-26.7	11.97	17.5
17.5-18	12	225	1775	1.7	0.78	-26.4	10.35	15.57
18.5-19	13	243	1757	1.7	0.75	-26.6	10.53	16.46
19.5-20	14	262	1738	1.6	0.73	-26.7	10.38	16.65
20.5-21	15	280	1720	1.4	0.83	-26.9	12.45	17.58
21.5-22	16	299	1701	1.2	0.76	-26.9	12.38	19.01
22.5-23	17	317	1683	1.6	0.64	-26.3	8.53	15.57
23-23.5	18	335	1665	1.7	0.68	-26.2	9.3	16.01
24-24.5	19	353	1647	1.5	0.66	-26.2	9	16.02
25-25.5	20	370	1630	1.7	0.61	-25.9	7.69	14.66
26-26.5	21	388	1612	1.5	0.62	-25.9	8.01	15.03
27-27.5	22	405	1595	1.3	0.72	-26.3	9.6	15.64
28-28.5	23	422	1578	1.2	0.69	-25.9	9.46	15.95
29-29.5	24	438	1562	1.5	0.69	-26.1	9.19	15.58
30-30.5	25	455	1545	1.3	0.7	-26.5	10.96	18.31
31-31.5	26	471	1529	1.5	0.64	-26.4	8.92	16.28
32-32.5	27	487	1513	1.4	0.64	-26.6	9.31	17.07
33-33.5	28	503	1497	1.3	0.62	-26.6	8.98	16.97
34-34.5	29	518	1482	1.6	0.41	-25.4	5.28	15.04
35-35.5	30	533	1467	2	0.57	-24.5	6.51	13.21
36-36.5	31	548	1452	1.8	0.59	-24.5	6.63	13.21
37-37.5	32	562	1438	1.8	0.55	-24.4	6.08	12.97
38-38.5	33	576	1424	2	0.55	-24.1	5.99	12.72
39-39.5	34	590	1410	1.9	0.55	-23.8	5.83	12.47
40-40.5	35	604	1396	1.9	0.54	-23.4	5.73	12.38
BAE10-2C-41	36	617	1383	1.6	0.51	-22.6	5.18	11.8
42	37	630	1370	1.6	0.52	-22.3	5.12	11.52
43	38	643	1357	1.7	0.51	-22.5	5.06	11.65
44	39	655	1345	1.7	0.5	-22.4	4.9	11.44
45	40	668	1332	1.8	0.49	-22.8	5.39	12.81
46	41	680	1320	1.6	0.5	-22.9	5.3	12.49
47	42	692	1308	1.6	0.53	-22.1	5.23	11.52
48	43	703	1297	1.6	0.5	-21.8	4.87	11.25
49	44	714	1286	1.6	0.51	-21.9	4.98	11.32
50	45	725	1275	1.6	0.49	-21.9	4.83	11.53
51	46	736	1264	1.7	0.48	-22	4.73	11.51
52-52.5	47	747	1253	1.7	0.49	-22.6	4.93	11.76
53-53.5	48	757	1243	1.7	0.49	-22.6	5.01	11.83
54	49	767	1233	1.8	0.51	-22.4	5.11	11.71
55	50	777	1223	1.9	0.51	-22.5	5.06	11.64
56	51	787	1213	1.6	0.5	-22.5	4.82	11.35
57	52	797	1203	1.7	0.52	-22.1	5.09	11.33
58	53	806	1194	1.6	0.5	-22.4	5.08	11.93
59	54	815	1185	1.7	0.46	-22.3	4.61	11.65
60	55	825	1175	1.7	0.48	-22.4	4.77	11.54

BAE10 proxy data

61	56	834	1166	1.7	0.48	-22.5	4.65	11.41
62	57	843	1157	1.8	0.5	-22.6	5.02	11.73
63	58	852	1148	1.6	0.52	-22.3	5.12	11.54
64-64.5	59	861	1139	1.8	0.49	-22.6	5	11.83
65-65.5	60	870	1130	1.7	0.52	-22.6	5.16	11.67
66	61	880	1120	1.7	0.51	-23.4	5.87	13.38
67	62	890	1110	1.7	0.49	-22.5	4.82	11.46
68	63	900	1100	1.7	0.46	-22.1	4.59	11.61
69	64	911	1089	1.5	0.41	-21.5	3.93	11.1
70	65	922	1078	1.5	0.44	-21.4	4.3	11.29
71	66	934	1066	1.6	0.44	-21.6	4.16	11.13
72	67	947	1053	1.5	0.36	-21.6	3.41	11.15
73	68	960	1040	1.5	0.25	-22.8	2.81	13.35
74	69	974	1026	1.4	0.4	-21.9	3.9	11.37
75	70	989	1011	0.7	0.31	-21.2	3.04	11.59
76-76.5	71	1004	996	1.5	0.29	-21.6	2.81	11.22
77-77.5	72	1021	979	1.4	0.36	-21.9	3.48	11.11
78	73	1038	962	1.7	0.37	-21.9	3.59	11.26
79	74	1057	943	1.6	0.43	-21.9	4.2	11.31
80	75	1077	923	1.6	0.38	-22.4	3.77	11.6
81	76	1098	902	1.4	0.31	-22.3	2.96	11.07
82	77	1120	880	1.4	0.23	-22.1	2.15	10.95
83	78	1144	856	1.5	0.42	-22.3	4.06	11.33
84	79	1169	831	1.6	0.7	-23	6.53	10.91
85	80	1195	805	1.5	0.48	-22.6	4.72	11.44
86	81	1222	778	1.5	0.47	-22.5	4.67	11.55
87	82	1251	749	1.3	0.48	-22.3	4.6	11.23
88-88.5	83	1281	719	1.5	0.48	-22.4	4.75	11.51
89-89.5	84	1311	689	1.4	0.47	-22.4	4.58	11.35
90	85	1343	657	1.4	0.49	-22.2	4.79	11.4
91	86	1376	624	1.4	0.5	-22.2	4.89	11.47
92	87	1409	591	1.4	0.46	-22.4	4.54	11.45
93	88	1444	556	1.5	0.48	-22.2	4.64	11.38
94	89	1479	521	1.3	0.48	-22.3	4.66	11.37
95	90	1515	485	1.3	0.45	-22.3	4.31	11.11
96	91	1551	449	1.1	0.42	-22.4	4.37	12.11
97	92	1588	412	1.3	0.44	-21.8	4.16	10.96
98	93	1626	374	1.3	0.33	-22.3	3.16	11.18
99	94	1664	336	1.3	0.23	-23	2.7	13.78
100-100.5	95	1702	298	1.3	0.46	-22.4	4.44	11.23
101-101.5	96	1741	259	1.3	0.48	-22.1	4.54	11.12
102-102.5	97	1780	220	1.3	0.5	-22.1	4.85	11.3
103-103.5	98	1819	181	1.2	0.51	-22.1	4.83	11.03

BAE10 proxy data

PIG depth	pig AD	Chlorins	Diatoms	BSi age	BSi uncalib
0.5	1997.5	0.2306	0.021587	2007	98.749
1.5	1978	0.73464	0.065364	1988	105.6
2.5	1958.5	0.68079	0.044759	1968	102.22
3.5	1939	0.73342	0.030034	1949	97.784
4.5	1919.5	1.0044	0.051191	1929	116.8
5.5	1900	0.99298	0.044422	1910	121.93
6.5	1880.5	0.92597	0.055411	1890	118.14
7.5	1861.5	0.74163	0.040224	1871	114.12
8.5	1842	0.50327	0.031137	1852	119.6
9.5	1822.5	0.50199	0.028314	1832	114.55
10.5	1803.5	0.55255	0.047473	1813	119.62
11.5	1784.5	0.11904	0.0074106	1794	108.81
12.5	1766	0.56268	0.030829	1775	116.43
13.5	1747.5	0.55761	0.040344	1757	126.76
14.5	1729	0.52611	0.027193	1738	119.11
15.5	1710.5	0.36149	0.021304	1720	122.88
16.5	1692	0.51015	0.021291	1701	112.96
17.5	1674	0.68431	0.034597	1683	120.9
18	1665	0.58	0.044198	1674	120.21
19	1647	0.61924	0.068289	1656	119.79
20	1630	0.80551	0.093723	1638.5	135.77
21	1612	0.96207	0.12938	1621	123.22
22	1595	0.31975	0.046142	1603.5	126.8
23	1578	0.8724	0.14811	1586.5	128.62
24	1562		0.19399	1570	117.64
26	1529	0.67801	0.081394	1553.5	117.39
27	1513	0.51421	0.049787	1537	102.31
28	1497	0.4247	0.038435	1521	108.4
29	1482	0.99486	0.077735	1505	107.19
30	1467	0.971	0.061909	1489.5	106.84
31	1452	0.91476	0.091682	1474.5	123.9
32	1438	0.82179	0.10725	1459.5	126.04
33	1424	1.0008	0.13655	1445	124.36
34	1410	0.92151	0.17841	1431	120.07
35	1396	0.93091	0.059721	1417	121.78
36	1383	1.0761	0.11827	1403	125.96
37	1370	1.0492	0.22108	1389.5	126.01
38	1357	1.3134	0.51996	1376.5	125.19
39	1345	1.2248	0.19299	1363.5	134.9
40	1332	1.1691	0.15326	1351	131.07
41	1320	1.3019	0.18454	1338.5	127
42	1308	1.3056	0.32385	1326	125.47
43	1297	1.4904	0.25793	1314	123.41
44.5	1280.5	1.4109	0.084539	1302.5	136.51
45	1275	1.0838	0.26073	1291.5	131.48
46	1264	1.1923	0.22006	1280.5	128.09
47	1253	1.2545	0.30799	1269.5	131.16
48	1243	1.2047	0.3312	1258.5	129.88
49	1233	0.33888	0.10727	1248	120.21
50	1223	1.3297	0.31491	1238	126.95
51	1213	1.3991	0.34589	1228	125.52
52	1203	1.2295	0.29126	1218	128.49
53	1194	1.068	0.36473	1208	137.07
54	1185	1.0793	0.35035	1198.5	127.68
55	1175	1.4215	0.45548	1189.5	124.71
56	1166	1.3951	0.40169	1180	117.56

BAE10 proxy data

57	1157	1.0744	0.37744	1170.5	118.92
58	1148	1.4293	0.48919	1161.5	123.65
59	1139	1.2711	0.42582	1152.5	122.13
60	1130	1.1399	0.37789	1143.5	120.71
61	1120	1.1117	0.35042	1134.5	117.63
62	1110	1.2142	0.32327	1125	116.14
63	1100	1.1716	0.26925	1115	122.92
64	1089	1.4489	0.33368	1105	120.85
65	1078	1.2479	0.32981	1094.5	120.37
66.5	1059.5	1.1886	0.092772	1083.5	132.56
67	1053	1.2743	0.33628	1072	120.64
68	1040	1.2482	0.28141	1059.5	114.09
69	1026	1.4075	0.20758	1046.5	96.899
70	1011	1.3996	0.36335	1033	112.96
71	996	1.5231	0.32598	1018.5	103.38
72	979	1.2331	0.22636	1003.5	115.23
73	962	1.4729	0.17735	987.5	112.21
74	943	1.2791	0.16894	970.5	108.17
75	923	1.3591	0.11307	952.5	124.08
76	902	1.4145	0.093986	933	119.21
77	880	1.3078	0.074491	912.5	114.3
78	856	1.4124	0.19428	891	99.843
79.5	818	1.1118	0.078876	868	126.01
80.5	791.5	1.1276	0.10809	843.5	123.61
81	778	0.96323	0.16166	818	134.61
82	749	1.2368	0.14811	791.5	125.96
83.5	704	1.223	0.1018	763.5	134.23
84.5	673	1.0606	0.10159	734	136.25
85.5	640.5	1.2538	0.12597	704	125.27
86.5	607.5	1.1984	0.10745	673	128.12
87.5	573.5	1.1927	0.11124	640.5	127.24
88.5	538.5	1.1095	0.11815	607.5	128.79
89.5	503	1.071	0.11626	573.5	128.56
90	485	0.99507	0.31299	538.5	139.96
91	449	1.1122	0.29242	503	136.44
92	412	1.1634	0.41037	467	136.11
93	374	1.2741	0.30113	430.5	117.25
94	336	1.5981	0.46919	393	125.64
95	298	1.3617	0.34256	355	102.54
96	259	1.2611	0.3585	317	135.98
97	220	1.075	0.20045	278.5	139.81
98	181	1.1961	0.2128	239.5	137.08
				200.5	138.27

TORF12 proxy data

depth age	min95%	max95%	best	ADYRS	accrate	Depth core	sed rate	DENS	MS
0	-65	-18	-47	1997	13.83	0		0.4352	25.999
2	-37	6	-19	1969	13.79	2	0.071429	1.0161	32.389
4	-7	40	8	1942	13.7	4	0.074074	1.1567	37.108
6	22	62	36	1914	13.56	6	0.071429	1.1439	40.889
8	50	85	63	1887	13.38	8	0.074074	1.1613	43.685
10	77	108	90	1860	13.16	10	0.074074	1.1346	44.858
12	104	129	116	1834	12.88	12	0.076923	1.1418	45.421
14	130	152	142	1808	12.56	14	0.076923	1.1398	46.228
16	156	174	167	1783	12.21	16	0.08	1.1476	47.345
18	181	197	191	1759	11.83	18	0.083333	1.163	48.461
20	204	223	215	1735	11.48	20	0.083333	1.1568	48.836
22	227	248	238	1712	11.16	22	0.086957	1.1538	48.705
24	243	272	260	1690	10.87	24	0.090909	1.1656	48.208
26	266	297	282	1668	10.59	26	0.090909	1.1464	47.72
28	287	319	303	1647	10.35	28	0.095238	1.1618	47.532
30	306	342	324	1626	10.13	30	0.095238	1.1651	46.537
32	325	364	344	1606	9.93	32	0.1	1.1558	46.228
34	344	386	364	1586	9.76	34	0.1	1.1583	45.29
36	363	409	383	1567	9.62	36	0.10526	1.1485	43.685
38	383	431	403	1547	9.5	38	0.1	1.1397	41.387
40	401	451	422	1528	9.41	40	0.10526	1.1404	38.778
42	420	472	440	1510	9.34	42	0.11111	1.1487	36.489
44	438	492	459	1491	9.3	44	0.10526	1.1514	35.185
46	457	513	478	1472	9.28	46	0.10526	1.1334	34.744
48	476	533	496	1454	9.29	48	0.11111	1.1425	34.678
50	495	553	515	1435	9.32	50	0.10526	1.1494	33.937
52	515	572	533	1417	9.38	52	0.11111	1.1371	32.389
54	534	591	552	1398	9.46	54	0.10526	1.1623	31.028
56	553	609	571	1379	9.57	56	0.10526	1.1461	30.465
58	574	628	590	1360	9.71	58	0.10526	1.1428	30.84
60	594	647	610	1340	9.87	60	0.1	1.1394	32.023
62	615	667	629	1321	10.05	62	0.10526	1.1588	34.002
64	634	673	650	1300	10.27	64	0.095238	1.1476	37.164
66	652	693	670	1280	10.48	66	0.1	1.1745	40.702
68	670	723	691	1259	10.61	68	0.095238	1.157	42.137
70	690	743	712	1238	10.64	70	0.095238	1.1562	40.58
72	712	762	734	1216	10.56	72	0.090909	1.1799	38.225
74	732	781	755	1195	10.38	74	0.095238	1.1583	36.855
76	753	798	775	1175	10.1	76	0.1	1.1591	37.971
78	772	815	796	1154	9.71	78	0.095238	1.1784	42.25
80	790	832	815	1135	3.69	80	0.10526	1.2272	48.893
	790	832	815	1135	3.69	82	0	1.2261	52.43
	790	832	815	1135	3.69	84	0	1.2003	49.512
85	808	849	834	1116	8.69	86	0.10526	1.1797	42.193
87	826	866	851	1099	8.22	88	0.11765	1.1479	35.804
89	843	886	867	1083	7.78	90	0.125	1.1637	31.891
91	858	904	883	1067	7.39	92	0.125	1.1489	30.034
93	872	921	898	1052	7.05	94	0.13333	1.1477	29.536
95	885	937	912	1038	6.76	96	0.14286	1.1486	29.78
97	899	954	925	1025	6.5	98	0.15385	1.136	30.09
99	911	968	938	1012	6.3	100	0.15385	1.1558	30.343
101	922	981	951	999	6.14	102	0.15385	1.1538	30.719
103	935	995	963	987	6.02	104	0.16667	1.1561	31.272
105	948	1009	975	975	5.96	106	0.16667	1.1684	32.079
107	961	1022	987	963	5.93	108	0.16667	1.1799	32.698
109	973	1036	999	951	5.95	110	0.16667	1.1889	32.83

TORF12 proxy data

111	985	1048	1011	939	6.02	112	0.16667	1.2136	32.389
113	998	1061	1023	927	6.13	114	0.16667	1.1845	31.15
115	1011	1074	1035	915	6.29	116	0.16667	1.2029	30.034
117	1025	1087	1048	902	6.5	118	0.15385	1.1782	29.471
119	1037	1099	1061	889	6.74	120	0.15385	1.1719	29.536
121	1052	1112	1074	876	7.04	122	0.15385	1.1682	30.399
123	1068	1125	1088	862	7.38	124	0.14286	1.1837	31.957
125	1083	1138	1103	847	3.88	126	0.13333	1.1465	33.008
129	1099	1151	1119	831	8.1	128	0.125	1.1195	33.946
131	1116	1166	1135	815	8.42	130	0.125	1.1523	34.997
133	1133	1181	1152	798	8.71	132	0.11765	1.1512	34.997
135	1150	1195	1169	781	8.96	134	0.11765	1.1439	34.059
137	1167	1210	1187	763	9.18	136	0.11111	1.1486	33.074
139	1184	1225	1205	745	9.36	138	0.11111	1.1142	32.576
141	1203	1243	1224	726	9.51	140	0.10526	1.1591	32.454
143	1221	1259	1243	707	9.63	142	0.10526	1.1471	31.957
145	1239	1279	1262	688	9.72	144	0.10526	1.1407	30.399
147	1257	1294	1282	668	9.77	146	0.1	1.0985	28.42
149	1277	1314	1301	649	9.8	148	0.10526	1.1402	26.872
151	1296	1334	1321	629	9.84	150	0.1	1.1237	25.812
153	1314	1356	1341	609	9.87	152	0.1	1.0993	24.826
155	1333	1377	1360	590	9.9	154	0.10526	1.1118	23.954
157	1356	1400	1380	570	9.93	156	0.1	1.1193	23.203
159	1375	1422	1400	550	9.96	158	0.1	1.1166	22.706
161	1393	1444	1420	530	9.99	160	0.1	1.1225	22.584
163	1411	1466	1440	510	10.01	162	0.1	1.1172	22.771
165	1428	1488	1460	490	10.04	164	0.1	1.1049	22.959
167	1446	1511	1480	470	10.07	166	0.1	1.1215	22.893
169	1463	1533	1500	450	10.09	168	0.1	1.1174	22.584
171	1481	1556	1520	430	10.12	170	0.1	1.1247	22.087
173	1500	1580	1541	409	10.14	172	0.095238	1.1176	21.589
175	1517	1602	1561	389	10.16	174	0.1	1.1176	21.158
177	1536	1626	1581	369	10.18	176	0.1	1.1236	21.092
179	1552	1648	1602	348	10.21	178	0.095238	1.1075	21.402
181	1570	1671	1622	328	10.23	180	0.1	1.1043	22.218
183	1588	1695	1642	308	10.25	182	0.1	1.1161	22.406
185	1606	1718	1663	287	10.26	184	0.095238	1.1107	21.843
187	1624	1741	1683	267	10.28	186	0.1	1.123	20.97
189	1642	1765	1704	246	10.3	188	0.095238	1.1036	20.538
191	1659	1787	1725	225	10.31	190	0.095238	1.1156	20.163
193	1676	1810	1745	205	10.33	192	0.1	1.1227	20.173
195	1695	1834	1766	184	10.34	194	0.095238	1.1282	20.782
197	1712	1857	1787	163	10.36	196	0.095238	1.1205	21.899
199	1731	1881	1807	143	10.37	198	0.1	1.1209	23.147
201	1748	1903	1828	122	10.38	200	0.095238	1.1199	24.817
203	1767	1927	1849	101	10.39	202	0.095238	1.1555	25.812
205	1785	1950	1870	80	10.4	204	0.095238	1.1215	24.883
207	1802	1972	1890	60	10.41	206	0.1	1.1323	23.325
209	1821	1995	1911	39	10.42	208	0.095238	1.1008	22.706
211	1840	2018	1932	18	10.43	210	0.095238	1.1413	22.959
213	1858	2040	1953	-3	10.43	212	0.095238	1.1375	23.888
215	1877	2063	1974	-24	10.44	214	0.095238	1.1345	25.436
217	1895	2085	1995	-45	10.44	216	0.095238	1.122	27.801
219	1915	2108	2016	-66	10.45	218	0.095238	1.1603	29.658
221	1934	2130	2036	-86	10.46	220	0.1	1.1215	29.039
223	1954	2152	2057	-107	10.46	222	0.095238	1.1293	27.425
225	1973	2174	2078	-128	10.47	224	0.095238	1.1223	26.562

TORF12 proxy data

227	1993	2196	2099	-149	10.49	226	0.095238	1.137	26.618
229	2013	2218	2120	-170	10.5	228	0.095238	1.1269	26.44
231	2034	2240	2141	-191	10.52	230	0.095238	1.1162	25.314
233	2053	2261	2162	-212	10.54	232	0.095238	1.1206	24.01
235	2074	2283	2183	-233	10.56	234	0.095238	1.1454	23.081
237	2094	2304	2204	-254	10.58	236	0.095238	1.1345	22.715
239	2114	2325	2226	-276	10.6	238	0.090909	1.0863	22.771
241	2136	2347	2247	-297	10.63	240	0.095238	1.1575	22.584
243	2157	2368	2268		10.66	242	0.095238	1.1359	22.152
245	2178	2389	2289		10.69	244	0.095238	1.1398	21.589
247	2199	2410	2311		10.72	246	0.090909	1.1504	21.036
249	2220	2431	2332		10.76	248	0.095238	1.1291	20.792
251	2242	2453	2354		10.8	250	0.090909	1.1319	21.036
253	2264	2474	2375		10.83	252	0.095238	1.1485	22.218
255	2286	2495	2397		10.88	254	0.090909	1.162	24.817
257	2308	2516	2419		10.92	256	0.090909	1.1856	27.303
259	2331	2538	2441		10.96	258	0.090909	1.2113	27.36
261	2353	2559	2462		11.01	260	0.095238	1.1699	25.633
263	2376	2581	2484		11.06	262	0.090909	1.1906	24.076
265	2400	2603	2507		11.11	264	0.086957	1.21	23.325
267	2422	2624	2529		11.16	266	0.090909	0.655	22.34
269	2446	2646	2551		11.22	268	0.090909	0.7658	22.396
271	2468	2667	2574		11.28	270	0.086957	0.8649	23.269
273	2492	2689	2596		11.34	272	0.090909	1.21	23.944
275	2517	2712	2619		11.4	274	0.086957	1.187	24.019
277	2540	2734	2642		11.46	276	0.086957	1.1372	24.198
279	2564	2756	2665		11.53	278	0.086957	1.1463	24.695
281	2589	2779	2688		11.6	280	0.086957	1.1377	25.07
283	2613	2801	2711		11.66	282	0.086957	1.1456	25.746
285	2638	2824	2734		11.74	284	0.086957	1.1398	27.116
287	2662	2846	2758		11.81	286	0.083333	1.1418	29.227
289	2688	2870	2781		11.89	288	0.086957	1.1527	30.653
291	2713	2893	2805		11.96	290	0.083333	1.1535	30.099
293	2738	2916	2829		12.04	292	0.083333	1.1444	29.283
295	2763	2938	2853		12.13	294	0.083333	1.1425	28.608
297	2789	2962	2877		12.21	296	0.083333	1.1451	27.979
299	2814	2984	2902		12.3	298	0.08	1.1387	27.669
301	2839	3007	2926		12.38	300	0.083333	1.1352	28.298
303	2866	3031	2951		12.47	302	0.08	1.1505	29.658
305	2893	3055	2976		12.57	304	0.08	1.1279	30.465
307	2920	3079	3001		12.66	306	0.08	1.1455	29.968
309	2946	3102	3026		12.76	308	0.08	1.1575	29.292
311	2974	3127	3052		12.86	310	0.076923	1.1453	30.212
313	3002	3151	3078		12.96	312	0.076923	1.1702	29.602
315	3030	3176	3104		13.06	314	0.076923	1.1126	27.425
317	3057	3200	3130		13.16	316	0.076923	1.1276	25.999
319	3086	3225	3156		13.27	318	0.076923	1.1453	25.933
321	3114	3250	3183		13.38	320	0.074074	1.1357	26.44
323	3143	3275	3209		13.49	322	0.076923	1.1445	26.618
325	3172	3300	3236		13.6	324	0.074074	1.0809	25.877
327	3202	3326	3264		13.72	326	0.071429	1.1459	25.38
329	3231	3352	3291		13.83	328	0.074074	1.1371	25.005
331	3260	3377	3319		13.95	330	0.071429	1.0708	24.883
333	3290	3403	3347		14.07	332	0.071429	1.1328	24.883
335	3321	3431	3375		14.2	334	0.071429	1.1282	24.939
337	3351	3457	3403		14.32	336	0.071429	1.1072	25.005
339	3381	3484	3432		14.45	338	0.068966	1.136	25.567

TORF12 proxy data

341	3412	3512	3461	14.58	340	0.068966	1.1602	26.431
343	3442	3540	3490	14.71	342	0.068966	1.1768	26.684
345	3472	3568	3519	14.84	344	0.068966	1.0417	26.374
347	3502	3597	3549	14.97	346	0.066667	1.153	25.877
349	3532	3627	3579	15.09	348	0.066667	1.1519	25.502
351	3562	3657	3609	15.19	350	0.066667	1.1527	24.883
353	3591	3687	3639	15.28	352	0.066667	1.1603	24.076
355	3621	3718	3670	15.36	354	0.064516	0.9976	23.334
357	3649	3748	3701	15.43	356	0.064516	1.1509	23.025
359	3679	3779	3731	15.48	358	0.066667	1.1514	22.893
361	3709	3810	3762	15.53	360	0.064516	1.1509	23.391
363	3739	3842	3794	15.56	362	0.0625	1.142	24.451
365	3768	3872	3825	15.58	364	0.064516	1.1611	25.38
367	3798	3904	3856	15.58	366	0.064516	1.1611	25.624
369	3828	3936	3887	15.58	368	0.064516	1.1684	25.38
371	3857	3967	3918	15.56	370	0.064516	1.1527	25.624
373	3887	4000	3949	15.53	372	0.064516	1.1523	26.365
375	3916	4031	3980	15.49	374	0.064516	1.1622	26.252
377	3947	4063	4011	15.43	376	0.064516	1.1623	26.252
379	3976	4094	4042	15.37	378	0.064516	1.1453	26.806
381	4005	4126	4073	15.29	380	0.064516	1.1738	29.105
383	4034	4157	4103	15.2	382	0.066667	1.1744	32.886
385	4063	4188	4134	15.09	384	0.064516	1.2115	37.849
387	4091	4219	4164	14.98	386	0.066667	1.2122	45.111
389	4119	4249	4194	5.94	388	0.066667	1.3881	49.014
	4119	4249	4194	5.94	390	0	1.2076	42.747
	4119	4249	4194	5.94	392	0	1.2058	36.048
394	4147	4280	4224	14.71	394	0.066667	1.1934	34.002
396	4176	4311	4253	14.58	396	0.068966	1.2187	35.804
398	4203	4340	4282	14.45	398	0.068966	1.1729	63.783
400	4232	4371	4311	14.33	400	0.068966	1.2287	53.978
402	4260	4401	4340	14.21	402	0.068966	1.2352	49.324
404	4287	4430	4368	14.11	404	0.071429	1.2115	49.821
406	4315	4459	4396	14	406	0.071429	1.2412	52.12
408	4342	4488	4424	13.9	408	0.071429	1.2237	48.836
410	4370	4517	4452	13.81	410	0.071429	1.1715	40.082
412	4397	4545	4480	13.73	412	0.071429	1.1702	33.139
414	4425	4574	4507	13.65	414	0.074074	1.1587	29.968
416	4451	4601	4535	13.57	416	0.071429	1.162	28.851
418	4478	4629	4562	13.5	418	0.074074	1.1451	28.795
420	4506	4658	4589	13.44	420	0.074074	1.1653	28.598
422	4533	4686	4616	13.38	422	0.074074	1.1542	27.303
424	4561	4714	4642	13.33	424	0.076923	1.1375	26.806
426	4588	4742	4669	13.29	426	0.074074	1.1541	27.116
428	4615	4769	4696	13.25	428	0.074074	1.1176	28.288
430	4642	4796	4722	13.22	430	0.076923	1.1672	30.343
432	4669	4824	4749	13.19	432	0.074074	1.1425	30.775
434	4696	4851	4775	13.17	434	0.076923	1.1432	28.973
436	4724	4878	4801	13.16	436	0.076923	1.1372	27.491
438	4750	4904	4828	13.15	438	0.074074	1.1386	26.994
440	4777	4931	4854	13.15	440	0.076923	1.148	31.394
442	4805	4958	4880	13.15	442	0.076923	1.1443	30.897
444	4832	4984	4907	13.16	444	0.074074	1.1495	31.516
446	4860	5012	4933	13.17	446	0.076923	1.1329	33.252
448	4888	5038	4959	13.19	448	0.076923	1.1479	34.19
450	4915	5064	4986	13.22	450	0.074074	1.1512	34.124
452	4943	5091	5012	13.25	452	0.076923	1.1419	33.571

TORF12 proxy data

454	4971	5118	5039	13.29	454	0.074074	1.1519	33.195
456	5000	5145	5065	13.34	456	0.076923	1.1325	33.261
458	5027	5171	5092	13.39	458	0.074074	1.1075	33.946
460	5055	5198	5119	13.45	460	0.074074	1.114	35.119
462	5084	5225	5145	13.51	462	0.076923	1.1338	36.236
464	5112	5251	5172	13.58	464	0.074074	1.1372	32.276
466	5140	5278	5200	13.65	466	0.071429	1.1377	32.276
468	5169	5305	5227	13.73	468	0.074074	1.1618	32.323
470	5197	5331	5254	13.82	470	0.074074	1.1481	32.37
472	5227	5359	5282	13.91	472	0.071429	1.1519	32.67
474	5255	5385	5310	14.01	474	0.071429	1.1489	33.411
476	5285	5413	5338	14.11	476	0.071429	1.1284	34.2
478	5314	5440	5366	14.22	478	0.071429	1.1535	34.396
480	5343	5468	5395	14.34	480	0.068966	1.1491	35.185
482	5372	5497	5423	14.46	482	0.071429	1.1617	36.376
484	5402	5527	5452	14.59	484	0.068966	1.1394	37.211
486	5431	5554	5481	14.72	486	0.068966	1.1655	37.802
488	5461	5584	5511	14.86	488	0.066667	1.137	38.394
490	5491	5612	5541	15.01	490	0.066667	1.1558	39.088
492	5522	5641	5571	15.14	492	0.066667	1.1695	39.482
494	5553	5671	5601	15.26	494	0.066667	1.144	39.876
496	5583	5700	5631	15.37	496	0.066667	1.1489	40.917
498	5613	5731	5662	15.47	498	0.064516	1.1716	41.312
500	5644	5763	5693	15.56	500	0.064516	1.1591	40.467
502	5674	5794	5724	15.64	502	0.064516	1.1407	39.482
504	5705	5826	5755	15.7	504	0.064516	1.1487	38.196
506	5735	5857	5787	15.76	506	0.0625	1.1458	36.714
508	5764	5888	5818	15.81	508	0.064516	1.1583	35.776
510	5795	5920	5850	15.85	510	0.0625	1.164	35.391
512	5825	5952	5882	15.87	512	0.0625	1.1642	35.832
514	5855	5984	5913	15.89	514	0.064516	1.1576	36.076
516	5884	6015	5945	15.9	516	0.0625	1.1555	36.573
518	5914	6047	5977	15.89	518	0.0625	1.1618	38.15
520	5944	6079	6009	15.87	520	0.0625	1.1437	39.041
522	5974	6111	6040	15.85	522	0.064516	1.1666	38.787
524	6004	6143	6072	15.81	524	0.0625	1.1626	39.135
526	6035	6175	6104	15.77	526	0.0625	1.1738	40.176
528	6065	6207	6135	15.71	528	0.064516	1.1561	40.917
530	6095	6238	6167	15.64	530	0.0625	1.1863	42.297
532	6124	6269	6198	15.56	532	0.064516	1.1137	42.944
534	6154	6300	6229	15.47	534	0.064516	1.1793	43.479
536	6183	6331	6260	15.37	536	0.064516	1.1398	44.868
538	6213	6362	6291	15.26	538	0.064516	1.1941	46.397
540	6241	6391	6321	15.14	540	0.066667	1.206	45.853
542	6270	6422	6352	15.01	542	0.064516	1.2	45.308
544	6299	6452	6382	14.87	544	0.066667	1.1998	45.064
546	6327	6481	6411	14.72	546	0.068966	1.2083	44.764
548	6355	6511	6441	14.56	548	0.066667	1.245	45.412
550	6383	6540	6470	14.38	550	0.068966	1.2639	45.064
552	6410	6569	6499	14.2	552	0.068966	1.2278	43.479
554	6438	6598	6527	14.01	554	0.071429	1.201	43.873
556	6465	6626	6555	5.52	556	0.071429	1.2013	48.771
	6465	6626	6555	5.52	558	0	1.2033	59.776
561	6493	6655	6583	13.6	560	0.071429	1.3039	68.071
563	6519	6682	6610	13.4	562	0.074074	1.1765	60.02
565	6545	6709	6637	13.21	564	0.074074	1.1773	52.223
567	6571	6736	6663	13.03	566	0.076923	1.185	48.423

TORF12 proxy data

569	6597	6762	6689	12.85	568	0.076923	1.1641	46.491
571	6623	6789	6715	12.69	570	0.076923	1.1837	45.215
573	6649	6815	6740	12.53	572	0.08	1.183	44.717
575	6674	6840	6765	12.38	574	0.08	1.1925	44.868
577	6698	6864	6790	12.23	576	0.08	1.1646	44.717
579	6724	6889	6815	12.1	578	0.08	1.1676	43.732
581	6748	6913	6839	11.97	580	0.083333	1.1801	42.156
583	6773	6937	6863	11.85	582	0.083333	1.1656	41.011
585	6797	6960	6886	11.73	584	0.086957	1.1676	40.861
587	6822	6984	6910	11.63	586	0.083333	1.1697	40.964
589	6846	7007	6933	11.53	588	0.086957	1.1588	40.964
591	6870	7029	6956	11.44	590	0.086957	1.1516	40.673
593	6893	7051	6979	11.36	592	0.086957	1.1763	40.026
595	6918	7074	7002	11.29	594	0.086957	1.123	38.59
597	6941	7096	7024	11.22	596	0.090909	1.1468	37.558
599	6964	7117	7047	11.16	598	0.086957	1.1621	37.211
601	6989	7139	7069	11.11	600	0.090909	1.1406	37.849
603	7012	7160	7091	11.07	602	0.090909	1.1561	38.347
605	7036	7182	7114	11.03	604	0.086957	1.1459	38.694
607	7060	7203	7136	11	606	0.090909	1.1445	39.332
609	7084	7224	7158	10.98	608	0.090909	1.1576	39.829
611	7108	7245	7180	10.97	610	0.090909	1.1613	39.932
613	7133	7266	7201	10.97	612	0.095238	1.1486	39.688
615	7157	7287	7223	10.97	614	0.090909	1.1481	39.482
617	7181	7307	7245	10.98	616	0.090909	1.1637	39.838
619	7205	7328	7267	11	618	0.090909	1.1613	39.651
621	7230	7349	7289	11.03	620	0.090909	1.1626	39.529
623	7254	7370	7311	11.06	622	0.090909	1.173	39.519
625	7277	7390	7334	11.1	624	0.086957	1.1373	39.585
627	7300	7411	7356	11.15	626	0.090909	1.177	40.214
629	7324	7432	7378	11.21	628	0.090909	1.166	40.889
631	7347	7453	7400	11.27	630	0.090909	1.1555	41.95
633	7369	7473	7423	11.35	632	0.086957	1.1521	42.813
635	7394	7495	7446	11.43	634	0.086957	1.1522	44.426
637	7416	7517	7469	11.52	636	0.086957	1.153	42.25
639	7436	7540	7492	11.61	638	0.086957	1.1456	41.443
641	7456	7565	7515	11.72	640	0.086957	1.1442	42.381
643	7476	7592	7538	11.83	642	0.086957	1.1561	44.37
645	7499	7623	7562	11.97	644	0.083333	1.1563	46.537
647	7519	7653	7586	12.13	646	0.083333	1.0687	47.842
649	7528	7683	7610	12.31	648	0.083333	1.1621	49.268
651	7552	7713	7635	12.51	650	0.08	1.1475	50.319
653	7581	7746	7660	12.74	652	0.08	1.1532	51.004
655	7604	7780	7685	12.98	654	0.08	1.1622	52.805
657	7626	7814	7711	13.24	656	0.076923	1.1661	54.353
659	7649	7849	7738	13.52	658	0.074074	1.1709	53.546
661	7673	7884	7765	13.83	660	0.074074	1.1764	51.754
663	7696	7920	7792	14.15	662	0.074074	1.1578	50.262
665	7720	7957	7821	14.5	664	0.068966	1.1724	49.821
667	7746	7996	7850	14.87	666	0.068966	1.1725	51.004
669	7771	8033	7879	15.25	668	0.068966	1.1633	52.43
671	7797	8072	7910	15.66	670	0.064516	1.1755	55.414
673	7822	8110	7941	16.09	672	0.064516	1.1908	58.388
675	7850	8150	7973	16.54	674	0.0625	1.186	58.951
677	7878	8190	8007	17.01	676	0.058824	1.1842	58.885
679	7906	8230	8041	17.5	678	0.058824	1.1815	60.058
681	7937	8272	8076	18.02	680	0.057143	1.1677	62.788

TORF12 proxy data

683	7968	8314	8112	18.55	682	0.055556	1.1815	68.812
685	8002	8358	8149	19.1	684	0.054054	1.2309	76.571
687	8035	8401	8187	19.68	686	0.052632	1.1944	78.495
689	8071	8447	8226	20.27	688	0.051282	1.1709	75.079
691	8107	8492	8267	20.89	690	0.04878	1.1687	73.907
693	8146	8539	8309	21.52	692	0.047619	1.1906	76.074
695	8186	8587	8352	22.18	694	0.046512	1.1966	77.5
697	8227	8635	8396	22.86	696	0.045455	1.2301	75.699
699	8270	8685	8442	23.56	698	0.043478	1.215	72.349
701	8316	8736	8489	24.27	700	0.042553	1.2407	69.741
703	8362	8788	8537	25.02	702	0.041667	1.2187	43.188
705	8410	8841	8587	25.78	704	0.04	1.2544	56.896
707	8459	8894	8639	26.56	706	0.038462	1.2536	65.96
709	8512	8950	8692	27.36	708	0.037736	1.2497	66.823
711	8566	9006	8747	28.18	710	0.036364	1.2291	65.584
713	8621	9062	8803	29.03	712	0.035714	1.2292	67.076
715	8679	9119	8861	29.89	714	0.034483	1.239	71.786
717	8739	9178	8921	30.78	716	0.033333	1.299	74.835
719	8801	9238	8982	31.68	718	0.032787	1.1869	74.216
721	8865	9298	9046	32.61	720	0.03125	1.199	72.903
723	8932	9360	9111	33.56	722	0.030769	1.1954	71.42
725	9002	9423	9178	34.52	724	0.029851	1.2213	70.426
727	9074	9487	9247	35.51	726	0.028986	1.1972	71.167
729	9148	9553	9318	36.52	728	0.028169	1.2308	74.704
731	9225	9621	9391	37.55	730	0.027397	1.256	78.86
733	9304	9690	9466	38.6	732	0.026667	1.239	81.657
735	9387	9760	9544	39.68	734	0.025641	1.2117	84.697
737	9472	9832	9623	40.77	736	0.025316	1.2391	88.177
739	9560	9905	9704	41.88	738	0.024691	1.2777	90.711
741	9651	9980	9788	43.01	740	0.02381	1.2381	95.927
743	9747	10061	9874	44.17	742	0.023256	1.2912	105.17
745	9846	10144	9963	45.35	744	0.022472	1.2238	115.28
747	9948	10231	10053	46.54	746	0.022222	1.2857	131.23
749	10052	10321	10146	47.76	748	0.021505	1.2783	147.05
751	10158	10413	10242	49	750	0.020833	1.3211	160.34
753	10254	10508	10340	3.47	752	0.020408	1.3322	174.73
	10254	10508	10340	3.47	754	0	1.4776	189.43
782	10328	10700	10440	51.48	782	0.28	1.3567	195.02
784	10403	10785	10543	52.63	784	0.019417		
786	10473	10893	10649	53.7	786	0.018868		
788	10549	10995	10756	54.69	788	0.018692		
790	10624	11094	10865	55.6	790	0.018349		
792	10703	11196	10977	56.43	792	0.017857		
794	10787	11302	11089	57.19	794	0.017857		
796	10878	11425	11204	57.86	796	0.017391		
798	10957	11546	11320	58.45	798	0.017241		
800	11037	11670	11436	58.97	800	0.017241		
802	11118	11795	11554	59.4	802	0.016949		
804	11198	11920	11673	59.76	804	0.016807		
806	11282	12053	11793	60.03	806	0.016667		
808	11365	12178	11913	60.23	808	0.016667		
810	11447	12306	12033	60.35	810	0.016667		
812	11530	12439	12154	60.39	812	0.016529		
814	11615	12572	12275	60.39	814	0.016529		
816	11697	12705	12395	60.39	816	0.016667		
818	11779	12842	12516	60.39	818	0.016529		
820	11860	12981	12637	60.39	820	0.016529		

TORF12 proxy data

822	11941	13121	12758	60.39	822	0.016529		
824	12021	13262	12879	60.39	824	0.016529		
826	12101	13403	12999	60.39	826	0.016667		
828	12181	13545	13120	60.39	828	0.016529		
830	12262	13686	13241	60.39	830	0.016529		
832	12342	13826	13362	60.39	832	0.016529		
834	12424	13968	13482	60.39	834	0.016667		
836	12505	14110	13603	60.39	836	0.016529		
838	12586	14252	13724	60.39	838	0.016529	1.4795	554.09
840	12668	14394	13845	60.39	840	0.016529	1.4332	523.5
842	12748	14536	13966	60.39	842	0.016529	1.4309	517.85
844	12829	14679	14086	60.39	844	0.016667	1.4856	526.11

TORF12 proxy data

%C	15N	13C	C/N	C:N at	Bsi	Bsi/TOC	TOC/Bsi	lut/diat	Diato 1
8.6393	-0.055	-21.596	9.6533	11.262		0		0.35601	0.1405
9.7679	-0.115	-20.779	9.5332	11.122	105.69	10.82	0.092425	0.28096	0.19813
9.8246	0.016	-21.734	10.123	11.81	104.65	10.652	0.093881	0.28532	0.15788
8.5189	-0.067	-21.183	9.4923	11.074	102.09	11.985	0.083441	0.37248	0.23236
8.2476	0.129	-21.815	9.6044	11.205	91.156	11.052	0.090478	0.29787	0.20057
9.257	-0.017	-21.662	9.6363	11.242	97.66	10.55	0.094789	0.32481	0.1982
9.1813	0.007	-21.757	9.61	11.212	101.48	11.053	0.090474	0.39739	0.21643
9.3437	0.17	-21.711	9.5465	11.138	109.32	11.7	0.085467	0.33647	0.20816
9.0584	-0.166	-21.779	9.5256	11.113	104.01	11.482	0.087095	0.40055	0.21462
8.5656	0.176	-22.165	9.4816	11.062	108.75	12.696	0.078765	0.32305	0.14501
7.8834	0.167	-22.495	9.4106	10.979	108.28	13.735	0.072807	0.32352	0.16474
8.8779	0.429	-23.053	9.4423	11.016	105.58	11.892	0.08409	0.33143	0.13692
9.2119	0.079	-22.837	10.295	12.011	109.91	11.932	0.08381	0.41406	0.14287
8.9509	-0.088	-22.129	9.7197	11.34	107.42	12.001	0.083329	0.32459	0.16272
8.51	0.174	-21.982	9.4248	10.996	101.96	11.981	0.083465	0.29231	0.15431
8.9337	-0.125	-21.923	9.5796	11.176	108.75	12.173	0.082151	0.30467	0.12708
8.6021	-0.25	-21.674	9.3801	10.943	111.08	12.913	0.077442	0.24304	0.13528
8.8935	-0.203	-21.455	9.5839	11.181	116.01	13.044	0.076662	0.30148	0.17118
8.6594	-0.23	-20.796	9.4658	11.043	110.38	12.747	0.078451		
8.8519	-0.269	-19.975	9.1447	10.669	114.94	12.985	0.077011	0.20476	0.27632
8.5766	-0.365	-19.9	9.3059	10.857	119.01	13.876	0.072069	0.21454	0.30902
8.5982	-0.273	-20.355	9.2095	10.744	116.22	13.517	0.073982	0.22488	0.25636
10.442	-0.837	-19.503	9.9382	11.595	109.63	10.499	0.095244	0.22014	0.098246
9.9842	-0.516	-20.101	9.4827	11.063	121.42	12.161	0.082229	0.22561	0.095702
10.014	-0.34	-20.551	9.7377	11.361	113.17	11.301	0.088485		
9.7798	-0.252	-19.963	9.356	10.915	111.15	11.365	0.08799		
9.219	-0.521	-20.016	9.1732	10.702	113.26	12.285	0.081398		
9.1497	-0.472	-19.592	8.8844	10.365	104.55	11.426	0.087517	0.29366	0.22595
9.2585	-0.621	-19.267	8.9896	10.488	130.31	14.074	0.071052	0.27791	0.30931
9.4639	-0.742	-19.126	9.1239	10.644	115.12	12.164	0.082208	0.24865	0.30275
9.1785	-0.507	-19.274	8.9437	10.434	110.78	12.07	0.082852	0.1761	0.11777
8.7192	-0.534	-19.497	9.3051	10.856	108.36	12.428	0.080466	0.24498	0.2873
8.4191	-0.496	-20.142	8.9411	10.431	112.73	13.39	0.074682	0.20416	0.24079
7.1038	-0.554	-20.628	9.1127	10.632	103.57	14.579	0.06859	0.19322	0.26912
7.231	-0.807	-20.954	9.1087	10.627	117.92	16.307	0.061323	0.20479	0.19638
6.9262	-0.686	-19.591	8.8904	10.372	104.77	15.126	0.066111	0.20669	0.13905
6.1512	-0.545	-19.033	8.4312	9.8364	126.07	20.496	0.04879	0.24877	0.21492
					124.85			0.25168	0.28404
7.497	-0.656	-18.609	8.5948	10.027	119.16	15.894	0.062917	0.26408	0.29747
6.4829	-0.277	-18.932	8.2558	9.6318	116.1	17.909	0.055838	0.20165	0.22801
5.3288	-0.673	-18.885	8.8416	10.315	115.37	21.65	0.046188	0.18147	0.19132
5.0906	-0.726	-19.303	8.5386	9.9617	105.56	20.736	0.048226	0.20436	0.17748
6.6885	-0.935	-20.017	9.8969	11.546	100.89	15.083	0.066298	0.21143	0.089917
8.7449	-0.543	-18.463	8.4259	9.8302	123.21	14.089	0.070978	0.20986	0.11935
8.4748	-0.586	-18.565	8.3581	9.7511	128.61	15.176	0.065893	0.19484	0.16954
8.6632	-0.599	-18.581	8.2767	9.6562	133.13	15.368	0.065071	0.24179	0.24348
8.4677	-0.488	-18.54	8.3032	9.6871	126.9	14.987	0.066725	0.22627	0.26524
8.4774	-0.489	-18.581	8.3681	9.7628	130.55	15.4	0.064937	0.2423	0.28791
8.6906	-0.529	-18.249	8.4725	9.8846	119.82	13.788	0.072529	0.24097	0.27743
8.3584	-0.578	-18.417	8.4004	9.8005	124.43	14.887	0.067171	0.23144	0.30078
					126.33			0.23223	0.26082
8.7204	-0.6	-18.891	8.7662	10.227	128.43	14.727	0.067901	0.23251	0.2918
8.1054	-0.512	-18.585	8.4711	9.8829	125.69	15.508	0.064484	0.24898	0.15546
10.247	-0.711	-21.127	10.536	12.292	138.08	13.476	0.074207	0.26642	0.14715
8.4895	-0.508	-18.831	8.4785	9.8916	127.34	15	0.066667	0.27811	0.17858
8.2756	-0.612	-18.239	8.441	9.8478	125.04	15.11	0.066183	0.27416	0.22417

TORF12 proxy data

8.0121	-0.728	-18.175	8.3813	9.7782	141.75	17.692	0.056524	0.23315	0.19665
7.5031	-0.797	-17.468	8.165	9.5258	124.07	16.536	0.060473		
8.0236	-0.517	-17.699	8.0164	9.3524	121.22	15.108	0.066192	0.2178	0.11879
8.0327	-0.685	-17.833	8.0931	9.4419	123.97	15.433	0.064796	0.19281	0.22096
8.0192	-0.598	-17.648	7.9789	9.3087	128.05	15.968	0.062626	0.19331	0.21756
7.718	-0.781	-17.673	8.0654	9.4097	127.42	16.509	0.060572	0.22213	0.18748
6.6067	-0.577	-17.547	7.9554	9.2813	116.38	17.616	0.056766	0.26856	0.24211
8.1868	-0.608	-17.198	7.9092	9.2274	124	15.147	0.066021		
5.599	-0.64	-17.713	8.1137	9.466	128.04	22.868	0.043729	0.22831	0.1703
6.7824	-0.731	-17.397	8.0319	9.3706	119.96	17.687	0.056539	0.25348	0.28429
8.7554	-0.59	-17.342	8.1369	9.4931	119.6	13.66	0.073208	0.22642	0.16241
9.4368	-0.592	-17.722	8.3859	9.7835	144.94	15.359	0.065109	0.24211	0.16945
8.5247	-0.62	-17.234	8.121	9.4745	145.22	17.036	0.058701	0.24725	0.18146
8.4149	-0.365	-17.343	8.1295	9.4844	135.84	16.143	0.061947	0.23827	0.14758
9.827	-0.573	-17.203	8.1916	9.5569	136.96	13.937	0.071749	0.24497	0.156
9.1873	-0.538	-17.702	8.082	9.429	127.6	13.888	0.072003	0.24158	0.18019
8.8717	-0.479	-17.354	8.0033	9.3372	130.14	14.669	0.06817	0.24077	0.12748
8.0151	-0.565	-17.426	8.1216	9.4752	136.38	17.015	0.058771	0.2566	0.31256
7.6955	-0.56	-17.709	8.1416	9.4986	130.96	17.017	0.058764	0.25342	0.26857
9.1125	-0.562	-17.265	8.1719	9.5339	124.9	13.706	0.07296	0.22092	0.24932
9.1296	-0.599	-17.283	8.0669	9.4114	126.55	13.862	0.072141	0.23171	0.23055
8.8912	-0.422	-17.212	7.9027	9.2198	131.42	14.781	0.067655	0.19375	0.1536
9.6797	-0.532	-17.213	8.0579	9.4009	134.69	13.915	0.071867	0.23969	0.26646
8.8	-0.581	-17.117	7.9514	9.2766	131.87	14.985	0.066732	0.23349	0.19392
9.0514	-0.703	-17.151	8.0762	9.4222	135.86	15.009	0.066625	0.21944	0.23946
8.8569	-0.572	-17.105	8.1133	9.4656	133.41	15.063	0.066388	0.23475	0.20468
9.0984	-0.587	-17.287	8.0257	9.3633	133.94	14.722	0.067927	0.25192	0.33587
8.9616	-0.664	-17.23	8.0425	9.383	132.07	14.738	0.067854	0.26927	0.31521
6.4957	-0.582	-17.083	8.0468	9.388	124.93	19.233	0.051993	0.26745	0.32928
9.3884	-0.816	-17.194	8.2361	9.6088	133.06	14.173	0.070558		
8.9892	-0.761	-16.944	8.176	9.5386	135.23	15.044	0.066473	0.25658	0.2747
9.0271	-0.529	-17.096	7.9891	9.3207	137.4	15.221	0.065699	0.23499	0.28022
7.1999	-0.614	-17.174	7.9231	9.2436	137.52	19.101	0.052354	0.21686	0.23627
8.2679	-0.668	-17.209	7.8737	9.1859	137.04	16.575	0.060331	0.17998	0.18465
8.2786	-0.497	-17.133	7.7778	9.0741	140.22	16.938	0.059039	0.27172	0.26369
8.6096	-0.713	-17.107	7.944	9.268	129.81	15.077	0.066325	0.33958	0.24919
8.9296	-0.74	-16.803	8.0666	9.411	138.48	15.509	0.064481	0.27481	0.16528
9.0791	-0.748	-16.916	7.9772	9.3067	133.39	14.693	0.068062	0.2625	0.1411
8.3393	-0.542	-16.998	7.9747	9.3038	144.25	17.298	0.05781	0.25701	0.18208
8.2094	-0.535	-16.998	7.9675	9.2954	139.78	17.027	0.05873	0.30999	0.27036
8.6555	-0.605	-16.856	7.9563	9.2823	142.43	16.455	0.060772	0.309	0.33581
8.3451	-0.647	-17.27	7.9023	9.2194	139.51	16.718	0.059816	0.28502	0.22303
7.9778	-0.631	-17.526	8.001	9.3345	135.77	17.019	0.058758	0.32571	0.27496
7.8606	-0.583	-17.831	8.0845	9.4319	141.26	17.971	0.055646	0.29414	0.2626
5.2925	-0.521	-17.746	8.0659	9.4103	142.39	26.904	0.037169		
6.3022	-0.642	-17.583	8.0253	9.3629	113.17	17.957	0.055689		
8.2354	-0.499	-17.51	8.2909	9.6727	139.68	16.961	0.05896	0.22474	0.43719
8.217	-0.511	-17.784	8.1437	9.501	135.77	16.523	0.06052	0.20867	0.34636
8.2861	-0.513	-17.843	8.0819	9.4288	137.12	16.548	0.060431	0.2153	0.3915
7.8658	-0.505	-17.812	8.0602	9.4036	130.46	16.586	0.060293	0.22616	0.31127
8.1012	-0.374	-17.677	8.138	9.4943	141.24	17.435	0.057357	0.26585	0.3129
8.178	-0.509	-18.187	8.2064	9.5742	137.21	16.778	0.059602	0.24017	0.4039
7.8158	-0.471	-17.844	8.1356	9.4915	132.96	17.011	0.058785	0.25857	0.30431
7.5758	-0.525	-17.768	7.9348	9.2572	135.97	17.949	0.055715	0.21635	0.1657
9.6928	-0.591	-18.03	7.8984	9.2148	141.1	14.557	0.068695	0.26412	0.27688
7.786	-0.462	-18.073	7.9472	9.2718	135.97	17.463	0.057263	0.24568	0.25096
7.6994	-0.52	-17.923	7.8527	9.1615	139.57	18.128	0.055164	0.24294	0.29679

TORF12 proxy data

8.6309	-0.556	-17.125	8.1404	9.4971	140.02	16.223	0.061643	0.24067	0.28354
6.9605	-0.545	-17.888	7.9938	9.3261	137.7	19.783	0.050549		
7.7595	-0.459	-18.463	8.2804	9.6605	133.24	17.171	0.058239	0.094194	0.31427
8.0159	-0.535	-17.809	8.0677	9.4124	136.65	17.047	0.058661		
8.5524	-0.544	-18.069	8.2073	9.5752	135.83	15.882	0.062963	0.19471	0.20914
8.6759	-0.438	-18.03	8.147	9.5048	139.33	16.059	0.062268		
8.2663	-0.43	-17.947	7.9097	9.228	132.23	15.996	0.062516	0.084596	0.30208
8.8312	-0.418	-17.839	8.1738	9.5361	136.04	15.405	0.064915		
8.3671	-0.542	-17.824	8.0039	9.3379	132.08	15.785	0.063351	0.24871	0.30471
8.6829	-0.522	-17.839	8.1156	9.4683	137.85	15.876	0.062987		
8.799	-0.294	-17.549	8.0359	9.3753	136.88	15.557	0.064281	0.11772	0.26118
8.637	-0.357	-17.872	8.1526	9.5114	138.23	16.004	0.062485		
8.6757	-0.342	-17.879	8.0669	9.4114	133.3	15.365	0.065082	0.13993	0.21609
8.6529	-0.406	-17.69	8.193	9.5585	137.64	15.907	0.062867		
8.3066	-0.337	-18.05	8.1965	9.5625	134.24	16.16	0.061881		
7.6259	-0.263	-18.326	8.136	9.492	118.88	15.589	0.064149		
7.692	-0.26	-18.55	8.1835	9.5474	132.24	17.192	0.058167	0.11795	0.2508
7.9	-0.255	-18.693	8.2177	9.5873	133.92	16.952	0.05899		
8.2015	-0.293	-18.33	8.1964	9.5625	133.24	16.246	0.061555	0.094929	0.24282
8.6893	-0.264	-17.973	8.2536	9.6292	126.53	14.561	0.068676		
8.3272	-0.374	-17.966	8.2834	9.664	143.08	17.182	0.058201		
7.8907	-0.228	-18.469	8.2695	9.6477	134	16.982	0.058887	0.11402	0.26242
7.8506	-0.345	-18.41	8.2287	9.6001	132.97	16.937	0.059042		
8.5821	-0.06	-18.395	8.0011	9.3346	131.17	15.284	0.065426	0.11017	0.27539
7.5821	-0.236	-18.688	8.0236	9.3609	129.97	17.141	0.058339		
7.6642	-0.254	-18.835	8.1511	9.5096	133.83	17.462	0.057267		
7.7853	-0.544	-18.743	8.1397	9.4963	140.29	18.02	0.055493	0.14382	0.34703
7.6307	-0.619	-18.737	8.1035	9.4541	129.4	16.958	0.058968		
7.1207	-0.403	-18.673	7.9429	9.2667	125.43	17.615	0.056769	0.1091	0.37707
7.1371	-0.293	-18.846	8.1026	9.453	127.65	17.885	0.055913		
6.9839	-0.413	-19.148	8.0739	9.4196	138.34	19.808	0.050485		
7.2016	-0.195	-18.551	8.4452	9.8527	128.1	17.788	0.056218	0.27967	0.31091
6.685	-0.19	-19.308	8.0183	9.3547	134.12	20.063	0.049843		
6.2782	-0.191	-19.27	7.8552	9.1644	132.67	21.132	0.047321	0.13983	0.30963
6.6087	-0.066	-18.763	8.047	9.3882	130.32	19.72	0.05071		
6.4441	-0.081	-18.988	7.9563	9.2823	123.12	19.106	0.052339	0.10122	0.2997
6.5681	-0.102	-19.271	8.0741	9.4198	133.99	20.4	0.04902		
5.7897	-0.173	-19.161	7.9324	9.2545	126.96	21.928	0.045603	0.092211	0.25309
6.6323	-0.144	-18.606	7.8337	9.1393	123.95	18.689	0.053509		
6.5422	-0.206	-18.489	7.9157	9.235	114.48	17.498	0.057149	0.11326	0.26239
6.6445	-0.365	-18.543	7.9089	9.2271					
5.8379	-0.448	-18.519	7.8708	9.1826	113.54	19.448	0.051418	0.10501	0.2113
8.4675	-0.368	-18.421	7.8671	9.1783					
8.2101	-0.161	-18.575	7.8699	9.1815	139.49	16.99	0.05886	0.10365	0.27736
8.2088	-0.252	-18.613	7.9199	9.2399					
8.2061	-0.412	-18.584	7.9513	9.2765	133.15	16.225	0.061632	0.13254	0.20146
8.1589	-0.262	-18.586	7.8971	9.2133					
10.088	-0.579	-17.846	8.5955	10.028	125.03	12.393	0.080688	0.12505	0.29446
8.5514	-0.402	-18.639	7.8544	9.1634					
9.037	-0.253	-19.143	7.8741	9.1864	125.46	13.882	0.072034	0.10787	0.24918
8.596	-0.187	-18.843	7.8754	9.188					
8.4903	-0.16	-18.74	7.9684	9.2965	143.91	16.95	0.058997	0.12286	0.16042
8.5937	-0.216	-18.807	7.9484	9.2732					
8.6341	-0.443	-18.557	8.0268	9.3646	132.82	15.383	0.065008	0.13349	0.14737
8.3158	-0.312	-18.813	7.9278	9.2491					
7.6713	-0.037	-19.218	7.7149	9.0007	134.57	17.541	0.057008	0.12058	0.24534

TORF12 proxy data

7.6905	-0.069	-19.416	7.6704	8.9488					
8.7134	-0.282	-18.96	7.7851	9.0826	132.16	15.168	0.065928	0.1186	0.16722
8.7222	-0.342	-19.099	7.7067	8.9911					
8.2457	-0.137	-19.631	7.7551	9.0476	131.47	15.945	0.062717	0.13706	0.25744
8.537	-0.123	-18.95	7.7916	9.0902					
8.3126	-0.265	-18.985	7.6366	8.9093	140.29	16.877	0.059253	0.11024	0.33102
8.4074	-0.252	-18.555	7.7121	8.9975					
8.593	-0.309	-18.475	7.6678	8.9458	140.16	16.311	0.061308	0.12065	0.36653
8.8619	-0.12	-18.23	7.7979	9.0975					
8.9456	-0.146	-18.276	7.7675	9.062	136.28	15.234	0.065643	0.10507	0.27572
8.0943	-0.222	-18.659	7.7235	9.0107					
8.109	-0.119	-18.682	7.7114	8.9967	134.22	16.551	0.060418	0.097682	0.31542
8.0344	-0.064	-18.813	7.5588	8.8186					
7.5684	-0.102	-19.065	7.7038	8.9878	148.29	19.594	0.051037	0.12893	0.28628
8.7209	-0.38	-17.969	7.8936	9.2092					
7.8642	-0.209	-18.377	7.7884	9.0864	137.63	17.5	0.057142	0.12499	0.23599
7.7778	-0.141	-18.53	7.683	8.9635					
8.2706	-0.271	-18.566	7.8568	9.1662	143.6	17.363	0.057595	0.11225	0.18917
8.6262	-0.337	-17.853	7.8852	9.1994					
7.6891	-0.175	-18.234	7.8975	9.2137	135.52	17.624	0.056739	0.12616	0.20244
7.2905	0.103	-18.762	7.7463	9.0374					
8.0037	-0.637	-17.174	8.6852	10.133	135.34	16.91	0.059136	0.15313	0.081216
5.715	-0.163	-18.426	8.1229	9.4768					
4.6474	0.181	-18.841	7.3812	8.6114	115.47	24.846	0.040248	0.10225	0.091064
7.6548	0.096	-18.145	7.6392	8.9124					
7.5861	-0.051	-18.377	7.6633	8.9405	145.88	19.23	0.052002	0.10809	0.35681
7.735	0.08	-18.06	7.7164	9.0025					
6.9551	0.04	-18.591	7.6519	8.9272	138.68	19.939	0.050152	0.10581	0.32733
7.2073	0.301	-18.205	7.3898	8.6214	135.14	18.751	0.053331	0.23497	0.22184
6.5244	0.23	-18.335	7.6552	8.931					
7.0549	0.221	-17.869	7.429	8.6672	131.56	18.648	0.053625	0.26589	0.24257
5.5013	0.138	-18.321	7.3	8.5166					
5.4005	0.113	-18.444	7.2899	8.5048	115.85	21.452	0.046615	0.2005	0.25898
7.263	0.179	-18.239	7.5133	8.7655					
7.8327	0.063	-17.767	7.6019	8.8689	139.55	17.816	0.05613	0.25897	0.26304
7.5117	0.2	-17.97	7.4708	8.716					
7.4996	0.192	-17.942	7.3943	8.6267	130.76	17.436	0.057354	0.27414	0.22498
7.9383	0.179	-17.915	7.4695	8.7144					
6.4856	0.151	-18.526	7.3385	8.5616	120.69	18.609	0.053737	0.28745	0.22939
7.9313	0.052	-17.918	7.3995	8.6328					
8.1627	0.059	-18.223	7.2485	8.4565	138.25	16.937	0.059044	0.15536	0.27931
8.695	0.066	-17.863	7.3723	8.601					
9.084	0.191	-17.806	7.4055	8.6397	135.89	14.959	0.066849		
7.6699	0.009	-18.18	7.4299	8.6683					
8.2972	-0.021	-17.969	7.2022	8.4025	135.7	16.354	0.061146		
8.9633	0.377	-17.927	6.998	8.1644					
8.6263	-0.043	-17.802	7.4745	8.7203	133.12	15.431	0.064803	0.19027	0.23273
8.8319	0.026	-17.669	7.6417	8.9153					
8.7303	-0.105	-17.639	7.8493	9.1575	138.72	15.889	0.062936	0.23223	0.22685
9.2037	-0.158	-17.031	8.0438	9.3844					
8.441	-0.036	-17.857	7.7007	8.9841	137.76	16.32	0.061274	0.17162	0.26467
8.824	0.081	-18.257	7.6637	8.941					
7.8055	-0.157	-18.443	7.6075	8.8755	127.88	16.383	0.061039	0.19272	0.25428
8.0079	0.172	-18.537	7.7562	9.0488					
7.7934	0.132	-18.621	7.6118	8.8804	150.21	19.274	0.051884	0.23826	0.32702
7.8618	0.251	-18.422	7.5244	8.7785					
7.5834	0.171	-18.598	7.5172	8.77	150.2	19.806	0.05049	0.085271	0.30546

TORF12 proxy data

7.5529	0.191	-18.956	7.6469	8.9214					
7.8166	0.204	-18.743	7.6139	8.8829	139.38	17.831	0.056081	0.099965	0.31425
7.3194	0.223	-18.927	7.7553	9.0478					
7.7726	0.457	-19.046	7.7391	9.029	137.35	17.67	0.056592	0.098428	0.32929
7.6868	0.326	-18.957	7.8902	9.2053					
7.4091	0.38	-18.639	7.8198	9.1231	136.02	18.359	0.054469	0.098122	0.31395
7.7321	0.359	-18.683	7.7288	9.017					
8.4899	0.628	-17.774	8.2824	9.6628	136.11	16.032	0.062376	0.092911	0.26949
7.2292	0.567	-18.683	7.7357	9.025					
7.9608	0.582	-18.475	7.7644	9.0585	133.66	16.789	0.059562	0.097061	0.29233
7.9608	0.582	-18.475	7.7644	9.0585					
7.61	0.948	-19.058	7.8051	9.1059	136.11	17.886	0.055911	0.11143	0.27161
7.6702	1.093	-18.775	7.903	9.2202					
7.1187	1.376	-19.001	7.8774	9.1903	134.18	18.849	0.053053	0.18362	0.18749
6.9528	2.142	-19.376	7.9196	9.2395					
6.4575	2.21	-19.659	8.0727	9.4181	130.79	20.254	0.049372	0.29851	0.17022
6.958	2.276	-19.64	7.9824	9.3128					
6.9972	2.229	-19.91	8.0455	9.3864	136.23	19.469	0.051363	0.24684	0.14368
6.9379	2.212	-19.422	8.0586	9.4017					
7.4513	2.263	-19.114	8.3869	9.7847	143.99	19.324	0.051749	0.2887	0.081356
6.5933	2.553	-19.915	7.8144	9.1168					
6.3774	2.421	-19.614	8.0028	9.3366	129.08	20.241	0.049405	0.38106	0.096747
7.9231	2.159	-18.814	8.406	9.807					
7.4802	2.254	-19.408	7.8306	9.1357	134.89	18.033	0.055455	0.26737	0.1465
8.0919	2.385	-18.823	8.4675	9.8788					
7.0155	2.283	-19.509	8.0496	9.3912	137.91	19.658	0.050871		
7.6133	2.267	-19.134	8.1235	9.4774					
6.7616	2.23	-19.514	8.1949	9.5607	138.35	20.462	0.048872	0.22183	0.16843
7.7341	2.257	-19.606	8.1018	9.4521					
7.5694	2.289	-19.411	8.108	9.4593	142.21	18.787	0.053227	0.28352	0.15938
7.8351	2.205	-18.66	8.2826	9.663					
7.5708	2.203	-18.812	8.1121	9.4641	142.39	18.808	0.053169	0.27614	0.1086
6.9978	2.194	-19.062	8.0108	9.346					
7.3015	2.138	-18.665	8.1442	9.5015	142.65	19.538	0.051183	0.28628	0.14232
7.7232	2.206	-18.755	8.331	9.7195					
9.1654	2.173	-19.568	9.2826	10.83	132.78	14.487	0.069029	0.30103	0.10772
7.1203	2.207	-18.977	8.4101	9.8117					
7.6841	1.99	-18.146	8.8538	10.329	129.38	16.838	0.05939	0.24648	0.069128
6.3606	2.497	-19.303	8.0384	9.3782					
7.5957	2.091	-18.528	8.4993	9.9158	100.71	13.259	0.075419	0.19497	0.087886
6.7448	2.01	-18.027	8.6287	10.067					
7.063	2.173	-19.247	8.0237	9.361	137.59	19.481	0.051332	0.21034	0.17673
7.3183	2.126	-18.578	8.7687	10.23					
7.2583	1.935	-18.806	7.9965	9.3292	135.9	18.724	0.053408	0.17964	0.19616
7.9882	1.299	-17.843	8.8309	10.303					
7.0187	1.611	-18.961	8.1828	9.5466	140.81	20.062	0.049845	0.37537	0.17968
6.6462	1.81	-19.273	8.0173	9.3535					
8.7454	1.678	-16.737	9.7244	11.345	124.42	14.226	0.070292	0.32855	0.19555
6.9599	2.273	-18.237	8.7947	10.26					
8.5791	1.968	-16.366	10.229	11.933	122	14.22	0.070323	0.18362	0.15092
6.6411	1.892	-17.869	9.1957	10.728					
7.2939	2.894	-19.473	8.304	9.688	123.24	16.897	0.059184		
7.3386	2.862	-19.317	8.4085	9.8099				0.28776	0.17774
9.0365	2.719	-20.462	9.5562	11.149	132.63	14.677	0.068135	0.20681	0.10395
7.1675	2.914	-19.704	8.3393	9.7292					
7.7059	3.13	-19.639	8.3449	9.7358	140.1	18.181	0.055001	0.19398	0.16599
7.8713	2.727	-19.016	8.4512	9.8597					

TORF12 proxy data

7.2787	2.65	-19.517	8.2893	9.6709	121.49	16.692	0.059911	0.27085	0.17748
7.2256	2.628	-19.41	8.1101	9.4618					
6.8855	2.308	-19.299	7.9577	9.2839	139.22	20.219	0.049459	0.32654	0.21319
7.0915	2.146	-18.983	8.0971	9.4466					
7.3642	2.229	-18.657	8.1516	9.5102	135.53	18.404	0.054335	0.33341	0.17353
8.2274	2.091	-18.912	8.3384	9.7281					
8.8527	1.808	-20.324	9.469	11.047	145.18	16.4	0.060977	0.27845	0.13848
7.3589	1.875	-19.062	8.1542	9.5132					
7.4726	1.697	-19.049	8.2399	9.6132	140.44	18.794	0.053208	0.19904	0.22887
7.0757	1.524	-18.551	8.3538	9.7462					
7.3244	0.911	-16.883	9.2783	10.825	124.23	16.962	0.058957	0.16294	0.13729
8.51	1.51	-17.656	8.9707	10.466					
7.4635	1.427	-18.429	8.4663	9.8773	140.75	18.859	0.053025	0.18126	0.27447
8.019	1.28	-17.98	8.6806	10.127					
7.8994	1.247	-17.207	8.9118	10.397	128.37	16.251	0.061534	0.17849	0.24697
7.63	1.171	-17.7	8.2728	9.6516					
7.45	1.23	-17.4	8.3668	9.7613	129.44	17.371	0.057566	0.16449	0.27817
7.79	1.12	-17.3	8.2048	9.5723					
6.84	1.111	-18.1	8.1249	9.479	131.67	19.243	0.051967	0.18969	0.20488
7.45	1.164	-17.7	8.009	9.3438					
7.76	0.945	-17.5	8.0901	9.4384	136.49	17.58	0.056884	0.20473	0.31142
7.85	0.899	-17.4	8.2078	9.5757					
7.91	0.946	-17.4	8.0837	9.431	132.88	16.79	0.059561	0.19152	0.20316
8.13	1.066	-17.2	7.9433	9.2672					
8.85	0.477	-16.4	8.6208	10.058	129.13	14.592	0.068529	0.19013	0.34185
7.88	1.01	-17.4	7.7072	8.9917					
8.64	0.9	-17.6	9.6331	11.239	127.88	14.805	0.067545	0.15747	0.31364
8.19	0.9	-17.5	9.0686	10.58					
8.46	0.8	-17.2	9.2821	10.829	136.55	16.142	0.061951	0.15154	0.39067
8.27	0.9	-17.6	9.032	10.537					
7.95	0.8	-17.5	8.98	10.477	133.54	16.803	0.059514	0.15515	0.3113
7.87	1	-17.3	9.103	10.62					
8.77	0.9	-19	10.256	11.966	138.93	15.833	0.06316	0.16081	0.25142
7.38	0.9	-17.3	9.0388	10.545					
7.68	0.9	-17.3	9.4063	10.974	134.22	17.467	0.057251	0.18187	0.37352
9.4	0.9	-16.2	10.18	11.876					
7.67	1.1	-17.9	9.4308	11.003	129.62	16.9	0.059171	0.19517	0.15079
8.05	1.1	-16.9	9.4321	11.004					
8.48	1.1	-16.3	10.459	12.202	128.04	15.093	0.066255	0.20443	0.25948
7.19	1.2	-17.5	9.2166	10.753					
7	1.2	-17.7	9.311	10.863	134.67	19.234	0.051992	0.22609	0.35963
8.97	0.9	-15.9	11.131	12.986					
6.92	1.1	-17.5	9.8476	11.489	132.61	19.15	0.052219		
6.8	1.1	-17.7	9.6451	11.253					
7.07	0.9	-17.6	9.6335	11.239	124.78	17.648	0.056665	0.2024	0.33016
6.89	0.8	-17.5	9.3639	10.925					
6.39	0.8	-17.9	9.4224	10.993	126.74	19.833	0.050421	0.17308	0.3074
6.24	0.8	-18.3	9.5582	11.151					
7.22	0.6	-18.3	10.066	11.743	134.69	18.649	0.053622	0.13883	0.26428
6.2	0.8	-18	9.1699	10.698					
6.52	1	-17.9	9.3841	10.948	111.16	17.038	0.058692	0.19734	0.17514
6.05	1	-17.7	9.7353	11.358					
5.75	1.1	-18	9.7016	11.318	123.96	21.572	0.046356	0.17086	0.26809
5.69	1.1	-18.2	9.6542	11.263					
6.03	1.2	-18.7	9.8331	11.472	126.8	21.035	0.047539	0.27631	0.21376
5.97	1.8	-19.8	10.2	11.9					
5.41	1.6	-20.4	9.964	11.625	112.06	20.731	0.048237	0.1625	0.19244

TORF12 proxy data

6.04	1.1	-19.3	9.4332	11.005					
6.86	1.1	-18.6	9.5552	11.148	118.35	17.249	0.057974	0.18096	0.2097
5.56	1.1	-19.3	9.2712	10.816					
5.76	1.1	-19.4	9.0815	10.595	121.81	21.158	0.047263	0.16808	0.25789
5.39	1	-19.6	8.9905	10.489					
4.83	0.8	-19.2	9.3646	10.925	131.76	27.283	0.036652	0.11089	0.40759
5.62	0.9	-19	9.5588	11.152					
4.43	1.1	-19.2	9.0108	10.513	131.04	29.605	0.033779	0.11933	0.37103
4.3	0.9	-19.4	9.1862	10.717	139.68	32.487	0.030782	0.10088	0.24291
4.91	0.9	-19.3	9.1064	10.624					
4.52	0.7	-19.2	9.1791	10.709	128.36	28.378	0.035238	0.081057	0.4671
5.18	0.8	-19	9.2629	10.807					
4.72	1	-19.1	9.0858	10.6	116.8	24.748	0.040407	0.080171	0.54755
4.01	1	-19.9	9.0809	10.594					
3.43	1	-19.7	9.0917	10.607	118.34	34.479	0.029003	0.074214	0.49822
5.37	1	-19.2	8.9604	10.454					
4.72	1.1	-19.3	9.0851	10.599	126.68	26.863	0.037225	0.088629	0.41502
5.59	1.2	-20.2	9.7856	11.417					
4.79	1	-19.2	9.1933	10.725	136.85	28.564	0.035009	0.09726	0.43608
4.78	1.3	-18.8	8.8692	10.347					
4.41	1.4	-18.5	8.6611	10.105	132.43	30.034	0.033296	0.083081	0.31673
5.29	1.3	-19.3	9.0515	10.56					
4.02	1.5	-18.7	8.7519	10.211	126.8	31.52	0.031726	0.1232	0.2474
4.31	1.6	-18.5	8.4781	9.8911					
3.48	1.3	-18.6	8.7205	10.174	123.57	35.471	0.028192	0.14411	0.2382
3.13	1.2	-18.6	8.3122	9.6975					
3.5	1.3	-18.3	8.3406	9.7307	135.99	38.891	0.025713		
3.11	1.3	-18.7	8.8233	10.294				0.11713	0.32046
3.73	1.5	-18.8	8.9131	10.399	123.35	33.072	0.030237		
2.41	1.2	-18.7	8.6787	10.125				0.10077	0.49166
2.69	1.4	-19.1	8.5285	9.95	113.53	42.144	0.023728		
2.08	1.2	-19	8.5543	9.9801				0.061815	0.39576
2.15	1.5	-18.8	8.4155	9.8181	103.62	48.153	0.020767		
1.29	2.4	-19.5	8.7316	10.187				0.031934	0.53196
2.82	1.8	-20.8	9.9207	11.574	93.5	33.19	0.03013		
1.57	2.1	-21.4	9.6982	11.315				0.10666	0.22599
1.81	0.8	-22.3	9.3393	10.896	90.449	49.876	0.02005		
2.55	1.4	-20.3	9.2822	10.829				0.081309	0.089161
2.59	1.4	-19.8	8.7987	10.265	112.34	43.304	0.023092		
1.68	1.1	-20.1	8.313	9.6985				0.070682	0.089059
1.73	1.3	-20.2	8.6633	10.107	119.03	68.813	0.014532		
1.85	1	-20.8	8.7984	10.265				0.098034	0.12194
1.87	1.4	-19.7	8.2667	9.6445	81.125	43.43	0.023026		
1.56	1.2	-20.1	7.9398	9.2631				0.11496	0.1775
1.84	1.1	-20.7	8.2965	9.6793	93.874	50.92	0.019639		
1.6	0.7	-20.3	7.6234	8.8939				0.093902	0.22459
1.74	0.6	-19.8	7.6418	8.9154	98.629	56.804	0.017604		
1.21	1	-20.8	7.8315	9.1367				0.089997	0.32254
1.3	0.7	-20.4	7.8074	9.1086	87.962	67.44	0.014828		
1.51	0.7	-20.3	7.8165	9.1193				0.090367	0.19448
1.5	0.4	-21.4	8.2491	9.624	95.703	63.665	0.015707		
1.46	0.2	-19.8	7.7722	9.0676				0.11773	0.44119
1.25	0.4	-21.2	7.4697	8.7146	84.874	67.985	0.014709		
1.46	0.2	-21.1	7.8511	9.1597				0.11045	0.73357
0.98	0.5	-18	6.8148	7.9506	91.045	92.978	0.010755		
1.18	0.9	-17.5	6.9437	8.101				0.10788	1.1411
1.24	0.6	-16.2	6.8433	7.9838	77.21	62.077	0.016109		

TORF12 proxy data

0.96	0.8	-17.2	6.0798	7.0931				0.13571	1.2653
1.23	1	-20.1	7.5345	8.7903	88.658	72.233	0.013844		
1.86	1	-20.7	10.222	11.926				0.1231	0.33188
0.85	1.1	-18.1	5.9914	6.99	79.766	94.395	0.010594		
0.98	0.9	-18.6	6.6321	7.7375				0.089404	1.2647
1.43	0.7	-19.6	7.2298	8.4348	91.599	63.874	0.015656		
1.24	0.7	-19.6	7.2454	8.4529				0.20936	0.91782
1.36	0.8	-18.8	7.0151	8.1843	96.107	70.472	0.01419		
1.51	0.5	-18.7	7.4171	8.6533				0.10087	0.78254
1.35	0.9	-19.5	7.2357	8.4416	95.647	70.819	0.014121		
1.36	0.2	-19.8	7.3924	8.6245				0.13245	1.0512
0.66	0.2	-18.7	5.3305	6.2189	81.642	124.14	0.0080555		
				0					

TORF12 proxy data

Lut 1	canth	bcar	Tot Chlorin	Diatom pig	Total pig	diato/total	lut/total	canth/total	bcar/total
0.049208	0.020431	0.010442	1.1404	0.1405	1.3451	0.10445	0.036584	0.015189	0.0077631
0.054766	0.021101	0.014085	1.1107	0.19813	1.3876	0.14279	0.039468	0.015207	0.01015
0.044319	0.015205	0.010673	0.92998	0.15788	1.1561	0.13657	0.038334	0.013152	0.0092317
0.085149	0.023768	0.021106	1.1819	0.23236	1.5302	0.15185	0.055645	0.015532	0.013793
0.058774	0.018668	0.013806	1.125	0.20057	1.4023	0.14303	0.041913	0.013313	0.009845
0.063334	0.018177	0.015016	1.1429	0.1982	1.4252	0.13907	0.044439	0.012754	0.010536
0.084613	0.017177	0.020193	1.3072	0.21643	1.6566	0.13065	0.051078	0.010369	0.012189
0.068907	0.018016	0.018347	1.1852	0.20816	1.4881	0.13989	0.046306	0.012107	0.012329
0.084573	0.018665	0.020098	1.1837	0.21462	1.5149	0.14167	0.055827	0.012321	0.013267
0.046086	0.01322	0.013501	0.82672	0.14501	1.0347	0.14015	0.044542	0.012777	0.013048
0.052434	0.013338	0.01316	0.92757	0.16474	1.1645	0.14147	0.045026	0.011454	0.011301
0.044643	0.012113	0.012215	0.87918	0.13692	1.0804	0.12673	0.041322	0.011212	0.011306
0.058199	0.013846	0.01386	0.98761	0.14287	1.211	0.11798	0.048058	0.011433	0.011445
0.051962	0.015694	0.016376	1.0085	0.16272	1.2428	0.13094	0.041812	0.012628	0.013177
0.044375	0.015056	0.012415	1.0709	0.15431	1.29	0.11962	0.034399	0.011672	0.0096238
0.038089	0.01227	0.0089875	0.92849	0.12708	1.1078	0.11471	0.034383	0.011076	0.008113
0.032346	0.012835	0.016244	0.79664	0.13528	0.98069	0.13794	0.032983	0.013088	0.016563
0.050771	0.015972	0.023174	1.0202	0.17118	1.2657	0.13525	0.040113	0.012619	0.018309
						0	0		
0.055661	0.022922	0.036044	1.3881	0.27632	1.7531	0.15761	0.03175	0.013075	0.02056
0.065225	0.02469	0.038075	1.5608	0.30902	1.9641	0.15733	0.033208	0.01257	0.019385
0.056715	0.025739	0.031534	1.3901	0.25636	1.7294	0.14824	0.032795	0.014883	0.018234
0.021277	0.0061057	0.011656	0.50415	0.098246	0.63302	0.1552	0.033613	0.0096453	0.018414
0.021241	0.010104	0.011371	0.49803	0.095702	0.62507	0.15311	0.033982	0.016164	0.018191
						0	0		
						0	0		
						0	0		
0.065279	0.016165	0.033319	1.0702	0.22595	1.3933	0.16218	0.046854	0.011602	0.023914
0.08457	0.019991	0.049371	1.1884	0.30931	1.626	0.19023	0.052012	0.012295	0.030364
0.074059	0.017023	0.027875	1.234	0.30275	1.6579	0.18261	0.044671	0.010268	0.016814
0.020403	0.010557	0.0046069	0.72852	0.11777	0.87945	0.13391	0.0232	0.012004	0.0052384
0.069244	0.017916	0.039741	1.1078	0.2873	1.499	0.19166	0.046192	0.011952	0.026511
0.048362	0.01682	0.038989	1.0349	0.24079	1.3687	0.17592	0.035333	0.012289	0.028486
0.051156	0.017962	0.058594	1.0988	0.26912	1.4605	0.18426	0.035025	0.012298	0.040118
0.039566	0.015512	0.031357	1.0799	0.19638	1.3469	0.14581	0.029377	0.011517	0.023282
0.028276	0.014118	0.011358	1.0822	0.13905	1.2721	0.10931	0.022227	0.011098	0.0089282
0.0526	0.018255	0	1.2047	0.21492	1.4984	0.14343	0.035104	0.012183	
0.070331	0.022451	0.017182	1.3198	0.28404	1.7078	0.16632	0.041182	0.013146	0.010061
0.077281	0.018227	0.021357	0.90881	0.29747	1.3175	0.22578	0.058657	0.013834	0.01621
0.045235	0.015358	0.01602	1.1673	0.22801	1.4681	0.15531	0.030812	0.010461	0.010912
0.034157	0.013111	0.010268	1.1303	0.19132	1.3786	0.13878	0.024777	0.0095107	0.0074485
0.035681	0.016504	0.015219	1.421	0.17748	1.6728	0.1061	0.02133	0.0098661	0.0090977
0.018704	0.0090763	0.0046354	0.80065	0.089917	0.92609	0.097093	0.020196	0.0098006	0.0050053
0.024642	0.010335	0.0050832	0.87677	0.11935	1.0344	0.11538	0.023822	0.0099907	0.004914
0.032497	0.015363	0.0064612	1.2027	0.16954	1.4223	0.1192	0.022848	0.010801	0.0045427
0.057919	0.017996	0.012664	1.1683	0.24348	1.492	0.16319	0.03882	0.012061	0.0084876
0.059043	0.016962	0.012711	1.1202	0.26524	1.4701	0.18042	0.040163	0.011538	0.0086464
0.068631	0.01763	0.019302	1.052	0.28791	1.4359	0.2005	0.047795	0.012278	0.013442
0.065772	0.01695	0.0097725	1.1294	0.27743	1.5019	0.18472	0.043793	0.011286	0.0065068
0.068485	0.019136	0.010791	1.1546	0.30078	1.5534	0.19362	0.044086	0.012318	0.0069463
0.059588	0.018295	0.0075131	1.1897	0.26082	1.543	0.16904	0.03862	0.011857	0.0048693
0.066748	0.01786	0.0095883	1.1598	0.2918	1.5451	0.18885	0.043199	0.011559	0.0062056
0.038081	0.01149	0.0046169	0.76592	0.15546	0.97737	0.15906	0.038962	0.011756	0.0047238
0.038569	0.011117	0.0043967	0.7498	0.14715	0.95436	0.15419	0.040414	0.011648	0.004607
0.048861	0.013821	0	0.93048	0.17858	1.19	0.15007	0.041061	0.011615	
0.060463	0.016858	0.0055829	0.96068	0.22417	1.3015	0.17225	0.046458	0.012953	0.0042897

TORF12 proxy data

0.045107	0.018621	0.0091837	1.155	0.19665	1.4286	0.13765	0.031574	0.013034	0.0064284
						0	0		
0.025455	0.019109	0.0059025	1.1729	0.11879	1.3419	0.088525	0.018969	0.01424	0.0043986
0.041915	0.020742	0.0052259	1.1639	0.22096	1.4579	0.15156	0.028749	0.014227	0.0035844
0.041376	0.020763	0.0047029	1.176	0.21756	1.4619	0.14882	0.028303	0.014203	0.003217
0.04097	0.021422	0.0072926	1.2841	0.18748	1.5411	0.12165	0.026585	0.013901	0.0047321
0.063967	0.019874	0.0067108	1.0368	0.24211	1.3912	0.17403	0.045981	0.014286	0.0048239
						0	0		
0.038253	0.01659	0.0081351	1.0124	0.1703	1.2485	0.13641	0.030639	0.013288	0.0065158
0.070896	0.023552	0.013304	1.4115	0.28429	1.834	0.15501	0.038656	0.012842	0.0072541
0.036176	0.017424	0.0077154	1.1186	0.16241	1.3517	0.12015	0.026764	0.01289	0.005708
0.040362	0.015192	0.0078207	0.96587	0.16945	1.2129	0.13971	0.033277	0.012525	0.0064479
0.044141	0.016918	0.0067488	0.97841	0.18146	1.2455	0.1457	0.035441	0.013583	0.0054187
0.034593	0.015264	0.0054998	1.0068	0.14758	1.2097	0.122	0.028597	0.012618	0.0045466
0.037597	0.015974	0.0060455	0.99768	0.156	1.2118	0.12874	0.031027	0.013183	0.0049891
0.042825	0.014957	0.005567	0.89528	0.18019	1.1399	0.15807	0.037569	0.013121	0.0048836
0.030195	0.014079	0.0031862	1.0179	0.12748	1.1918	0.10696	0.025336	0.011813	0.0026735
0.078903	0.021397	0.021744	1.077	0.31256	1.4995	0.20844	0.052619	0.014269	0.0145
0.066959	0.021972	0.01211	1.1145	0.26857	1.4807	0.18138	0.045222	0.014839	0.0081784
0.054187	0.023097	0.010869	1.2841	0.24932	1.6152	0.15435	0.033547	0.0143	0.0067292
0.052555	0.021462	0.0091689	1.1519	0.23055	1.4657	0.15729	0.035856	0.014643	0.0062556
0.029279	0.018417	0.0061982	1.104	0.1536	1.3044	0.11776	0.022446	0.014119	0.0047517
0.062834	0.022972	0.0091534	1.228	0.26646	1.5882	0.16777	0.039563	0.014464	0.0057633
0.044545	0.020935	0.0079214	1.148	0.19392	1.4058	0.13794	0.031686	0.014892	0.0056346
0.051697	0.018979	0.0082759	1.1859	0.23946	1.5052	0.15909	0.034345	0.012609	0.0054981
0.047271	0.019462	0.0096877	1.1346	0.20468	1.4068	0.14549	0.033602	0.013834	0.0068863
0.083241	0.021723	0.023136	1.0007	0.33587	1.4584	0.2303	0.057077	0.014895	0.015864
0.0835	0.021714	0.021674	1.1483	0.31521	1.58	0.1995	0.052849	0.013743	0.013718
0.08664	0.022239	0.018394	1.2627	0.32928	1.7173	0.19175	0.050453	0.01295	0.010711
						0	0		
0.069341	0.018796	0.013802	1.1992	0.2747	1.5703	0.17493	0.044157	0.011969	0.0087895
0.064784	0.018208	0.012071	1.2988	0.28022	1.6681	0.16798	0.038836	0.010915	0.0072365
0.050408	0.021208	0.010894	1.4837	0.23627	1.8007	0.13121	0.027993	0.011777	0.0060497
0.032695	0.021525	0.0090502	1.6732	0.18465	1.9161	0.096365	0.017063	0.011234	0.0047232
0.070489	0.01942	0.010122	1.3641	0.26369	1.7315	0.15229	0.04071	0.011216	0.0058459
0.08325	0.016551	0.019861	1.1923	0.24919	1.5648	0.15925	0.053204	0.010577	0.012693
0.044686	0.016886	0.011717	1.2134	0.16528	1.4446	0.11441	0.030932	0.011689	0.0081107
0.036439	0.016708	0.0052552	1.3663	0.1411	1.5597	0.090465	0.023363	0.010712	0.0033693
0.046039	0.017573	0.0069933	1.3068	0.18208	1.5509	0.11741	0.029686	0.011331	0.0045093
0.082454	0.02189	0.017245	1.2641	0.27036	1.6416	0.16469	0.050226	0.013334	0.010505
0.10208	0.028094	0.019436	1.5332	0.33581	1.9971	0.16815	0.051115	0.014067	0.009732
0.062538	0.022162	0.0099249	1.2667	0.22303	1.5695	0.1421	0.039845	0.01412	0.0063235
0.088107	0.02499	0.019849	1.3639	0.27496	1.7511	0.15702	0.050315	0.014271	0.011335
0.075993	0.019154	0.011674	1.3434	0.2626	1.7047	0.15405	0.044579	0.011236	0.006848
						0	0		
						0	0		
0.096663	0.022835	0.04265	1.3705	0.43719	1.9547	0.22366	0.049451	0.011682	0.021819
0.071104	0.01837	0.028478	1.1699	0.34636	1.626	0.21301	0.043729	0.011298	0.017514
0.082927	0.018998	0.025926	1.1664	0.3915	1.6777	0.23335	0.049428	0.011324	0.015453
0.069257	0.017066	0.015587	1.0769	0.31127	1.4954	0.20815	0.046313	0.011412	0.010423
0.08184	0.017381	0.021973	1.025	0.3129	1.4847	0.21075	0.055121	0.011707	0.014799
0.095434	0.019483	0.045818	1.0918	0.4039	1.6391	0.24641	0.058223	0.011886	0.027953
0.077412	0.016294	0.031878	0.94421	0.30431	1.372	0.2218	0.056423	0.011876	0.023235
0.035268	0.010372	0.0083968	0.72178	0.1657	0.94115	0.17606	0.037473	0.01102	0.0089218
0.071946	0.015022	0.013417	1.0453	0.27688	1.4303	0.19359	0.050302	0.010503	0.0093809
0.060658	0.012832	0.015362	0.81831	0.25096	1.1599	0.21636	0.052295	0.011063	0.013244
0.070933	0.015809	0.015208	1.0166	0.29679	1.4145	0.20982	0.050147	0.011176	0.010752

TORF12 proxy data

0.067134	0.015255	0.022422	0.94075	0.28354	1.3192	0.214940	0.050890	0.011564	0.016997
0.029123	0.0074595	0.023035	1.3339	0.31427	1.7187	0.182850	0.016945	0.0043402	0.013403
0.040063	0.01717	0.0089727	1.161	0.20914	1.4315	0.14610	0.027987	0.011995	0.0062681
0.02514	0.017671	0.0089185	1.1744	0.30208	1.5229	0.198360	0.016509	0.011604	0.0058565
0.074557	0.020159	0.026725	1.1829	0.30471	1.5956	0.190970	0.046728	0.012634	0.01675
0.030248	0.020809	0.025334	1.0306	0.26118	1.348	0.193750	0.02244	0.015437	0.018794
0.029747	0.018345	0.01463	1.1132	0.21609	1.3918	0.155250	0.021373	0.013181	0.010512
0.029102	0.019617	0.038619	1.0859	0.2508	1.4142	0.177350	0.020579	0.013872	0.027309
0.022677	0.019536	0.024914		0.24282		0	0		
0.029436	0.01962	0.022354	1.1025	0.26242	1.4287	0.183680	0.020604	0.013733	0.015647
0.029849	0.020725	0.01953	1.2743	0.27539	1.6226	0.169720	0.018396	0.012773	0.012036
0.049102	0.02338	0.035369	1.4543	0.34703	1.91	0.181690	0.025708	0.012241	0.018518
0.04047	0.021866	0.029079	1.5941	0.37707	2.0729	0.181910	0.019524	0.010549	0.014028
0.085543	0.025435	0.043883	1.5247	0.31091	1.9841	0.15670	0.043114	0.012819	0.022117
0.042596	0.022698	0.028196	1.6446	0.30963	2.0652	0.149930	0.020626	0.010991	0.013653
0.029845	0.02092	0.044655	1.4416	0.2997	1.8139	0.165220	0.016454	0.011533	0.024618
0.02296	0.021969	0.044159	1.4687	0.25309	1.7879	0.141550	0.012842	0.012287	0.024699
0.029236	0.021823	0.028169	1.2532	0.26239	1.5848	0.165560	0.018447	0.01377	0.017774
0.02183	0.017117	0.034158	1.0738	0.2113	1.3406	0.157620	0.016284	0.012768	0.02548
0.028282	0.022791	0.039576	1.3191	0.27736	1.6723	0.165860	0.016912	0.013629	0.023666
0.02627	0.022061	0.035493	1.2681	0.20146	1.5283	0.131820	0.017189	0.014435	0.023224
0.036225	0.018945	0.050982	1.1936	0.29446	1.5618	0.188540	0.023194	0.01213	0.032643
0.026444	0.020492	0.046136	1.2966	0.24918	1.6122	0.154560	0.016403	0.012711	0.028617
0.01939	0.018481	0.022372	1.3316	0.16042	1.5335	0.104610	0.012644	0.012051	0.014589
0.019353	0.018984	0.033188	1.2782	0.14737	1.4715	0.100150	0.013152	0.012902	0.022554
0.029104	0.023897	0.046253	1.4592	0.24534	1.7829	0.13761	0.016324	0.013403	0.025942

TORF12 proxy data

						0	0		
0.019512	0.017955	0.029023	1.1813	0.16722	1.3936	0.11999	0.014001	0.012884	0.020826
						0	0		
0.034713	0.024707	0.056219	1.2446	0.25744	1.5707	0.16391	0.022101	0.01573	0.035792
						0	0		
0.035901	0.023076	0.079067	1.3894	0.33102	1.8155	0.18233	0.019775	0.012711	0.043552
						0	0		
0.043508	0.024104	0.12951	1.5727	0.36653	2.049	0.17888	0.021233	0.011764	0.063203
						0	0		
0.028502	0.02052	0.059262	1.5383	0.27572	1.8877	0.14606	0.015098	0.01087	0.031393
						0	0		
0.030312	0.025174	0.076611	1.7632	0.31542	2.1621	0.14588	0.014019	0.011643	0.035433
						0	0		
0.036312	0.027553	0.09219	1.5748	0.28628	1.9549	0.14644	0.018575	0.014094	0.047159
						0	0		
0.029019	0.022073	0.070523	1.5857	0.23599	1.8985	0.1243	0.015285	0.011627	0.037146
						0	0		
0.020892	0.018003	0.036785	1.421	0.18917	1.6713	0.11319	0.0125	0.010772	0.02201
						0	0		
0.025126	0.021606	0.05793	1.569	0.20244	1.8381	0.11013	0.013669	0.011754	0.031516
						0	0		
0.012235	0.015226	0.02129	1.3049	0.081216	1.4249	0.056997	0.0085865	0.010685	0.014941
						0	0		
0.0091606	0.0091753	0.024103	0.71473	0.091064	0.83022	0.10969	0.011034	0.011052	0.029032
						0	0		
0.037943	0.025737	0.060511	1.7615	0.35681	2.1889	0.16301	0.017334	0.011758	0.027644
						0	0		
0.034073	0.034003	0.12493	1.8055	0.32733	2.199	0.14886	0.015495	0.015463	0.056812
0.051284	0.023225	0.014984	1.4405	0.22184	1.737	0.12772	0.029524	0.013371	0.0086264
						0	0		
0.063451	0.026228	0.015507	1.5125	0.24257	1.8504	0.13109	0.034291	0.014174	0.0083803
						0	0		
0.051084	0.025396	0.013913	1.9243	0.25898	2.2576	0.11471	0.022627	0.011249	0.0061625
						0	0		
0.067017	0.029537	0.019641	1.555	0.26304	1.9139	0.13743	0.035016	0.015433	0.010262
						0	0		
0.060676	0.028452	0.03294	1.7256	0.22498	2.0494	0.10978	0.029606	0.013883	0.016073
						0	0		
0.06487	0.028521	0.034948	1.7963	0.22939	2.1284	0.10777	0.030478	0.0134	0.01642
						0	0		
0.042691	0.021766	0.020986	2.0221	0.27931	2.3702	0.11784	0.018011	0.0091832	0.0088542
						0	0		
						0	0		
						0	0		
						0	0		
						0	0		
0.043565	0.026328	0.05164	1.5193	0.23273	1.8249	0.12753	0.023873	0.014427	0.028298
						0	0		
0.051828	0.027829	0.060201	1.5941	0.22685	1.9091	0.11882	0.027147	0.014577	0.031534
						0	0		
0.044687	0.025654	0.054889	1.6742	0.26467	2.0102	0.13167	0.02223	0.012762	0.027305
						0	0		
0.04821	0.028043	0.067922	1.7635	0.25428	2.0975	0.12123	0.022984	0.013369	0.032382
						0	0		
0.076653	0.026761	0.059726	1.6024	0.32702	2.0432	0.16005	0.037517	0.013098	0.029232
						0	0		
0.025625	0.024607	0.057712	1.7917	0.30546	2.1547	0.14176	0.011892	0.01142	0.026784

TORF12 proxy data

						0	0		
0.030905	0.025767	0.067558	1.5456	0.31425	1.9268	0.16309	0.016039	0.013372	0.035062
						0	0		
0.031887	0.025994	0.082887	1.4272	0.32929	1.8388	0.17908	0.017341	0.014136	0.045076
						0	0		
0.030307	0.0217	0.060002	1.4462	0.31395	1.8329	0.17129	0.016535	0.011839	0.032736
						0	0		
0.024633	0.021981	0.041049	1.2087	0.26949	1.5255	0.17666	0.016148	0.01441	0.026909
						0	0		
0.027914	0.025707	0.072655	1.3667	0.29233	1.7107	0.17089	0.016318	0.015027	0.042472
						0	0		
0.029774	0.025885	0.059806	1.2378	0.27161	1.5657	0.17348	0.019017	0.016533	0.038198
						0	0		
0.033869	0.025215	0.055553	1.2143	0.18749	1.4606	0.12836	0.023188	0.017263	0.038034
						0	0		
0.049989	0.033638	0.049802	1.4593	0.17022	1.7005	0.1001	0.029397	0.019782	0.029287
						0	0		
0.034892	0.02676	0.039197	1.3718	0.14368	1.5654	0.091784	0.022289	0.017094	0.025039
						0	0		
0.023107	0.022409	0.028987	1.171	0.081356	1.2878	0.063174	0.017943	0.017401	0.022508
						0	0		
0.036269	0.034926	0.046054	1.6987	0.096747	1.852	0.05224	0.019584	0.018859	0.024867
						0	0		
0.038536	0.027157	0.040094	1.3924	0.1465	1.5976	0.091702	0.024121	0.016999	0.025096
						0	0		
						0	0		
						0	0		
0.036757	0.028529	0.045772	1.4072	0.16843	1.6332	0.10313	0.022506	0.017468	0.028025
						0	0		
0.044456	0.022495	0.046119	1.3032	0.15938	1.5305	0.10414	0.029046	0.014698	0.030133
						0	0		
0.029503	0.023999	0.035142	1.0467	0.1086	1.2017	0.09037	0.02455	0.01997	0.029243
						0	0		
0.040084	0.02427	0.041088	1.224	0.14232	1.426	0.099803	0.028109	0.01702	0.028814
						0	0		
0.031901	0.018318	0.035806	0.91218	0.10772	1.068	0.10086	0.02987	0.017152	0.033526
						0	0		
0.016763	0.020232	0.024378	1.0865	0.069128	1.1891	0.058134	0.014097	0.017014	0.020501
						0	0		
0.016858	0.023374	0.025672	1.0434	0.087886	1.161	0.0757	0.01452	0.020133	0.022112
						0	0		
0.03657	0.024935	0.063813	1.2012	0.17673	1.4457	0.12224	0.025296	0.017247	0.04414
						0	0		
0.034667	0.024266	0.056579	1.2015	0.19616	1.4619	0.13418	0.023713	0.016599	0.038702
						0	0		
0.066353	0.039314	0.049196	0.97241	0.17968	1.2401	0.14489	0.053504	0.031702	0.03967
						0	0		
0.063209	0.03514	0.04009	0.9122	0.19555	1.1895	0.1644	0.053138	0.029542	0.033703
						0	0		
0.027263	0.017837	0.029008	0.92792	0.15092	1.1223	0.13448	0.024293	0.015893	0.025848
						0	0		
						0	0		
0.050319	0.022922	0.026996	1.193	0.17774	1.4435	0.12313	0.034859	0.015879	0.018702
0.021151	0.021736	0.034449	1.0146	0.10395	1.1559	0.089935	0.018298	0.018804	0.029803
						0	0		
0.031677	0.027074	0.040028	1.3501	0.16599	1.5709	0.10567	0.020165	0.017235	0.025481
						0	0		

TORF12 proxy data

0.047292	0.036679	0.043719	1.1376	0.17748	1.3838	0.128250	0.034176	0.026506	0.031593
0.068487	0.036301	0.05049	1.1897	0.21319	1.4983	0.142290	0.045711	0.024229	0.033699
0.056919	0.027529	0.033392	1.1703	0.17353	1.418	0.122370	0.040139	0.019414	0.023548
0.037934	0.025508	0.033818	0.87888	0.13848	1.0718	0.12920	0.035393	0.023799	0.031553
0.044818	0.026944	0.046063	1.3854	0.22887	1.6794	0.136290	0.026688	0.016044	0.027429
0.022007	0.021798	0.037814	1.5331	0.13729	1.7084	0.0803610	0.012882	0.012759	0.022134
0.048946	0.025095	0.030043	1.5895	0.27447	1.9362	0.141760	0.02528	0.012961	0.015517
0.043366	0.029129	0.040856	1.3465	0.24697	1.6593	0.148830	0.026135	0.017554	0.024622
0.045015	0.029972	0.043976	1.5995	0.27817	1.9475	0.142840	0.023115	0.015391	0.022581
0.038233	0.03024	0.047198	1.5976	0.20488	1.8607	0.110110	0.020547	0.016252	0.025366
0.062724	0.028791	0.051004	1.2229	0.31142	1.6336	0.190640	0.038397	0.017625	0.031222
0.038278	0.023311	0.041699	0.95104	0.20316	1.2106	0.167820	0.03162	0.019257	0.034446
0.063943	0.037942	0.074635	1.617	0.34185	2.0519	0.16660	0.031163	0.018491	0.036373
0.04859	0.026656	0.04933	1.054	0.31364	1.4409	0.217660	0.033721	0.018499	0.034235
0.058244	0.032338	0.062476	1.0862	0.39067	1.5657	0.249510	0.037199	0.020654	0.039901
0.047517	0.030818	0.059835	1.1044	0.3113	1.4935	0.208440	0.031816	0.020635	0.040063
0.039776	0.02656	0.042897	0.95717	0.25142	1.2725	0.197580	0.031258	0.020872	0.033711
0.066833	0.040972	0.07053	1.3512	0.37352	1.8289	0.204240	0.036544	0.022403	0.038565
0.028954	0.026072	0.040214	1.2294	0.15079	1.4273	0.105650	0.020285	0.018267	0.028175
0.052185	0.025596	0.046745	1.2365	0.25948	1.5779	0.164440	0.033072	0.016221	0.029625
0.079992	0.03578	0.075349	1.2974	0.35963	1.7813	0.2019000	0.044907000	0.020087	0.042301
0.065741	0.037406	0.074361	1.2434	0.33016	1.6783	0.196730	0.039172	0.022289	0.044308
0.052343	0.039708	0.062192	1.2104	0.3074	1.6018	0.191910	0.032678	0.02479	0.038826
0.036096	0.029243	0.042266	1.0384	0.26428	1.3656	0.193520	0.026432	0.021413	0.030949
0.034003	0.031333	0.053948	0.91907	0.17514	1.1541	0.151750	0.029462	0.027149	0.046745
0.045064	0.033844	0.060637	1.1659	0.26809	1.5142	0.177050	0.029761	0.022351	0.040045
0.058106	0.032713	0.042255	1.003	0.21376	1.3099	0.163190	0.044359	0.024974	0.032258
0.030765	0.020994	0.027437	0.93732	0.19244	1.1937	0.16121	0.025772	0.017587	0.022984

TORF12 proxy data

						0	0		
0.037332	0.013254	0.070094	1.2102	0.2097	1.485	0.1412	0.025138	0.0089247	0.0472
						0	0		
0.042645	0.028696	0.043739	1.2703	0.25789	1.6053	0.16065	0.026565	0.017876	0.027247
						0	0		
0.044467	0.029261	0.051541	1.2835	0.40759	1.788	0.22796	0.024869	0.016365	0.028825
						0	0		
0.04356	0.025245	0.036264	1.2144	0.37103	1.6789	0.221	0.025946	0.015037	0.0216
0.024109	0.019437	0.01748	1.1075	0.24291	1.4039	0.17302	0.017172	0.013844	0.01245
						0	0		
0.037249	0.019635	0.026485	1.148	0.4671	1.7091	0.2733	0.021794	0.011489	0.015496
						0	0		
0.043187	0.020563	0.037649	1.253	0.54755	1.9104	0.28661	0.022606	0.010763	0.019707
						0	0		
0.036376	0.019917	0.040576	1.3558	0.49822	1.9648	0.25358	0.018514	0.010137	0.020652
						0	0		
0.036187	0.018052	0.031876	1.0586	0.41502	1.5646	0.26525	0.023128	0.011537	0.020373
						0	0		
0.041726	0.020376	0.029491	1.2098	0.43608	1.7561	0.24832	0.023761	0.011603	0.016794
						0	0		
0.025888	0.016644	0.028981	1.0768	0.31673	1.4637	0.21639	0.017687	0.011371	0.0198
						0	0		
0.029986	0.019958	0.017108	1.1734	0.2474	1.4872	0.16635	0.020162	0.01342	0.011503
						0	0		
0.03377	0.021035	0.023483	1.0246	0.2382	1.3267	0.17953	0.025453	0.015854	0.0177
						0	0		
						0	0		
0.036927	0.024049	0.031163	1.0147	0.32046	1.4149	0.22649	0.026099	0.016997	0.022025
						0	0		
0.04874	0.041652	0.085191	1.9098	0.49166	2.5277	0.19451	0.019283	0.016478	0.033704
						0	0		
0.024068	0.018	0.031037	1.5982	0.39576	2.069	0.19128	0.011633	0.0086999	0.015001
						0	0		
0.016712	0.013988	0.031389	1.9448	0.53196	2.5839	0.20588	0.006468	0.0054137	0.012148
						0	0		
0.023714	0.016906	0.05848	1.7631	0.22599	2.0479	0.11035	0.011579	0.008255	0.028555
						0	0		
0.0071322	0.0090021	0.0079063	1.4292	0.089161	1.5359	0.058051	0.0046436	0.005861	0.0051476
						0	0		
0.0061929	0.0093251	0.0078749	1.4857	0.089059	1.5943	0.055862	0.0038845	0.0058491	0.0049395
						0	0		
0.011761	0.016427	0.023954	1.41	0.12194	1.5596	0.078187	0.0075409	0.010533	0.015359
						0	0		
0.020075	0.013704	0.014474	1.8997	0.1775	2.1389	0.082988	0.0093857	0.0064069	0.0067668
						0	0		
0.020748	0.018049	0.018631	2.4225	0.22459	2.6979	0.083248	0.0076905	0.0066901	0.0069058
						0	0		
0.028558	0.020847	0.019047	3.3306	0.32254	3.7501	0.086009	0.0076152	0.0055591	0.005079
						0	0		
0.01729	0.015816	0.036648	2.848	0.19448	3.0937	0.062863	0.0055887	0.0051123	0.011846
						0	0		
0.051099	0.018833	0.032737	2.6586	0.44119	3.2299	0.1366	0.015821	0.0058309	0.010135
						0	0		
0.079713	0.019048	0.093773	3.8481	0.73357	4.8155	0.15233	0.016553	0.0039555	0.019473
						0	0		
0.12112	0.065807	0.18285	6.579	1.1411	7.9848	0.14292	0.015168	0.0082415	0.0229
						0	0		

TORF12 proxy data

0.16893	0.017263	0.16761	6.6236	1.2653	8.1879	0.154530	0.020630	0.0021084	0.02047
0.040193	0.072164	0.067512	4.2633	0.33188	4.6814	0.070893	0.0085857	0.015415	0.014421
0.11124	0.045521	0.16362	7.4734	1.2647	8.9555	0.141220	0.012421	0.005083	0.01827
0.18904	0.088113	0.1994	5.7285	0.91782	6.9238	0.132560	0.027303	0.012726	0.028799
0.077653	0.079956	0.11164	2.6988	0.78254	3.6213	0.21610	0.021444	0.02208	0.03083
0.13698	0.11514	0.17603	4.3852	1.0512	5.685	0.18491	0.024094	0.020252	0.030964

TORF12 proxy data

chlorin/total	diatom/tot	8k pca age	8k pca factor 1
0.84783	0.10445	-19	19.412
0.80044	0.14279	8	22.806
0.80441	0.13657	36	26.755
0.77235	0.15185	63	37.635
0.80228	0.14303	90	32.708
0.80194	0.13907	116	29.701
0.78909	0.13065	142	23.366
0.79648	0.13989	167	28.494
0.78137	0.14167	191	24.958
0.79901	0.14015	215	25.492
0.79652	0.14147	238	27.907
0.81377	0.12673	260	23.961
0.81552	0.11798	282	25.771
0.81153	0.13094	303	30.315
0.83015	0.11962	324	24
0.83814	0.11471	344	21.778
0.81232	0.13794	364	17.07
0.806	0.13525	403	15.872
		422	11.004
0.79177	0.15761	440	12.27
0.79466	0.15733	459	17.429
0.80383	0.14824	478	7.0485
0.79642	0.1552	552	19.543
0.79675	0.15311	571	-2.9465
		590	10.341
		610	14.67
		629	17.742
0.76813	0.16218	650	15.583
0.73087	0.19023	670	25.155
0.74434	0.18261	691	13.533
0.82838	0.13391	712	23.955
0.73899	0.19166	734	4.1066
0.7561	0.17592	775	10.212
0.75235	0.18426	796	14.859
0.80182	0.14581	815	18.602
0.85073	0.10931	815	28.865
0.80399	0.14343	815	31.898
0.77281	0.16632	834	9.0337
0.68978	0.22578	851	1.0739
0.79514	0.15531	867	-4.7982
0.81988	0.13878	883	-0.40135
0.84949	0.1061	898	-3.7893
0.86454	0.097093	912	5.5894
0.84759	0.11538	925	1.7377
0.8456	0.1192	951	-1.2943
0.78302	0.16319	963	1.2402
0.76197	0.18042	975	-8.5291
0.73262	0.2005	999	2.5936
0.75196	0.18472	1011	-12.092
0.74325	0.19362	1035	4.3807
0.77108	0.16904	1048	1.7285
0.75061	0.18885	1061	-1.7756
0.78365	0.15906	1074	-0.83551
0.78566	0.15419	1088	9.2851
0.78195	0.15007	1119	-0.027739
0.73815	0.17225	1135	7.7648

TORF12 proxy data

0.80847	0.13765	1152	8.3846
		1169	-13.814
0.87403	0.088525	1187	-14.726
0.7983	0.15156	1205	-6.8958
0.80443	0.14882	1224	-7.7614
0.83323	0.12165	1243	0.013751
0.74526	0.17403	1262	-3.0382
		1282	-9.5416
0.81088	0.13641	1301	-5.6858
0.76964	0.15501	1321	-0.8379
0.82753	0.12015	1341	-2.766
0.79633	0.13971	1360	-7.4406
0.78558	0.1457	1380	-10.549
0.83227	0.122	1400	-8.484
0.82333	0.12874	1420	-11.946
0.78538	0.15807	1440	-9.7665
0.85408	0.10696	1460	-10.09
0.71822	0.20844	1480	-8.5336
0.75267	0.18138	1500	-2.9485
0.79498	0.15435	1541	-11.933
0.78588	0.15729	1561	-14.015
0.84635	0.11776	1581	-14.444
0.77322	0.16777	1602	-13.687
0.81658	0.13794	1622	-16.016
0.78787	0.15909	1642	-6.8883
0.80649	0.14549	1663	-14.627
0.68614	0.2303	1683	-10.665
0.72679	0.1995	1704	-20.34
0.73532	0.19175	1725	-16.696
		1745	-18.921
0.76366	0.17493	1766	-16.112
0.77862	0.16798	1787	-12.356
0.82394	0.13121	1807	-16.448
0.87321	0.096365	1870	-14.153
0.7878	0.15229	1890	-11.565
0.76197	0.15925	1911	-13.029
0.83991	0.11441	1932	-7.2212
0.876	0.090465	1953	-16.017
0.84264	0.11741	1974	-11.705
0.77004	0.16469	1995	-6.9058
0.76769	0.16815	2016	-8.6117
0.80706	0.1421	2036	-13.039
0.77888	0.15702	2057	-9.6927
0.78808	0.15405	2078	-13.275
		2099	-13.522
		2141	-8.385
0.7011	0.22366	2183	-11.67
0.71948	0.21301	2226	-8.7781
0.69524	0.23335	2268	-8.9552
0.72012	0.20815	2311	-13.622
0.69038	0.21075	2354	-10.533
0.66609	0.24641	2441	-6.4864
0.68821	0.2218	2574	-10.059
0.76691	0.17606	2619	-7.1545
0.73081	0.19359	2688	-14.586
0.70548	0.21636	2734	-0.8441
0.71872	0.20982	2805	-1.599

TORF12 proxy data

0.71313	0.21494	2853	-6.4916
		2902	1.324
0.77609	0.18285	2951	-1.14
		3001	9.9661
0.81104	0.1461	3052	10.745
		3104	-12.634
0.77117	0.19836	3156	-7.9247
		3209	-0.38994
0.74134	0.19097	3264	-1.4346
		3319	-17.688
0.76458	0.19375	3375	-8.0855
		3432	-9.3889
0.79981	0.15525	3490	-6.6027
		3549	-6.4421
		3609	-14.595
		3670	-15.267
0.76788	0.17735	3731	-12.103
		3794	-9.6265
		3856	-21.242
		3918	-12.025
		3980	-16.772
		4042	-9.6335
0.77167	0.18368	4103	-6.3684
		4164	16.301
0.78536	0.16972	4194	-10.467
		4224	-8.8254
		4253	-4.8235
0.76141	0.18169	4311	7.4951
		4368	18.588
0.76903	0.18191	4424	-1.8845
		4480	-2.367
		4535	3.982
0.76843	0.1567	4589	-11.029
		4749	-5.4385
0.79636	0.14993	4801	-11.928
		4854	-9.1413
0.79477	0.16522	4907	-0.61838
		4959	-18.512
0.82144	0.14155	5012	-18.867
		5065	-9.6292
0.79072	0.16556	5119	-6.9039
		5172	-7.3033
0.80101	0.15762	5227	-7.2103
		5282	-4.9733
0.78882	0.16586	5338	-6.3253
		5395	-4.2462
0.82975	0.13182	5452	-0.37455
		5511	-4.3356
0.76423	0.18854	5571	-10.424
		5631	2.9701
0.80424	0.15456	5693	-2.0629
		5818	-7.5793
0.86835	0.10461	5882	-10.722
		5945	-10.534
0.86867	0.10015	6009	-9.5668
		6072	-0.60495
0.81844	0.13761	6135	2.9144

TORF12 proxy data

		6198	28.698
0.84766	0.11999	6260	-2.2382
		6321	-0.26583
0.79237	0.16391	6382	-4.94
		6441	9.5814
0.76533	0.18233	6499	10.657
		6583	14.347
0.76753	0.17888	6637	-0.48545
		6689	12.575
0.81491	0.14606	6740	-3.7536
		6790	-0.50645
0.81549	0.14588	6839	-9.7387
		6886	-6.6718
0.80556	0.14644	6933	7.2424
		6979	-7.4075
0.83523	0.1243	7024	2.0353
		7069	1.1746
0.85021	0.11319	7114	-0.40008
		7158	-3.8422
0.85356	0.11013	7201	-0.778
		7245	2.6009
0.91574	0.056997	7289	3.6263
		7334	-3.8879
0.86089	0.10969	7378	-0.68997
		7423	-4.0949
0.80475	0.16301	7469	-0.62843
		7515	3.4464
0.82107	0.14886	7562	6.9855
0.82932	0.12772	7610	2.4584
		7711	13.615
0.81744	0.13109	7765	10.469
		7821	2.8385
0.85237	0.11471	7879	24.326
		7941	16.112
0.81249	0.13743	8007	14.035
0.842	0.10978		
		0	
0.84397	0.10777		
0.85313	0.11784		
0.83256	0.12753		
0.83498	0.11882		
0.83284	0.13167		
0.84076	0.12123		
0.78428	0.16005		
0.8315	0.14176		